EPRI | ELECTRIC POWER RESEARCH INSTITUTE

# Materials Reliability Program: Crack Growth Rates for Evaluating Primary Water Stress Corrosion Cracking (PWSCC) of Thick-Wall Alloy 600 Materials and Alloy 82, 182, and 132 Welds (MRP-420, Revision 1)

2018 TECHNICAL REPORT

# Materials Reliability Program: Crack Growth Rates for Evaluating Primary Water Stress Corrosion Cracking (PWSCC) of Thick-Wall Alloy 600 Materials and Alloy 82, 182, and 132 Welds (MRP-420, Revision 1)

**3002014244**

Final Report, July 2018

EPRI Project Manager
P. Crooker



ELECTRIC POWER RESEARCH INSTITUTE
3420 Hillview Avenue, Palo Alto, California 94304-1338 ▪ PO Box 10412, Palo Alto, California 94303-0813 ▪ USA
800.313.3774 ▪ 650.855.2121 ▪ askepri@epri.com ▪ www.epri.com

## DISCLAIMER OF WARRANTIES AND LIMITATION OF LIABILITIES



THE FOLLOWING ORGANIZATION, UNDER CONTRACT TO EPRI, PREPARED THIS REPORT:

**Dominion Engineering, Inc.**



## NOTE

For further information about EPRI, call the EPRI Customer Assistance Center at 800.313.3774 or e-mail askepri@epri.com.

# ACKNOWLEDGMENTS

The following organization, under contract to the Electric Power Research Institute (EPRI), prepared this report:

Dominion Engineering, Inc.
12100 Sunrise Valley Drive
Reston, VA 20191

Principal Investigators
A. Jenks
G. White
M. Burkardt

This report describes research sponsored by EPRI.

Valuable input and review comments were received from many sources, in particular from the following people:

The Data Evaluation Group of the Expert Panel: Peter Andresen (GE-GRC; retired), Lola Gomez-Briceño (CIEMAT), Anders Jenssen (Studsvik), Stuart Medway (AMEC-FW), F.J. Perosanz (CIEMAT), Denise Paraventi (NNL)

The Applications Group of the Expert Panel: Warren Bamford (Westinghouse), Pål Efsing (Ringhals), Stephen Fyfitch (AREVA), David Morton (NNL), Raj Pathania (EPRI), Toshio Yonezawa (Tohoku University)

Input and review from Martin Morra (GE-GRC), Rickard Shen (Royal Institute of Technology), and Gary Stevens (EPRI) are also acknowledged.

This publication is a corporate document that should be cited in the literature in the following manner:

*Materials Reliability Program: Crack Growth Rates for Evaluating Primary Water Stress Corrosion Cracking (PWSCC) of Thick-Wall Alloy 600 Materials and Alloy 82, 182, and 132 Welds (MRP-420, Revision 1).* EPRI, Palo Alto, CA: 2018. 3002014244.

# ABSTRACT

Primary water stress corrosion cracking (PWSCC) of Alloy 600 and its weld metals, Alloys 82, 182, and 132, has been a known issue throughout the nuclear industry for decades. In 2002 and 2004, MRP-55 and MRP-115 were published, which presented PWSCC crack growth rate (CGR) equations for Alloys 600 and 82/182/132, respectively. There were insufficient data at those times to characterize various factors that affect PWSCC susceptibility, such as the stress intensity factor exponent for Alloy 600 or the effects of dissolved hydrogen for both the wrought and weld metals. Since the early 2000s, additional CGR data have been produced and there are now sufficient data to quantify these and other effects.

Therefore, to revise the disposition equations for Alloys 600 and 82/182/132, an international PWSCC CGR Expert Panel was organized by EPRI. A total of over 440 Alloy 600 CGR data points and over 530 Alloy 82/182/132 CGR data points were compiled, including data from the original MRP-55 and MRP-115 efforts. The data were screened for data quality and assessed to determine the effects of key parameters, such as the crack-tip stress intensity factor, temperature, yield strength, and crack growth orientation. This report presents revised CGR disposition equations for Alloys 600 and 82/182/132 that were developed from these data, as well as a full CGR model for Alloy 600 that has a greater range of applicability than the disposition equation for that alloy.

**Keywords**
Alloy 600
Alloy 82/182/132
Primary water stress corrosion cracking
Crack growth rate

**Deliverable Number: 3002014244**

**Product Type: Technical Report**

# Product Title: Materials Reliability Program: Crack Growth Rates for Evaluating Primary Water Stress Corrosion Cracking (PWSCC) of Thick-Wall Alloy 600 Materials and Alloy 82, 182, and 132 Welds (MRP-420, Revision 1)

**PRIMARY AUDIENCE:** PWR Plant Owners, Utilities, Licensees, Engineering Experts

**SECONDARY AUDIENCE:** Regulators, Codes and Standards, Vendors

## KEY RESEARCH QUESTION

Primary water stress corrosion cracking (PWSCC) of thick-wall Alloy 600 and its weld metals, Alloys 82/182/132, has been a known issue throughout the nuclear industry for decades. MRP-55 and MRP-115 addressed this issue through the development of crack growth rate (CGR) equations that could be used to evaluate flaws identified during in-service inspections of thick-wall components. Since 2002 and 2004, a substantial amount of new PWSCC CGR data have been produced for Alloy 600 and Alloy 82/182, respectively, such that reevaluation of the disposition curves was deemed appropriate. This report presents a summary of the analysis to reevaluate the CGR equations for Alloys 600 and 82/182/132.

## RESEARCH OVERVIEW

This report summarizes laboratory testing by an international group of experts to quantify the stress corrosion crack growth rates of Alloy 600 and its weld metals, Alloys 82, 182, and 132, in simulated PWR primary water. Variables known to affect PWSCC were assessed and included in the CGR model and/or disposition equations: the stress intensity factor, the test temperature, the yield strength of the component, the electrochemical potential, the orientation of the crack growth, and the alloy. The data were assessed by an Expert Panel and then were used to update the CGR disposition equations presented for these alloys in MRP-55 and MRP-115. Changes to the original equations include the removal of a stress intensity factor threshold, the modification of the stress intensity factor exponent, and the addition of a dissolved hydrogen term. A full CGR model was also developed for Alloy 600, in which terms for yield strength and crack growth orientation were added. When compared to the original MRP-55 and MRP-115 disposition equations, the new equations are generally similar.

## KEY FINDINGS

- The validity of the original disposition equations for Alloy 600 and Alloy 82/182/132 is supported by reevaluation of the original data used to develop the equations presented in MRP-55 and MRP-115 and assessments of additional newly compiled data.
- Added deformation results in increased susceptibility to PWSCC, and crack growth rates are strongly dependent on yield strength, stress intensity factor, and temperature.
- The effects of key engineering parameters are illustrated, along with the bases for their selection.
- An updated CGR disposition equation, which is directly applicable to plant conditions, and a full CGR model, which includes additional factors, are presented separately for Alloy 600. An updated disposition equation is also presented for Alloy 82/182/132.

ELECTRIC POWER RESEARCH INSTITUTE

# EXECUTIVE SUMMARY

## WHY THIS MATTERS

Crack growth rate disposition equations for Alloy 600 and Alloy 82/182/132 were developed approximately 15 years ago that could be used to evaluate flaws identified during in-service inspections of thick-wall components. Subsequently, these equations were incorporated into the ASME Boiler and Pressure Vessel (B&PV) Code Section XI for continued-service evaluation of detected PWSCC flaws or those postulated to exist. This report reevaluates these equations in light of newly compiled data.

## HOW TO APPLY RESULTS

This report presents both a full crack growth rate model that incorporates key engineering variables that affect the stress corrosion crack growth rate, and a simplified disposition curve that is directly applicable to plant component conditions. Applications of this work may include determining component design lives, setting inspection intervals, optimizing SCC mitigation repairs, and dispositioning any crack-like indications relative to degradation via stress corrosion cracking.

## LEARNING AND ENGAGEMENT OPPORTUNITIES

- MRP-386 (EPRI 3002010756) documents the Expert Panel effort to develop factors of improvement (FOIs) for Alloys 690 and 52/152 versus Alloys 600 and 82/182/132, respectively.
- MRP-55 (EPRI 1006695) and MRP-115 (EPRI 1006696) developed the original disposition equations for Alloys 600 and 82/182/132, respectively, that were subsequently incorporated into the ASME Boiler and Pressure Vessel Code Section XI. The databases and analyses developed for these reports form the basis for this current report.

**EPRI CONTACTS:** Paul Crooker, Principal Technical Leader, pcrooker@epri.com

**PROGRAM:** Materials Reliability Program, 41.01.04

**IMPLEMENTATION CATEGORY:** Category 2 – Plant optimization



**Electric Power Research Institute**
3420 Hillview Avenue, Palo Alto, California 94304-1338 • PO Box 10412, Palo Alto, California 94303-0813 USA
800.313.3774 • 650.855.2121 • askepri@epri.com • www.epri.com

# RECORD OF REVISIONS

| Revision Number | Revision Description |
|---|---|
| MRP-420 | Original Report (Revision 0) |
| MRP-420 Rev. 1 | This report as originally published (MRP-420) was revised to incorporate updated Alloy 82/182/132 dissolved hydrogen parameter dependencies. All changes, except corrections to typographic errors and minor editorial changes, are summarized below.<br><br>**Record of Revisions:** Added to reflect changes from MRP-420 Rev. 0.<br><br>**Section 5.3:** Updated to incorporate modifications to the Alloy 82/182/132 dissolved hydrogen parameter values.<br><br>**Section 6.1.3:** Corrected reference temperature and reference yield strength within Table 6-2.<br><br>**Section 6.2:** Updated to incorporate modifications to the Alloy 82/182/132 dissolved hydrogen parameter values.<br><br>**Appendix C:** Added to provide explanation of the updated approach to the Alloy 82/182/132 dissolved hydrogen parameter values. |

# ACRONYMS

| | |
|---|---|
| AMIS | Average misorientation |
| ANL | Argonne National Laboratory |
| ANS | American Nuclear Society |
| ASME | American Society of Mechanical Engineers |
| BMI | Bottom-mounted instrumentation (nozzle) |
| CEA | Le Commissariat à l'Energie Atomique |
| CGR | Crack growth rate |
| CIEMAT | Centro de Investigaciones Energéticas, Medioambientales y Tecnológicas |
| CK | Constant stress intensity factor |
| CL | Constant load |
| CMTR | Certified material test report |
| CRDM | Control rod drive mechanism |
| CT | Compact tension (specimen geometry) |
| CW | Cold work |
| DCPD | Direct current potential drop |
| EBSD | Electron backscatter diffraction |
| ECP | Electrochemical potential |
| EDF | Électricité de France |
| EPRI | Electric Power Research Institute |
| FCC | Face-centered cubic |
| FOI | Factor of improvement |
| GE | General Electric |
| GE-GRC | General Electric – Global Research Center |
| GOS | Grain orientation spread |
| HAZ | Heat-affected zone |

| | |
|---|---|
| HK | Knoop hardness |
| HRC | Rockwell C hardness |
| HT | Heat treatment |
| HTMA | High temperature mill anneal |
| ID | Inner diameter |
| IG | Intergranular |
| IGSCC | Intergranular stress corrosion cracking |
| K | Stress intensity factor |
| KAM | Kernel average misorientation |
| KAPL | Knolls Atomic Power Laboratory |
| $K_{TH}$ | Threshold stress intensity factor |
| LTMA | Low temperature mill anneal |
| MA | Mill anneal |
| MHI | Mitsubishi Heavy Industries |
| MRP | Materials Reliability Program |
| NNL | Naval Nuclear Laboratory |
| OD | Outer diameter |
| PMZ | Partially melted zone |
| PNNL | Pacific Northwest National Laboratory |
| PORV | Power operated relief valve |
| PPU | Periodic partial unloading |
| PV | Pressure vessel |
| PWHT | Post-weld heat treatment |
| PWR | Pressurized water reactor |
| PWSCC | Primary water stress corrosion cracking |
| RT | Room temperature |
| SCC | Stress corrosion cracking |
| STP | Standard temperature and pressure |
| TT | Thermally treated |
| UMZ | Unmixed zone |
| YS | Yield strength |

# CONTENTS

# LIST OF FIGURES

# LIST OF TABLES

# 1
# INTRODUCTION

Primary water stress corrosion cracking (PWSCC) of thick-wall Alloy 600 and its weld metals Alloys 82/182/132 has been a known issue throughout the nuclear industry for decades. PWSCC of control rod drive mechanism (CRDM) nozzles and associated J-groove welds, among other locations, in the 1990s highlighted the need for crack growth rate (CGR) equations that could be used to evaluate flaws identified during in-service inspections of thick-wall components. This need was addressed in 2002 for Alloy 600 with the publication of MRP-55 ([1], [2]) and in 2004 for Alloy 82/182/132 with the publication of MRP-115 ([3], [4]).

For both of the original reports, an EPRI Materials Reliability Program (MRP) CGR review team consisting of an international panel of experts in the area of SCC crack growth was assembled to review the CGR data from which CGR equations were developed. Subsequently, these equations were incorporated into the ASME Boiler and Pressure Vessel (B&PV) Code Section XI for continued-service evaluation of detected PWSCC flaws or those postulated to exist.

Since 2002 and 2004, a substantial amount of new PWSCC CGR data have been produced for Alloy 600 and Alloy 82/182,[1] respectively, such that it was deemed prudent to reevaluate the CGR equations at this time. With the newly obtained data, as well as some data that were available at the time but excluded from the MRP-55 and MRP-115 databases for various reasons, there is now sufficient information to investigate several parameters, some for the first time and some in greater depth, that had not been possible previously. These parameters include:

- Stress intensity factor exponent (Alloys 600 and 82/182/132)
- Stress intensity factor threshold (Alloy 600)
- Dissolved hydrogen concentration (Alloys 600 and 82/182/132)
- Cold work and/or yield strength (Alloy 600)
- Heat-affected zone (Alloy 600)

For this effort, a new Expert Panel was organized by EPRI. The purpose of this Expert Panel was two-fold. First, they were tasked with determining if the original equations should be revised based on preliminary analyses showing the effect of the newly included data on the previous statistical assessments, as well as the availability of data covering a wider range of parameters than had previously been investigated. Second, if such revisions were warranted, the experts were to guide the analysis process to develop new CGR equations.

[1] No new Alloy 132 PWSCC CGR data have been produced since the publication of MRP-115.

## 1.1 Objective

The objectives of this report are to present updated crack growth rate disposition equations for Alloy 600 and Alloy 82/182/132 based on expanded CGR databases that are generally applicable to thick-wall plant components, as well as CGR models that are valid under a variety of material and environmental conditions.

This report will also detail the Expert Panel's activities to compile, evaluate, and analyze the data to support these goals.

## 1.2 Report Organization

This report is organized as follows:

- Section 1 presents the background for predicting PWSCC crack growth rates of Alloy 600 and Alloy 82/182/132, as well as the objective of this report.
- Section 2 describes the Expert Panel role and the approach taken to compiling and scoring the Alloy 600 and Alloy 82/182/132 CGR databases.
- Section 3 provides a description of the Alloy 600 and Alloy 82/182/132 PWSCC CGR databases post-screening by the Expert Panel.
- Section 4 addresses the applicability of laboratory testing conditions to plant components.
- Section 5 details the selection and development of the PWSCC CGR parameters and functional dependencies.
- Section 6 presents the PWSCC CGR disposition equations and full models for Alloy 600 and Alloy 82/182/132.
- Section 7 contains the conclusions of this report.
- Section 8 lists the references cited.
- Appendix A documents the screened Alloy 600 and Alloy 82/182/132 PWSCC CGR databases.
- Appendix B explains the quantification of the relationships between cold work, yield strength, and hardness for Alloy 690.
- Appendix C discusses the updated approach for the Alloy 82/182/132 dissolved hydrogen parameter development included in Revision 1 of this report.

# 2
# EXPERT PANEL APPROACH

## 2.1 Introduction

Members of the EPRI-organized Expert Panel were required to have expertise in the metallurgical, mechanical, and environmental aspects of primary water stress corrosion cracking (PWSCC) of nickel-base alloys and weldments. The panel was structured into two groups: the Data Evaluation Group, which dealt primarily with evaluating the laboratory data, and the Applications Group, which dealt with analyzing the data and developing the crack growth rate (CGR) equations. The Data Evaluation Group had the lead responsibility for scoring the laboratory data. The Applications Group had the lead responsibility for identifying the applicable material conditions relevant to plant components and for guiding the statistical approach to be applied to the scored data. Several members had expertise in both areas but served only in a single group, and many had been involved with the original MRP-55 and MRP-115 efforts.

Decisions throughout the process were made by consensus of the experts within the two groups.

## 2.2 Expert Panel Members and Roles

The Data Evaluation Group experts have substantial experience performing PWSCC crack growth rate testing and detailed analysis of raw laboratory data. These experts evaluated the compiled database to score for data quality from a testing perspective. These experts include:

- Dr. Stuart Medway, AMEC-Foster Wheeler
- Ms. Lola Gomez-Briceño and Mr. F.J. Perosanz, CIEMAT
- Dr. Peter Andresen, General Electric – Global Research Center (now retired)
- Dr. Denise Paraventi, Naval Nuclear Laboratory
- Mr. Anders Jenssen, Studsvik

The Applications Group experts' experience is with nickel-base components in pressurized water reactors (PWRs), including knowledge of material processing, component fabrication, incidents of PWSCC detected in PWR plant components, and application of CGR equations to plant scenarios. These experts evaluated the applicability of material, mechanical, and environmental conditions used in the laboratory testing to plant conditions, and they guided the statistical approach to evaluating the data and developing the CGR models and disposition curves. These experts include:

- Mr. Stephen Fyfitch, AREVA
- Dr. Raj Pathania, EPRI
- Dr. David Morton, Naval Nuclear Laboratory

- Mr. Pål Efsing, Ringhals
- Prof. Toshio Yonezawa, Tohoku University
- Mr. Warren Bamford, Westinghouse

## 2.3 Data Compilation

The bases for the CGR data compilation for Alloys 600 and 82/182/132 were the MRP-55 and MRP-115 databases. The MRP-55 database included 158 Alloy 600 test segments from 137 specimens and 28 heats. The MRP-115 database included 77 Alloy 82/182/132 test segments from 42 specimens and 19 welds. In addition, the database of excluded data from MRP-115 was obtained, and some of those data were reevaluated for inclusion into the final database used for developing the CGR model, as described in Section 2.4.

Data that were not included in MRP-55 and MRP-115–most of which were produced after the publication of those reports–were compiled by Dominion Engineering, Inc., from various publicly available documents, including conference proceedings, EPRI reports, and NUREG reports. The publications are included as References [5] through [29]. In some cases, investigators provided laboratory reports and/or additional as-yet unpublished data. Over 280 new Alloy 600 and Alloy 600 heat-affected zone (HAZ) test segments were collected from 190 specimens and 19 heats. Over 290 new Alloy 82/182 test segments were collected from 201 specimens and 24 welds. A total of 42 attributes were recorded for each test segment, as listed in Table 2-1.

CGR data were obtained from 12 laboratories in six countries, including:

- Argonne National Laboratory (ANL; United States)
- AREVA GmbH (Germany)
- Bettis Atomic Power Laboratory (now Naval Nuclear Laboratory (NNL); United States)
- CEA (France)
- Centro de Investigaciones Energéticas, Medioambientales y Tecnológicas (CIEMAT; Spain)
- Électricité de France (EdF; France)
- General Electric – Global Research Center (GE-GRC; United States)
- Lockheed Martin (now Naval Nuclear Laboratory (NNL); United States)
- Mitsubishi Heavy Industries (MHI; Japan)
- Pacific Northwest National Laboratory (PNNL; United States)
- Studsvik (Sweden)
- Westinghouse (United States)

The Alloy 600 and Alloy 82/182/132 data compiled for this effort, as well as the compositions of the heats and welds included, are tabulated in Appendix A. Details of the scoring procedure and the criteria for inclusion of data for model development can be found in Sections 2.4 and 2.5, respectively.

**Table 2-1**
**Attributes recorded for CGR database compilation**

| Specimen Identification | Specimen Properties | Test Parameters | Test Results |
|---|---|---|---|
| Laboratory | As Received Condition | Total Test Time (h) | %Width Used for Δa Calc |
| Material | Product Form | ID for Test Segment | Δa (mm) Avg. for Segment |
| Overall Test ID | Post-Supplier Thickness Reduction (%) | Time of Test Segment (h) | Δa (mm) Max. for Segment |
| Heat/Weld | Post-Supplier Processing Method | Duration of Test Segment (h) | % Engaged |
| Supplier | Post-Supplier Processing Details | Load Type | % Intergranular |
| | Crack Orientation vs. Product Form | K (MPa√m) | Post-Test Correction Factor |
| | Crack Orientation vs. Deformation Plane | K Range (MPa√m) if >5% | Correction Technique |
| | Crack Orientation vs. Banding (where applicable) | Test Temp (°C) | Range in SCC CGR (mm/s) (optional) |
| | Yield Strength (MPa) | Dissolved $H_2$ (cc/kg) | Reported SCC CGR (mm/s) |
| | Hardness (HV) | B (ppm) | Δa/Δt (mm/s) |
| | Misorientation (deg) | Li (ppm) | % Difference Between Δa/Δt and Reported CGR |
| | CT Size | PPU Details | Laboratory Notes |
| | Control vs. Tandem CT | | |

## 2.4 Data Screening and Scoring

Screening of the newly compiled Alloy 600 and 82/182 data was based on the same criteria used in MRP-115. For that effort, test segments were screened out of the database to be used for CGR equation development if they failed to meet any of the following criteria:

1. Crack growth increment during the test segment of at least 0.5 mm (0.02 in.).
2. Crack front engagement of at least 50%.
3. Nominal PWR primary water chemistry (particularly dissolved hydrogen content).
4. Constant loading conditions, including constant load, stress intensity factor, or crack opening displacement (collectively referred to as "CL/CK"), or cyclic loading with at least 1 hour hold time at CL/CK during each cycle.
5. Average, rather than maximum, crack increment reported. (Unless otherwise specified, it was assumed that reported crack growth increments and CGRs were the average values.)

The last four criteria were accepted by the Data Evaluation Group as still being appropriate for screening of the newly compiled data. However, it was decided by consensus that the minimum crack increment requirement was too restrictive. This was in large part because testing methods have improved since the 1990s, when the MRP-55 and MRP-115 data were generated, such that the experts had greater confidence in the quality and accuracy of the new data with lower crack increments. Such improvements included more careful transitioning from fatigue to SCC, more widespread use of sensitive DCPD monitoring, and better stability of the environment and loading parameters. Thus, the data screening process was amended as follows:

1. Screen the newly compiled data based on the five screening criteria above.
2. If the test segment passed all five screening criteria, it was included in the final database to be used for CGR equation development.
3. If the test segment failed any of criteria #2 – #5 (i.e., failed any criterion excluding that for minimum crack growth increment), it was excluded from the equation development database.
4. If the test segment passed criteria #2 – #5 but failed #1 (i.e., passed all criteria except that for the minimum crack growth increment), it was evaluated (scored) in more detail by the Data Evaluation Group to determine suitability for inclusion in the equation development database.

The experts also decided that any of the original Alloy 82/182/132 data that had been screened out of MRP-115 solely because they did not meet the minimum crack increment requirement should be reevaluated and scored by the experts. The fully detailed database of excluded data from MRP-55 was not available, so no original Alloy 600 data were reevaluated.

After this screening process was applied, of the 285 newly compiled Alloy 600 test segments, 108 were screened in, 45 were screened out, and 132 were "low crack increment" data. Of the 293 newly compiled Alloy 82/182 test segments, 141 were screened in, 34 were screened out, and 118 were "low crack increment" data. Of the 167 test segments that were scored out in MRP-115, 12 were determined to be "low crack increment" data but otherwise acceptable and were reevaluated.

### 2.4.1 Scoring of Low Crack Increment Data

The low crack increment data were evaluated by the Data Evaluation experts on the basis of experimental technique and overall data quality and testing credibility. Expert evaluation was to be based on the details of the test and not on an expectation of what the data should show based, for example, on the effect of temperature or stress intensity factor, or on prior observations (either at constant stress intensity factor (K)/load or during cycling/transitioning). Any implications regarding material applicability to plant components or to parameter dependencies (such as the K exponent, for example) were to be addressed in the statistical analysis and modeling processes, rather than during scoring.

Numerous factors were assessed to determine the quality of the test segment in question, as well as the overall test, and a score was assigned by each expert. Scores ranged from 1 to 5, inclusive, with 1 representing the highest quality data. Only data with an average expert score above a certain threshold were used in the development of the CGR models, although the effects of adjusting this threshold were investigated.

The issues that were considered when scoring the low increment data included:

- Crack increment, test time, and crack growth rate interactions
- Crack front engagement and intergranular morphology percentage
- Loading condition
- Environment
- Transitioning steps from fatigue to SCC
- DCPD availability and noise, and crack growth behavior as shown by DCPD
- Post-test correction

## 2.5 Criteria for Inclusion of Data in Equation Development

Data could be included in the equation development database in one of three ways:

1. Were included in the original MRP-55 or MRP-115 analyses,
2. Passed all five of the first set of screening criteria listed in Section 2.4, or
3. Failed only the minimum crack growth increment criterion in Section 2.4 and received an average score better than a specified threshold value

A threshold average value of 3 was selected, such that any data with an average score of the threshold value or better were included and any data with a worse average score were excluded.

The scoring process for Alloy 600 resulted in approximately 11% of the low crack increment data being removed due to low average scores, resulting in a final database consisting of 371 test segments. For Alloy 82/182/132, approximately 8% of the low crack increment data were scored out, leaving 314 test segments available for model development. Details on these screened databases are described in Section 3.

# 3
# SUMMARY OF SCREENED CGR DATABASES

The screened databases used for CGR equation development include data that a) were originally included in MRP-55 or MRP-115, b) were not in MRP-55 or MRP-115 (i.e., were typically generated more recently) and passed the MRP-115 screening criteria, or c) passed all of the MRP-115 screening criteria except for minimum crack increment and passed the threshold for average score selected by the current Expert Panel. The following sections describe the properties of the Alloy 600 and Alloy 82/182/132 databases, including important variable distributions.

## 3.1 Alloy 600 Screened CGR Database

The Alloy 600 screened CGR database contains 371 test segments from 277 specimens and 33 heats. All data from the original MRP-55 database were included except for 13 points obtained under periodic partial unloading (PPU) with hold times less than one hour. (The PPU hold time minimum was first implemented in MRP-115, after MRP-55 had been published.) The breakdown by testing laboratory is shown in Table 3-1. A total of 14 of the 33 heats were tested by multiple laboratories, with the most extensive testing (in terms of number of test segments included) being performed on heat NX5853G11, a mill annealed plate. Table 3-2 lists the ranges for a variety of testing parameters, and Figure 3-1 shows cumulative distribution plots of these variables to illustrate the spread of the data. Figure 3-2 plots all of the as-reported (i.e., not adjusted) Alloy 600 data and Figure 3-3 separates the original MRP-55 data from the newly compiled data. Both of these plots include the MRP-55 75$^{th}$ percentile curve for non-cold worked Alloy 600 for reference. As seen in Figure 3-3, the old and new data with similar yields strength (YS) ranges are generally very similar.

**Table 3-1**
**Distribution of Alloy 600 CGR data points, specimens, and heats by testing laboratory**

| | ANL | Bettis | CEA | CIEMAT | EDF | GE-GRC |
|---|---|---|---|---|---|---|
| No. Points | 34 | 78 | 22 | 50 | 23 | 33 |
| No. Specimens | 5 | 78 | 22 | 38 | 23 | 15 |
| No. Heats | 2 | 2 | 3 | 6 | 7 | 3 |
| | **Lockheed Martin** | **PNNL** | **Studsvik** | **Westinghouse** | | **Total*** |
| No. Points | 28 | 24 | 34 | 45 | | **371** |
| No. Specimens | 28 | 4 | 28 | 36 | | **277** |
| No. Heats | 2 | 2 | 9 | 11 | | **33** |

*Total numbers of points and specimens are a sum of the respective values for each of the testing laboratories. Some heats were tested by multiple laboratories, however, so the total number of heats is less than the sum of those tested at each laboratory.

**Table 3-2**
**Range of several key parameters and responses for Alloy 600 CGR data**

| Parameter | Minimum Value | Maximum Value | Units |
|---|---|---|---|
| K | 7 | 69 | MPa√m |
| T | 252 | 363 | °C |
| $[H_2]$ | 3 | 239 | cc/kg |
| $\Delta ECP_{Ni/NiO}$ | -50 | 61 | mV |
| CW | 0 | 32 | % |
| YS | 166 | 827 | MPa |
| t | 5 | 7000 | hr |
| Δa | 0.003 | 7.0 | mm |
| IG | 50 | 100 | % |

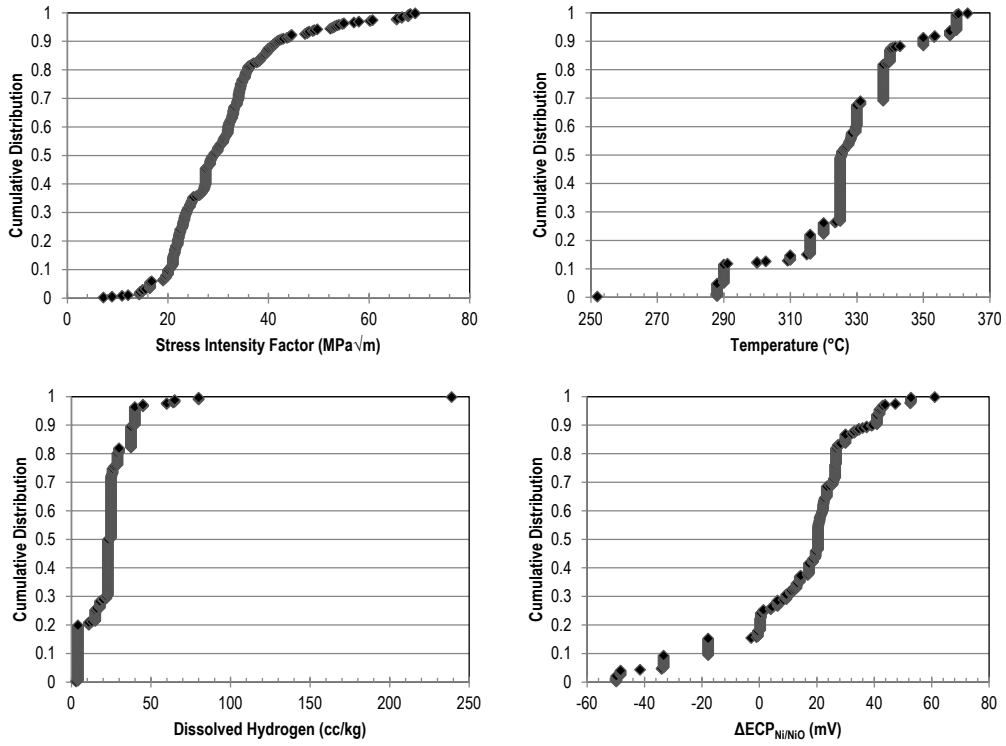


**Figure 3-1**
**Cumulative distribution plots for several key parameters and responses for Alloy 600 data**

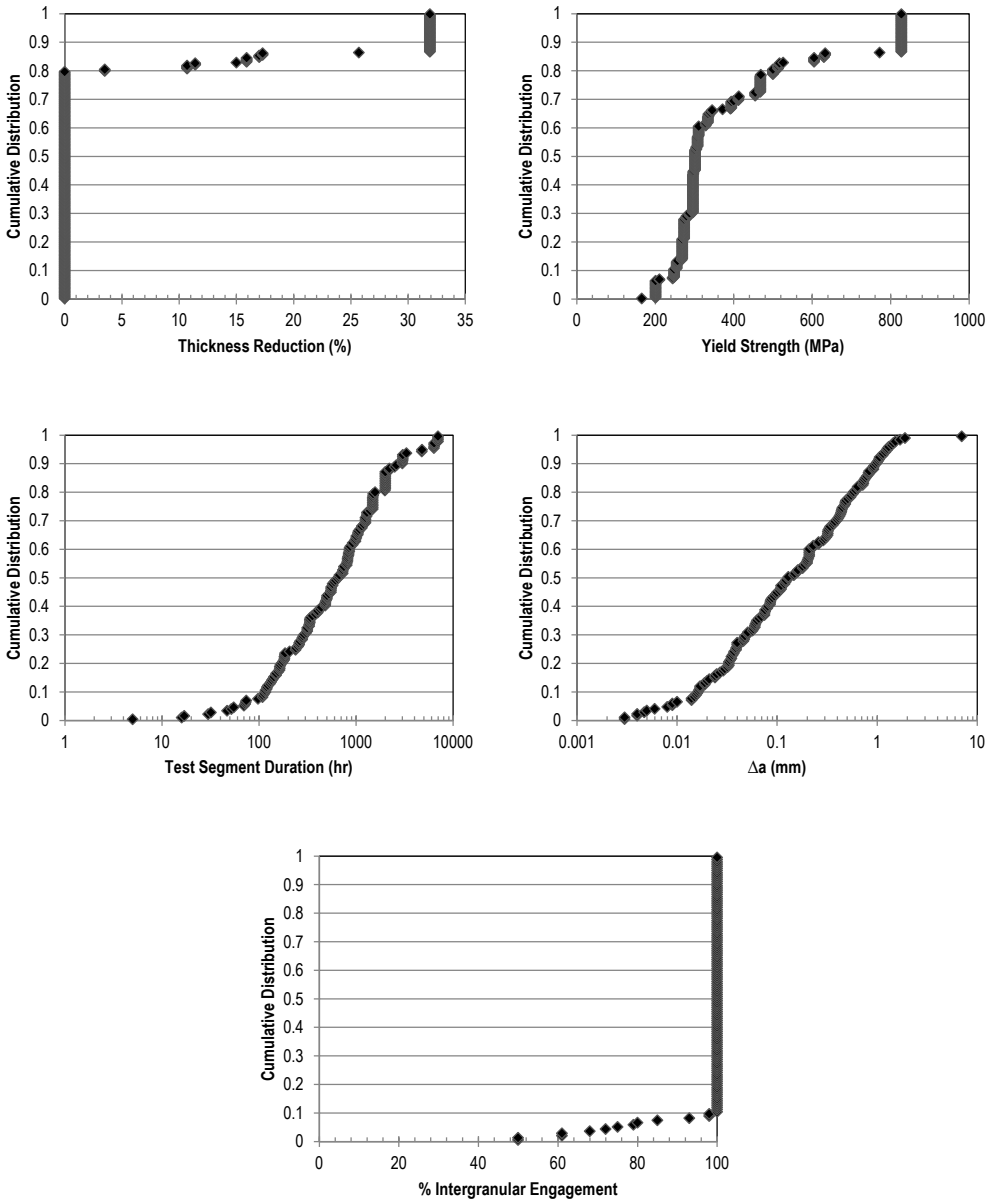


**Figure 3-1 (continued)**
**Cumulative distribution plots for several key parameters and responses for Alloy 600 data**

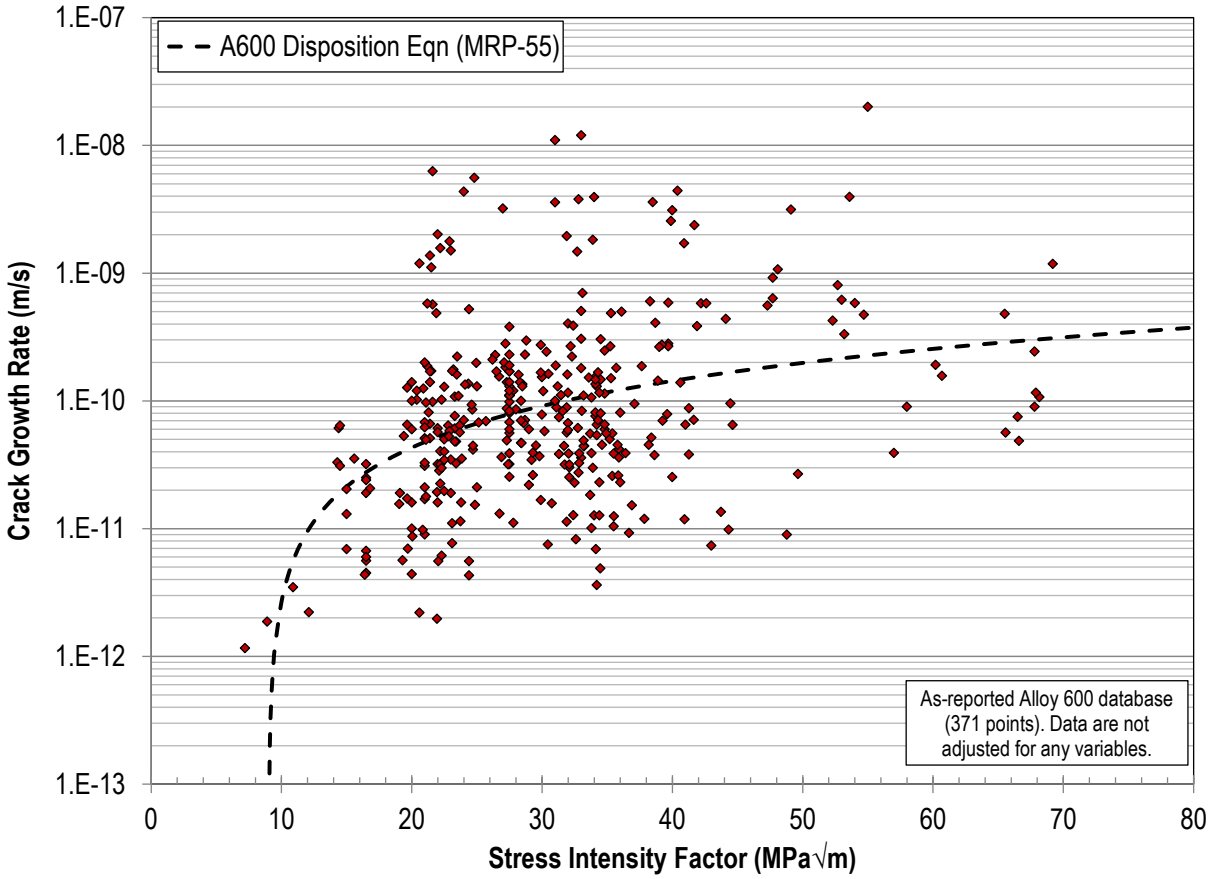


**Figure 3-2**
**Screened Alloy 600 database: All data, unadjusted for temperature, dissolved hydrogen, cold work level, etc.**

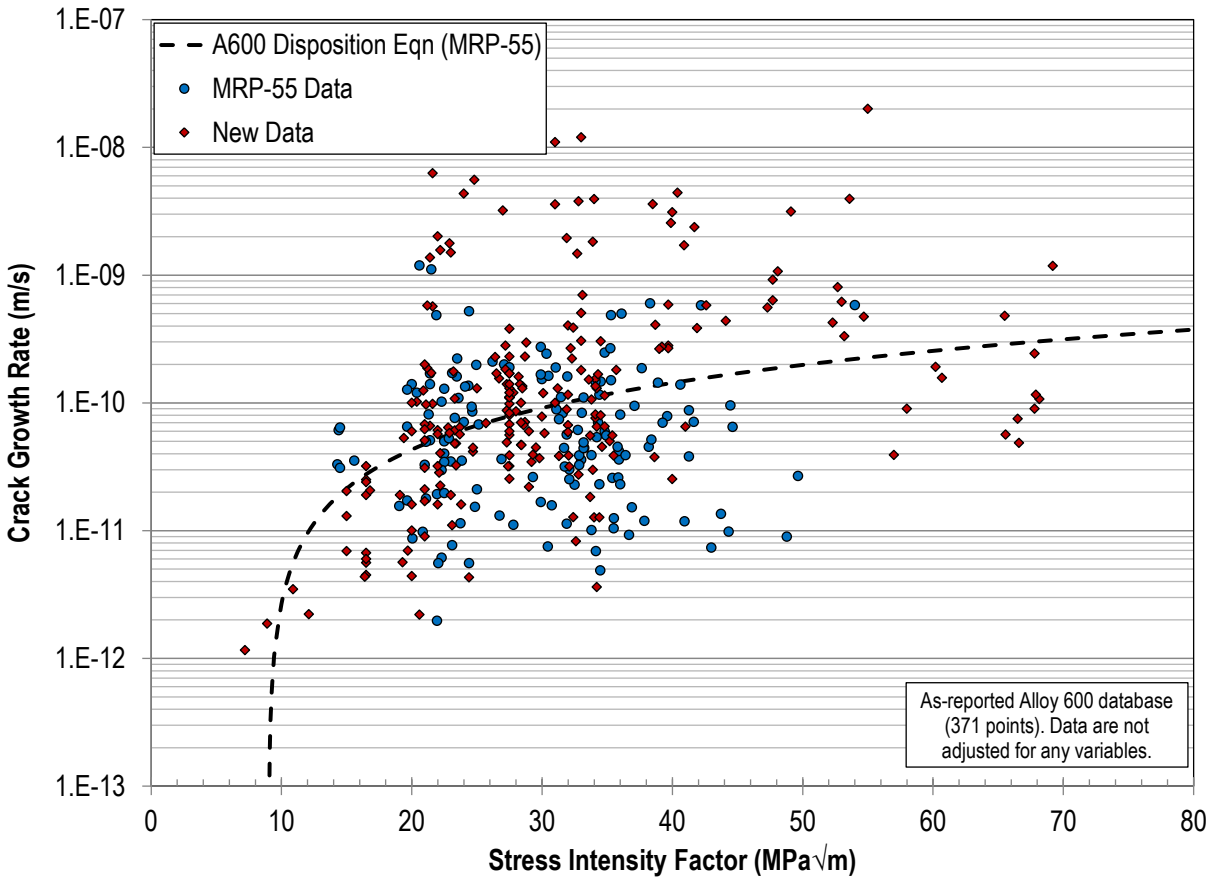


**Figure 3-3**
**Screened Alloy 600 database: All data, unadjusted for temperature, dissolved hydrogen, cold work level, etc. Comparison is shown between MRP-55 data and newly compiled data.**

## 3.2 Alloy 600 Disposition Equation Database

The disposition equation for Alloy 600 is meant to be utilized for cracks growing in plant components. This means that the material and environmental conditions of the CGR data used to develop the equation must be broadly representative of plant components, as discussed in Section 4, particularly with regard to yield strength being below 600 MPa.

The full Alloy 600 CGR database of 371 points was reduced to 308 points for the disposition equation development, limiting the data to those directly relevant to plant component scenarios (namely YS <600 MPa). No original MRP-55 data were excluded (except for the 13 PPU points with short hold times that were excluded from the full database). The reduction in data (63 points) was due to limitations on the maximum YS (and by extent, CW level). Table 3-3 and Figure 3-4 show the distribution of various characteristics of the disposition equation database. Figure 3-5 plots all of the as-reported (i.e., not adjusted) Alloy 600 data and Figure 3-6 separates the original MRP-55 data from the newly compiled data.

**Table 3-3**
**Range of several key parameters and responses for Alloy 600 CGR data used for development of the disposition equation**

| Parameter | Minimum Value | Maximum Value | Units |
|---|---|---|---|
| K | 7 | 69 | MPa√m |
| T | 288 | 363 | °C |
| $[H_2]$ | 3 | 239 | cc/kg |
| $\Delta ECP_{Ni/NiO}$ | -50 | 61 | mV |
| CW | 0 | 15 | % |
| YS | 166 | 526 | MPa |
| t | 30 | 7000 | hr |
| Δa | 0.003 | 7.0 | mm |
| IG | 50 | 100 | % |

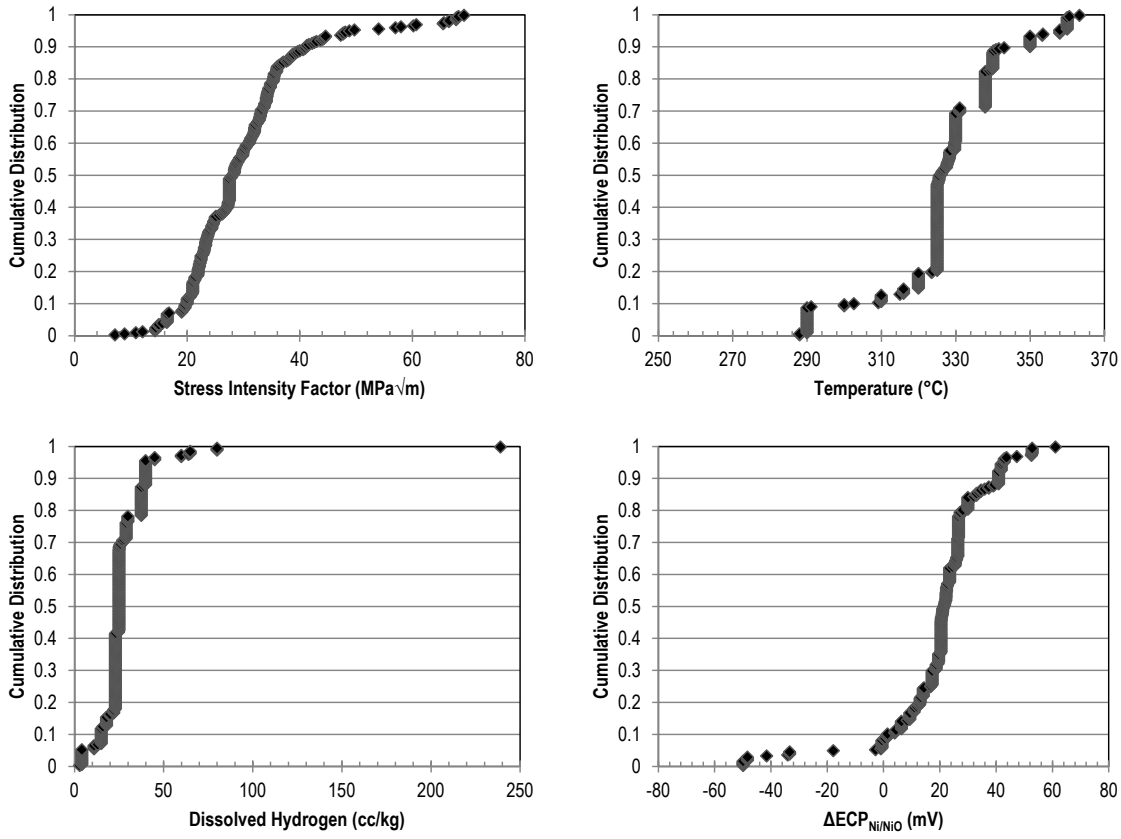


**Figure 3-4**
**Cumulative distribution plots for several key parameters and responses for Alloy 600 data used for development of the disposition equation**

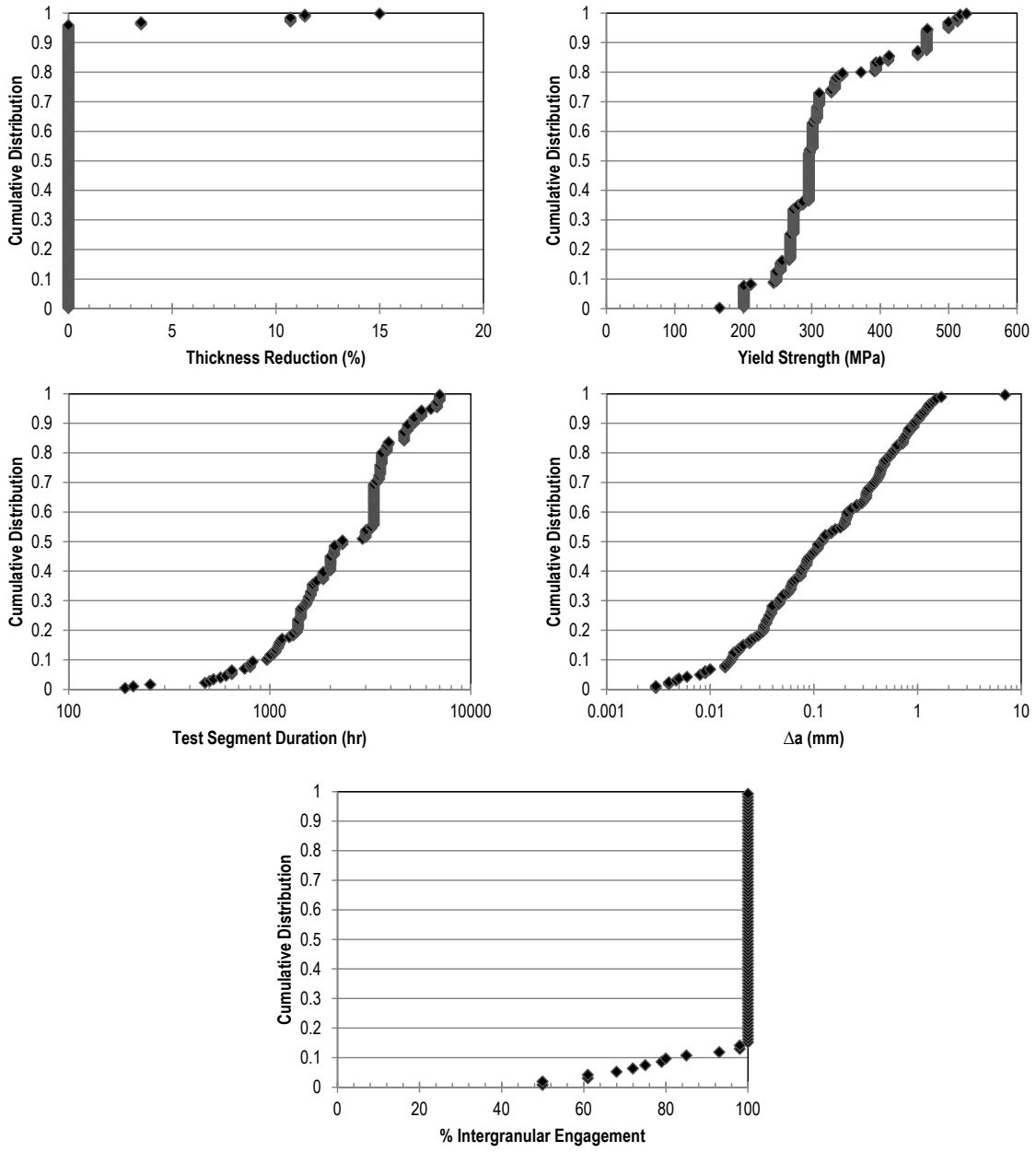


**Figure 3-4 (continued)**
**Cumulative distribution plots for several key parameters and responses for Alloy 600 data used for development of the disposition equation**

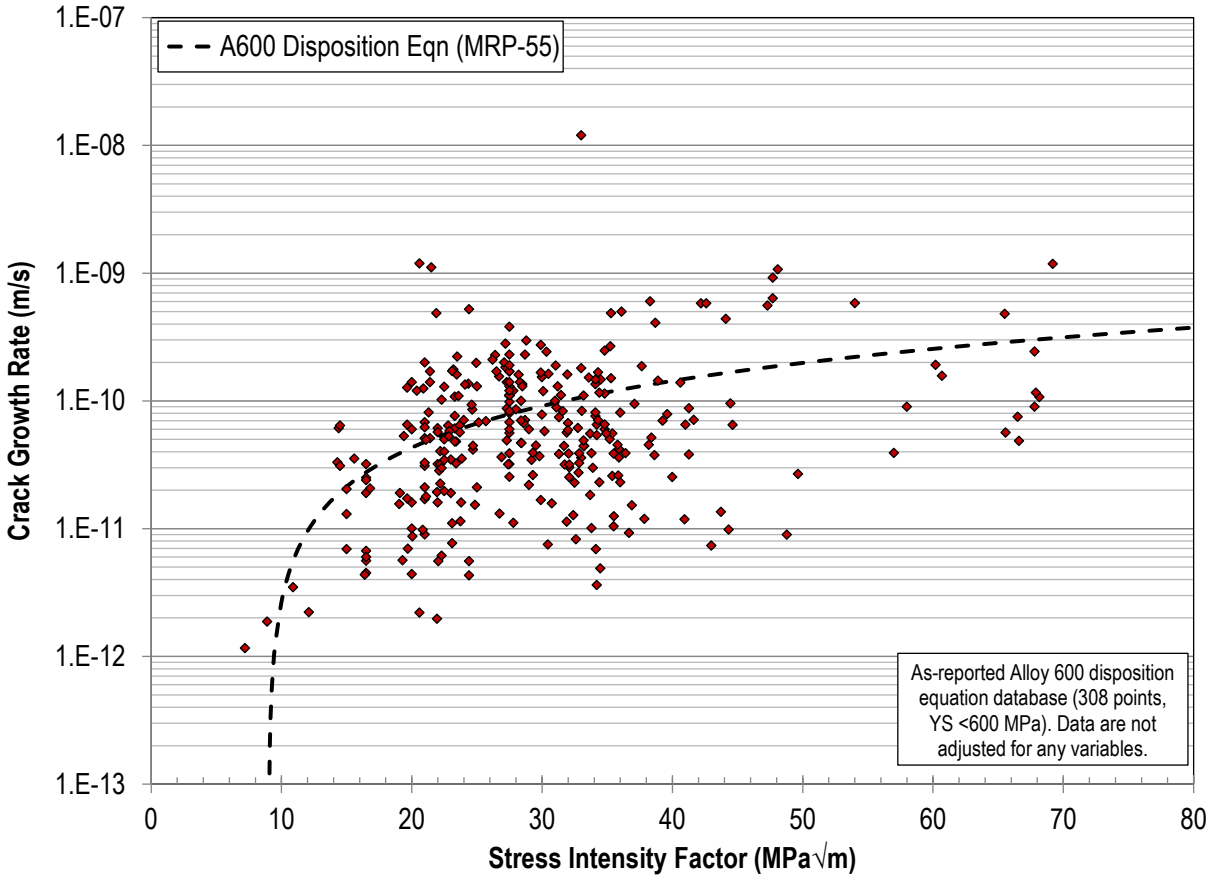


**Figure 3-5**
**Screened Alloy 600 database: Only data used for the development of the disposition equation are shown (308 points). Data are unadjusted for temperature, dissolved hydrogen, cold work level, etc.**

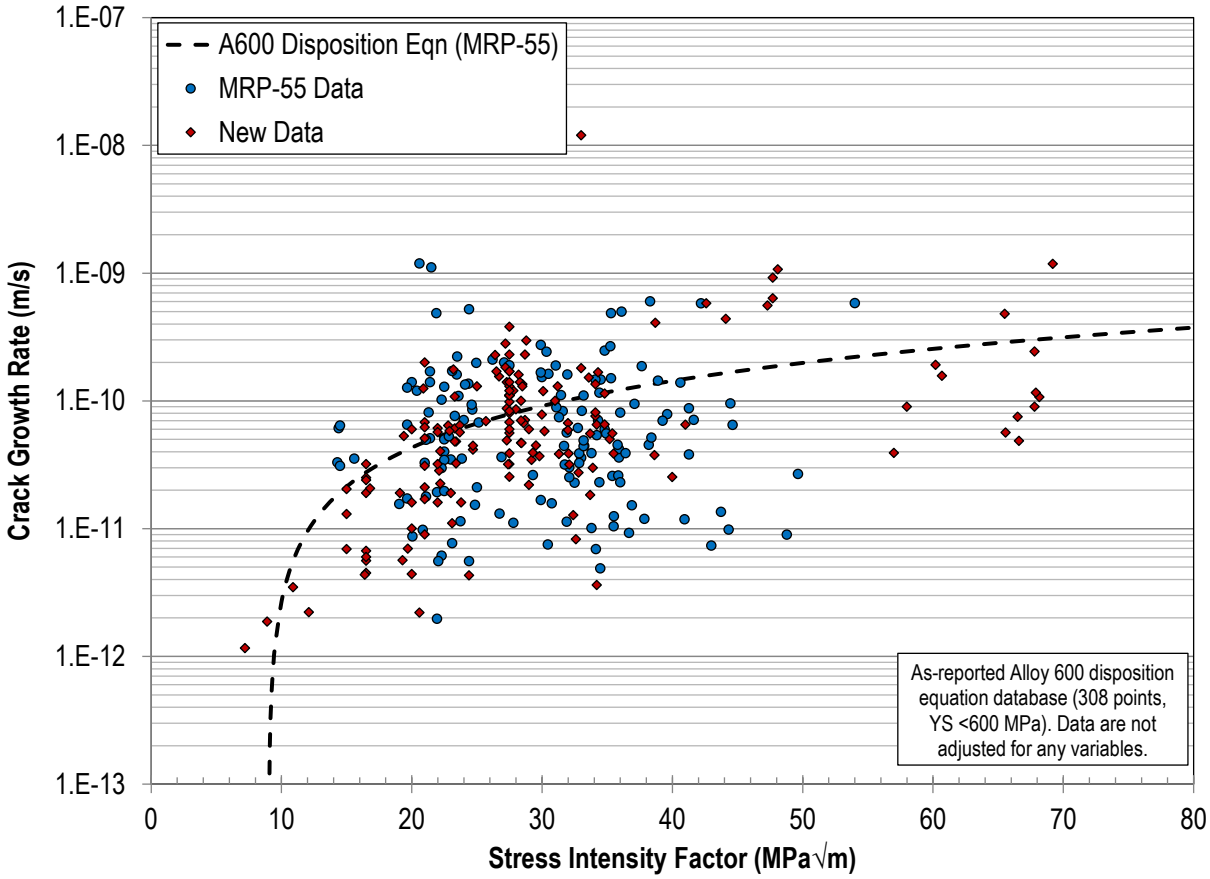


**Figure 3-6**
**Screened Alloy 600 database: All data, unadjusted for temperature, dissolved hydrogen, cold work level, etc. Comparison is shown between MRP-55 data and newly compiled data.**

## 3.3 Alloy 82/182/132 Screened CGR Database

The Alloy 82/182/132 screened CGR database contains 314 test segments from 188 specimens and 41 welds. All data from the original MRP-115 database are included. The breakdown by testing laboratory is shown in Table 3-4. One of the 41 welds was tested by multiple laboratories, although the most extensive testing (in terms of number of test segments included) was performed on Alloy 182 weld 414998 by a single laboratory. Table 3-5 shows the distribution of weld alloys included in the database. Table 3-6 lists the ranges for a variety of testing parameters, and Figure 3-7 shows cumulative distribution plots of these variables to illustrate the spread of the data. Figure 3-8 plots all of the as-reported (i.e., unadjusted) Alloy 82/182/132 data, and Figure 3-9 separates the original MRP-115 data from the newly compiled data. Both plots include the MRP-115 75$^{th}$ percentile curves for Alloys 82 and 182 for reference. As seen in Figure 3-9, the old and new data are generally very similar.

All Alloy 82/182/132 data are applicable to plant components, as discussed in Section 4. Therefore, there is no difference between the full and disposition equation databases for Alloy 82/182/132, and so no separate Alloy 82/182/132 disposition equation database was developed.

**Table 3-4**
**Distribution of Alloy 82/182/132 CGR data points, specimens, and welds by testing laboratory**

| | ANL | AREVA | Bettis | GE-GRC | Lockheed Martin |
|---|---|---|---|---|---|
| No. Points | 35 | 2 | 99 | 72 | 30 |
| No. Specimens | 11 | 2 | 89 | 16 | 6 |
| No. Welds | 6 | 1 | 12 | 6 | 6 |
| | **MHI** | **PNNL** | **Studsvik** | **Westinghouse** | **Total*** |
| No. Points | 9 | 10 | 39 | 18 | **314** |
| No. Specimens | 7 | 1 | 39 | 17 | **188** |
| No. Welds | 2 | 1 | 5 | 3 | **41** |

*Total numbers of points and specimens are a sum of the respective values for each of the testing laboratories. Some welds were tested by multiple laboratories, however, so the total number of welds is less than the sum of those tested at each laboratory.

**Table 3-5**
**Distribution of tested variants of weld metals Alloys 82, 182, and 132**

| Weld Alloy | No. Points | No. Specimens | No. Welds |
|---|---|---|---|
| 82 | 134 | 91 | 17 |
| 182 | 171 | 90 | 22 |
| 132 | 9 | 7 | 2 |

**Table 3-6**
**Range of several key parameters and responses for Alloy 82/182/132 CGR data**

| Parameter | Minimum Value | Maximum Value | Units |
|---|---|---|---|
| K | 14 | 77 | MPa√m |
| T | 290 | 360 | °C |
| $[H_2]$ | 1 | 80 | cc/kg |
| $\Delta ECP_{Ni/NiO}$ | -81 | 53 | mV |
| t | 67 | 5798 | hr |
| Δa | 0.004 | 11.4 | mm |
| IG | 50 | 100 | % |

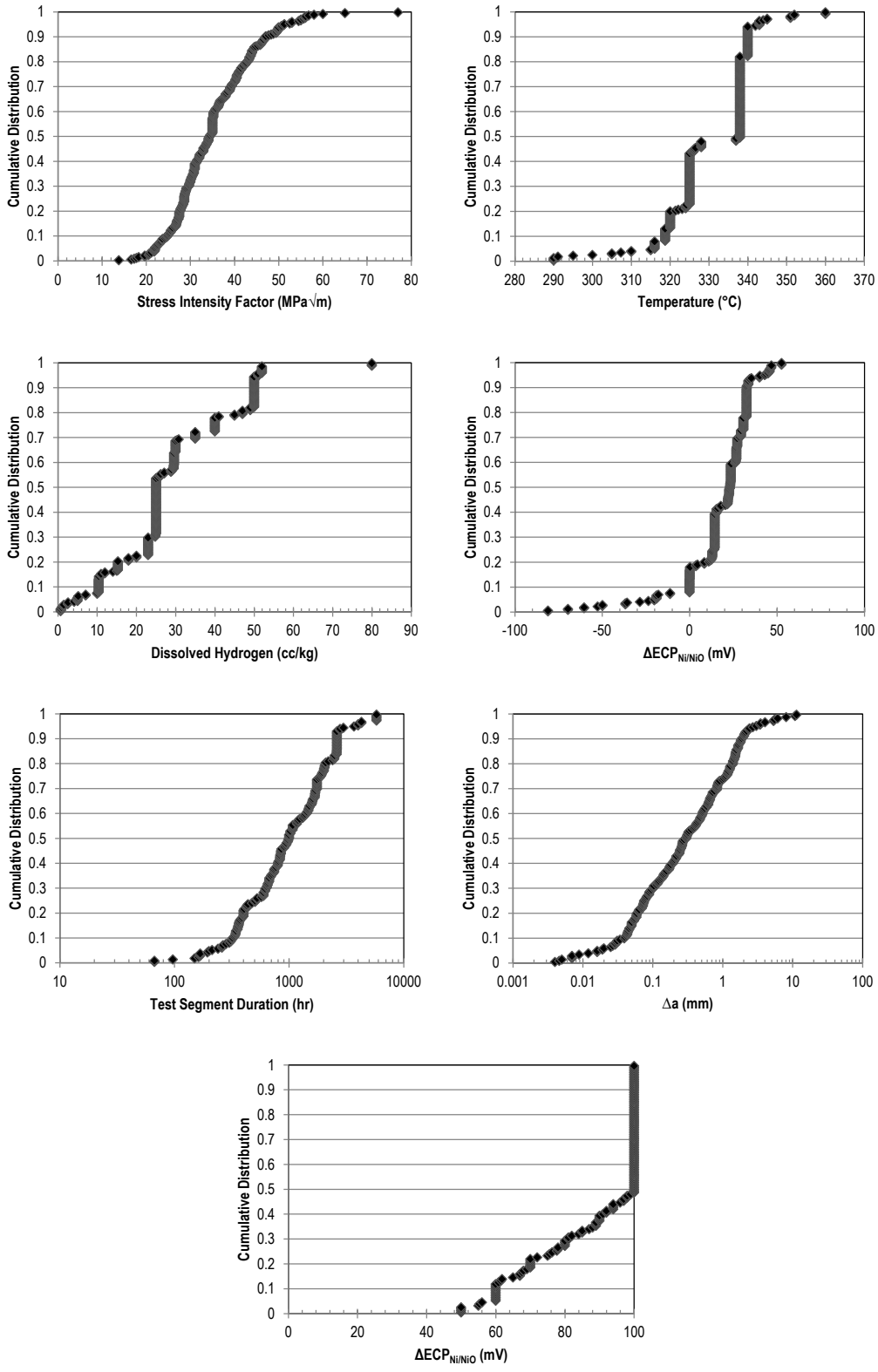


**Figure 3-7**
**Cumulative distribution plots for several key parameters and responses for Alloy 82/182/132 data**

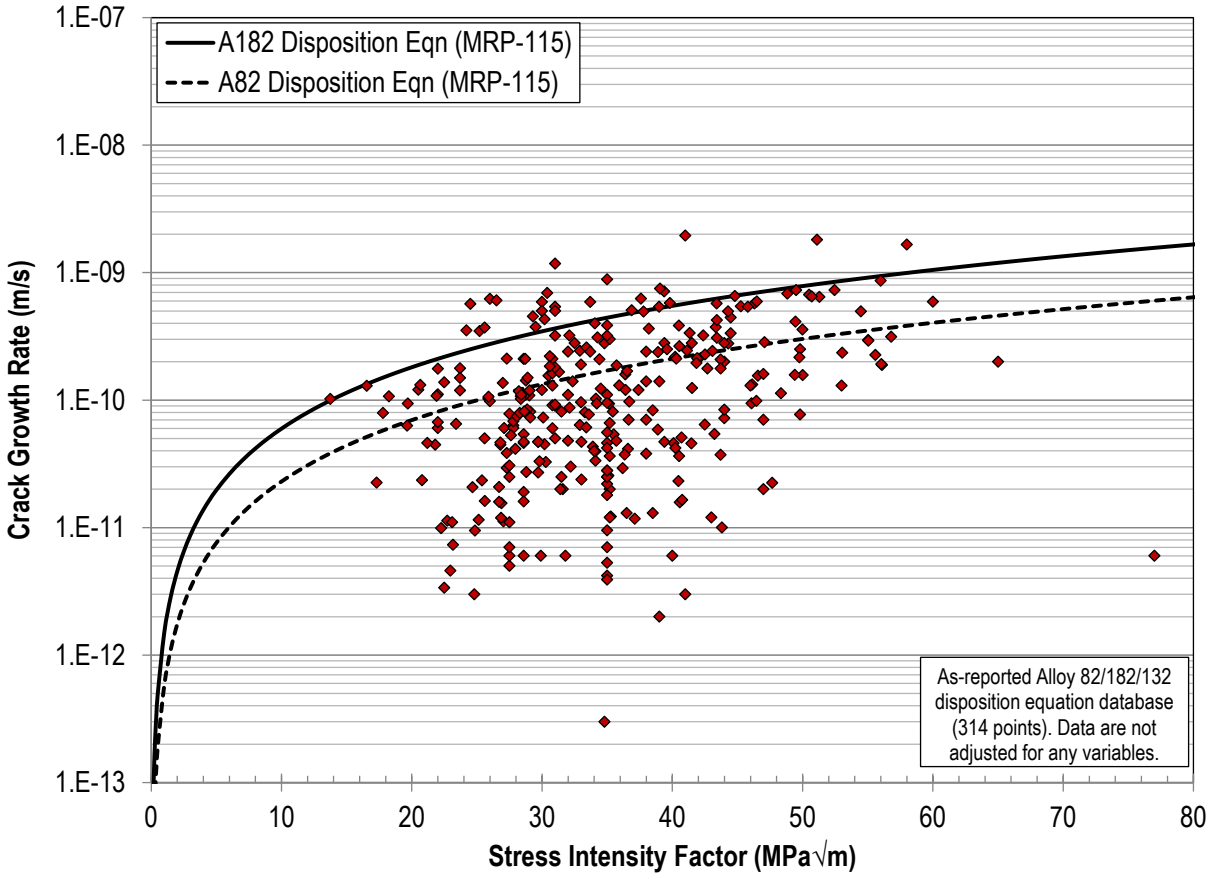


**Figure 3-8**
**Screened Alloy 82/182/132 database: All data, unadjusted for temperature, dissolved hydrogen, etc.**

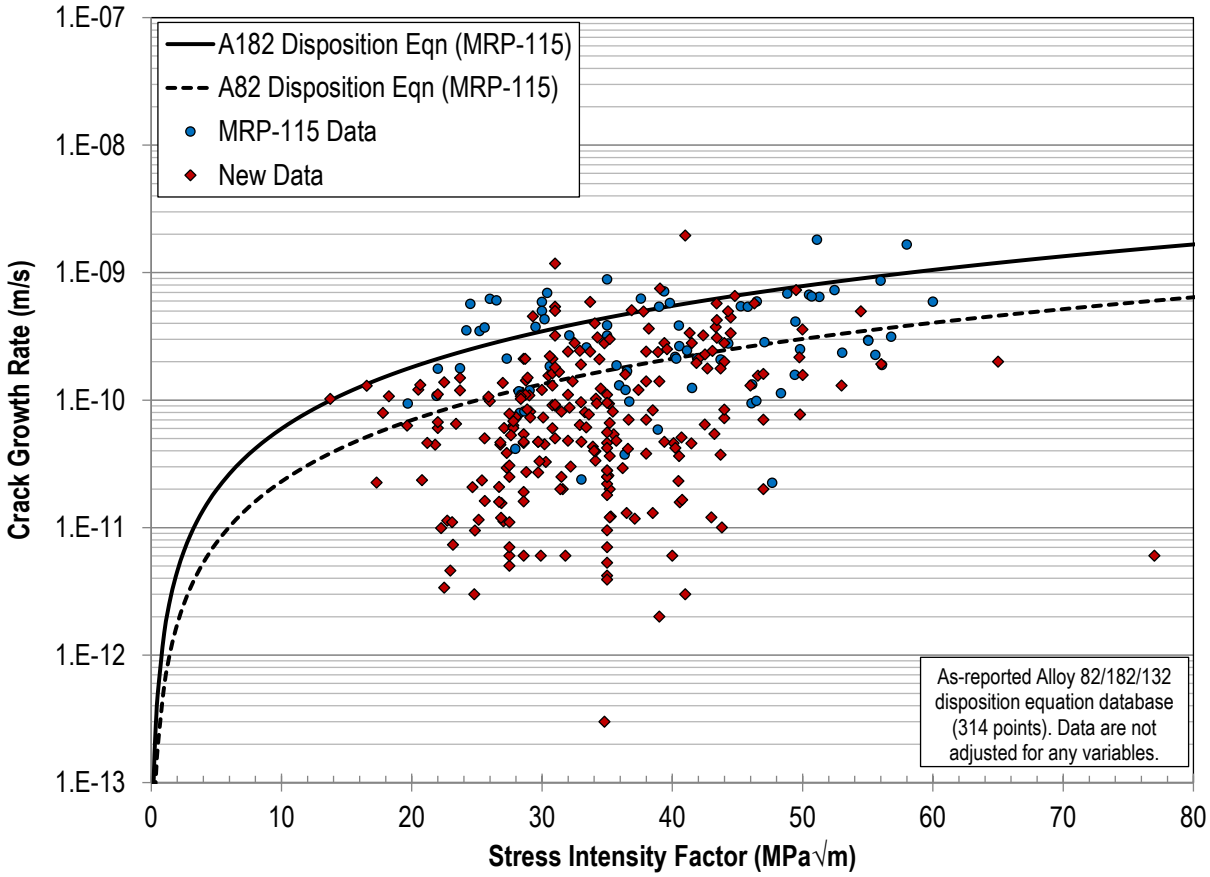


**Figure 3-9**
**Screened Alloy 82/182/132 database: All data, unadjusted for temperature, dissolved hydrogen, etc. Comparison is shown between MRP-115 data and newly compiled data.**

# 4
# APPLICABILITY OF TESTING CONDITIONS TO PLANT COMPONENTS

Because the target user base of this report is the commercial nuclear power industry, any results obtained from laboratory data must be relevant to industry applications. While many of the testing attributes, such as using a simulated PWR primary water environment, are directly applicable for the vast majority of the data, some attributes, such as the level of added deformation, are not directly comparable to what is typically seen in plant components, particularly for thick-wall tubing.

This section lists the attributes that may not be directly relevant, details the differences between the laboratory and plant conditions, and explains if and how any data that are not directly relevant can still be used in the statistical analysis process. In most cases, materials and environmental conditions not expected in plants are valuable to improve precision and confidence in dependencies and clarify how the PWSCC behavior changes for conditions that drift outside of expected plant conditions.

## 4.1 Environmental Conditions

The testing environments used for obtaining the laboratory CGR data generally simulate typical PWR primary water environment conditions. As shown in Table 3-2, for the laboratory Alloy 600 CGR data, the temperature range is 252-363˚C (486-685˚F) and the dissolved hydrogen range is 3-239 cc/kg. For the laboratory Alloy 82/182/132 CGR data, shown in Table 3-6, the temperature range is 290-360˚C (554-680˚F) and the dissolved hydrogen range is 1-80 cc/kg.

Alloy 600/82/182/132 materials are used in locations that span the PWR cold leg and hot leg temperature range of approximately 285-329˚C (545-625˚F), as well as the typical pressurizer temperature of 345°C (653°F). Crack growth rates vary with temperature, so the activation energy (Q) was determined from the laboratory testing. Because of the sensitivity of PWSCC CGRs to the hydrogen concentration (see Appendix C of MRP-115 [3]), dissolved hydrogen concentrations are often controlled in laboratory tests to maintain electrochemical potential (ECP) conditions close to the nickel/nickel oxide (Ni/NiO) phase boundary to maximize the SCC susceptibility (unless a specific ΔECP value is used to evaluate its effect on the CGR). PWR primary water chemistry conditions are maintained in the range of 25-50 cc/kg at standard temperature and pressure, which corresponds to ECP conditions in the nickel-stable regime at the relevant temperatures.

Other environmental conditions such as impurity levels (e.g., chloride and sulfates), pH, and boron and lithium values are well controlled in laboratory tests and are within the limits of typical PWR primary water chemistry conditions.

## 4.2 Mechanical Deformation

An increase in the strength level (yield and tensile strengths) resulting from cold work (CW) has been known for many years to increase PWSCC CGRs of wrought nickel-base alloys [30]. As a result of this understanding, CW and elevated temperatures are used in laboratory experiments as accelerating factors for Alloy 600 wrought materials, as well as to simulate the cold work or plastic strain that may exist in the weld heat-affected zone of Alloy 600. Because as-received Alloy 600 is susceptible to PWSCC, only about 20% of the data in the CGR database compiled for this effort has some degree of added CW, with thickness reduction levels of up to 32%.

Increased levels of cold work clearly cause corresponding increases in CGRs. Therefore, to appropriately apply the PWSCC CGR results from materials with high levels of added cold work (i.e., >12%) when developing a CGR model to be applied to the low added CW levels seen in plant components (see Section 4.2.3), an adjustment factor is needed.

### *4.2.1 Cold Work vs. Warm Work*

When evaluating the effects of added deformation on PWSCC CGRs, the type of deformation, and particularly the temperature at which the deformation was introduced, has a notable effect. Cold work, such as the rolling and forging introduced in some wrought Alloy 600 laboratory materials, is defined as deformation occurring at or near room temperature, while warm work can be defined as a process that occurs at temperatures near half of the homologous melting temperature, which is around 690°C (1275°F) for Alloy 600. Because of the ability at increased temperatures for the material to better accommodate or recover the damage associated with deformation, warm work is often less detrimental to the material than cold work.

For multipass welds, a more complex thermo-mechanical history in the weld metal or base metal HAZ is developed as the weld is completed, such that neither “cold” nor “warm” work alone can accurately define the processing history. For example, consider a thick section multipass gas tungsten arc weld shown schematically in Figure 4-1 [31]. The right plot shows the time-temperature cycles for Bead 1, the first bead deposited in the weld, due to the deposition of three nearby weld beads. Because of the close proximity to Bead 1, Bead 3 likely anneals Bead 1. Bead 9 might cause warm working effects, while the strains on Bead 1 induced by the deposition of Bead 15 could be considered to be cold work because of the increased distance between the two weld beads. Although broadly accurate, this a fairly simplistic description of the welding-induced strains; when the deposition of all weld beads is considered, the actual deformation throughout the weld becomes a complex function of the weld restraint (including differences in material strength, thermal expansion, and thermal conductivity in dissimilar metal welds) and overall heating and cooling cycles.

This simplistic description of the combination of warm and cold work present in welds also translates to the HAZ of the adjacent base material. Depending on the number, location, and heat input of the weld beads, the HAZ likely experiences annealing from the deposition of weld beads immediately adjacent to the base metal, warm work strains as adjacent weld beads solidify, and cold work-type effects from the deposition of distant weld beads. This combination of effects at various temperatures leads to the possibility that crack growth in these regions (i.e., welds and HAZs) may be slower than in bulk base metal that has been cold worked to a comparable level of residual strain.

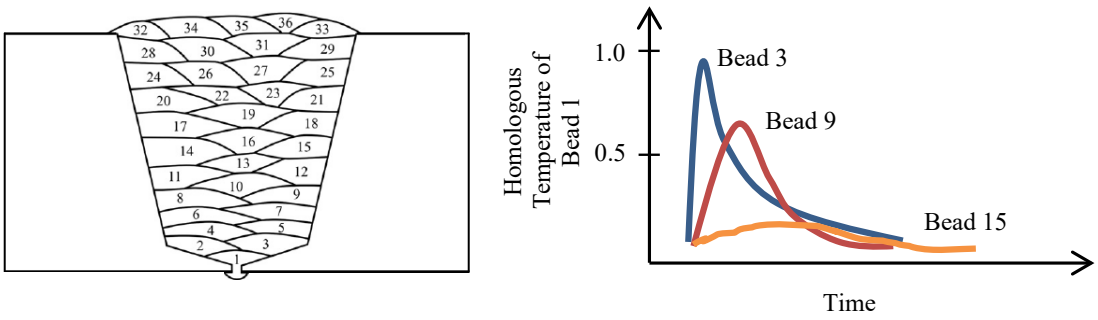


**Figure 4-1**
**Left: Illustration of a typical weld bead sequence for a multipass weld [31]**
**Right: Schematic representation of the time-temperature cycles that Bead 1 undergoes due to the deposition of Beads 3, 9, and 15**

### *4.2.2 Surface Cold Work*

The majority of the effects of cold working described in this report pertain to relatively uniform working distributed through the bulk of the subject materials. However, some special effects of cold working can occur when it is constrained to the surface regions of materials. Several examples of surface cold work have been observed in operating plants, including the following cases:

- CRDM and other nozzles may have near-surface cold worked layers from gun drilling or other forms of aggressive machining and post-weld grinding.
- Steam generator divider plates may have compressive layers induced by planing and/or grinding that are pulled into tension during the initial hydrotest.

The hardness and, by extension, PWSCC susceptibility in a cold worked surface layer may be greater than that of the undeformed bulk base metal. However, this cold worked layer is typically very thin, often less than 100 μm (4 mils) [32], and is thus more of consequence for PWSCC initiation rather than growth. As such, it is expected that even if a crack initiates in a highly cold worked surface layer, by the time it reaches the softer bulk material, the CGR will become negligibly small due to the reduction in the driving mechanism, provided the bulk residual strain levels are low.

This principle was investigated at Tohoku University [33], where the relationship between the IGSCC growth rate and Vickers hardness was measured for Alloy 690 specimens that had either been conventionally unidirectionally cold rolled or functionally graded cold rolled. Functionally graded cold rolling is defined as an intentional change in the reduction in thickness within a single specimen. For this investigation, specimens were fabricated such that the post-cold worked specimens were uniform in thickness, which meant the initial thickness within a single specimen varied according to the desired final thickness reduction level, as shown schematically in Figure 4-2 [33]. Two ranges of functionally graded cold rolling were tested: 30%–0% and 20%–5%. Conventionally cold rolled materials (i.e., those with a uniform thickness reduction) were cold worked to 15%, 26%, and 30%.

PWSCC growth rate tests were conducted on 0.7T compact tension (CT) Alloy 690 specimens machined from each of the cold rolled materials, and Vickers hardness measurements were taken

approximately 1 mm (0.04 in.) adjacent to the crack plane after the conclusion of the PWSCC tests. From this, a correlation between Vickers hardness and the average CGR was obtained, as shown in Figure 4-3 [34].

From these test results, it was concluded that stresses in heavily cold worked surface layers are sufficiently large that the possibility of PWSCC initiation increases. However, once the crack grows past the surface layer into the softer bulk material, the CGR may become negligibly small and could possibly arrest if the bulk residual strain is low and K has not increased significantly. Similar behaviors of self-arresting cracks would be expected in the surface work hardened regions of actual plant components.

The hardness profile extending between the surface and bulk material is also available for ex-service Alloy 600 materials. Two bottom mounted instrumentation (BMI) nozzles from South Texas Project (STP) Unit 1 were removed after boric acid deposits were found at those locations, and they subsequently were examined in detail in the laboratory [35].

During the examination of the two nozzles, full-thickness microhardness profiles were obtained, which clearly revealed the presence of thin cold worked surface layers on both the inner diameter (ID) and outer diameter (OD) of the nozzles. The measured Knoop microhardness values were converted to Vickers (HV) in the reference, from which the level of cold work was estimated using a HV-CW relationship developed from laboratory data (see Section 5.2.4) in Table 4-1.

Both optical metallography and microhardness profiles were used to determine the thickness of the ID cold worked layer. The microhardness profiles suggested a greater thickness of the cold worked layer than those measured by optical metallography, with cold worked layer thicknesses of 0.05 mm (0.002 in.) and 0.18 mm (0.007 in.) based on hardness for the two nozzles. The OD cold worked layer thickness was 0.013 mm (0.0001 in.) deep on one nozzle and indiscernible in the other.

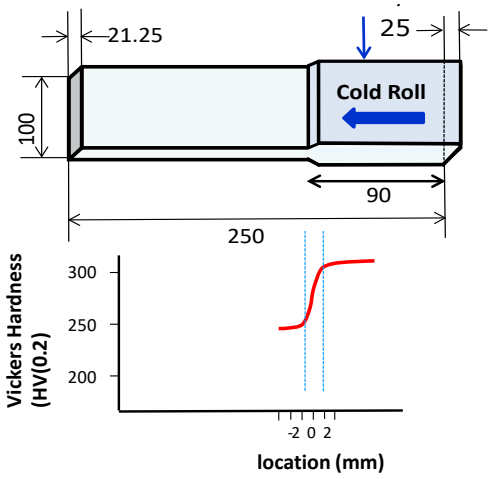


**Figure 4-2**
**Top: Schematic of a functionally cold rolled specimen prior to rolling**
**Bottom: Post-CW hardness profile near the transition region [33]**

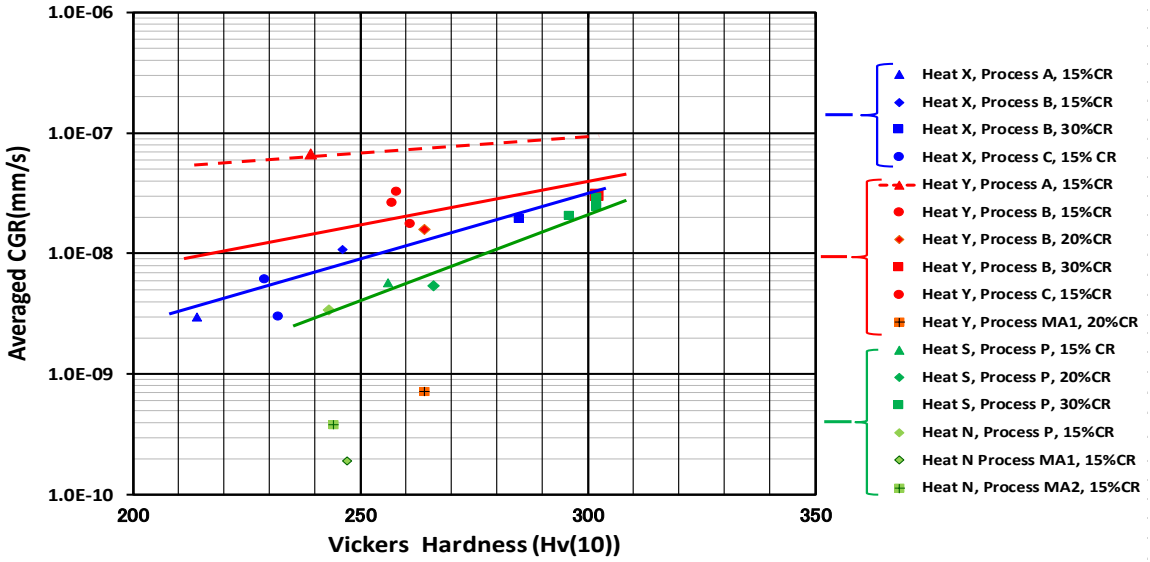


**Figure 4-3**
**Relationship between CGR and Vickers hardness for Alloy 690 cold rolled to various thickness reduction levels [34]**

**Table 4-1**
**Measured hardness values and estimated cold work levels for two BMI nozzles [35]**

| Location | Knoop 500g | Vickers | CW (%) |
|---|---|---|---|
| ID | 300 – 325 | 266 – 285 | 19.5 – 24.0 |
| Mid-wall | 220 – 240 | 192 – 210 | 3.5 – 7.5 |
| OD | 250 – 260 | 220 – 230 | 9.5 – 12.0 |

### *4.2.3 Cold Work in Plant Components*

In general, component fabrication from Alloy 600 materials with fabrication-induced bulk cold work of over 5% is prohibited by all of the vendors involved in nuclear component manufacturing. ASME B&PV Code Section III, Division 1, Subsection NH, Paragraph NH-4212 limits fabrication-induced local strains to 5%. A footnote to this paragraph states that strain resulting from final straightening operations performed on materials furnished in the solution annealed or heat treated condition do not need to be considered when applying the 5% limit. As such, manufacturers would need to limit the maximum bending strain to 5%, calculated from the actual distortion values associated with any mechanical nozzle straightening subsequent to nozzle installation. This level of deformation is not expected to be approached during cold straightening of typical components. On this basis, a post-fabrication heat treatment as called out per NH-4212 would likely not be required, although it may be performed regardless.

Each vendor controls the amount of cold work in the material using a variety of proprietary specifications, processes, and other limitations. Note, however, that the limitations apply to *intentionally added* bulk cold work; unintentional deviations may occur that increase the

effective cold work level to over the maximum allowed limit. Such examples are not expected to be common.

To estimate the actual levels of deformation/residual strain in plant components, data from ex-service Alloy 600 materials were compiled. In many cases, only hardness or yield strength were reported, so it was necessary to develop a method to convert from these measurable material properties to cold work level. These conversion equations were developed from the newly compiled Alloy 600 data in the CGR database, as well as additional data from other references, as described in Section 5.2.4.

For the new Alloy 600 data produced after MRP-55 was published, the test specimens with 0% added cold work (and not in the HAZ) had YS values of 201-340 MPa (29-49 ksi) and hardness values of 160-187 HV. Therefore, any plant data with YS or HV values within those respective ranges can be assumed to have 0% added CW. Above these ranges, the equations developed in Section 5.2.4 of this report and duplicated below should be used to estimate the levels of added CW based on materials property measurements for Alloy 600:

$$\boldsymbol{YS\ (MPa) = -0.455 \cdot \%CW^2 + 31.2 \cdot \%CW + 287} \qquad \textbf{Eq. 4-1}$$

$$\boldsymbol{HV = -0.064 \cdot \%CW^2 + 5.79 \cdot \%CW + 172} \qquad \textbf{Eq. 4-2}$$

$$\boldsymbol{HV = 0.189 \cdot YS\ (MPa) + 129} \qquad \textbf{Eq. 4-3}$$

Three sets of data from ex-service Alloy 600 materials are available for comparison to determine actual cold work levels in plant components, in addition to weld mockups of Alloy 690/52/152 materials, as described in the following paragraphs.

**Davis-Besse [36]**

A CRDM nozzle made from heat M3935 was removed from Davis-Besse. The YS for this heat was listed at 334 MPa (48 ksi) on the CMTR, which is within the 0% added CW range for Alloy 600 of 201-340 MPa (29-49 ksi). A hardness profile was obtained across the thickness of the nozzle, with an average value of 175 HV (200 HK) and a maximum value of 194 HV (221 HK). These values correspond to added cold work levels of 0% and 4%, respectively, as calculated from Eq. 4-2. These hardness levels are within the scatter of values for as-received material with no intentionally added cold work.

**South Texas Project [35]**

Two bottom mounted instrumentation (BMI) nozzles were removed from STP Unit 1. The heats of these nozzles were H-979 and L-090. Hardness profiles across the thickness of the nozzles indicated values of 192-210 HV in the bulk portion of the nozzle (i.e., not in the surface layers), which correspond to added cold work values of 3.5-7%, as calculated from Eq. 4-2. These hardness levels are within the scatter of values for as-received material with no intentionally added cold work.

**Palisades [37]**

A crack in the HAZ of an Alloy 600 pressurizer power operated relief valve (PORV) safe end was identified at Palisades, which resulted in removal, repair, and reinstallation of the safe end. The safe end was produced from heat NX-5222, which had a “very high yield strength” (531 MPa (77 ksi)) and “high hardness” (22 HRC). (It is unclear from the reference whether these measurements were obtained in the HAZ or bulk material.) The YS value is estimated to be

equivalent to 9% added cold work, as calculated from Eq. 4-1. The reference noted that the material was procured to SB-166 prior to 1987 and that the post-forging heat treatment was likely low (1600-1700°F (871-927°C)). Improved procurement specifications and practices since that time means that this high hardness is unlikely for newer Alloy 600 materials in service.

**EPRI Mockups ([38], [39])**

EPRI sponsored the production of several weld mockups (many were unconstrained, though some were minimally or fully constrained), as discussed in more detail in Section 4.6. Although these mockups were produced from Alloy 690 materials, they are still relevant to Alloy 600 materials due to the similar applicable specifications. In addition to the residual strain measurements in the weld material presented in that section, residual strain measurements were also taken on the base metal, in both the bulk and HAZ regions. Figure 4-4 illustrates the cumulative distribution of the 45 bulk Alloy 690 measurements and 44 HAZ Alloy 690 measurements. Table 4-2 lists the strains for the bulk region, HAZ region, and overall (combined bulk and HAZ data) for select percentile values, as well as the minimum and maximum values. The table shows that all of the bulk material and almost 75% of the HAZ material has the equivalent of less than 10% added CW.

Hardness measurements on Alloy 600 HAZ specimens in the current CGR database support the EPRI mockups residual strain measurements in that region. The hardness of only one HAZ specimen in the database was measured; it was reported as 210 HV, which is equivalent to 7% cold work, per Eq. 4-2.

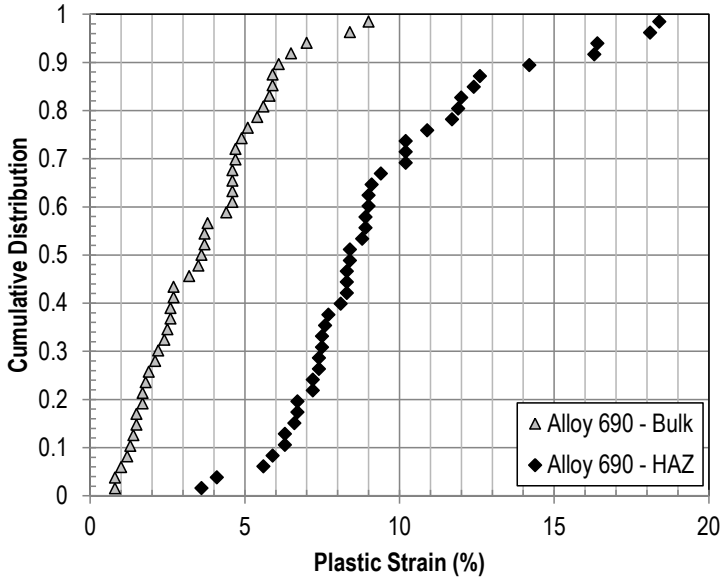


**Figure 4-4**
**Residual strain measurements from bulk and HAZ regions of Alloy 690 material ([38], [39])**

**Table 4-2**
**Summary of residual strain measurements from bulk and HAZ regions of Alloy 690 material ([38], [39])**

| Percentile | Bulk | HAZ | Overall |
|---|---|---|---|
| min | 0.8 | 3.6 | 0.8 |
| 0.50 | 3.6 | 8.4 | 6.1 |
| 0.75 | 5.0 | 10.7 | 8.6 |
| 0.80 | 5.6 | 11.9 | 9.0 |
| 0.90 | 6.3 | 15.3 | 11.9 |
| 0.95 | 8.0 | 17.7 | 15.3 |
| max | 9.0 | 18.4 | 18.4 |

#### 4.2.3.1 Conclusions

With the above specifications and requirements in place, it is concluded that extensive bulk cold work (i.e., >15%) is unlikely to occur in base materials, including in HAZ regions. Thus, crack growth rates resulting from specimens with relatively high bulk cold work are not anticipated to be directly applicable to Alloy 600 component replacements or repairs that are in service.

The Alloy 600 disposition curve is intended to be applicable for HAZ regions in addition to the bulk material, and it is also intended to be a 75$^{th}$ percentile conservative best-fit equation, not a bounding equation. Therefore, relevant levels of added cold work for Alloy 600 for the purpose of developing a disposition curve are limited to 12% added deformation, as defined by the YS equivalent of approximately 600 MPa, for CGR test specimens. Residual strain levels typical for Alloy 600 HAZ material are included in this value, so no special considerations are needed to account for crack growth in that region. For Alloy 82/182 weld metals, no additional cold work is necessary because the test data encompass representative levels of strain; i.e., machined test specimens will generally retain the plastic strain produced during welding (although some of the residual stresses are relieved during the specimen preparation from the weldment and not all mockups were prototypically constrained).

## 4.3 Crack Growth Orientation

Crack growth orientation has been found to affect CGRs in nickel-base alloys, as these materials are not mechanically isotropic, even if no added deformation has been introduced. The crack growth orientation in a compact tension (CT) specimen is described by two directions: the direction normal to the plane of the crack and the direction of crack growth. Additionally, orientation can be described relative to either of two attributes: product form and added deformation. Both orientations (i.e., both with respect to product form and with respect to added deformation) are needed to fully describe the orientation of a crack when cold work has been added to the material, particularly as the two orientations may not be aligned.

For the Alloy 600 specimens in the CGR database, only one orientation was reported. For the approximately 80% of data with no added deformation, this is the product form orientation. For the approximately 20% of data with cold work, this is the added deformation orientation. In the majority of these cases, the orientations with respect to added deformation and product form were coincident.

For Alloy 82/182/132 specimens in the CGR database, no cold work was introduced to any specimens, so the reported orientation is with respect to product form (weld geometry).

### 4.3.1 Product Form Orientation

Figure 4-5 shows the nomenclature for CT specimen orientations with respect to a cylindrical product form, such as an extruded CRDM nozzle. Because cracks in plant components can grow in both length and width, the orientation of an in-service crack propagating through-wall can be represented by the C-R or C-L orientations for an axial crack and by the L-R or L-C orientations for a circumferential crack. The R-L and R-C orientations are parallel to the pressurized surface, often termed the laminar direction; flaws in these orientations have never been observed in service. This is because radial stresses must be in equilibrium with the stress at the surface. The stress at the surface is either zero or compressive and is equal in magnitude to the internal pressure for a pressurized cylinder.

Figure 4-6 shows the nomenclature for CT specimen orientations with respect to a plate product form. The orientation of an in-service crack propagating through-wall can be represented by the T-S or T-L orientations for an axial crack and by L-S or L-T for a transverse crack. The S-L and S-T orientations are located in the laminar direction, in which no cracks have been observed in service.

For welds, the product form orientation is often more straightforward due to the formation of similarly oriented dendrites, particularly in the center of the weld. Fusion welding leads to the formation of dendrites growing opposite the direction of the heat flow and perpendicular to the solid material on which the weld is deposited. Most structural welds of interest are made with multiple passes. The grain structure of dendrites in subsequent passes is typically related to that of previous passes as a result of epitaxy and preferred growth (⟨100⟩ for FCC metals), i.e., by the tendency of a crystal forming on a substrate to have the same crystallographic orientation as the substrate. This results in dendrites of the same orientation persisting through many weld passes.

The nomenclature used to describe the crack orientation in welds is illustrated in Figure 4-7. Here, the welding direction is taken as the longitudinal direction, L; the weld width as T; and the weld thickness as S. Cracks growing along the dendrite growth direction typically have higher CGRs than those growing perpendicular to the dendrite growth direction. As shown in Figure 4-7, the T-S and L-S orientations are parallel to dendrite growth and so are termed the “fast” directions. The T-L and L-T orientations are perpendicular to dendrite growth, but cracks in these orientations can still grow intergranularly. Thus, these directions are moderate growth directions. The slowest directions are the S-T and S-L orientations, as cracks must cut across dendrites in order to advance.

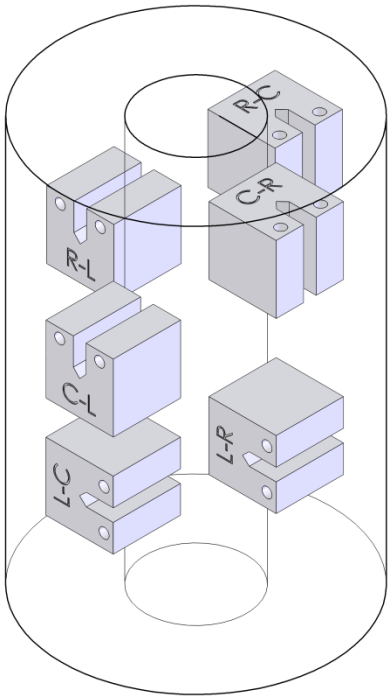


**Figure 4-5**
**Specimen orientations for a cylindrical product form**

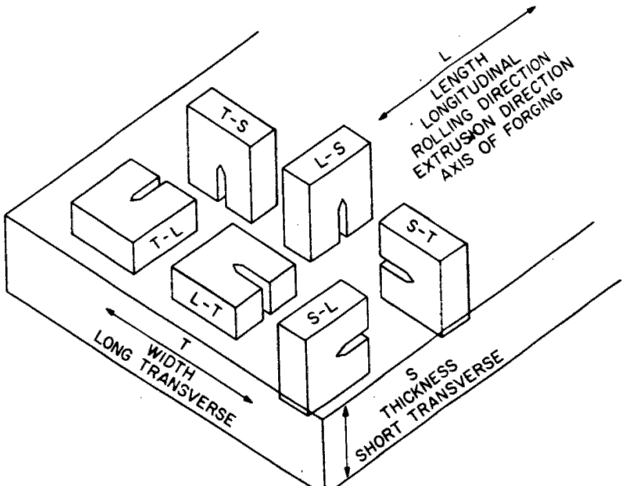


**Figure 4-6**
**Specimen orientations for a plate product form**

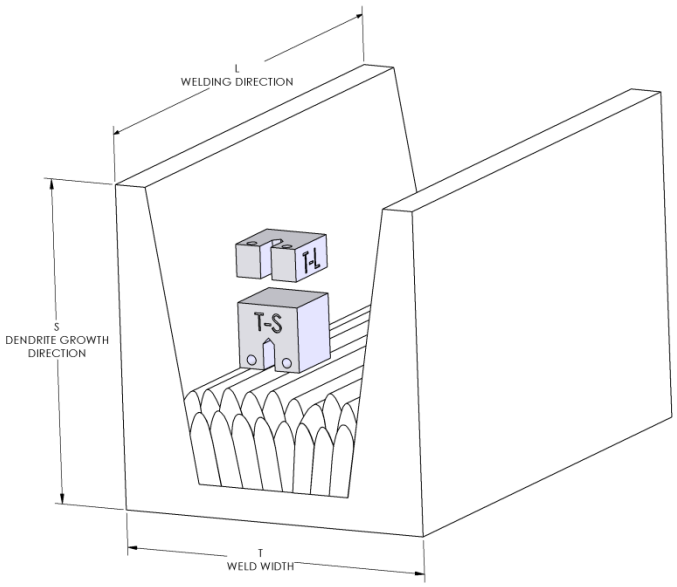


**Figure 4-7**
**Specimen orientations for a weld product form (simplified schematic showing exaggerated weld dendrite growth)**

### *4.3.2 Added Deformation Orientation*

Different processing methods induce deformation in different orientations, such that a new set of nomenclature is needed to accurately describe the crack growth orientation with respect to the added deformation, regardless of the original product form. The added deformation orientation can be described in terms of a combination of the primary direction of grain lengthening and the primary direction of thickness reduction resulting from the deformation process. (This description substantially simplifies the actual microstructure effects, but it provides an intuitive interpretation of the added deformation nomenclature.) Similar to how the L direction for product form is equivalent to the rolling or extrusion direction, the L direction for added deformation is equivalent to the primary direction of relative grain lengthening[2]. Additionally, just as the S direction for product form is the thickness, or short transverse direction, of the component, the S direction for added deformation is the direction in which the greatest thickness reduction occurs. The specific nomenclatures for three processing methods (rolling, forging, and tensile straining) are described in the following subsections.

Note that the cold work levels added by laboratories (and potentially added during component installation/straightening in plants) is often much greater than those introduced during production of the original product. As would be expected, as the post-supplier added cold work increases, its effect on the microstructure and resulting PWSCC behavior becomes more pronounced.

[2] Grain lengthening is generally limited unless the material is cold rolled to a large thickness reduction level (e.g., >20%) where elongation occurs mostly in the length direction. Unlike rolling, forging tends to produce 2D deformation. It is not clear whether grain lengthening directly affects SCC, but it is a convenient and intuitive basis for discussing orientation.

### 4.3.2.1 Rolling

The nomenclature for unidirectional rolling is the same as that for product form orientation for a plate, as shown in Figure 4-8. The direction of primary grain lengthening is L. The reduction in thickness direction is S. If the T direction is unconstrained such that elongation in the L and T directions are similar (not a typical scenario), then those two directions may be interchangeable (i.e., the L-S orientation would be equivalent to the T-S orientation). However, if the T direction is constrained or otherwise undergoes much lower deformation than the L direction, all six orientation designations are unique.

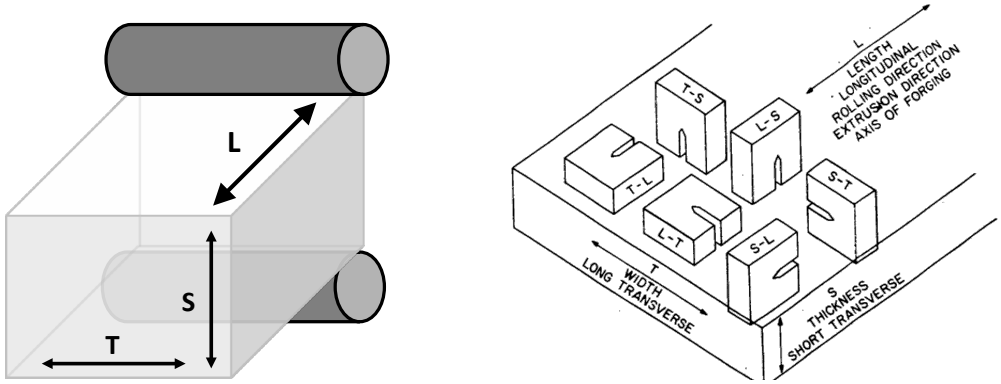


**Figure 4-8**
**Specimen orientations for unidirectional rolling**

### 4.3.2.2 Forging

The direction of thickness reduction in a forging, whether of a plate or a cylinder is the S direction, as shown in Figure 4-9. When unconstrained and similar in dimension, the L and T directions expand essentially identically and so, if the starting material is randomly oriented, are interchangeable in the nomenclature. If the starting material contained significant crystallographic texture, this simplification may not be justified. For cylindrical specimens, while the L and T directions are the radial direction R, the use of L or T (which are interchangeable in this case) over R is preferred to facilitate comparison between various processing methods.

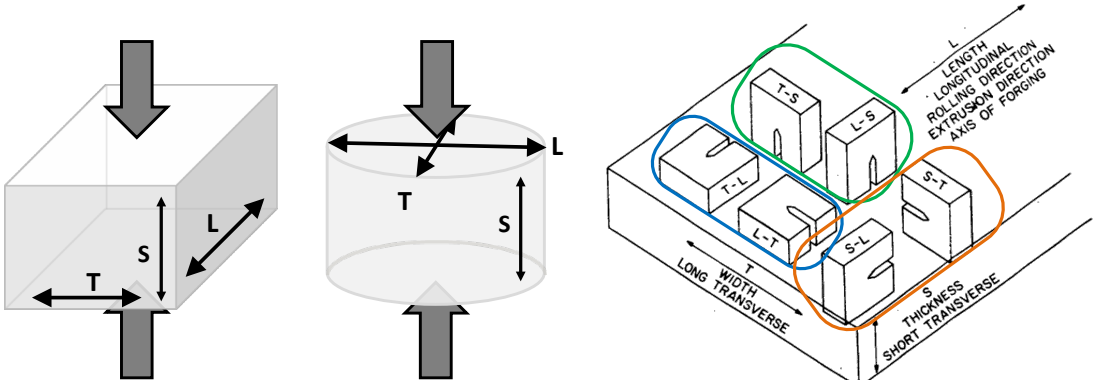


**Figure 4-9**
**Specimen orientations for forging; circled pairs of orientations in the far right schematic are considered equivalent and can be interchangeable under certain conditions**

### 4.3.2.3 Tensile Straining

Tensile straining orientations are similar to forging orientations, except that the direction of primary interest–the direction of tensile strain–is the L direction because of the grain elongation in that direction, as shown in Figure 4-10. Again, if the starting material is randomly oriented, then the S and T directions contract essentially identically and so are interchangeable in the nomenclature. For cylindrical specimens, while the S and T directions are the radial direction R, the use of S or T (which are interchangeable in a cylinder) over R is preferred to facilitate comparison between various processing methods.

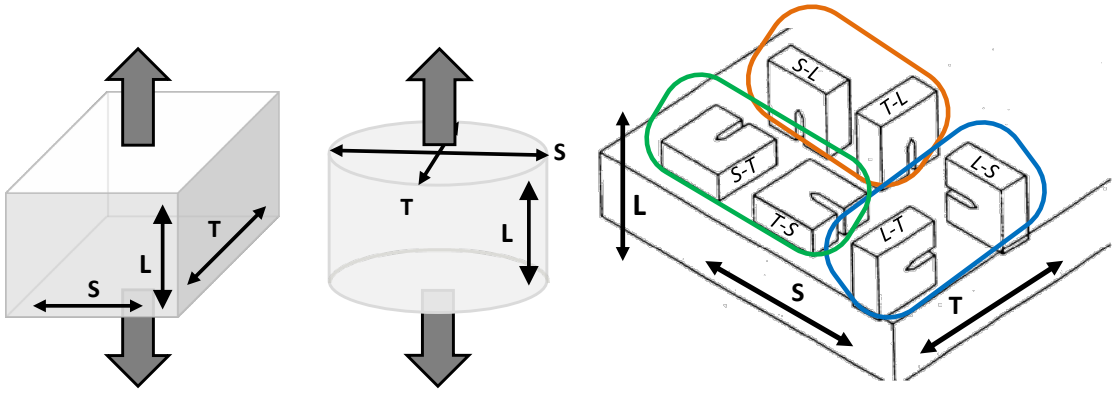


**Figure 4-10**
**Specimen orientations for tensile straining; circled pairs of orientations in the far right schematic are considered equivalent and can be interchangeable under certain conditions**

### 4.3.2.4 Conclusions

Greater levels of added deformation increase the anisotropy in the material relative to its original, as-received state. Therefore it is expected that as the added deformation level increases from 0%, the added deformation orientation effects become more pronounced, quickly overtaking the product form orientation as the primary factor for crack growth direction. However, it is generally not as easy to characterize the orientation of added deformation induced through methods such as bending or straightening in plant components as it is in laboratory specimens. Therefore, because the actual orientation with respect to added deformation is often unknown, all deformation orientations are potentially relevant to plant components, and thus it is inappropriate to discount any orientations during the development of the CGR equations.

## 4.4 Product Form

Alloy 600 CGR data have been obtained from several different product forms, including plate, CRDM tubing, bar, and billet. The majority of CGR data were obtained on either CRDM tubing or plate material, while few tests were performed on bar and billet materials. Each of these product forms are processed in different ways during production with different resulting effects on the microstructure. Still, the production and installation of Alloy 600 plant components may introduce stresses and strains that are not confined to a single product form. Therefore, all product forms are considered to be applicable without adjustment needed to differentiate among the data obtained from the various product forms.

It is noted that a billet is not a final product form, so it may not be appropriate to treat billet specimens the same as those from bar, CRDM nozzle, or plate product forms. However, there are insufficient data in the current CGR database to investigate this fully, and obtaining more data on billets and the other product forms would be necessary to reliably determine the effect of this product form. No data from billet specimens were included in the development of the disposition equation, but there were billet data included for the CGR model.

Alloy 82/182/132 data have been obtained from several different weld geometries (e.g., J-groove, V-groove, buildup), but all geometries are considered to be applicable.

## 4.5 Material Heat Treatment

### *4.5.1 Alloy 600*

The Alloy 600 materials used for CGR testing were generally received in a mill annealed (MA) condition, although the mill annealing temperature (i.e., whether it was a high temperature mill anneal (HTMA) or low temperature mill anneal (LTMA)) was not consistently specified. No materials were reported as being thermally treated (TT), but because the as-received condition was not specified for all materials, no comprehensive statement that no TT materials are included in the database can be made.

The original Alloy 600 materials used for plant components were typically produced in the MA condition, although when the high PWSCC susceptibility of this condition was recognized, the TT condition was developed and used instead. The TT condition, which precipitates carbides on grain boundaries, is well known to enhance PWSCC resistance of Alloy 600. However, because of the lack of data in the CGR database, no factor was developed to credit this greater resistance of the TT condition over the MA condition, as discussed in Section 5.2.7.

### *4.5.2 Alloy 82/182/132*

The Alloy 82/182/132 materials used for CGR testing were generally tested in the as-received, as-welded condition without any subsequent heat treatments. Heat treatments were applied to some data, typically at 556°C (1033°F) although some were at 607°C (1125°F) or 1093°C (2000°F). As-welded conditions are typical for many repair and replacement components welded with these materials that are currently in service. One exception to this is the buttering used with low-alloy steel (e.g., as part of the J-groove weld of CRDM nozzles in replacement reactor vessel heads); in that case, a post-weld heat treatment (PWHT) at about 620°C (1150°F) is performed on the entire reactor vessel head following the buttering, before the CRDM nozzle is welded into place. Therefore, welds both with and without PWHT are potentially relevant to plant components. A lack of PWHT data, however, means that the difference between the two conditions cannot be determined at this time, as discussed in Section 5.3.6.

## 4.6 Welding Residual Strains

The EPRI Materials Reliability Program (MRP) sponsored a study of residual plastic strain measurements in weld mockups made of Alloys 690 and 52/152 by Morra et al. at GE-GRC ([38], [39]). The mockups were prepared from commercial Alloy 690 plate material welded with Alloy 52 or Alloy 152 filler metal provided by various organizations, including EPRI, KAPL, ENSA, and MHI. A CRDM J-groove weld produced by Valinox was also examined. Various

levels of constraint were used when producing the mockups, including no constraint at all. The objectives of this work were to characterize the composition, microstructure, and plastic strains in the weld metal, heat-affected zone (HAZ), and bulk base metal. The strains measured are defined as the equivalent residual (i.e., internal) strain in the material. The results regarding the Alloy 690 bulk and HAZ materials were discussed in Section 4.2.3; the results from the weld metal are described below. Despite these results being for the high-Cr materials, they are generally applicable to Alloy 600/82/182/132, as well.

The weld material was examined using electron backscatter diffraction (EBSD), which quantifies the amount of strain experienced during processing by measuring the amount of average intra-grain misorientation (AMIS). The samples for EBSD examination were slices of material perpendicular to the fusion line that were ground and given a final polish using a vibratory polisher with 0.05 μm colloidal silica to produce a surface with minimal preparation-induced surface strain. Figure 4-11 shows an example of the plastic strain profile in Alloy 52 weld metal, weld dilution zone, partially melted and unmelted heat-affected zones, and base metal.

Table 4-3 through Table 4-5 show the results of residual plastic strain measurements in the weld material, HAZ, and base metal from eleven weld mockups. The strains were measured at three different locations through the thickness: at the weld crown near the OD (Table 4-3), at the weld middle (Table 4-4), and at the weld root near the ID (Table 4-5). Figure 4-12 presents the cumulative distributions of the strains in the HAZ at the three locations, and Table 4-6 lists the strain values at select percentiles of the distributions.

The divider plate weld mockup made by ENSA and the CRDM J-groove weld by Valinox were also characterized along with a CRDM J-groove weld mockup manufactured by MHI by Efsing and Shen at KTH Royal Institute of Technology [40]. The method was similar to the EBSD-based method used at GE-GRC. The most significant differences were in the heat treatment of calibration specimens and the choice of misorientation metric. A longer solution anneal of 1050°C (1922°F) for four hours was used while the 500°C (932°F) stress relief for 100 hours after specimen machining was omitted. Instead of using AMIS as the misorientation metric, one based on kernel average misorientation (KAM) and one using grain orientation spread (GOS) were used in parallel. Both of the latter misorientation metrics produced the same results, which were slightly lower than the EBSD-based method used at GE-GRC for the same mockups.

Residual strain measurements on other mockups were obtained by Tohoku University. To obtain a correlation between residual strain and tensile applied strain for Alloy 690/52/152, KAM values were measured on 0%, 5%, 10%, 15%, 20%, and 30% tensile pre-strained specimens, as shown in Figure 4-13. Figure 4-14 shows the typical residual strain for the center of the Alloy 152 weld metal and the first layer of the Alloy 152 weld metal near the Alloy 690 base metal for the as-welded Alloy 690/152 mockup. Near the first layer of the Alloy 690/152 weld joint, the highest residual strain was measured to be less than 12% equivalent strain [41].

The mockups tested at the various laboratories included both constrained and unconstrained welds, including repair welds. The degree of constraint is an important detail because it can affect the location and magnitude of plastic strains that develop. Constrained welds tend to have higher residual strains, but many plant welds, such as the J-groove welds used to attach CRDM nozzles, tend to have lower residual strains because fewer weld passes are required to manufacture the weld compared to mockup joints.

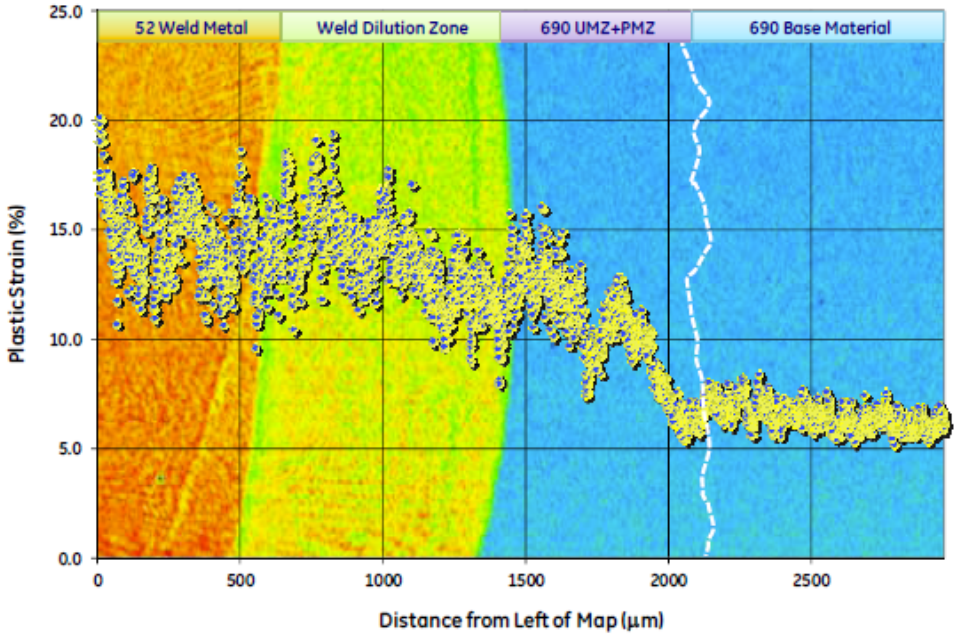


**Figure 4-11**
**Example of residual strain distribution from Alloy 690 base metal through the partially melted zone (PMZ) and unmixed zone (UMZ) and into the first two welding passes. The color mapping is for Mn, which is low in the base metal and high in the weld metal [38].**

**Table 4-3**
**Plastic strain in weld mockups at the weld crown height**

| Weld No. | Alloy | Product Form | Producer | Plastic Strain at Weld Crown Height, % (Approximate Distance from Interface) | | | |
|---|---|---|---|---|---|---|---|
| | | | | 52/Variant | 152/Variant | 690 Interface | 690 Base Metal |
| DJI19508A | 52M | A690 Plate<br>NG V-Groove | KAPL | 14.7<br>(4.2 mm) | — | 6.3 | 3.7<br>(3.9 mm) |
| CRDM J Weld | | PG&E<br>CRDM J-Groove Mockup | Valinox | — | — | — | — |
| 187775 | 52i | A690 Plate<br>V-Groove | EPRI | 12.3<br>(1.4 mm) | — | 10.2 | 7.0<br>(1.4 mm) |
| NX4721TK | 52M | 2" A690 plate (WP547)<br>ESW clad with 3 52M<br>filler metal layers | ENSA | 8.4<br>(Location 1: 1.0 mm) | — | 3.6 | 1.7<br>(17.4 mm) |
| MLT-3-Cr | | KAPL<br>V-groove | KAPL | 14.2<br>(3.5 mm) | — | 8.1 | 2.6<br>(16.4 mm) |
| | | | | 14.9<br>(3.0 mm) | | 6.7 | 2.6<br>(16.0 mm) |
| WC10E7 | 152 | V-groove | | — | 12.2<br>(~2.0 mm) | 6.3 | 1.4<br>(11.8 mm) |
| | | | | | 10.1<br>(~1.0 mm) | 7.2 | 1.2<br>(15.3 mm) |
| MU508 R690 | 52 | | MHI | — | — | — | — |
| MHI Mockup | | 2 V-groove welds | MHI | 18.9<br>(A weld: 1.1 mm) | — | A weld: 7.4 | 6.1<br>(0.8 mm) |
| | | | | 19.3<br>(B weld: 2.3 mm) | | B weld: 7.4 | 5.1<br>(0.96 mm) |
| NX2579JK | | U-bath tub | | 11.5<br>(0.1 mm) | — | 9.1 | 1.9<br>(12.2 mm) |
| | | | | 13.4<br>(1.6 mm) | | 10.9 | 3.7<br>(9.4 mm) |
| ENSA Divider Plate MU | 52M | Divider plate weld<br>52M filler metal | ENSA | 12.9<br>(2.8 mm) | — | 8.3 | 4.6<br>(1 mm) |
| | | | | 10.3<br>(2.6 mm) | | 8.4 | 4.6<br>(1 mm) |
| NX6523JK | 52M | V-groove | EPRI | 11.4<br>(0.8 mm) | — | 5.9 | 4.7<br>(0.9 mm) |

**Table 4-4**
**Plastic strain in weld mockups at the weld middle height**

| Weld No. | Alloy | Product Form | Producer | Plastic Strain at Weld Middle Height, % (Approximate Distance from Interface) | | | |
|---|---|---|---|---|---|---|---|
| | | | | 52/Variant | 152/Variant | 690 Interface | 690 Base Metal |
| DJI19508A | 52M | A690 Plate<br>NG V-Groove | KAPL | 23.6<br>(2.1 mm) | — | 8.3 | 3.6<br>(3.7 mm) |
| CRDM J Weld | | PG&E<br>CRDM J-Groove Mockup | Valinox | 15.7<br>(3.1 mm) | — | 7.6 | 2.7<br>(12.4 mm) |
| 187775 | 52i | A690 Plate<br>V-Groove | EPRI | 13.8<br>(1.0 mm) | — | 10.2 | 5.6<br>(1.6 mm) |
| NX4721TK | 52M | 2" A690 plate (WP547)<br>ESW clad with 3 52M<br>filler metal layers | ENSA | 8.0<br>(Location 2: 2.6 mm) | — | 4.1 | 1.5<br>(17.4 mm) |
| MLT-3-Cr | | KAPL<br>V-groove | KAPL | 16.9<br>(2.2 mm) | — | 8.8 | 2.4<br>(8.5 mm) |
| | | | | 17.2<br>(2.9 mm) | | 10.2 | 2.7<br>(9.1 mm) |
| WC10E7 | 152 | V-groove | | — | 9.5<br>(0.8 mm) | 9 | 1.7<br>(14.9 mm) |
| | | | | | 15.6<br>(2.5 mm) | 8.9 | 0.8<br>(17.3 mm) |
| MU508 R690 | 52 | | MHI | 12.2<br>(0.4 mm) | — | 12.6 | 4.7<br>(1.0 mm) |
| MHI Mockup | | 2 V-groove welds | MHI | 36<br>(A weld: 1.5 mm) | — | A weld: 8.9 | 4.6<br>(0.9 mm) |
| | | | | 19.5<br>(B weld: 2.5 mm) | | B weld: 7.5 | 4.6<br>(0.8 mm) |
| NX2579JK | | U-bath tub | | 14.9<br>(2.4 mm) | — | 16.4 | 2.1<br>(14 mm) |
| | | | | 18.1<br>(1.5 mm) | | 12 | 3.2<br>(11.1 mm) |
| ENSA Divider Plate MU | 52M | Divider plate weld<br>52M filler metal | ENSA | — | — | — | — |
| NX6523JK | 52M | V-groove | EPRI | 13.7<br>(1.9 mm) | — | 7.2 | 4.9<br>(1.1 mm) |

**Table 4-5**
**Plastic strain in weld mockups at the weld root height**

| Weld No. | Alloy | Product Form | Producer | Plastic Strain at Weld Root Height, % (Approximate Distance from Interface) | | | |
|---|---|---|---|---|---|---|---|
| | | | | 52/Variant | 152/Variant | 690 Interface | 690 Base Metal |
| DJI19508A | 52M | A690 Plate<br>NG V-Groove | KAPL | 38.6<br>(0.17 mm) | — | 6.7 | 3.8<br>(0.4 mm) |
| CRDM J Weld | | PG&E<br>CRDM J-Groove Mockup<br>(*region over LOF defect) | Valinox | 8.9<br>(0.9 mm) | — | 7.5 | 4.4<br>(1.6 mm) |
| | | | | 30.0*<br>(0.2 mm) | | 13.8* | 2.5<br>(13.4 mm) |
| 187775 | 52i | A690 Plate<br>V-Groove | EPRI | 19.6<br>(1.2 mm) | — | 12.4 | 5.9<br>(1.3 mm) |
| NX4721TK | 52M | 2" A690 plate (WP547)<br>ESW clad with 3 52M<br>filler metal layers | ENSA | 11.4<br>(Location 3: 0.68 mm) | — | 5.6 | 1.5<br>(16.8 mm) |
| MLT-3-Cr | | KAPL<br>V-groove | KAPL | 15.5<br>(3.7 mm) | — | 8.4 | 1.3<br>(15.2 mm) |
| | | | | 15.8<br>(3.5 mm) | | 8.3 | 1.8<br>(16.5 mm) |
| WC10E7 | 152 | V-groove | | — | 12.9<br>(1.6 mm) | 9 | 1.0<br>(16.7 mm) |
| | | | | | 19.3<br>(2.1 mm) | 9.4 | 0.8<br>(17.2 mm) |
| MU508 R690 | 52 | | MHI | 17.5<br>(1.9 mm) | — | 7.7 | 3.5<br>(1.2 mm) |
| MHI Mockup | | 2 V-groove welds | MHI | 48.1<br>(A weld: 1.3 mm) | — | A weld: 18.1 | 6.5<br>(1.3 mm) |
| | | | | 48.8<br>(B weld: 2.4 mm) | | B weld: 11.9 | 5.8<br>(1.0 mm) |
| NX2579JK | | U-bath tub | | 8.3<br>(1.2 mm) | — | 14.2 | 2.2<br>(14.7 mm) |
| | | | | 11.9<br>(0.5 mm) | | 11.7 | 5.9<br>(6.4 mm) |
| ENSA Divider Plate MU | 52M | Divider plate weld<br>52M filler metal | ENSA | 52.2<br>(Mid weld: 1.5 mm) | — | Mid weld: 16.3 | 8.4<br>(1.5 mm) |
| | | | | 37.9<br>(End weld: 2.9 mm) | | End weld: 18.4 | 9.0<br>(1.6 mm) |
| NX6523JK | 52M | V-groove | EPRI | 18.1<br>(1.7 mm) | — | 6.6 | 5.4<br>(0.9 mm) |

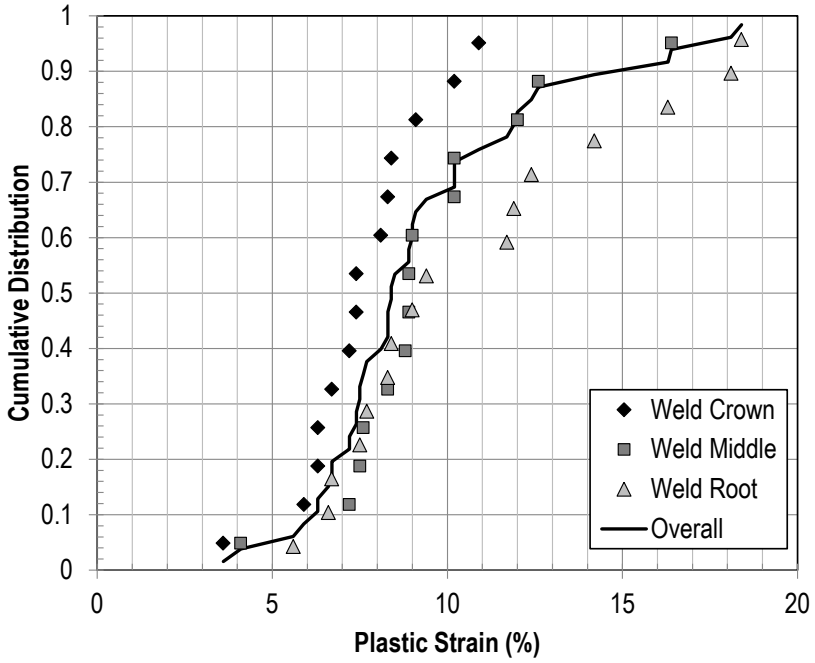


**Figure 4-12**
**Cumulative distribution of HAZ strains in weld mockups**

**Table 4-6**
**50th, 75th, and 95th percentile values of HAZ strains (%) in weld mockups**

| | 50th Percentile | 75th Percentile | 95th Percentile |
|---|---|---|---|
| Weld Crown | 7.4 | 8.6 | 10.9 |
| Weld Middle | 8.9 | 10.7 | 16.3 |
| Weld Root | 9.2 | 13.8 | 18.4 |
| Overall | 8.4 | 10.7 | 17.7 |

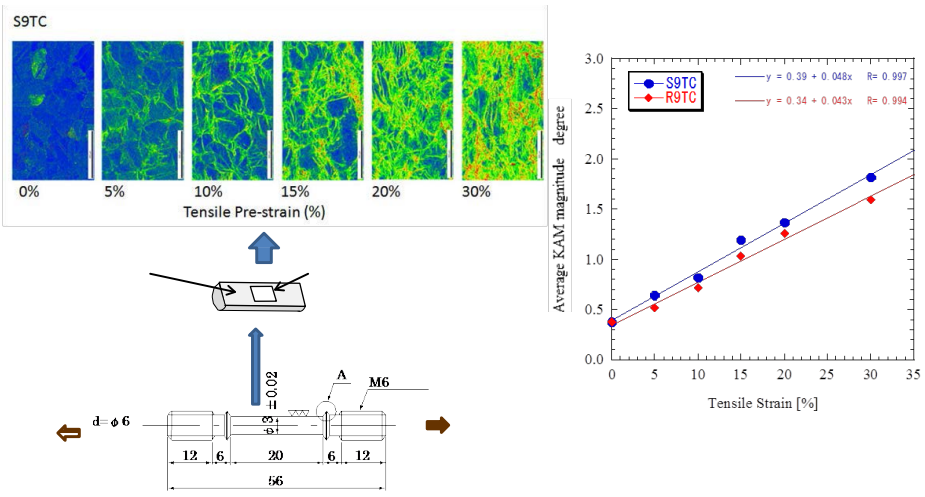


**Figure 4-13**
**KAM values measured on tensile pre-strained specimens with increasing amounts of cold work [42]**

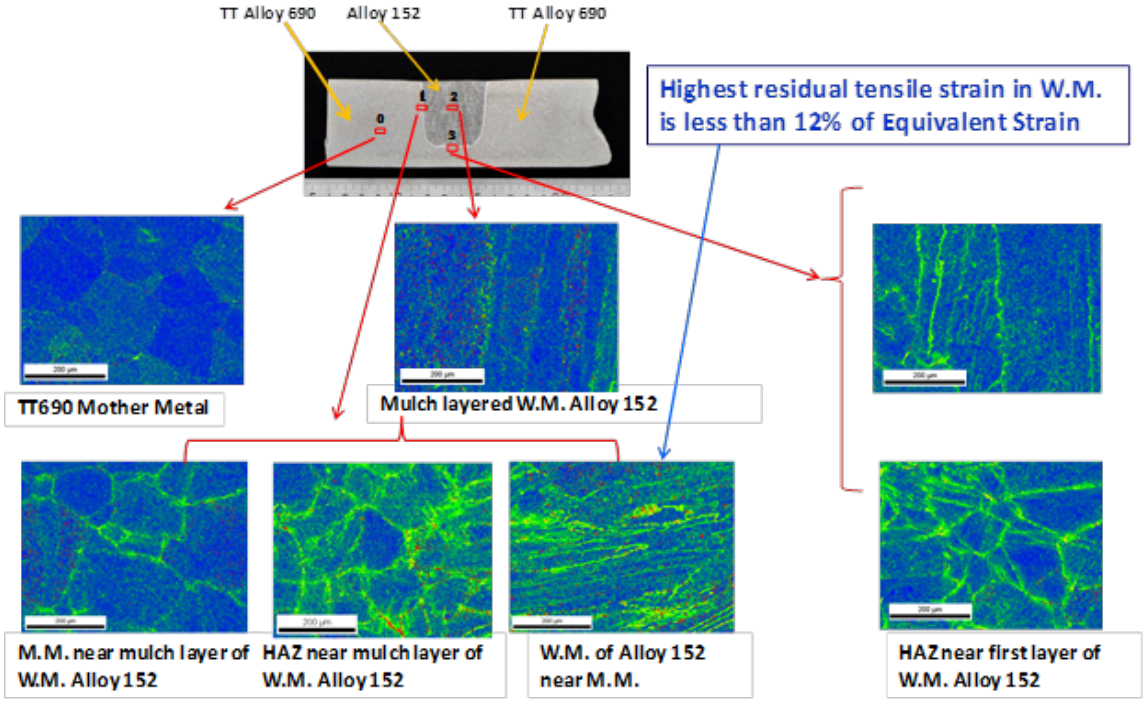


**Figure 4-14**
**Typical residual strain values for a weld joint mockup [42]**

# 5
# DETERMINATION OF PWSCC CGR PARAMETERS

Several parameters were investigated for inclusion in the CGR equations, based on which factors were included in the original MRP-55 and MRP-115 equations, other factors that are known to affect PWSCC CGRs, and what data are available to support quantifying the effects of such additional factors. For Alloy 600 and Alloy 82/182/132, parameters such as stress intensity factor, temperature, and dissolved hydrogen content were selected for inclusion in all revised CGR equations.

Section 5.1 describes the general modeling process used to determine the functional form of the parameter dependencies as well as the specific values. Section 5.2 details the factors selected for the Alloy 600 CGR equations, and how the parameter forms and values were selected. Similarly, Sections 5.3 presents the factors selected for the Alloy 82/182/132 CGR equations. Finally, Section 5.4 discusses how variability and uncertainty are inherently incorporated into the CGR equations.

## 5.1 Modeling Process Used

Three complementary methods were used to evaluate the CGR model dependencies for Alloy 600 and Alloy 82/182/132 and are described in detail in the following paragraphs:

1. The use of individual specimens and/or otherwise similar subgroups of data where only one variable was studied at a time ("*one-variable evaluations*"), where all datasets are weighted equally
2. A *generalized statistical analysis* using the same individual specimens or subgroups of data as the first method, but where the datasets are not weighted equally
3. An *aggregate statistical analysis* using the full database

The first method of *one-variable evaluations* was used because of the high scatter observed when analyzing numerous specimens from multiple heats, laboratories, and test conditions. This scatter can be much greater than the dependencies being investigated and can obfuscate the true parameter value. Therefore, the error in the parameter estimates was reduced as much as possible by evaluating subsets of data, ideally single specimens if available, from the same heat, tested by the same lab, and having all other variables kept constant except for the single parameter being investigated. The dependencies observed from single specimens with "on-the-fly" changes were typically stronger with greater correlation ($R^2$) values than those determined from larger datasets, where variability appears to reduce the clarity of the effects. The result from this analysis method was the median value of the subsets of data, thereby weighting each dataset equally, regardless of the number of points or the range of the investigated parameter within any given dataset.

The second method–the *generalized statistical analysis* method–supplemented the one-variable evaluations in that the same individual specimens or subsets of data were analyzed. However,

rather than calculating the median parameter value, the data were transformed to a linear dependence on the variable in question (e.g., to ln(CGR) vs. ln(K) from CGR vs. K) and used as input into statistical software, which fit a generalized linear model to the data. A categorical "dataset ID" parameter was also included to account for differences in heat, T, K, YS, etc., that varied among the datasets (but were consistent within each dataset). This allowed datasets with greater numbers of points and/or larger parameter ranges to be weighted more heavily, as opposed to the equal weighting assumed by simply calculating a median.

The third method used for data analysis was an *aggregate statistical analysis* in which the full database was used as input into the statistical software. This method was generally employed to determine the values of various parameters that either had insufficient data for the one-variable evaluation and/or generalized statistical analysis methods to be used, or those that varied on a heat-to-heat/weld-to-weld basis (e.g., alloy variation for the welds). The desired categorical (discrete) and quantitative (continuous) parameters were identified for each analysis case. Categorical variables are those that do not have distinct numerical values, such as heat or crack growth orientation. Quantitative variables, in contrast, do have numerical values that can vary continuously, such as stress intensity factor or temperature. After transforming the data to a linear dependence on the variable(s) in question (e.g., into ln(CGR) vs. ln(K) for the K dependency), a generalized linear model was fit to the data. Certain parameters were preset to values identified using the one-variable evaluation or generalized statistical analysis methods by normalizing the measured CGR prior to inputting the database into the statistical software. The output of the analysis software included values for the quantitative variables, values for the categorical variable factors, and factors for each heat (or weld) to account for heat-to-heat (or weld-to-weld) variability. The higher scatter in the data used for this method (due to the use of the larger database) led to lower confidence (i.e., weaker fits) for the dependences, including larger confidence intervals for the parameter values. Nevertheless, the values resulting from this method were often deemed most appropriate to include in the CGR model, based on expert judgment. The method used to determine the final value for each of the parameters is provided in each of the respective subsections that follow.

## 5.2 Alloy 600 PWSCC CGR Parameters

The parameters investigated for Alloy 600, and discussed in the following subsections, include:

$f_K$ = factor for stress intensity factor
$f_T$ = factor for temperature
$f_{H2}$ = factor for dissolved hydrogen concentration
$f_{YS}$ = factor for yield strength
$f_{orient}$ = factor for crack growth orientation
$f_{HAZ}$ = factor for crack growth in the heat-affected zone
$f_{HT}$ = factor for heat treatment
$f_{heat}$ = factor for heat-to-heat variation

### *5.2.1 Stress Intensity Factor*

The general form of the stress intensity factor (K) dependency is the same as that used in MRP-55 and is the basic power-law relationship often used to model stress corrosion crack growth:

$$f_K = K^{\beta} \qquad \text{Eq. 5-1}$$

where β is defined as the stress intensity factor exponent. The K threshold, $K_{th}$, was removed for this revision of the Alloy 600 CGR equations because new data are available that show crack growth is possible at K values below the previous threshold of 9 MPa√m (8 ksi√in.); the current CGR database includes test segments down to 7 MPa√m (6 ksi√in.). Additionally, cracks in plant components must develop through the low-K regime if they are to grow to significant depths. The Expert Panel decided by consensus that because there is no theoretical basis for why a K threshold should exist, $K_{th}$ should be removed rather than revised to a lower value.

The K exponent was investigated using all three analysis methods. For the one-variable evaluation and generalized statistical analysis methods, 12 datasets were identified with a K ratio ($K_{max}/K_{min}$) >1.5, as listed in Table 5-1. This ratio value was selected to allow for a sufficient number of datasets to be included while still requiring a large enough K range for the resulting dependency to be meaningful. For each of these 12 datasets, a linear estimate of the ln(CGR)-ln(K) transformation was calculated–an example is shown in Figure 5-1–and the median value of β derived from all of the individual dataset results was calculated to be 1.6 for all data or 1.5 for data with YS <600 MPa (87 ksi). Inputting these data into the statistical software for a generalized statistical analysis resulted in β=1.5 for all data or 1.3 for data with YS <600 MPa (87 ksi).

The aggregate statistical analysis method was also performed using the full database for comparison. The CGRs were normalized for temperature, dissolved hydrogen, yield strength, and/or orientation for various test cases where the K exponent was investigated. Numerous fits using varying values for the other parameters resulted in values of β of 2.0-2.2. From this, a final value of 2.0 was selected.

**Table 5-1**
**Datasets included in one-variable evaluations for β for Alloy 600**

| Set ID | Lab | Heat | Processing | Orientation | YS | K | K Ratio | T | [H2] | No. Points | β | $R^2$ |
|---|---|---|---|---|---|---|---|---|---|---|---|---|
| [—] | [—] | [—] | [—] | [—] | [MPa] | [MPa√m] | [—] | [°C] | [cc/kg] | [—] | [—] | [—] |
| A | Lockheed Martin | NX5853G11 | 0% None | L-T | 201 | 17 - 68 | 4.06 | 338 | 40 | 14 | 1.07 | 0.87 |
| B | CEA | WH220 | 0% None | — | 394 | 14 - 32 | 2.21 | 310 | — | 4 | 1.27 | 0.99 |
| C | Lockheed Martin | 44639 | 0% HAZ | S-L | 255 | 29 - 48 | 1.66 | 338 | 22 | 4 | 1.43 | 0.95 |
| D | Studsvik | 22474 | 0% None | L-T | 311 | 7 - 16 | 2.28 | 340 | 25 | 5 | 1.51 | 0.81 |
| E | Bettis | NX5853G11 | 31.9% CR | S-T | 827 | 22 - 40 | 1.84 | 338 | 4 | 8 | 1.56 | 0.90 |
| F | CEA | WH220 | 0% None | — | 394 | 14 - 35 | 2.42 | 330 | — | 3 | 1.56 | 1.00 |
| G | Bettis | NX5853G11 | 31.9% CR | L-T | 827 | 21 - 52 | 2.48 | 316 | 4 | 6 | 1.65 | 0.99 |
| H | Bettis | NX5853G11 | 31.9% CR | S-T | 827 | 33 - 54 | 1.64 | 316 | 4 | 7 | 1.79 | 0.83 |
| I | Bettis | NX5853G11 | 31.9% CR | L-T | 827 | 21 - 40 | 1.87 | 338 | 4 | 3 | 1.83 | 1.00 |
| J | Bettis | NX5853G11 | 31.9% CR | S-T | 827 | 20 - 53 | 2.61 | 288 | 4 | 12 | 1.86 | 0.70 |
| K | Lockheed Martin | NX5853G11 | 0% None | L-T | 201 | 30 - 68 | 2.30 | 338 | 40 | 3 | 2.20 | 0.97 |
| L | PNNL | M7929 | 0% None | C-R | 296 | 21 - 33 | 1.57 | 325 | 29 | 5 | 2.80 | 0.78 |

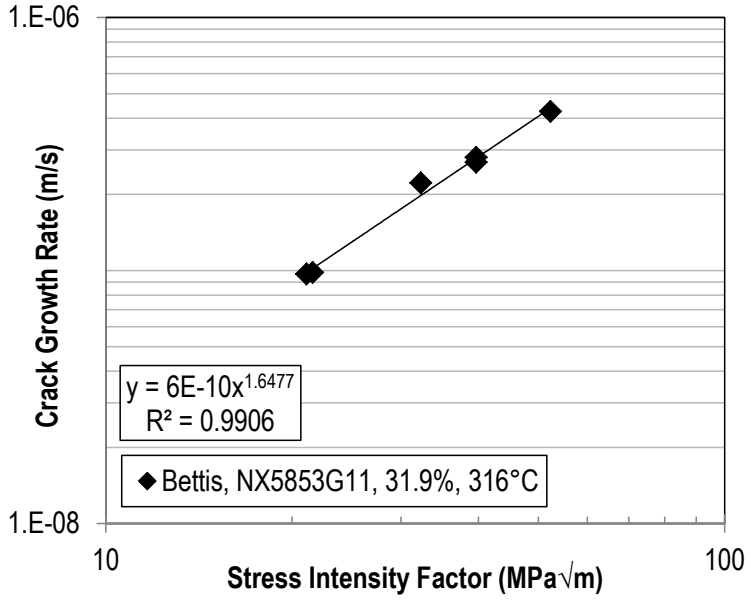


**Figure 5-1**
**Example calculation of the K exponent, β, for Alloy 600 that results in β=1.65**

### *5.2.2 Temperature*

A standard Arrhenius temperature dependence was retained from the MRP-55 Alloy 600 equation:

$$f_T = exp\left(\frac{-Q}{RT}\right) \qquad \text{Eq. 5-2}$$

where:

Q = thermal activation energy in kJ/mol
R = ideal gas constant = 0.008314 kJ/mol-K
T = test temperature in K

The thermal activation energy (Q) value is dependent on whether the dissolved hydrogen concentration versus the electrochemical potential (ECP) is maintained as the temperature changes. Two types of activation energies can be calculated: the *inherent* activation energy and the *apparent* activation energy. The *inherent* activation energy describes the true activation energy of the stress corrosion process and is calculated at a constant electrochemical potential relative to the Ni/NiO transition ($\Delta ECP_{Ni/NiO}$). The *apparent* Q, on the other hand, approximates the temperature dependence at a given hydrogen concentration (or over a specific $[H_2]$ range). The *apparent* Q is used when no $[H_2]/\Delta ECP$ term is included in the equation (such as for the MRP-55 disposition equation), while the *inherent* Q is used when the $[H_2]/\Delta ECP$ term is included. Both variations on Q were investigated for Alloy 600.

The *inherent* activation energy was investigated using all three analysis methods. A total of seven datasets were identified with a T ratio ($T_{max}/T_{min}$, where T is in °C) >1.1, as listed in Table 5-2. This ratio value was selected to allow for a sufficient number of datasets to be included while still requiring a large enough T range for the resulting dependency to be meaningful. All CGRs were normalized to $\Delta ECP_{Ni/NiO}=0$ at the respective test temperatures using the $[H_2]$ functional form and parameter values in Section 5.2.3 before calculating Q. Then, a linear

estimate of the ln(CGR) vs. 1/RT transformation was calculated for each dataset–an example is shown in Figure 5-2–and the median value derived from all of the individual dataset results was calculated to be 125 kJ/mol (29.9 kcal/mol). Inputting these data into the statistical software for a generalized statistical analysis resulted in Q=118 kJ/mol (28.2 kcal/mol). The aggregate statistical analysis resulted in Q=119 kJ/mol (28.4 kcal/mol). From these analyses, an inherent Q value of 120 kJ/mol (29 kcal/mol) was selected.

The overall temperature dependence must remain the same throughout the temperature range of interest, regardless of whether a dissolved hydrogen term (which also includes some temperature effects) is included in the model. In other words, the overall temperature dependence of $f_{Tinherent} f_{H2}$ must be equivalent to that of $f_{Tapparent}$ at all temperatures. Therefore, because the *apparent* and *inherent* Q values are directly correlated, one of the terms can be calculated if the other term and the hydrogen dependency are known by minimizing the difference in the overall temperature effect between the two methods over the temperature and hydrogen range of interest. Solving for $Q_{apparent}$ using an inherent Q of 120 kJ/mol (29 kcal/mol) (as discussed above), a reference $[H_2]$ level of 30 cc/kg, hydrogen parameters of P=3.0 and c=31 mV (per Section 5.2.3), and a temperature range of interest of 273-346°C (525-655°F) results in a value of 149 kJ/mol (35.6 kcal/mol). Therefore, the apparent Q–to be used when a dissolved hydrogen term is not included in the CGR equation–of 150 kJ/mol (36 kcal/mol) was judged to be appropriate by the Expert Panel for application within the relevant temperature and dissolved hydrogen conditions from which it was developed.

As identified in Section 4.1, the full range of temperatures represented in the laboratory data is not directly applicable to plant components (e.g., 360°C (680°F) is higher than standard operating temperatures). However, because the temperature dependence is known, the data can be normalized to a relevant reference temperature. Therefore, no data were excluded from the development of the disposition equation for this reason.

**Table 5-2**
**Datasets included in one-variable evaluations for inherent Q for Alloy 600**

| Set ID | Lab | Heat | Processing | Orientation | YS | K | T | T Ratio | [H2] | No. Points | Q | $R^2$ |
|---|---|---|---|---|---|---|---|---|---|---|---|---|
| [—] | [—] | [—] | [—] | [—] | [MPa] | [MPa√m] | [°C] | [—] | [cc/kg] | [—] | [kJ/mol] | [—] |
| A | CIEMAT | NX8664 | 0% None | — | — | 37 | 290 - 330 | 1.14 | varied; adj to ΔECP=0 at respective temp | 3 | 85 | 0.99 |
| B | EDF | WF675 | 0% None | — | 468 | 32 | 290 - 325 | 1.12 | | 6 | 97 | 0.69 |
| C | CIEMAT | NX8664 | 0% None | — | — | 33 | 290 - 330 | 1.14 | | 3 | 102 | 0.98 |
| D | CIEMAT | 746301 | 0% None | — | 302 | 35 | 290 - 330 | 1.14 | | 5 | 108 | 0.78 |
| E | PNNL | M7929 | 0% None | C-R | 296 | 21 | 300 - 360 | 1.20 | | 6 | 123 | 0.89 |
| F | PNNL | M7929 | 0% None | C-R | 296 | 21 | 300 - 360 | 1.20 | | 7 | 127 | 0.62 |
| G | Lockheed Martin | 44639 | 0% HAZ | S-L | 255 | 41 | 288 - 338 | 1.17 | | 4 | 163 | 0.98 |

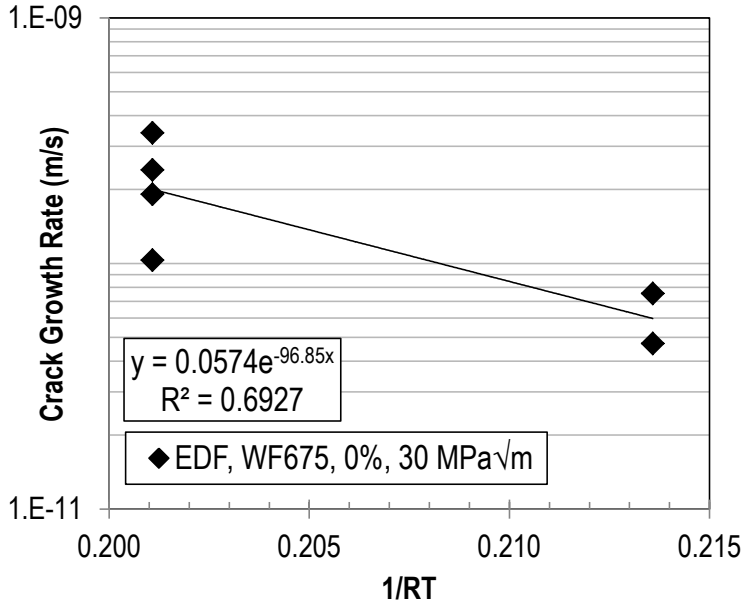


**Figure 5-2**
**Example calculation of inherent activation energy, Q, for Alloy 600 that results in Q=97 kJ/mol (23 kcal/mol)**

### *5.2.3 Dissolved Hydrogen*

Dissolved hydrogen is a new factor for the Alloy 600 CGR equations. MRP-55 noted that hydrogen likely had an effect on SCC CGRs of Alloy 600, but it did not elaborate beyond this statement. MRP-115 included a short section on this topic for Alloy 600 and presented data supporting a small (2.5-3X) enhancement of CGRs near the Ni/NiO phase boundary, but no specific values were recommended for Alloy 600. Therefore, because the available Alloy 600 data were produced at varying dissolved hydrogen concentrations, it is desirable to include a parameter to quantify these effects.

The functional form for the effect of dissolved hydrogen on Alloy 600 CGR behavior was adopted from MRP-263 [43], which investigated the effects of $[H_2]$ on the CGRs of Alloys 600 and 82/182/132. The same type of dependency on $[H_2]$ has been observed for Alloy X-750 and is believed to apply to all Ni-(15-30)Cr alloys:

$$f_{H2} = \frac{1}{P} + \frac{(P-1)}{P} exp\left(-0.5\left(\frac{\Delta ECP_{Ni/NiO}}{c}\right)^2\right) \quad \text{Eq. 5-3}$$

where:

$P$ = peak height; ratio of maximum to minimum expected CGRs
$c$ = peak width, mV

The electrochemical potential (ECP) term, $\Delta ECP_{Ni/NiO}$, is the difference in ECP between the Ni/NiO transition and the test condition, and it is given by the following equation:

$$\Delta ECP_{Ni/NiO} = 29.58\left(\frac{T}{298.15}\right) log_{10}\left(\frac{[H_2]}{[H_2]_{Ni/NiO}}\right) \quad \text{Eq. 5-4}$$

where:

$T$ = test temperature, K

$[H_2]$ = hydrogen concentration at the test condition in cc/kg $H_2O$ at standard temperature and pressure

$[H_2]_{Ni/NiO}$ = hydrogen concentration at the Ni/NiO transition at the temperature of interest in cc/kg $H_2O$, and is given by the following equation, with T in K:

$$= 10^{(0.0111(T-273.15)-2.59)}$$

This model is a Gaussian distribution centered at $\Delta ECP_{Ni/NiO}$=0 mV. The overall $[H_2]$ term is written in terms of the peak-to-shelf ratio, P, and peak width, c. P and c values were calculated for each dataset by varying P and c and minimizing the difference between the measured CGR and the predicted CGR using a least squares fit to the nonlinear equation and verifying visually by plotting the results. This was performed using Microsoft Excel's Solver function. Because of the relative complexity of these two interacting parameters, a general linear model could not be used to calculate these values. Therefore, only the one-variable evaluation method was used for this factor.

Four datasets, listed in Table 5-3, were identified where the $\Delta ECP_{Ni/NiO}$ (i.e., dissolved hydrogen and/or temperature) varied while all other parameters were held constant and the data obviously followed a Gaussian dependence. Figure 5-3 shows an example dataset with the Gaussian curve fit to the data. A median P value of 3.1 was identified, which was rounded to 3.0 to reflect the uncertainty in the precise value. This value of P was then assumed for all datasets and the Gaussian distributions were re-fit to each dataset to determine c. This analysis resulted in parameter values of P=3.0 and c=31 mV.

As identified in Section 4.1, the full range of dissolved hydrogen contents represented in the laboratory data is not directly applicable to plant components. However, because the $[H_2]$ dependence is known, the data can be normalized so that no data would have to be excluded from the disposition equation development for this reason.

**Table 5-3**
**Datasets included in one-variable evaluation analyses for P and c for Alloy 600**

| Set ID | Lab | Heat | Processing | Orientation | YS | K | T | ΔECP | No. Points | P | c |
|---|---|---|---|---|---|---|---|---|---|---|---|
| [—] | [—] | [—] | [—] | [—] | [MPa] | [MPa√m] | [°C] | [mV] | [—] | [—] | [mV] |
| A | GE-GRC | 93510 | 0% None | C-L | 269 | 28 | 325 | 17 - 53 | 3 | 1.8 | 22 |
| B | GE-GRC | 93510 | 0% None | C-L | 269 | 28 | 325 | 17 - 53 | 3 | 1.9 | 20 |
| C | GE-GRC | 93510 | 0% None | C-L | 269 | 28 | 325 | 9 - 27 | 4 | 4.3 | 29 |
| D | GE-GRC | 93510 | 0% None | C-L | 269 | 28 | 340 | 4 - 44 | 3 | 5.9 | 22 |

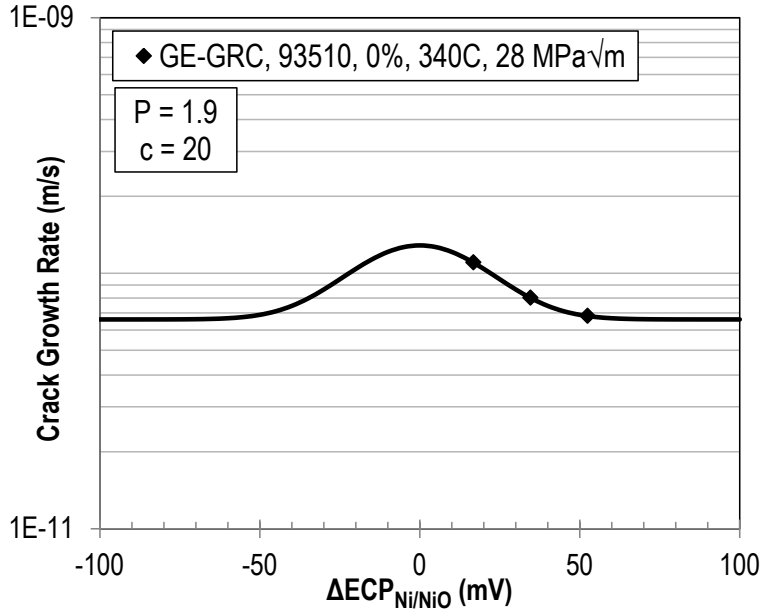


**Figure 5-3**
**Example calculation of [$H_2$] parameters for Alloy 600 that results in P=1.9 and c=20 mV**

### *5.2.4 Yield Strength*

Added cold work (CW) and yield strength (YS) were excluded from the MRP-55 analysis, as it was assumed at the time that no materials with added cold work were installed in plants. The consensus of the current Expert Panel is that while extensive cold work is not *intentionally* added to plant component materials, there may be some deformation that is unintentionally imparted, which should be accounted for, as discussed in Section 4.2.3.

A yield strength term was selected for inclusion into the Alloy 600 CGR model to reflect the fact that materials with higher yield strengths, whether in the as-received condition or with deformation added after supplier processing, tend to have higher CGRs. Yield strength (YS) has a positive correlation with deformation level and hardness, as shown in Figure 5-4 through Figure 5-6, so theoretically any of these three parameters could have been used. However, the scatter in the yield strengths associated with a single cold work value suggests that either the particular cold working method (e.g., the method type, strain rate, number of passes) may influence the strength and/or there may be some residual strain in the material that is not accounted for in the cold work value. For example, there may be residual strain left in the material during manufacturing and the material can still be classified as "as-received material," i.e., CW=0%, as discussed in Section 4.2.3. The YS of the as-received material, on the other hand, would reflect any of this residual strain.

The best fit equations relating added deformation (i.e., cold work, in percentage reduction from original thickness), yield strength (in MPa), and hardness (in Vickers (HV)) were developed from Alloy 600 CGR test data for which at least two of these values were reported, as well as a few additional references ([16], [41], [44], [45]). The data used to develop the equations are shown in Figure 5-4 through Figure 5-6, and the equations are presented below. YS was not reported for 13 test segments, nor hardness for numerous others, so the missing values were estimated using these equations:

$$YS\ (MPa) = -0.455 \cdot \%CW^2 + 31.2 \cdot \%CW + 287 \quad \text{Eq. 5-5}$$

$$HV = -0.064 \cdot \%CW^2 + 5.79 \cdot \%CW + 172 \quad \text{Eq. 5-6}$$

$$HV = 0.189 \cdot YS\ (MPa) + 129 \quad \text{Eq. 5-7}$$

The limits of applicability for both the YS vs. CW and HV vs. CW relationships are CW levels of 0-32%, equivalent to the range of the majority of the data. All of the Alloy 600 data included in the CGR database fall within these limits of applicability.

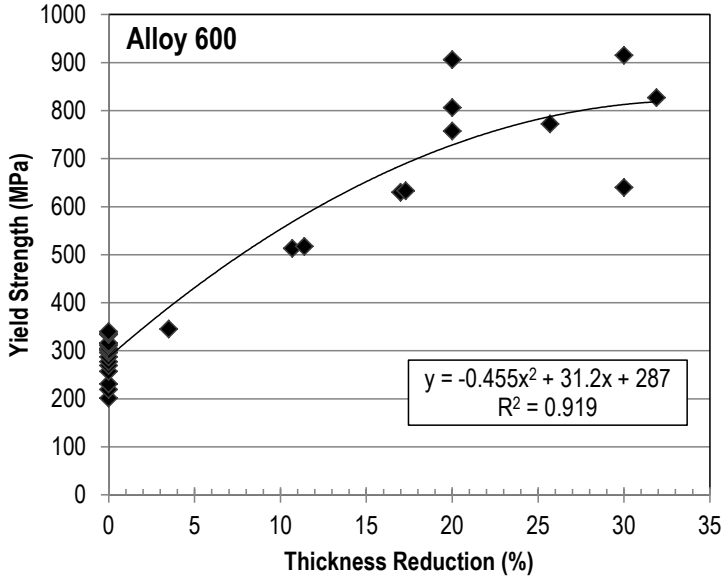


**Figure 5-4**
**Correlation between yield strength and thickness reduction (CW) from Alloy 600 test data**

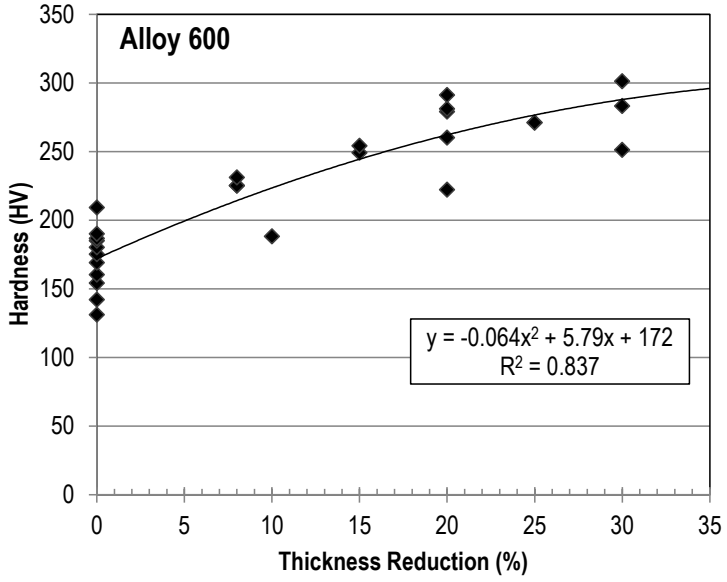


**Figure 5-5**
**Correlation between hardness and thickness reduction (CW) from Alloy 600 test data**

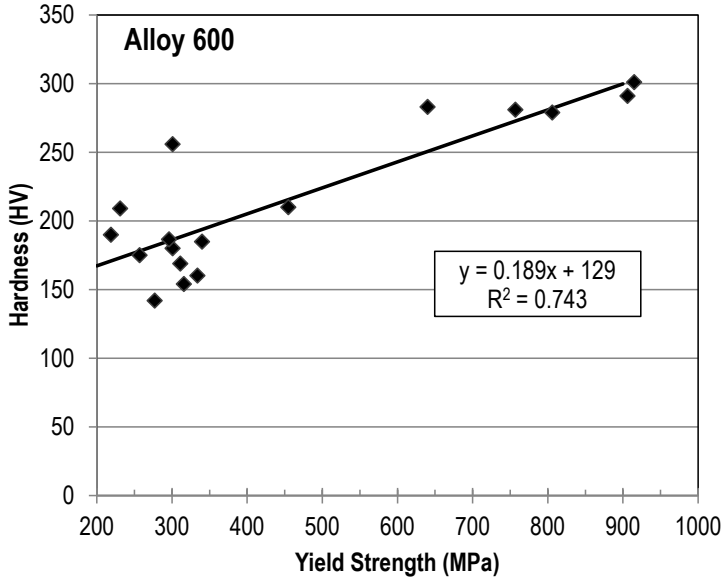


**Figure 5-6**
**Correlation between hardness and yield strength from Alloy 600 test data**

The general form of the YS dependency was selected as the following:

$$f_{YS} = YS^{\gamma} \qquad \text{Eq. 5-8}$$

where γ is defined as the yield strength exponent.

The YS exponent was investigated using all three analysis methods. For the one-variable evaluation and generalized statistical analysis methods, four datasets were identified with a YS ratio ($YS_{max}/YS_{min}$) ≥1.2, as listed in Table 5-4. This ratio value was selected to allow for a sufficient number of datasets to be included while still requiring a large enough YS range for the resulting dependency to be meaningful. Only specimens with the same deformation process were included in a single dataset. For each of these four datasets, a linear estimate of the ln(CGR) vs. ln(YS) transformation was calculated–an example is shown in Figure 5-7. The median value derived from all of the individual dataset results was calculated to be 2.7. Inputting these data into the statistical software for a generalized statistical analysis resulted in γ=2.4.

An aggregate statistical analysis using the full database was also performed for comparison. CGRs were normalized for stress intensity factor, temperature, dissolved hydrogen, and/or orientation for various test cases where the YS exponent was investigated. Numerous fits using varying values for the other parameters resulted in values of γ of 2.8-3.2. From this, a final value of γ=3.0 was selected.

Section 4.2.3 concluded that the conservative best estimate (approximately 75$^{th}$ percentile) of relevant added deformation levels for Alloy 600 is 12%, including HAZ regions. Because added deformation levels in plant components are not often known but yield strengths of the original materials may be available (e.g., from CMTRs), the 12% CW level was converted to YS using Eq. 5-5; 12% CW corresponds to a YS of approximately 600 MPa (87 ksi). Plant materials have a distribution of yield strengths, so rather than adjusting all Alloy 600 laboratory data to a relevant reference yield strength value, only data from specimens with YS values <600 MPa (87 ksi) were used in the development of the disposition curve without adjustment. This reduced

the database to 308 data points. For the model, all data were used and a term to adjust YS is included in the model equation. This allows CGRs at any given yield strength up to 820 MPa (120 ksi; 32% CW–the maximum CW level used for the YS dependence development) to be estimated.

**Table 5-4**
**Datasets included in one-variable evaluations for γ for Alloy 600**

| Set ID | Lab | Heat | Orientation | Processing | YS | YS Ratio | K | T | [H2] | No. Points | γ | $R^2$ |
|---|---|---|---|---|---|---|---|---|---|---|---|---|
| [—] | [—] | [—] | [—] | [—] | [MPa] | [—] | [MPa√m] | [°C] | [cc/kg] | [—] | [—] | [—] |
| A | Bettis | NX5853G11 | L-T | TS | 201 - 345 | 1.72 | 33.0 | 360 | 4.1 | 5 | 1.8 | 0.90 |
| B | Bettis | NX5853G11 | L-T | TS | 345 - 630 | 1.83 | 33.0 | 358 | 4.1 | 6 | 2.2 | 0.61 |
| C | Bettis | NX5853G11 | L-T | TS | 517 - 772 | 1.49 | 34.0 | 288 | 4.1 | 3 | 3.1 | 0.75 |
| D | Bettis | NX5853G11 | L-T | TS | 513 - 633 | 1.23 | 34.0 | 338 | 4.1 | 6 | 4.6 | 0.67 |

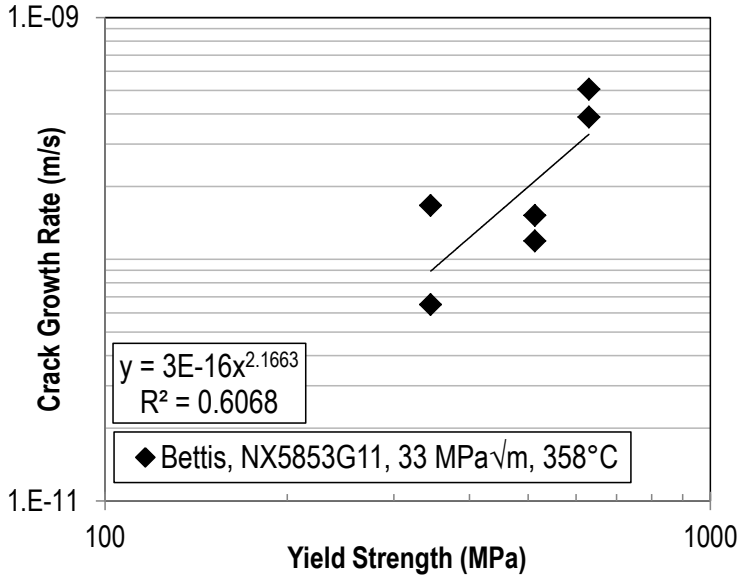


**Figure 5-7**
**Example calculation of yield strength exponent, γ, for Alloy 600 that results in γ=2.2**

### *5.2.5 Crack Growth Orientation*

The general form of the crack growth orientation dependency was selected as the following:

$$f_{orient} = \delta_{orient} \quad \text{Eq. 5-9}$$

where $\delta_{orient}$ is a function of the yield strength of the material.

Due to the anisotropy of Alloy 600 materials resulting from manufacturing processes and added deformation, cracks will grow faster in certain orientations than in others, as described in Section 4.3. The effects of orientation with respect to product form can only be seen at low cold work levels. Thus, for materials with YS ≤340 MPa (49 ksi; upper limit of 0% CW materials, as shown in Figure 5-4), CGRs for test segments in a "fast" orientation (S-L and S-T for plate materials; R-L and R-C for cylindrical materials) were compared to those from test segments in a "slow" orientation (T-S, T-L, L-S, L-T for plate materials; L-C, L-R, C-L, C-R for cylindrical materials). However, there were insufficient data to have confidence in the result because all nine

fast test segments were from a single HAZ heat, compared to 124 test segments from six different heats in the slow orientation. Therefore, no orientation factor for material with no added deformation was included in the model.

For orientation with respect to added deformation, it was predicted that the orientation effect would increase with deformation level due to the increasing damage imposed in the microstructure. To test this, CGRs for all data with added CW (YS >340 MPa (49 ksi)) were normalized for K, T, and $H_2$, then separated into subsets with similar YS values. A generalized statistical analysis using the subgroups of data was performed to determine the ratios between CGRs in the S-L or S-T orientations, as available, and the T-L orientation. Table 5-5 lists the subsets of data used, the number of data points per orientation per set, and the orientation factor.

Lack of data at multiple yield strengths, and especially between 340 MPa and 630 MPa (49 ksi and 91 ksi), resulted in the calculation of a best fit line through the two available data points that is anchored at a factor of 1 at 340 MPa (49 ksi), as shown in Figure 5-8. The full orientation factor was determined to be $f_{orient} = \max\{1, 0.013*YS - 3.42\}$, which has a minimum of 1 for YS values <340 MPa (49 ksi).

Section 4.3.2 concluded that all crack orientations with respect to added deformation are relevant to plant components because straightening, for example, can induce strains in multiple orientations. Therefore, no data were removed from the disposition equation database due to irrelevant CW orientation. Of the 12 points in the disposition equation database that had recorded added cold work, 11 were in the L-T orientation and one was in the S-L orientation. An additional 49 as-received points were recorded as having 0% added deformation but had YS values >340 MPa (49 ksi). No orientations were recorded for any of these data.

**Table 5-5**
**Subsets of data used for the Alloy 600 added deformation orientation factor development**

| YS Range | YS Average | No. Points / Orientation | | | | Ratio vs. L-T |
|---|---|---|---|---|---|---|
| | | S-L | S-T | L-T | Total | |
| 630 - 668 | 649 | 6 | 0 | 6 | 12 | 5.4 |
| 827 - 827 | 827 | 0 | 35 | 15 | 50 | 7.2 |

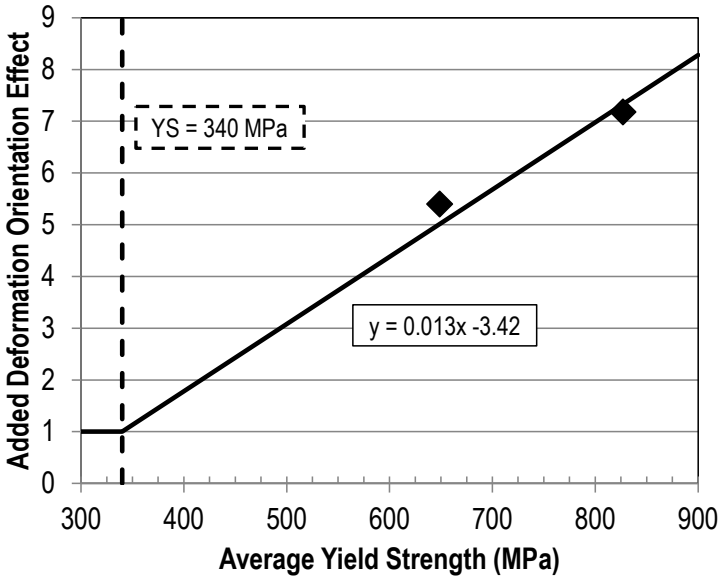


**Figure 5-8**
**Effect of added deformation orientation on CGRs for Alloy 600 data at various yield strengths**

### 5.2.6 Heat-Affected Zone

The HAZ term is a constant term to be included if the crack growth is confirmed to be in the heat-affected zone (HAZ) of Alloy 600:

$$f_{HAZ} = \delta_{HAZ} \quad \text{Eq. 5-10}$$

Because there were too few data to compare CGRs in the HAZ and in the undeformed bulk material for the same heat, this factor was determined using the aggregate analysis method with the full Alloy 600 CGR database. CGRs were normalized to a common reference condition using the parameters identified in the previous subsections, with an assumed HAZ YS of 287 MPa (42 ksi, equivalent 0% CW). Thus the only factor investigated in the analysis was the effect of HAZ (heat-to-heat variability was also accounted for by using a heat ID as an additional input), which resulted in a value of $\delta_{HAZ}$=1.7. This value was rounded to 2.0 for the CGR model to reflect the uncertainty in the precise value.

The Alloy 600 HAZ is clearly an important region for plant components, and cracks in this region should be covered by the disposition equation. A total of 17 HAZ data points are included in the disposition equation database. No factor is included in the disposition curve to differentiate these points or to adjust for crack growth in the HAZ rather than in the bulk material, but an HAZ factor is included in the model so that crack growth in the HAZ can be estimated under varying conditions.

### 5.2.7 Heat Treatment / As-Received Condition

A constant heat treatment term was considered to reflect the influence of a thermal treatment compared to a mill anneal:

$$f_{HT} = \delta_{HT} \quad \text{Eq. 5-11}$$

However, there were insufficient data to determine this factor, so it is not included in any Alloy 600 CGR equation.

### 5.2.8 Heat-to-Heat Variability

Heat-to-heat variability is reflected in a factor that is applied to all specimens of a given heat to account for the effect of inherent differences (e.g., composition and mill processing) on CGRs. These unique factors are determined by including heat as a categorical variable in the aggregate statistical analysis. Because only a limited subset of all Alloy 600 heats have been tested and it is typically unknown where a particular heat falls within the broad range of variability, the distribution of heat factors was evaluated. The 75$^{th}$ percentile of the heat factors distribution was calculated to define the overall model constant, α. The 75$^{th}$ percentile curve can be interpreted as the median of the upper half of the distribution describing the variability in CGR due to material heat. Thus, the resulting equations are considered to be conservative best estimate equations. The distributions of Alloy 600 heat factors obtained from the final disposition equation and full model analyses and adjusted to the reference condition of 325°C, 30 cc/kg $H_2$, and 287 MPa (42 ksi) YS (0% CW; only for the model) are presented in Section 6.1.

### 5.2.9 Additional Factors

There are numerous additional factors that may affect the PWSCC behavior of Alloy 600. However, these additional factors were not characterized sufficiently during testing, and some factors are not generally known for plant components. This includes the levels of trace elements, presence and extent (size and distribution) of grain boundary carbides, as well as grain size distribution. These factors, and others, are accounted for in the heat factors. Should additional testing be performed to isolate the effects of one or more of these variables, the CGR equations can be revised to include new factors.

## 5.3 Alloy 82/182/132 PWSCC CGR Parameters

The parameters investigated for Alloy 82/182/132, and discussed in the following subsections, include:

$f_K$ = factor for stress intensity factor
$f_T$ = factor for temperature
$f_{H2}$ = factor for dissolved hydrogen concentration
$f_{orient}$ = factor for crack growth orientation with respect to dendrite solidification
$f_{alloy}$ = factor for alloy variation
$f_{PWHT}$ = factor for post-weld heat treatment
$f_{weld}$ = factor for weld-to-weld variation

### *5.3.1 Stress Intensity Factor*

The general form of the stress intensity factor (K) dependency is the same as that used in MRP-115 and is the basic power-law relationship often used to model stress corrosion crack growth:

$$f_K = K^{\beta} \qquad \text{Eq. 5-12}$$

where β is defined as the stress intensity factor exponent.

The K exponent was investigated using all three analysis methods. For the one-variable evaluation and generalized statistical analysis methods, 14 datasets were identified with a K ratio ($K_{max}/K_{min}$) >1.5, as listed in Table 5-6. This ratio value was selected to allow for a sufficient number of datasets to be included while still requiring a large enough K range for the resulting dependency to be meaningful. For each of these 14 datasets, a linear estimate of the ln(CGR)-ln(K) transformation was calculated–an example is shown in Figure 5-9–and the median value derived from all of the individual dataset results was calculated to be 2.3. Inputting these data into the statistical software for a generalized statistical analysis resulted in β=2.5.

An aggregate statistical analysis using the full database was also performed for comparison. CGRs were normalized for temperature, dissolved hydrogen, and orientation to investigate the K exponent. This resulted in a K exponent of 2.0, which was selected as the final value.

**Table 5-6**
**Datasets included in one-variable analyses for β for Alloy 82/182/132**

| Set ID | Lab | Alloy | Weld | Orientation | K | K Ratio | T | [H2] | Load | No. Points | β | $R^2$ |
|---|---|---|---|---|---|---|---|---|---|---|---|---|
| [—] | [—] | [—] | [—] | [—] | [MPa√m] | [—] | [°C] | [cc/kg] | [—] | [—] | [—] | [—] |
| A | ANL | 182 | CT933 | T-L | 22 - 50 | 2.29 | 320 | 23 | CL/CK | 4 | 1.5 | 0.94 |
| B | ANL | 182 | VCS-182 | C-R | 21 - 34 | 1.63 | 320 | 23 | CL/CK | 4 | 1.5 | 0.78 |
| C | Bettis | 182 | Bettis-182 | T-S | 22 - 35 | 1.58 | 337 | 49 | PPU | 4 | 1.5 | 0.90 |
| D | Studsvik | 182 | 194 | T-S | 14 - 39 | 2.84 | 340 | 25 | CL/CK | 6 | 1.9 | 0.92 |
| E | Bettis | 82H | Bettis-82H | — | 22 - 36 | 1.63 | 338 | 50 | PPU | 4 | 2.1 | 0.99 |
| F | Bettis | 82H | Bettis-82H | — | 23 - 37 | 1.62 | 316 | 50 | PPU | 3 | 2.1 | 0.98 |
| G | Bettis | 82 | 16 | T-S | 28 - 54 | 1.92 | 338 | 25 | PPU | 7 | 2.3 | 0.87 |
| H | Bettis | 82 | 16 | T-S | 28 - 47 | 1.67 | 338 | 50 | PPU | 4 | 2.4 | 0.78 |
| I | Bettis | 82 | 7D | T-S | 22 - 38 | 1.74 | 338 | 50 | PPU | 3 | 3.1 | 1.00 |
| J | Lockheed Martin | 82 | LM82-3 | T-S | 28 - 50 | 1.79 | 338 | 40 | CL/CK | 5 | 3.4 | 0.97 |
| K | ANL | 182 | CT31 | T-S | 31 - 50 | 1.62 | 320 | 23 | CL/CK | 3 | 3.4 | 0.88 |
| L | Bettis | 82 | NGW-1 | T-S | 28 - 43 | 1.57 | 338 | 25 | PPU | 8 | 3.7 | 0.96 |
| M | Bettis | 82 | 8D | T-S | 29 - 46 | 1.59 | 338 | 25 | PPU | 5 | 4.0 | 0.89 |
| N | Westinghouse | 182 | PP751 | T-S | 17 - 32 | 1.86 | 325 | 25 | PPU | 4 | 4.1 | 0.82 |

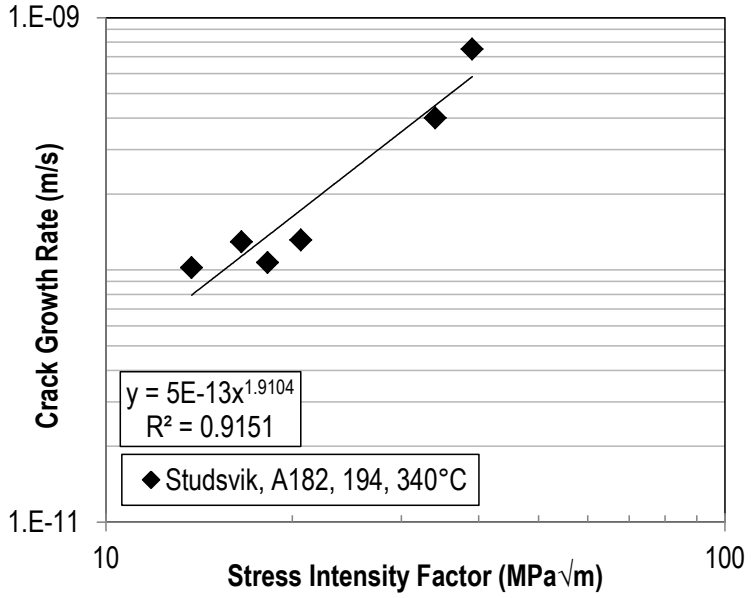


**Figure 5-9**
**Example calculation of the K exponent, β, for Alloy 82/182/132 that results in β=1.9**

### *5.3.2 Temperature*

A standard Arrhenius temperature dependence was retained from the MRP-115 Alloy 82/182/132 equation:

$$f_T = exp\left(\frac{-Q}{RT}\right) \qquad \text{Eq. 5-13}$$

where:

Q = thermal activation energy in kJ/mol

R = universal gas constant = 0.008314 kJ/mol-K

T = test temperature in K

The thermal activation energy (Q) value is dependent on whether the dissolved hydrogen concentration versus the electrochemical potential (ECP) is maintained as the temperature changes. As discussed in Section 5.2.2, the *inherent* activation energy describes the true activation energy of the stress corrosion process and is calculated at a constant electrochemical potential relative to the Ni/NiO transition ($\Delta ECP_{Ni/NiO}$), while the *apparent* Q approximates the temperature dependence at a given hydrogen concentration (or over a specific $[H_2]$ range). The *apparent* Q is used when no $[H_2]/\Delta ECP$ term is included in the equation (such as for the MRP-115 disposition equation for Alloy 82/182/132), while the *inherent* Q is used when the $[H_2]/\Delta ECP$ term is included. Both variations on Q were investigated for Alloy 82/182/132.

The *inherent* activation energy was investigated using all three analysis methods. A total of eight datasets were identified with a T ratio ($T_{max}/T_{min}$, where T is in °C) >1.1, as listed in Table 5-7. This ratio value was selected to allow for a sufficient number of datasets to be included while still requiring a large enough T range for the resulting dependency to be meaningful. All CGRs were normalized to $\Delta ECP_{Ni/NiO}=0$ at the respective test temperatures using the $H_2$ functional

form and parameter values in Section 5.3.3 before calculating Q. Then, a linear estimate of the ln(CGR) vs. 1/RT transformation was calculated for each dataset–an example is shown in Figure 5-10–and the median value derived from all of the individual dataset results was calculated to be 109 kJ/mol (26 kcal/mol). Inputting these data into the statistical software for a generalized statistical analysis resulted in Q=141 kJ/mol (34 kcal/mol). (Removing an outlier dataset that showed 251 kJ/mol (60 kcal/mol) results in an overall Q=128 kJ/mol (31 kcal/mol).) The aggregate statistical analysis resulted in Q=69 kJ/mol (16 kcal/mol). From these analyses, an inherent Q value of 120 kJ/mol (29 kcal/mol) was selected, the same as that for Alloy 600, as it is reasonable to expect that the base and weld metals of the same alloy family would exhibit a similar inherent temperature dependence.

The overall temperature dependence must remain the same throughout the temperature range of interest, regardless of whether a dissolved hydrogen term (which also includes some temperature effects) is included in the model. In other words, the overall temperature dependence of $f_{Tinherent} f_{H2}$ must be equivalent to that of $f_{Tapparent}$ at all temperatures. Therefore, because the *apparent* and *inherent* Q values are directly correlated, one term can be calculated if the other term and the hydrogen dependency are known by minimizing the difference in the overall temperature effect between the two methods over the temperature and hydrogen range of interest. Solving for $Q_{apparent}$ using an inherent Q of 120 kJ/mol (29 kcal/mol) (as discussed above), a reference $[H_2]$ level of 30 cc/kg, hydrogen parameters of P=7.5 and c=14 mV (per Section 5.3.3), and a temperature range of interest of 273-346°C (525-655°F) results in a value of 176 kJ/mol (42 kcal/mol). Therefore, the apparent Q–to be used when a dissolved hydrogen term is not included in the CGR equation–of 175 kJ/mol (42 kcal/mol) was judged to be appropriate for application within the relevant temperature and dissolved hydrogen conditions from which it was developed.

As identified in Section 4.1, the full range of temperatures represented in the laboratory data is not directly applicable to plant components (e.g., 360°C (680°F) is greater than typical operating temperatures). However, because the temperature dependence is known, the data can be normalized to a relevant reference temperature so no data would have to be excluded from the development of the disposition equation for this reason.

**Table 5-7**
**Datasets included in one-variable evaluations for inherent Q for Alloy 82/182/132**

| Set ID | Lab | Weld | Alloy | Orientation | Load | K | T | T Ratio | $[H_2]$ | No. Points | Q | $R^2$ |
|---|---|---|---|---|---|---|---|---|---|---|---|---|
| [—] | [—] | [—] | [—] | [—] | [—] | [MPa√m] | [°C] | [—] | [cc/kg] | [—] | [kJ/mol] | [—] |
| A | Bettis | Bettis-82H | 82H | — | PPU | 36.0 | 316 - 338 | 1.1 | varied; adj to ΔECP=0 at respective temp | 4 | 68 | 0.96 |
| B | Bettis | Bettis-82H | 82H | — | PPU | 23.0 | 316 - 338 | 1.1 | | 3 | 69 | 0.95 |
| C | Studsvik | 194 | 182 | T-S | CL | 32.0 | 290 - 319 | 1.1 | | 4 | 85 | 0.76 |
| D | Bettis | Bettis-182 | 182 | T-S | PPU | 22.0 | 315 - 337 | 1.1 | | 3 | 89 | 0.92 |
| E | Bettis | Bettis-182 | 182 | T-S | PPU | 34.0 | 315 - 337 | 1.1 | | 4 | 130 | 0.74 |
| F | ANL | CT933 | 182 | T-S | CL | 29.0 | 291 - 352 | 1.2 | | 3 | 134 | 0.92 |
| G | Westinghouse | PP751 | 182 | T-S | PPU | 23.0 | 290 - 342 | 1.2 | | 5 | 161 | 0.89 |
| H | ANL | A182-1 | 182 | T-S | CL | 35.0 | 291 - 322 | 1.1 | | 4 | 251 | 0.98 |

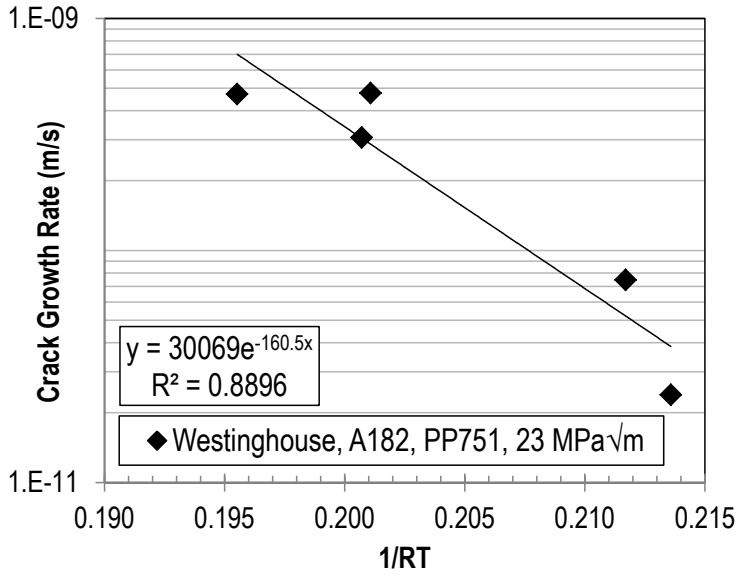


**Figure 5-10**
**Example calculation of inherent activation energy, Q, for Alloy 82/182/132 that results in Q=161 kJ/mol**

### *5.3.3 Dissolved Hydrogen*

Dissolved hydrogen is a new factor for the Alloy 82/182/132 CGR equations. MRP-115 noted that hydrogen likely had an effect on SCC CGRs of Alloy 82/182/132, but there were insufficient data at the time to confidently quantify the effects. There are now sufficient data to develop a dissolved hydrogen factor.

The functional form for the effect of dissolved hydrogen on Alloy 82/182/132 CGR behavior was adopted from MRP-263 [43], which investigated the effects of $[H_2]$ on the CGRs of Alloys 600 and 82/182/132. The same type of dependency on $[H_2]$ has been observed for Alloy X-750 and is believed to apply to all Ni-(15-30)Cr alloys:

$$f_{H2} = \frac{1}{P} + \frac{(P-1)}{P} exp\left(-0.5\left(\frac{\Delta ECP_{Ni/NiO}}{c}\right)^2\right) \quad \text{Eq. 5-14}$$

where:

$P$ = peak height; ratio of maximum to minimum expected CGRs
$c$ = peak width, mV

The electrochemical potential (ECP) term, $\Delta ECP_{Ni/NiO}$, is the difference in ECP between the Ni/NiO transition and the test condition, and it is given by the following equation:

$$\Delta ECP_{Ni/NiO} = 29.58\left(\frac{T}{298.15}\right) log_{10}\left(\frac{[H_2]}{[H_2]_{Ni/NiO}}\right) \quad \text{Eq. 5-15}$$

where:

$T$ = test temperature, K
$[H_2]$ = hydrogen concentration at the test condition in cc/kg $H_2O$ at standard temperature and pressure

$[H_2]_{Ni/NiO}$ = hydrogen concentration at the Ni/NiO transition at the temperature of interest in cc/kg, and is given by the following equation, with T in K:

$$= 10^{(0.0111(T-273.15)-2.59)}$$

This model is a Gaussian distribution centered at $\Delta ECP_{Ni/NiO}$=0 mV. The overall [$H_2$] term is written in terms of the peak-to-shelf ratio, P, and peak width, c. P and c values were calculated for each dataset by varying P and c and minimizing the difference between the measured CGR and the predicted CGR using a least squares fit to the nonlinear equation and verifying visually by plotting the results. This was performed using Microsoft Excel's Solver function. Because of the relative complexity of these two interacting parameters, a general linear model could not be used to calculate these values. Therefore, only the one-variable evaluation method was used for this factor.

Five datasets, listed in Table 5-8, were identified where the $\Delta ECP_{Ni/NiO}$ (i.e., dissolved hydrogen and/or temperature) varied while all other parameters were held constant and the data obviously followed a Gaussian dependence. Figure 5-11 shows an example dataset with the Gaussian curve fit to the data. The median P value of 7.5 was then assumed for all datasets and the Gaussian distributions were re-fit to each dataset to determine c, and the median c value was selected. Identifying P from the respective Gaussian distributions, rather than taking the ratio of CGRs obtained at peak and shelf ΔECP values, minimizes the effect of random data scatter. This resulted in final parameter values of P=7.5 and c=14 mV.

As identified in Section 4.1, the full range of dissolved hydrogen contents represented in the laboratory data is not directly applicable to plant components. However, because the [$H_2$] dependence is known, the data can be normalized so that no data would have to be excluded from the disposition equation development for this reason.

**Table 5-8**
**Datasets included in one-variable evaluations for P and c for Alloy 82/182/132**

| Set ID | Lab | Alloy | Weld | Orientation | K | T | ΔECP | No. Points | P | c |
|---|---|---|---|---|---|---|---|---|---|---|
| [—] | [—] | [—] | [—] | [—] | [MPa√m] | [°C] | [mV] | [—] | [—] | [mV] |
| A | GE-GRC | 82H | HD78-1 | T-S | 28.0 | 340 | 0 - 29 | 3 | 3.8 | 11 |
| B | GE-GRC | 182 | 688879 | T-S | 28.0 | 325 | -60 - 27 | 7 | 6.0 | 15 |
| C | GE-GRC | 182 | 414998 | T-S | 31.0 | 340 | -28 - 44 | 5 | 7.5 | 14 |
| D | GE-GRC | 182 | 414988 | T-S | 33.0 | 325 | -60 - 0 | 4 | 8.6 | 21 |
| E | GE-GRC | 82H | HD78-1 | T-S | 31.0 | 340 | -81 - 29 | 9 | 25.6 | 13 |

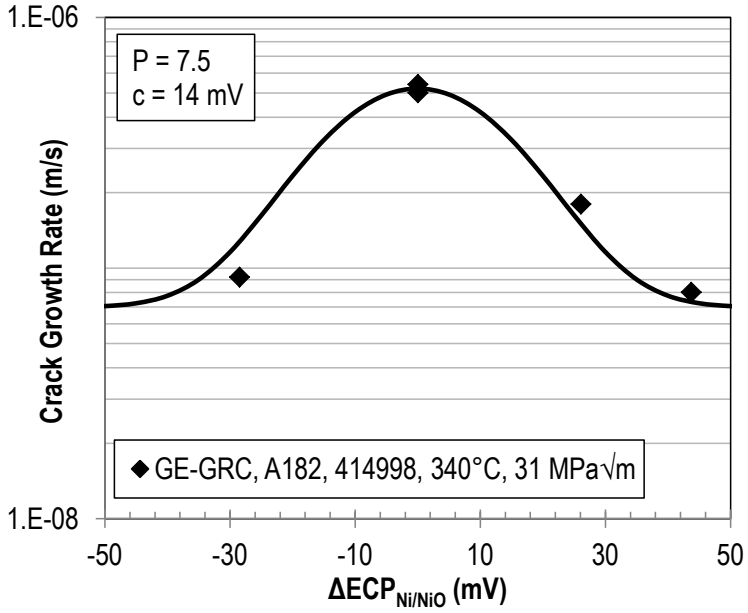


**Figure 5-11**
**Example calculation of [$H_2$] parameters for Alloy 82/182/132 that results in P=7.5 and c=14 mV**

### *5.3.4 Orientation*

For weld metals, crack growth orientation is defined with regard to the dendrite solidification direction. Cracks growing along the dendrite growth direction typically have higher CGRs than those growing perpendicular to the dendrite growth direction. As shown in Figure 4-7, the T-S and L-S orientations are parallel to dendrite growth, so they are termed the "fast" directions. The T-L and L-T orientations are perpendicular to dendrite growth, but cracks in these orientations can still grow intergranularly. Thus, these directions are moderate growth directions. The slowest directions are the S-T and S-L orientations, as cracks must cut across dendrites in order to advance. No welds were tested in the S-T or S-L orientations, so T-L and L-T are the slowest orientations tested and are referred to as the "slow" orientations for the CGR model.

The general form of the crack growth orientation dependency was selected as the following:

$$f_{orient} = \delta_{orient} \qquad \text{Eq. 5-16}$$

Six datasets were identified in which nominally identical specimens under nominally identical testing conditions were tested in different orientations. For each of the six datasets, listed in Table 5-9, about half of the test segments were obtained from cracks growing in a fast orientation and the other half from cracks growing in a slow orientation. No further distinction between orientations falling under the same category (e.g., between T-L and L-T in the "slow" category) was investigated.

The orientation factor was investigated using one-variable evaluations and generalized statistical analyses. For the one-variable evaluations, the ratio of the average CGR for slow-orientation test segments to the average CGR for fast-orientation segments within each dataset was calculated. A median ratio of 0.5 was identified. Inputting these data into the statistical software for a generalized statistical analysis resulted in $f_{orient}$=0.3. These analyses confirm that the orientation

factor of 0.5 determined in MRP-115 for Alloy 82/182/132 is still appropriate to use in the new equations.

As described in more detail in Section 4.3, cracks have been observed in all orientations in service and a crack may change direction as it grows to stay on low energy grain boundaries as much as possible. Therefore, it should be conservatively assumed that crack growth in Alloy 82/182/132 weld materials occurs in the fast orientation unless it can be proven otherwise.

**Table 5-9**
**Datasets included in one-variable evaluations for $f_{orient}$ for Alloy 82/182/132**

| Set ID | Lab | Weld | Alloy | K | T | [H2] | No. Points | $f_{orient}$ |
|---|---|---|---|---|---|---|---|---|
| [—] | [—] | [—] | [—] | [MPa√m] | [°C] | [cc/kg] | [—] | [—] |
| A | ANL | CT933 | 182 | 36 | 320 | 23 | 2 | 0.16 |
| B | Westinghouse | D545/582 | 182 | 28 | 325 | 25 | 7 | 0.21 |
| C | MHI | MHI-132 | 132 | 35 | 325 | 30 | 2 | 0.50 |
| D | ANL | CT933 | 182 | 29 | 320 | 23 | 4 | 0.51 |
| E | Bettis | 7D | 82 | 39 | 338 | 52 | 2 | 0.66 |
| F | Bettis | 7D | 82 | 22 | 338 | 50 | 2 | 0.90 |

### *5.3.5 Alloy Type*

An alloy factor was introduced in MRP-115 to reflect the slower growth of Alloy 82 compared to Alloy 182/132, likely due to the increased chromium content in the former alloy:

$$f_{alloy} = \delta_{alloy} \qquad \text{Eq. 5-17}$$

A generalized statistical analysis was performed on a laboratory basis to investigate this factor to remove any laboratory-to-laboratory variability. CGRs were normalized for K, T, $H_2$, and orientation using the values selected in Section 5.3 and were used as input to the statistical software to calculate the ratio between Alloy 82 and Alloy 182/132. The distribution of data is listed in Table 5-10. The median value was identified as 0.395 (i.e., cracks in Alloy 182/132 grow 1/0.395=2.5 times faster than those in Alloy 82). This supports the value of 0.385 used in MRP-115, and thus 0.385 was selected for the revised Alloy 82/182/132 CGR equations.

**Table 5-10**
**Distribution of data used to determine $f_{alloy}$ for Alloy 82/182/132**

| | Alloy 182 | | Alloy 82 | | |
|---|---|---|---|---|---|
| Laboratory | No. Welds | No. Points | No. Welds | No. Points | Alloy Factor |
| ANL | 5 | 33 | 1 | 2 | 0.51 |
| Bettis | 1 | 7 | 10 | 54 | 0.43 |
| GE-GRC | 5 | 53 | 1 | 19 | 0.36 |
| Lockheed | 3 | 11 | 3 | 19 | 0.27 |

### *5.3.6 Post-Weld Heat Treatment*

A constant factor was considered to credit the benefit of post-weld heat treatment (PWHT) on Alloy 82/182/132 CGRs:

$$f_{PWHT} = \delta_{PWHT} \qquad \text{Eq. 5-18}$$

While a few Alloy 82 datasets were identified that showed an effect of PWHT, there was limited variation in conditions between the sets (only two heats from a single laboratory), only Alloy 82H was represented (i.e., the full range of possible compositions for Alloy 82 was not covered), and the heat treatment applied was not directly applicable to commercial PWR components. These available datasets suggested a factor of 6 benefit for post-weld heat treatment on CGRs, but for all of the reasons mentioned above, a PWHT factor for Alloy 82 is not recommended.

No PWHT Alloy 182 data were included in the CGR database. A literature search identified two early studies on PWHT of Alloy 182, each of which supported a factor of 2 benefit ([46], [47]). However, neither dataset is included in the CGR database due to insufficient information on specific test segment duration, crack increment (Δa), or IG morphology/engagement, and [$H_2$] was only reported as "25-50 cc/kg." Additionally, one reference only reported maximum CGRs, whereas average CGRs were used for this effort (and for MRP-115). Therefore, because of the insufficient data available for these tests, which were performed prior to development of current best testing practices, the Expert Panel does not recommend including a PWHT factor for Alloy 182 at this time.

### 5.3.7 Weld-to-Weld Variability

Weld-to-weld variability is reflected in a factor that is applied to all specimens of a given weld to account for the effect of inherent differences (e.g., composition and welding process) on CGRs. These unique factors are determined by including weld as a categorical variable in the aggregate statistical analysis. Because only a limited subset of all Alloy 82/182/132 welds have been tested and it is typically unknown where a particular weld falls within the broad range of variability, the distribution of weld factors was evaluated. The 75$^{th}$ percentile of the weld factors distribution was calculated to define the overall model constant, α, so the resulting equations would be conservative best estimate equations. The distribution of Alloy 82/182/132 weld factors obtained from the final disposition equation analysis and adjusted to the reference condition of 325°C, 30 cc/kg $H_2$, fast orientation, and Alloy 182 is presented in Section 6.2.

### 5.3.8 Additional Factors

There are numerous additional factors that may affect the PWSCC behavior of Alloy 82/182/132. However, these additional factors were not characterized sufficiently during testing, and some factors are not generally knowable for plant components. This includes the levels of trace elements, presence and extent (size and distribution) of carbides, and welding parameters. These factors, and others, are accounted for in the weld factors. Should additional testing be performed to isolate the effects of one or more of these variables, the CGR equations can be revised to include new factors.

## 5.4 Treatment of Variability and Uncertainty

Developing empirical models from large databases always involves some degree of uncertainty. This uncertainty and variability in results was addressed in the following ways.

First, multiple analysis methods were used to obtain the values for all parameters where possible. Higher confidence was given to those parameters for which consistency in the value was maintained over multiple analysis methods. Where values varied significantly among analysis methods, expert judgement and consensus was used to determine which values were the most

realistic and/or reasonable. For this, prior experience of the Expert Panel members and outside studies were considered.

Additionally, comparisons to the original MRP-55 and MRP-115 equations were made for all factors where possible. These original disposition equations have been used throughout the industry for almost 15 years to date, and they have proven to successfully characterize crack growth in Alloy 600/82/182/132 plant components. The fact that prior parameter values were either confirmed or were changed only slightly due to the updated analyses supports that the new equations appropriately represent the true Alloy 600/82/182/132 PWSCC behavior.

Finally, much of the variability among heats that exists for reasons not explicitly accounted for in the CGR model is absorbed into the heat/weld factors. By including heat/weld factors in the generalized and aggregate statistical analyses, some of the variability among heats/welds is removed so the true dependencies can be identified. The variability among heats/welds is why the 75th percentile of heat/weld factors was used (instead of, for example, the median, or 50th percentile) to develop the leading constant term, α. The disposition equations and models were not intended to be bounding curves, but rather to be conservative best estimates, i.e., 75th percentile equations.

# 6
# PWSCC CRACK GROWTH RATE EQUATIONS

Three types of PWSCC CGR equations for Alloys 600 and 82/182/132 were developed in this effort and are presented in the following two subsections:

1. *New Disposition Equation for Original MRP-55/MRP-115 Data.* A new disposition equation for the original MRP-55 Alloy 600 CGR database (excluding 13 short hold time PPU data points, as discussed in Section 3.1) was created using the parameter values for the K exponent and threshold and for Q developed in Section 5.2 of this report. As described in MRP-55, the original K exponent of 1.16 and K threshold of 9 MPa√m (8 ksi√in.) were adopted from the Scott equation that was developed for steam generator tubing, and the activation energy of 130 kJ/mol (31 kcal/mol) was recommended based on literature and a general consensus of the CGR review team, rather than evaluation of the data compiled specifically for that effort. Therefore, it was desirable to reevaluate the original MRP-55 CGR equation in light of the parameter values that were developed from those (and additional) data. This equation only includes factors for stress intensity factor and temperature.

   For the original MRP-115 Alloy 82/182/132 CGR equation, the K exponent of 1.6 was calculated from the database compiled for that effort, but the activation energy of 130 kJ/mol (31 kcal/mol) was adopted from the MRP-55 Alloy 600 equation due to the similar compositions of the alloys and the supporting literature. Similar to the case for Alloy 600, there are sufficient Alloy 82/182/132 data in the current database to reevaluate these parameters (as discussed in Section 5.3 of this report) and to update the CGR equation for the original MRP-115 data.

2. *Revised Disposition Equation for All Compiled Data.* Revised disposition equations were developed for all currently compiled Alloy 600 and Alloy 82/182/132 data. As disposition equations, they have direct plant relevance and as such have limited ranges of applicability, particularly in terms of yield strength or added deformation applied to Alloy 600 materials. These equations include factors for stress intensity factor, temperature, and dissolved hydrogen, and all parameter values were developed within this effort.

3. *Full CGR Model for All Compiled Data.* The third type of CGR equation is the full CGR model. The model has a broader range of applicability than the respective disposition equation for the same alloy and it includes all terms for which dependencies were identified, even if they are not necessarily relevant or known for plant conditions or plant materials. The model is intended to be used when information about PWSCC behavior for conditions outside of typical plant conditions exist. For Alloy 600, highly cold worked materials (>12% CW) were used for the development of the CGR model, and the model includes factors for yield strength (YS), crack growth orientation, and crack growth in the heat-affected zone (HAZ) of the base material. For Alloy 82/182/132, all data were directly relevant to plant applications and all factors for which dependencies were identified were included in the

disposition equation, so it was not necessary to develop a CGR model with additional data or factors for the weld metal.

The variables included in the CGR equations presented in Sections 6.1 and 6.2 are defined as follows:

$\dot{a}$ = crack growth rate, m/s

$\alpha$ = crack growth constant

$f_K$ = factor for stress intensity factor, for K in MPa√m

= $K^{\beta}$

$K$ = crack tip stress intensity factor, MPa√m

$\beta$ = stress intensity factor exponent

$f_T$ = factor for temperature, for T in K

= $exp\left(\frac{-Q}{R}\left(\frac{1}{T}-\frac{1}{T_{ref}}\right)\right)$

$Q$ = thermal activation energy for crack growth, kJ/mol

$R$ = universal gas constant = 0.008314 kJ/mol-K

$T$ = absolute operating temperature at the location of the crack, K

$T_{ref}$ = absolute reference temperature used to normalize data = 598.15 K (325°C)

$f_{H2}$ = factor for dissolved hydrogen

= $\frac{1}{P}+\frac{P-1}{P}exp\left(-0.5\left(\frac{\Delta ECP_{Ni/NiO}}{c}\right)^2\right)$

$P$ = peak height

$c$ = peak width, mV

$\Delta ECP_{Ni/NiO}$ = electrochemical potential difference from the Ni/NiO transition line at the operating temperature, mV

= $29.58\left(\frac{T}{298.15}\right)log\left(\frac{[H_2]}{[H_2]_{Ni/NiO}}\right)$

$f_{H2ref}$ = reference dissolved hydrogen factor used to normalize data;

= $f_{H2}$ evaluated at $\Delta ECP_{ref}$ = 27.3 mV (30 cc/kg $H_2$ at 325°C)

$f_{YS}$ = factor for yield strength, for YS in MPa

= $YS^{\gamma}$

$\gamma$ = yield strength exponent

$f_{orient}$ = factor for crack growth orientation

$f_{HAZ}$ = factor for crack growth in the base metal heat-affected zone

$f_{alloy}$ = factor for weld alloy type

## 6.1 Alloy 600 CGR Equations

### *6.1.1 New Disposition Equation for MRP-55 Data*

Using the parameters identified in Section 5.2 ($K_{th}$=0 MPa√m, β=2.0, $Q_{app}$=149 kJ/mol), the constant term, α, was refit to the original MRP-55 data (excluding the 13 short hold time PPU points). The new fit is defined as follows and is shown in Figure 6-1, along with the original MRP-55 fit for comparison:

$$\dot{a} = \alpha K^{\beta} exp\left(\frac{-Q}{R}\left(\frac{1}{T}-\frac{1}{T_{ref}}\right)\right) \qquad \textbf{Eq. 6-1}$$

where:

$\alpha$ = $1.14 \times 10^{-13}$ at 325°C for $\dot{a}$ in m/s, K in MPa√m, and T in K

$\beta$ = 2.0

$Q$ = 149 kJ/mol

The new fit yields faster CGRs than the original fit at low K values, as expected due to the removal of the K threshold. The new fit is within 10% of the original fit between 17 MPa√m and 29 MPa√m. The higher K exponent in the updated fit causes the new equation to increase more rapidly over the MRP-55 equation as the K value increases beyond 30 MPa√m.

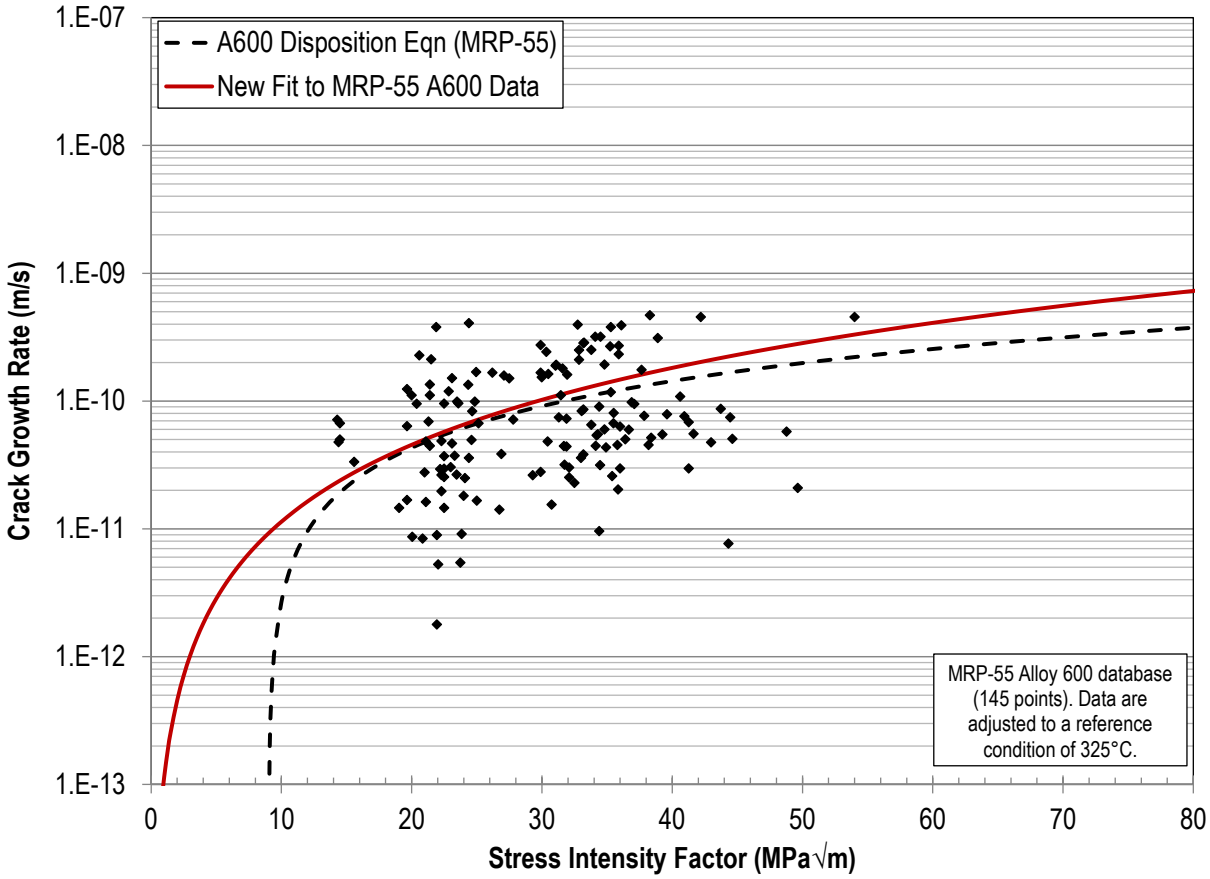


**Figure 6-1**
**New disposition equation for MRP-55 Alloy 600 data, shown with data adjusted to a reference condition of 325°C. The original MRP-55 disposition equation is shown for reference.**

### *6.1.2 Alloy 600 Revised Disposition Equation*

The Alloy 600 revised disposition equation was developed from guidance of the full Expert Panel. The parameter values used in this equation are those that were selected by the experts, as discussed in Section 5.2.

The Alloy 600 revised disposition equation is presented in Eq. 6-2, with the parameters defined at the beginning of this section and the values listed after Eq. 6-2. The constant term, α, was calculated to be equivalent to the 75$^{th}$ percentile of the log-normal heat factor distribution for the Alloy 600 disposition equation database, shown in Figure 6-3. Table 6-1 evaluates the dissolved hydrogen term, $\frac{f_{H2}}{f_{H2ref}}$, at various temperature and [$H_2$] combinations for convenience. The Alloy 600 disposition equation data, normalized to a reference condition of 30 cc/kg $H_2$ at 325°C (617°F) using the dependencies for this equation, are plotted along with the disposition equation in Figure 6-2, as well as the original MRP-55 Alloy 600 disposition equation. The applicability of these equations is limited to materials with YS values <600 MPa (87 ksi), as discussed in Section 4.2.3.

$$\dot{a} = \alpha K^{\beta} \exp\left(\frac{-Q}{R}\left(\frac{1}{T}-\frac{1}{T_{ref}}\right)\right)\frac{f_{H2}}{f_{H2ref}} \qquad \textbf{Eq. 6-2}$$

where:

$\alpha$ = $1.19 \times 10^{-13}$ at 325°C and 30 cc/kg $H_2$ for $\dot{a}$ in m/s, K in MPa√m, and T in K

$\beta$ = 2.0

$Q$ = 120 kJ/mol

$P$ = 3.0

$c$ = 31 mV

**Table 6-1**

**Values of the dissolved hydrogen term, $\frac{f_{H2}}{f_{H2ref}}$, at various temperature-[$H_2$] combinations for Alloy 600. Values at intermediate temperatures and/or hydrogen concentrations can be linearly interpolated.**

| | | Temperature | | | | | | | | | | | | | |
|---|---|---|---|---|---|---|---|---|---|---|---|---|---|---|---|
| | °F | 525 | 535 | 545 | 555 | 565 | 575 | 585 | 595 | 605 | 615 | 625 | 635 | 645 | 655 |
| | °C | 274 | 279 | 285 | 291 | 296 | 302 | 307 | 313 | 318 | 324 | 329 | 335 | 341 | 346 |
| [$H_2$] | 25 | 0.64 | 0.67 | 0.71 | 0.75 | 0.80 | 0.85 | 0.90 | 0.96 | 1.01 | 1.06 | 1.12 | 1.16 | 1.20 | 1.24 |
| | 30 | 0.59 | 0.62 | 0.65 | 0.69 | 0.73 | 0.78 | 0.83 | 0.88 | 0.93 | 0.99 | 1.04 | 1.10 | 1.15 | 1.19 |
| | 35 | 0.56 | 0.58 | 0.61 | 0.65 | 0.68 | 0.72 | 0.77 | 0.82 | 0.87 | 0.92 | 0.98 | 1.04 | 1.09 | 1.14 |
| | 40 | 0.54 | 0.56 | 0.58 | 0.61 | 0.64 | 0.68 | 0.72 | 0.76 | 0.81 | 0.87 | 0.92 | 0.98 | 1.04 | 1.09 |
| | 45 | 0.52 | 0.53 | 0.56 | 0.58 | 0.61 | 0.64 | 0.68 | 0.72 | 0.77 | 0.82 | 0.87 | 0.93 | 0.98 | 1.04 |
| | 50 | 0.50 | 0.52 | 0.54 | 0.56 | 0.58 | 0.61 | 0.65 | 0.69 | 0.73 | 0.78 | 0.83 | 0.88 | 0.94 | 1.00 |

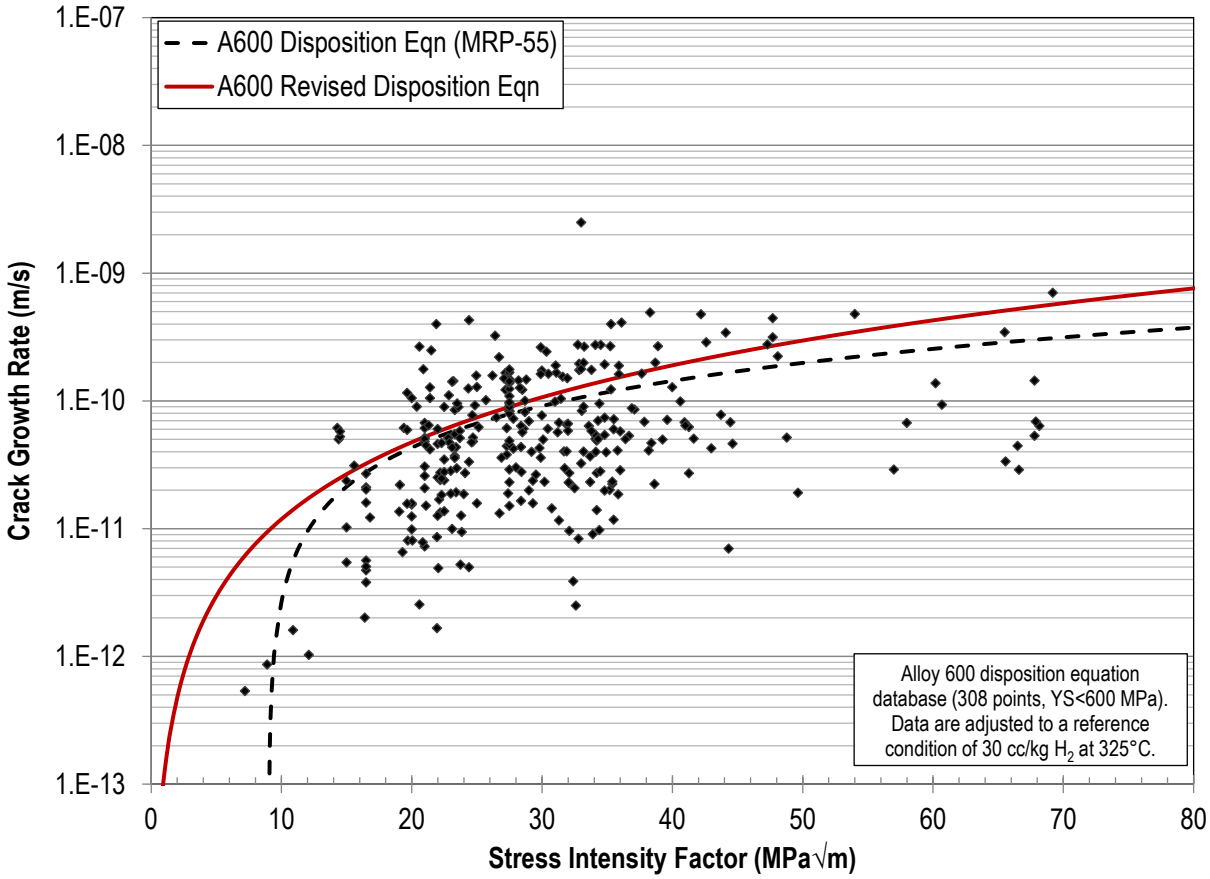


**Figure 6-2**
**Alloy 600 revised disposition equation, shown with data adjusted to a reference condition of 30 cc/kg $H_2$ at 325°C. The MRP-55 disposition equation is also shown for reference.**

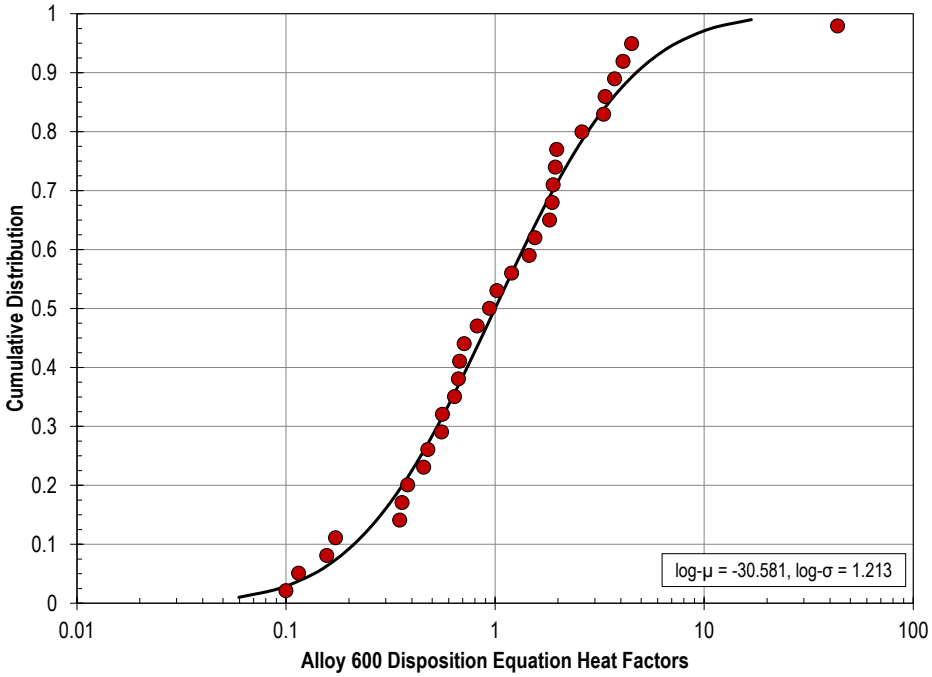


**Figure 6-3**
**Log-normal distribution of 33 heat factors for Alloy 600 data used for the revised disposition equation development. Log-μ is the log-mean of the distribution (i.e., the log of the 50th percentile α); log-σ is the standard deviation of heat factors in log space.**

### *6.1.3 Alloy 600 CGR Model*

The Alloy 600 CGR database includes data that are not directly relevant to plant conditions or to dispositioning a real or postulated flaw. This includes no-growth data as well as highly cold worked materials. From these data, it is possible to develop a CGR model that extends beyond the range of applicability of the disposition equation and includes additional terms that may be unknown in plant applications or may not be relevant to plant scenarios.

The full Alloy 600 model is of the form:

$$\dot{a} = f_K \cdot f_T \cdot f_{H2} \cdot f_{YS} \cdot f_{orient} \cdot f_{HAZ} \cdot f_{heat} \qquad \text{Eq. 6-3}$$

where each of the factors are as listed in Table 6-2. Note that the factors for K, T, and $H_2$ are identical to those in the revised disposition equation. The dissolved hydrogen term is evaluated at various conditions in Table 6-1 for convenience. The model, evaluated at a reference condition of 325°C (617°F), 30 cc/kg $H_2$, 287 MPa (42 ksi; 0% CW), fast orientation (i.e., S-L or S-T) relative to deformation, and 75th percentile of heat factors, is plotted in Figure 6-4, along with the Alloy 600 CGR data adjusted to the same conditions. The MRP-55 75th percentile disposition equation is shown for reference. The cumulative distribution of Alloy 600 heat factors is plotted in Figure 6-5.

The Alloy 600 disposition equation is equivalent to the Alloy 600 CGR model evaluated at approximately 1.1% CW, with all other reference conditions remaining the same.

**Table 6-2**
**Effect forms and parameter values for the Alloy 600 CGR model**

| Factor | Form | Variable | Units | Value |
|---|---|---|---|---|
| $f_K$ | $K^{\beta}$ | β | [—] | 2.0 |
| $f_T$ | $e^{\left(\frac{-Q}{R}\left(\frac{1}{T}-\frac{1}{T_{ref}}\right)\right)}$ | Q, $T_{ref}$ | [kJ/mol], [K] | Q = 120<br>$T_{ref}$ = 598.15 |
| $f_{H2}$ | $\left(\frac{1}{P}+\frac{P-1}{P}exp\left(-0.5\left(\frac{\Delta ECP}{c}\right)^2\right)\right)\cdot\frac{1}{f_{H2ref}}$ | P, c, $f_{H2ref}$ | [—], [mV], [—] | P = 3.0<br>c = 31<br>$f_{H2ref}$ = 0.79 |
| $f_{YS}$ | $\left(\frac{YS}{YS_{ref}}\right)^{\gamma}$ | γ, $YS_{ref}$ | [—], [MPa] | γ = 3.0<br>$YS_{ref}$ = 287 |
| $f_{orient}$ | ≤340 MPa: 1<br>>340 MPa: ε*YS – $\varepsilon_0$ | ε, $\varepsilon_0$ | [$MPa^{-1}$], [—] | ε = 0.013<br>$\varepsilon_0$ = 3.42 |
| $f_{HAZ}$ | $\delta_{HAz}$ | $\delta_{HAZ}$ | [—] | 2.0 |
| $f_{heat}$ | α | α | [(m/s)(MPa√m)$^{-\beta}$(MPa)$^{-\gamma}$]<br>(for CGR in m/s) | $8.48\times10^{-14}$ |

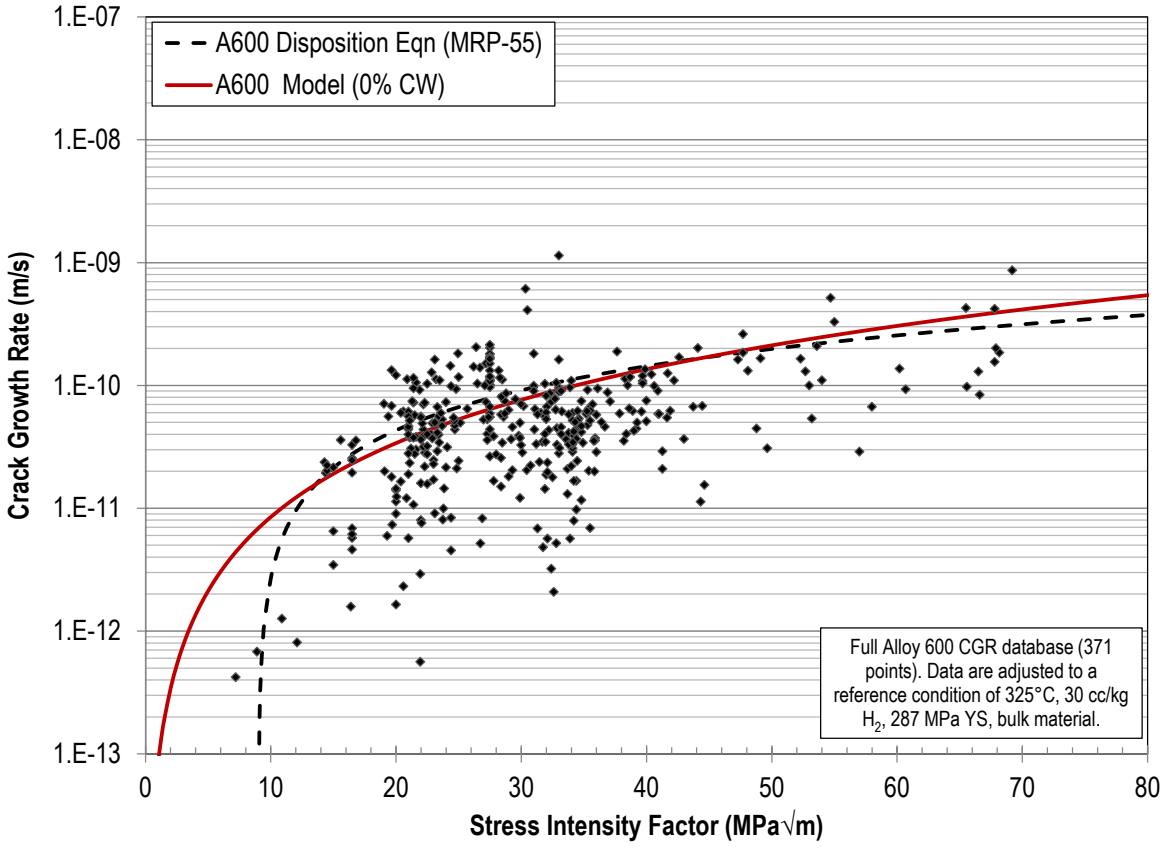


**Figure 6-4**
**Alloy 600 model, shown with data adjusted to a reference condition of 287 MPa (0% CW), 325°C, 30 cc/kg $H_2$, and fast orientation. The MRP-55 equation is shown for reference.**

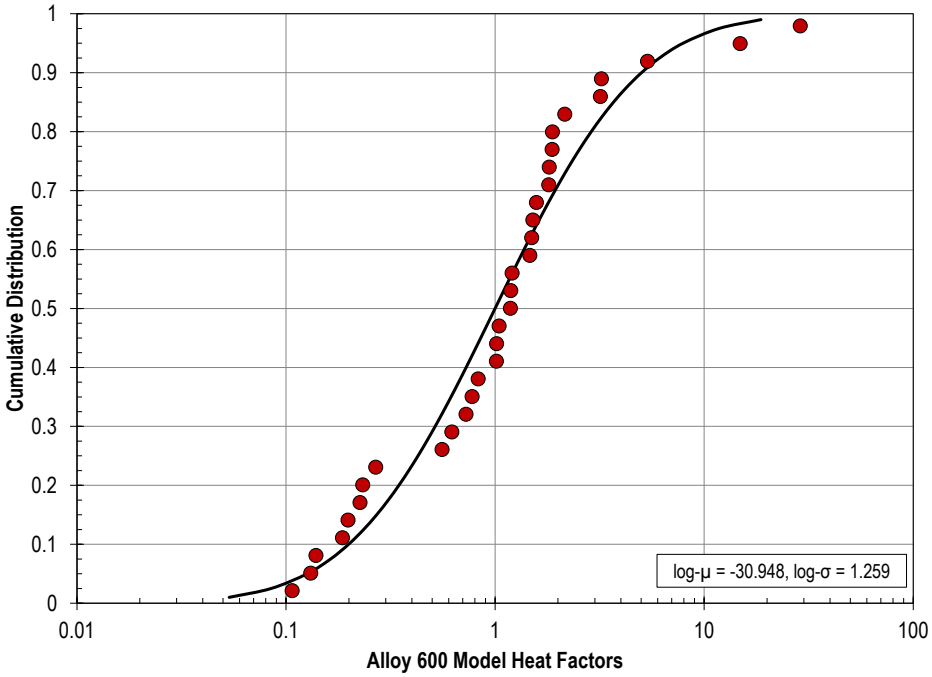


**Figure 6-5**
**Log-normal distribution of 33 heat factors for Alloy 600 data used for the CGR model development. Log-μ is the log-mean of the distribution (i.e., the log of the 50th percentile α); log-σ is the standard deviation of heat factors in log space.**

## 6.2 Alloy 82/182/132 CGR Equations

### *6.2.1 New Disposition Equation for MRP-115 Data*

Using the parameters identified in Section 5.3 (β=2.0, Q=175 kJ/mol, $f_{orient}$=0.5, $f_{alloy}$=0.385), the constant term, α, was refit to the original MRP-115 database. The new fit is defined as follows and is shown in Figure 6-6, along with the original MRP-115 fit for comparison:

$$\dot{a} = \alpha K^{\beta} exp\left(\frac{-Q}{R}\left(\frac{1}{T}-\frac{1}{T_{ref}}\right)\right) f_{orient} f_{alloy} \qquad \textbf{Eq. 6-4}$$

where:

$\alpha$ = 3.01x10$^{-13}$ at 325°C for $\dot{a}$ in m/s, K in MPa√m, and T in K
$\beta$ = 2.0
$Q$ = 175 kJ/mol
$f_{orient}$ = 0.5 for crack growth in the slow orientation
$f_{alloy}$ = 0.385 for crack growth in Alloy 82

The new fit is lower than the original MRP-115 fit for K values up through about 55 MPa√m (50 ksi√in.). The higher K exponent in the new fit causes the new equation to increase more rapidly as K increases. It is concluded that despite having different values for several parameters, both the original MRP-115 fit and the new fit to the MRP-115 data are good descriptors of the PWSCC CGR behavior of as-received Alloy 82/182/132 data.

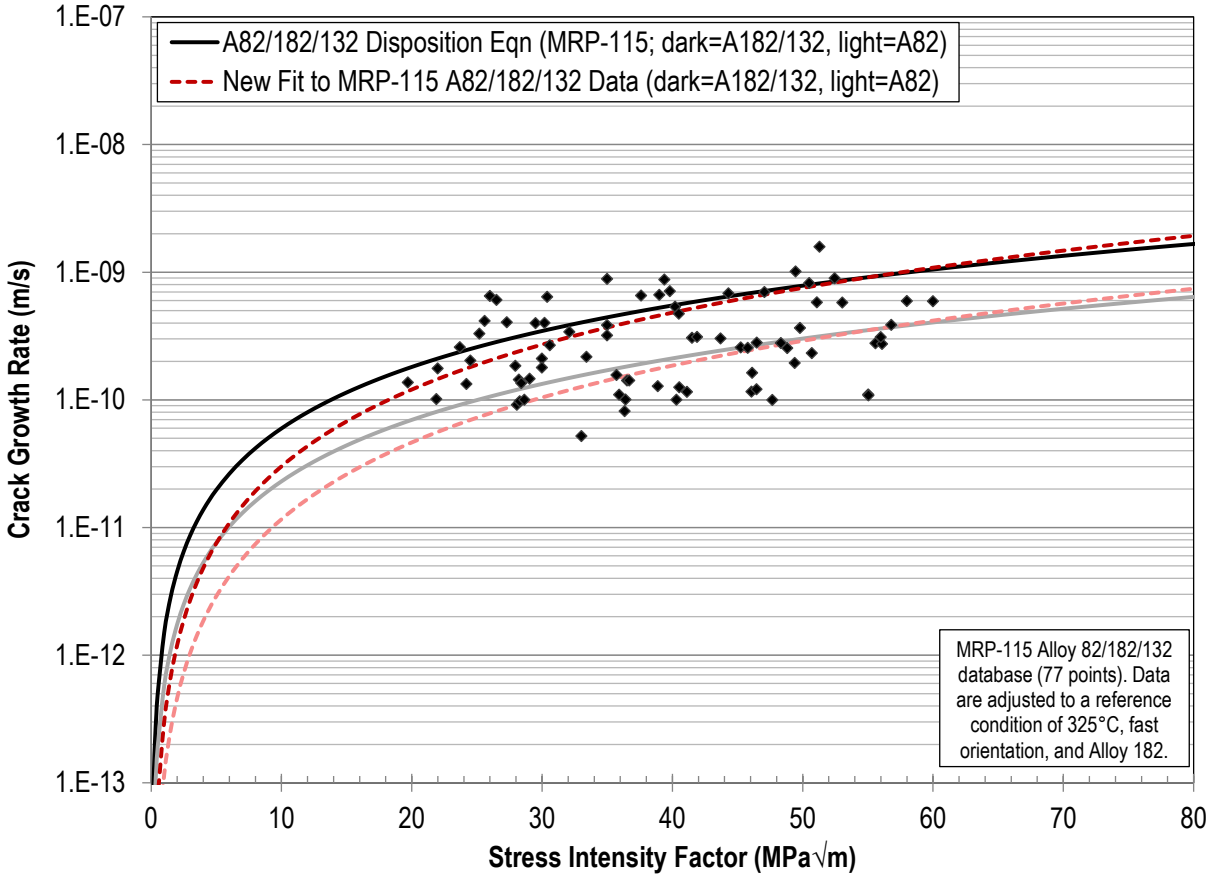


**Figure 6-6**
**New disposition equations for MRP-115 Alloy 82 and Alloy 182/132 data, shown with data adjusted to a reference condition of 325°C, fast orientation, and Alloy 182. The original MRP-115 disposition equations are shown for reference.**

### *6.2.2 Alloy 82/182/132 Revised Disposition Equation*

The Alloy 82/182/132 revised disposition equation was developed from guidance of the full Expert Panel. The parameter values used in this equation are those that were determined in Section 5.3.

The Alloy 82/182/132 revised disposition equation is presented in Eq. 6-5, with the parameters defined at the beginning of this section and the values listed after Eq. 6-5. The constant term, α, was calculated to be equivalent to the 75$^{th}$ percentile of the log-normal weld factor distribution for the Alloy 82/182/132 disposition equation database, shown in Figure 6-8. Table 6-3 evaluates the dissolved hydrogen term, $\frac{f_{H2}}{f_{H2ref}}$, at various temperature and [$H_2$] combinations for convenience. The Alloy 82/182/132 disposition equation data, normalized to a reference condition of 30 cc/kg $H_2$, 325°C (617°F), fast orientation, and Alloy 182 using the dependencies in this equation, are plotted along with the disposition equations in Figure 6-7, as well as the original MRP-115 Alloy 82 and Alloy 182/132 disposition equations.

$$\dot{a} = \alpha K^{\beta} \exp\left(\frac{-Q}{R}\left(\frac{1}{T}-\frac{1}{T_{ref}}\right)\right)\frac{f_{H2}}{f_{H2ref}} f_{orient} f_{alloy} \qquad \textbf{Eq. 6-5}$$

where:

$\alpha$ = $1.92 \times 10^{-13}$ at 325°C and 30 cc/kg $H_2$ for $\dot{a}$ in m/s, K in MPa√m, and T in K

$\beta$ = 2.0

$Q$ = 120 kJ/mol

$P$ = 7.5

$c$ = 14 mV

$f_{orient}$ = 0.5 for crack growth in the slow orientation

$f_{alloy}$ = 0.385 for crack growth in Alloy 82

As discussed at the beginning of this section, no CGR model for Alloy 82/182/132 was developed, as all compiled data are directly relevant to plant applications and all investigated factors are included in the disposition equation.

**Table 6-3**

**Values of the dissolved hydrogen term, $\frac{f_{H2}}{f_{H2ref}}$, at various temperature-[$H_2$] combinations for Alloy 82/182/132. Values at intermediate temperatures and/or hydrogen concentrations can be linearly interpolated.**

| | | Temperature | | | | | | | | | | | | | |
|---|---|---|---|---|---|---|---|---|---|---|---|---|---|---|---|
| | °F | 525 | 535 | 545 | 555 | 565 | 575 | 585 | 595 | 605 | 615 | 625 | 635 | 645 | 655 |
| | °C | 274 | 279 | 285 | 291 | 296 | 302 | 307 | 313 | 318 | 324 | 329 | 335 | 341 | 346 |
| [$H_2$] | 25 | 0.51 | 0.51 | 0.52 | 0.54 | 0.57 | 0.62 | 0.70 | 0.84 | 1.04 | 1.33 | 1.72 | 2.18 | 2.70 | 3.19 |
| | 30 | 0.51 | 0.51 | 0.51 | 0.52 | 0.53 | 0.55 | 0.59 | 0.66 | 0.78 | 0.95 | 1.22 | 1.57 | 2.02 | 2.53 |
| | 35 | 0.51 | 0.51 | 0.51 | 0.51 | 0.52 | 0.53 | 0.55 | 0.58 | 0.65 | 0.75 | 0.92 | 1.17 | 1.51 | 1.95 |
| | 40 | 0.51 | 0.51 | 0.51 | 0.51 | 0.51 | 0.52 | 0.53 | 0.54 | 0.58 | 0.64 | 0.75 | 0.92 | 1.17 | 1.52 |
| | 45 | 0.51 | 0.51 | 0.51 | 0.51 | 0.51 | 0.51 | 0.52 | 0.53 | 0.55 | 0.58 | 0.65 | 0.76 | 0.94 | 1.20 |
| | 50 | 0.51 | 0.51 | 0.51 | 0.51 | 0.51 | 0.51 | 0.51 | 0.52 | 0.53 | 0.55 | 0.59 | 0.67 | 0.79 | 0.99 |

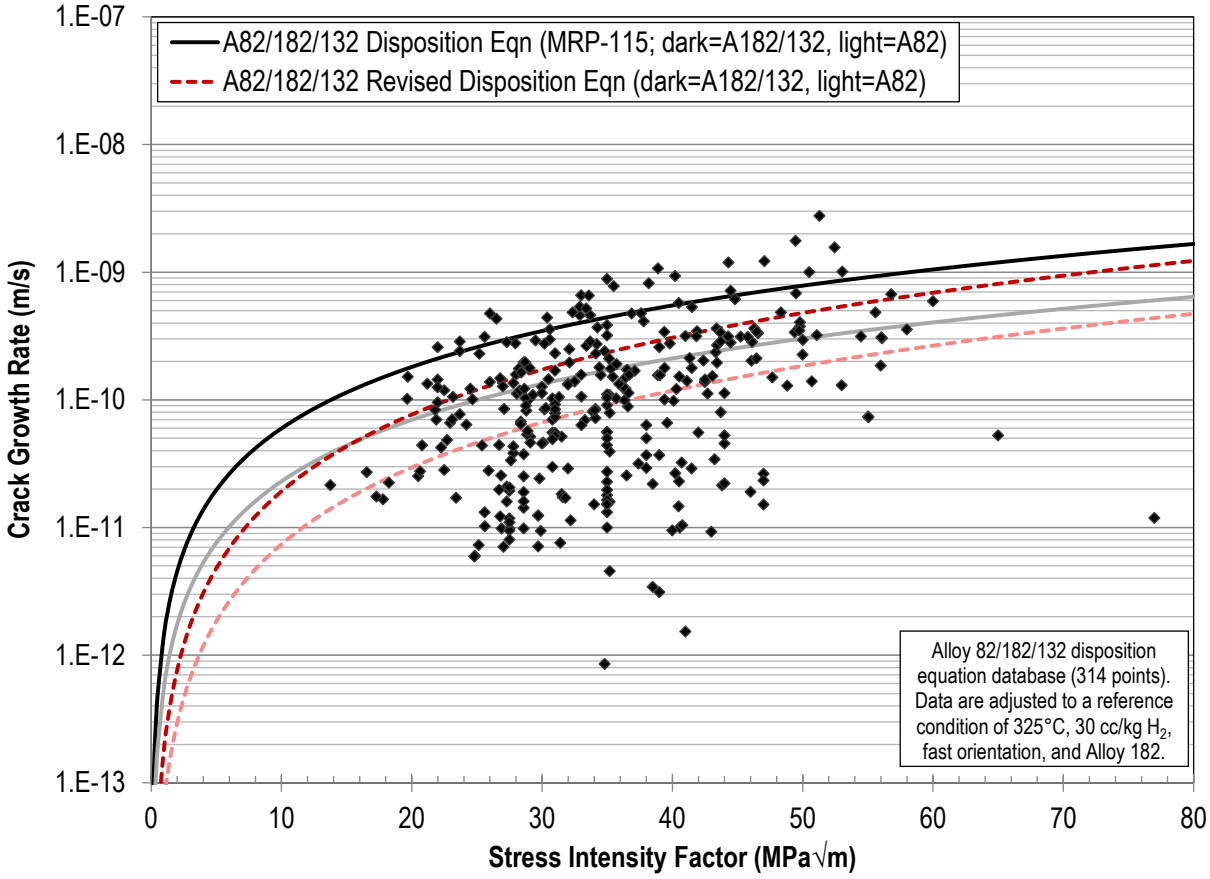


**Figure 6-7**
**Alloy 82 and Alloy 182/132 revised disposition equations, shown with data adjusted to a reference condition of 325°C, 30 cc/kg $H_2$, fast orientation, and Alloy 182. The MRP-115 disposition equations are also shown for reference.**

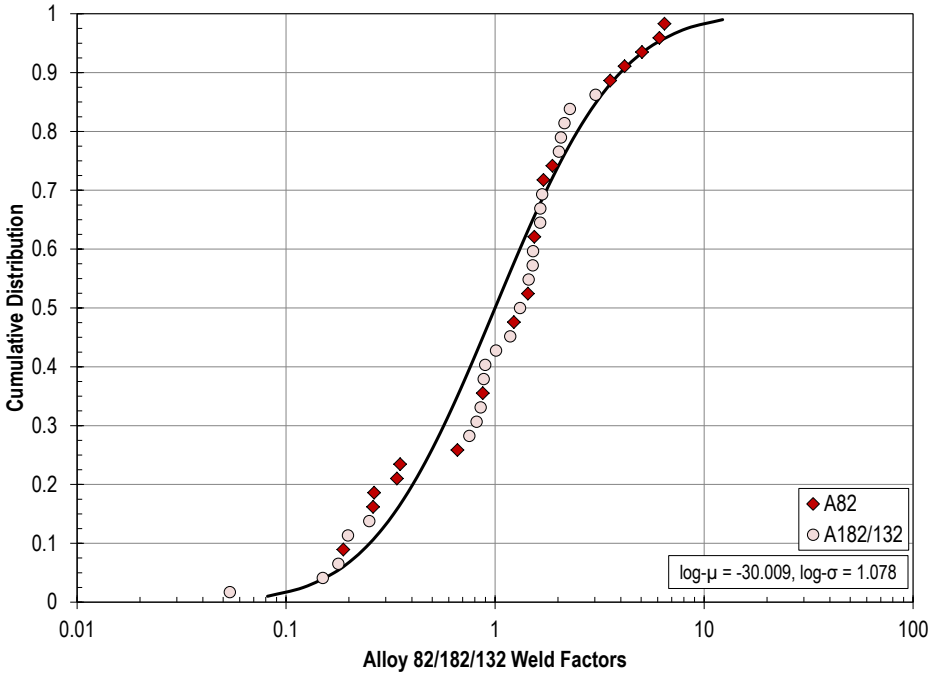


**Figure 6-8**
**Log-normal distribution of the 41 weld factors for Alloy 82/182/132 data used for the revised disposition equation development. Log-μ is the log-mean of the distribution (i.e., the log of the 50$^{th}$ percentile α); log-σ is the standard deviation of heat factors in log space.**

# 7
# CONCLUSIONS

The following are key conclusions regarding the development of CGR disposition equations and models for Alloy 600 and 82/182/132:

- An international Expert Panel was formed to evaluate newly compiled PWSCC CGR data to ensure that only the most reliable test data were used to develop the CGR models, determine applicability conditions for the relevant plant components, and guide the data manipulation and modeling processes to develop CGR disposition equations and models.
- Data were screened using the criteria developed in MRP-115, with the addition that expert evaluation was used to score low crack increment data on the basis of experimental techniques, overall data quality, and testing credibility.
- The relevant levels of added deformation in bulk base metal used for inservice components, including HAZ regions, is up to 12% deformation.
- Three equations were developed for Alloy 600: a new disposition equation for the original MRP-55 database, a revised disposition equation for all compiled data that is directly applicable to plant conditions, and a full model that has a broader range of applicability and includes additional factors. Two equations were developed for Alloy 82/182: a new disposition equation for the original MRP-115 database and a revised disposition equation for all compiled data that is directly applicable to plant conditions (no non-applicable data were compiled that could have extended the range of applicability).
- The Alloy 600 and Alloy 82/182/132 disposition equations include terms accounting for the effects of crack tip stress intensity factor, temperature, hydrogen concentration, and variability associated with different heats/welds. The full Alloy 600 model also contains terms for room temperature yield strength, crack growth orientation, and crack growth in the HAZ. The Alloy 82/182/132 disposition curve also contains terms for crack growth orientation and alloy.
- The new Alloy 600 and 82/182/132 disposition equations are generally similar to those developed in MRP-55 and MRP-115, respectively. The Alloy 600 equation is slightly higher at all K values, while the Alloy 82/182 equation is slightly lower for K values up through about 55 MPa$\sqrt{m}$ (50 ksi$\sqrt{in.}$).

# 8
# REFERENCES


1. *Materials Reliability Program (MRP) Crack Growth Rates for Evaluating Primary Water Stress Corrosion Cracking (PWSCC) of Thick-Wall Alloy 600 Materials (MRP-55) Revision 1*, EPRI, Palo Alto, CA: 2002. 1006695.
2. White, G.A., J. Hickling, and L.K. Mathews, "Crack Growth Rates for Evaluating PWSCC of Thick-Wall Alloy 600 Material," *Proceedings of the 11th International Conference of Environmental Degradation of Materials in Nuclear Power Systems – Water Reactors*, pp. 166 – 179, 2003.
3. *Materials Reliability Program Crack Growth Rates for Evaluating Primary Water Stress Corrosion Cracking (PWSCC) of Alloy 82, 182, and 132 Welds (MRP-115)*, EPRI, Palo Alto, CA: 2004. 1006696.
4. White, G.A., N.S. Nordmann, J. Hickling, and C.D. Harrington, "Development of Crack Growth Rate Disposition Curves for Primary Water Stress Corrosion Cracking (PWSCC) of Alloy 82, 182, and 132 Weldments," *Proceedings of the 12th International Conference on Environmental Degradation of Materials in Nuclear Power Systems–Water Reactors*, TMS, pp. 511 – 531, 2005.
5. B. Alexandreanu, Y. Chen, K. Natesan, and W.J. Shack, "Crack Growth Rate Testing of Alloy 600 Nozzle Sections from the Replacement Pressure Vessel Head at Davis-Besse Reactor," ANL Report ANL-12/21, February 2012.
6. W.C. Moshier and C.M. Brown, "Effect of Cold Work and Processing Orientation on Stress Corrosion Cracking Behavior of Alloy 600," *Corrosion*, Vol. 56, No. 3, pp. 307-320, 2000.
7. E. Richey, D.S. Morton, and W.C. Moshier, "Influence of Specimen Size on the SCC Growth Rate of Ni-Alloys Exposed to High Temperature Water," *Corrosion 2006*, Paper 06513, NACE, 2006.
8. K. Norring, M. Konig, and J. Lagerstrom, "Stress Intensity and Temperature Dependence for Crack Growth Rate in Weld Metal Alloy 182 in Primary PWR Environment," *Proceedings of the 12th International Conference on Environmental Degradation of Materials in Nuclear Power Systems–Water Reactors,* TMS, pp. 533-539, 2005.
9. D.J. Paraventi and W.C. Moshier, "The Effect of Cold Work and Dissolved Hydrogen in the Stress Corrosion Cracking of Alloy 82 and Alloy 182 Weld Metal," *Proceedings of the 12th International Conference on Environmental Degradation of Materials in Nuclear Power Systems–Water Reactors*, TMS, pp. 543-553, 2005.

10. G.A. Young, W.W. Wilkening, D.S. Morton, E. Richey, and N. Lewis, "The Mechanism and Modeling of Intergranular Stress Corrosion Cracking of Nickel-Chromium-Iron Alloys Exposed to High Purity Water," *Proceedings of the 12th International Conference on Environmental Degradation of Materials in Nuclear Power Systems–Water Reactors*, TMS, pp. 913-922, 2005.

11. D.S. Morton, S.A. Attanasio, E. Richey, and G.A. Young, "In Search of the True Temperature and Stress Intensity Factor Dependencies for PWSCC," *Proceedings of the 12th International Conference on Environmental Degradation of Materials in Nuclear Power Systems–Water Reactors,* TMS, pp. 977-986, 2005.

12. K. Norring, P. Efsing, and P.O. Andersson, "Influence of Boron and Lithium on the Crack Growth Rate of Alloy 600 in PWR Primary Environment," *Proceedings of the 13th International Conference on Environmental Degradation of Materials in Nuclear Power Systems–Water Reactors*, Paper 0015, CNS, 2007.

13. D.J. Paraventi and W.C. Moshier, "Assessment of the Interaction of Variables in the Intergranular Stress Corrosion Crack Growth Rate Behavior of Alloys 600, 82, and 182," *Proceedings of the 13th International Conference on Environmental Degradation of Materials in Nuclear Power Systems–Water Reactors*, Paper 0063, CNS, 2007.

14. P.L. Andresen, J. Hickling, K.S. Ahluwalia, and J.A. Wilson, "Effects of PWR Primary Water Chemistry on PWSCC of Ni Alloys," *Proceedings of the 13th International Conference on Environmental Degradation of Materials in Nuclear Power Systems–Water Reactors,* Paper 0123, CNS, 2007.

15. S.M. Bruemmer, J.S. Vetrano, and M.B. Toloczko, "Microstructure and SCC Crack Growth of Nickel-Base Alloy 182 Weld Metal in Simulated PWR Primary Water," *Proceedings of the 13th International Conference on Environmental Degradation of Materials in Nuclear Power Systems – Water Reactors*, Paper 0140, CNS, 2007.

16. T. Couvant, F. Vaillant, and E. Lemaire, "Stress Corrosion Crack Growth Rate in Rolled Alloy 600 Exposed to Primary PWR Environment," *Proceedings of the 14th International Conference on Environmental Degradation of Materials in Nuclear Power Systems–Water Reactors*, ANS, pp. 54-66, 2009.

17. D.J. Paraventi, B.M. Capell, and S.R. Claves, "Effect of Low Temperature Thermal Treatment on SCC Growth Rates In Alloy 82," Presented at the *14th International Conference on Environmental Degradation of Materials in Nuclear Power Systems–Water Reactors,* ANS, 2009.

18. D.J. Paraventi and W.C. Moshier, "Interaction of Microstructure, Composition, and Cold Work on the Stress Corrosion Cracking of Alloy 82 Weld Metal," *Proceedings of the 15th International Conference on Environmental Degradation of Materials in Nuclear Power Systems–Water Reactors*, TMS, pp. 1087-1101, 2011.

19. C. Guerre, C. Duhamel, M. Sennour, J. Crépin, M. Le Calvar, "SCC Crack Growth Rate of Alloy 82 in PWR Primary Water Conditions – Effect of a Thermal Treatment," *Proceedings of the 15th International Conference on Environmental Degradation of Materials in Nuclear Power Systems–Water Reactors*, TMS, pp. 1127-1139, 2011.

20. A. Jenssen, M. König, D. Déforge, S. Miloudi, E. Le Maire, F. Vaillant, "SCC Testing of Alloy 600 Divider Plates from Decommissioned Steam Generators," *Proceedings of the 16th International Conference on Environmental Degradation of Materials in Nuclear Power Systems–Water Reactors*, Paper 3257, NACE, 2013.

21. A. Jenssen and P. Efsing, "Crack Growth Rate Measurements in Alloy 182 in PWR Primary Water at Low Stress Intensity," *Proceedings of the 17th International Conference on Environmental Degradation of Materials in Nuclear Power Systems–Water Reactors,* Paper 116, CNS, 2015.

22. *Materials Reliability Program: Effects of B/Li/pH on PWSCC Growth Rates in Ni-Base Alloys (MRP-217).* EPRI, Palo Alto, CA: 2007. 1015008.

23. *Materials Reliability Program: Crack Growth Rate Studies in Weld Heat-Affected Zones of Alloy 600 and 690 Materials (MRP-283).* EPRI, Palo Alto, CA: 2010. 1021019.

24. *Materials Reliability Program: Low Stress Intensity Factor Crack Growth Rate Testing for Alloys 82, 182, and 600: Copyright Version (MRP-305)*. EPRI, Palo Alto, CA: 2011. 1022665.

25. *Materials Reliability Program: Determination of Crack Growth Rates for Alloy 82 at Low K Values Under PWR Primary Water Environment: 2013 Final Report (MRP-374)*. EPRI, Palo Alto, CA: 2013. 3002002181.

26. *Crack Growth Rates of Nickel Alloy Welds in a PWR Environment*, NUREG/CR-6907, 2006.

27. *Crack Growth Rates in a PWR Environment of Nickel Alloys from the Davis-Besse and V.C. Summer Power Plants*, NUREG/CR-6921, 2006.

28. *Crack Growth Rates and Metallographic Examinations of Alloy 600 and Alloy 82/182 from Field Components and Laboratory Materials Tested in PWR Environments,* NUREG/CR-6964, 2008.

29. S.M. Bruemmer, M.J. Olszta, D.K. Schreiber, N.R. Overman, and M.B. Toloczko, "Characterizations and Stress Corrosion Cracking Evaluations of Alloy 600 CRDM Nozzle Heats from the Davis Besse Nuclear Power Plant," Office of Nuclear Regulatory Research Project JCN-N6925, NRC Accession No. ML14316A029.

30. R. Magdowski, F. Vaillant, C. Amzallag, and M.O. Speidel, "Stress Corrosion Crack Growth Rates of Alloy 600 in Simulated PWR Coolant," *Proceedings of the 8th International Conference on the Environmental Degradation of Materials in Nuclear Power Systems–Water Reactors*, August 1997.

31. A. Skouras, A. Paradowska, M.J. Peel, P.E.J. Flewitt, and M.J. Pavier, "Residual Stress Measurements in a Ferritic Steel/In625 Superalloy Dissimilar Metal Weldment Using Neutron Diffraction and Deep-Hole Drilling," *International Journal of Pressure Vessels and Piping,* Vol. 101, pp. 143-153, January 2013.

32. P. Scott, M.C. Meunier, F. Steltzlen, O. Calonne, M. Foucault, P. Combrade, and C. Amzallag, "Comparison of Laboratory and Field Experience of PWSCC in Alloy 182 Weld Metal," *Proceedings of the 13th International Conference on Environmental Degradation of Materials Degradation of Materials in Nuclear Power Systems–Water Reactors*, CNS, 2007.

33. T. Yonezawa, "Study on the Possibility of PWSCC Initiation for TT Alloy 690," *Alloy 690/52/152 PWSCC Research Collaboration Meeting*, Tampa, FL, 2015.

34. T. Yonezawa, M. Watanabe, and A. Hashimoto, "The Mechanistic Study on the Stress Corrosion Crack Propagation for Heavily Cold Worked TT Alloy 690 in Simulated PWR Primary Water," *Alloy 690/52/152 PWSCC Research Collaboration Meeting*, Tampa, FL, 2016.

35. *Materials Reliability Program: South Texas Project Unit 1 Bottom Mounted Instrumentation Nozzles (#1 and #46) Analysis Reports and Related Documentation (MRP-102)*, EPRI, Palo Alto, CA, and South Texas Project Nuclear Operating Company: 2003. 1009309.

36. *Examination of the Reactor Vessel (RV) Head Degradation at Davis-Besse,* Framatome ANP, Inc., Document 31-5029337-02, BWXT Technologies, Inc., November 2003, NRC Accession No. ML033350327.

37. *Pressurizer Safe End Crack Engineering Analysis and Root Cause Evaluation*, Consumers Power Company, October 1993.

38. M. Morra, M. Othon, I. Dempster, S. McCracken, and A. Ahluwalia, "Simulated Alloy 690 HAZ Material," *Alloy 690/52/152 PWSCC Research Collaboration Meeting*, EPRI, Tampa, FL, 2013.

39. Email from M. Morra (GE-GRC) to R. Pathania (EPRI), "RE: PWSCC Expert Panel: Applications Group," June 30, 2016.

40. R. Shen, "Spatial Correlation Between Local Misorientations and Nanoindentation Hardness in Nickel-Base Alloy 690," *Materials Science and Engineering* A, Vol. 674, pp. 171-177, 2016.

41. T. Yonezawa, T. Maeguchi, T. Goto, and H. Juin "Quantitative Residual Strain Analyses on Strain Hardened Nickel Based Alloy," *Proceedings of the 15th International Conference on Environmental Degradation of Materials in Nuclear Power Systems–Water Reactors*, ANS, pp. 1759-1771, 2011.

42. T. Yonezawa, "Residual Strain and Dilution Zone of CRDM Tube J-Weld Mock Up," *Alloy 690/52/152 PWSCC Research Collaboration Meeting*, EPRI, Tampa, FL, December 2015.

43. *Materials Reliability Program: Technical Bases for the Chemical Mitigation of Primary Water Stress Corrosion Cracking in Pressurized Water Reactors (MRP-263 NP).* EPRI, Palo Alto, CA: 2012. 1025669.

44. T. Shoji, Z. Lu, and S. Yamazaki, "The Effect of Strain-Hardening on PWSCC of Nickel-Base Alloys 600 and 690," *Proceedings of the 14th International Conference on Environmental Degradation of Materials in Nuclear Power Systems–Water Reactors,* ANS, pp. 220-238, 2009.

45. A. Molander, K. Norring, P.O. Andersson, and P. Efsing, "Environmental Effects on PWSCC Initiation and Propagation in Alloy 600," *Proceedings of the 15th International Conference on Environmental Degradation of Materials in Nuclear Power Systems–Water Reactors*, TMS, pp. 1699-1711, 2011.

46. S. Le Hong, J.M. Boursier, C. Amzallag, and J. Daret, "Measurements of Stress Corrosion Cracking Growth Rates in Weld Alloy 182 in Primary Water of PWR," *Proceedings of the 10th International Conference on Environmental Degradation of Materials in Nuclear Power Systems–Water Reactors*, NACE, 2001.

47. T. Cassagne, D. Caron, J. Daret, and Y. Lefevre, "Stress Corrosion Crack Growth Rate Measurements in Alloys 600 and 182 in Primary Water Loops Under Constant Load," *Proceedings of the 9th International Conference on Environmental Degradation of Materials in Nuclear Power Systems–Water Reactors*, TMS, pp. 217-224, 1999.

# A
# SCREENED ALLOY 600 AND ALLOY 82/182/132 PWSCC CGR DATABASES

The tables presented in this appendix are:

Table A-1: Scored-in Alloy 600 PWSCC CGR data

Table A-2: Scored-out Alloy 600 PWSCC CGR data

Table A-3: Chemical compositions of all Alloy 600 heats tested in the CGR database

Table A-4: Scored-in Alloy 82/182/132 PWSCC CGR data

Table A-5: Scored-out Alloy 82/182/132 PWSCC CGR data

Table A-6: Chemical compositions of all Alloy 82/182/132 welds tested in the CGR database

## Table A-1
## Alloy 600 CGR database–Scored-in data

| Laboratory | Overall Test ID | Heat | As Received Condition | Thickness Reduction (%) | Processing Method | Product Form | Orientation | Yield Strength (MPa) | Hardness (HV) | Test Segment ID | Test Segment Duration (h) | Load Type | K (MPa√m) | Temperature (°C) | Dissolved $H_2$ (cc/kg) | Hold Time (s) | Load Ratio | % Engaged | Post-Test Correction Factor | Measured Δa (mm) | Reported SCC CGR (mm/s) |
|---|---|---|---|---|---|---|---|---|---|---|---|---|---|---|---|---|---|---|---|---|---|
| ANL | DB-3 | M7929 | MA | 0 | None | CRDM | C-R | 296 | | 16 | 73 | CL | 19.1 | 320 | 23 | | | 100 | 1.11 | 0.005 | 1.90E-08 |
| ANL | DB-3 | M7929 | MA | 0 | None | CRDM | C-R | 296 | | 20 | 182 | PPU | 19.7 | 320 | 23 | 3600 | 0.5 | 100 | 1.11 | 0.009 | 6.96E-09 |
| ANL | DB-3 | M7929 | MA | 0 | None | CRDM | C-R | 296 | | 21 | 314 | CL | 20.6 | 320 | 23 | | | 100 | 1.11 | 0.003 | 2.20E-09 |
| ANL | DB-3 | M7929 | MA | 0 | None | CRDM | C-R | 296 | | 28 | 163 | CL | 19.3 | 320 | 23 | | | 100 | 1.11 | 0.004 | 5.65E-09 |
| ANL | DB-3 | M7929 | MA | 0 | None | CRDM | C-R | 296 | | 37 | 334 | CL | 19.4 | 320 | 23 | | | 100 | 1.11 | 0.076 | 5.30E-08 |
| ANL | DB-3 | M7929 | MA | 0 | None | CRDM | C-R | 296 | | 8-10 | 383 | CL | 15 | 320 | 23 | | | 100 | 1.11 | 0.035 | 2.04E-08 |
| ANL | DB-4 | M7929 | MA | 0 | None | CRDM | C-L | 296 | | 6 | 207 | PPU | 24.7 | 320 | 23 | 7200 | 0.5 | 100 | 1.31 | 0.070 | 4.15E-08 |
| ANL | DB-4 | M7929 | MA | 0 | None | CRDM | C-L | 296 | | 9 | 259 | CL | 24.4 | 320 | 23 | | | 100 | 1.31 | 0.010 | 4.30E-09 |
| ANL | DB-4 | M7929 | MA | 0 | None | CRDM | C-L | 296 | | 10 | 238 | PPU | 24.7 | 320 | 23 | 7200 | 0.5 | 100 | 1.31 | 0.037 | 4.46E-08 |
| ANL | DB-4 | M7929 | MA | 0 | None | CRDM | C-L | 296 | | 12 | 158 | PPU | 28.7 | 320 | 23 | 7200 | 0.5 | 100 | 1.31 | 0.017 | 7.06E-08 |
| ANL | DB-4 | M7929 | MA | 0 | None | CRDM | C-L | 296 | | 14 | 280 | PPU | 29 | 320 | 23 | 7200 | 0.5 | 100 | 1.31 | 0.048 | 5.99E-08 |
| ANL | DB-4 | M7929 | MA | 0 | None | CRDM | C-L | 296 | | 15 | 241 | CL | 29.2 | 320 | 23 | | | 100 | 1.31 | 0.019 | 3.45E-08 |
| ANL | DB-4 | M7929 | MA | 0 | None | CRDM | C-L | 296 | | 17 | 733 | CL | 29.8 | 320 | 23 | | | 100 | 1.31 | 0.047 | 3.69E-08 |
| ANL | DB-5 | M7929 | MA | 0 | None | CRDM | C-L | 296 | | 5 | 72 | CL | 23.1 | 325 | 23 | | | 100 | 1.22 | 0.003 | 1.10E-08 |
| ANL | DB-5 | M7929 | MA | 0 | None | CRDM | C-L | 296 | | 7 | 121 | PPU | 23.3 | 325 | 23 | 7200 | 0.5 | 100 | 1.22 | 0.033 | 6.08E-08 |
| ANL | DB-5 | M7929 | MA | 0 | None | CRDM | C-L | 296 | | 8 | 265 | CL | 23.4 | 325 | 23 | | | 100 | 1.22 | 0.004 | 4.80E-08 |
| ANL | DB-5 | M7929 | MA | 0 | None | CRDM | C-L | 296 | | 10 | 120 | PPU | 23.7 | 325 | 23 | 7200 | 0.5 | 100 | 1.22 | 0.033 | 6.42E-08 |
| ANL | DB-5 | M7929 | MA | 0 | None | CRDM | C-L | 296 | | 11 | 130 | PPU | 23.7 | 325 | 23 | 7200 | 0.5 | 100 | 1.22 | 0.024 | 5.66E-08 |
| ANL | DB-5 | M7929 | MA | 0 | None | CRDM | C-L | 296 | | 14 | 30 | PPU | 27.2 | 325 | 23 | 7200 | 0.5 | 100 | 1.22 | 0.025 | 1.83E-07 |
| ANL | DB-5 | M7929 | MA | 0 | None | CRDM | C-L | 296 | | 15 | 329 | CL | 27.5 | 325 | 23 | | | 100 | 1.22 | 0.040 | 3.20E-08 |
| ANL | DB-5 | M7929 | MA | 0 | None | CRDM | C-L | 296 | | 17 | 124 | PPU | 28.2 | 325 | 23 | 7200 | 0.5 | 100 | 1.22 | 0.075 | 1.60E-07 |
| ANL | DB-5 | M7929 | MA | 0 | None | CRDM | C-L | 296 | | 18 | 171 | PPU | 28.5 | 325 | 23 | 7200 | 0.5 | 100 | 1.22 | 0.087 | 1.35E-07 |
| ANL | DB-5 | M7929 | MA | 0 | None | CRDM | C-L | 296 | | 19 | 74 | CL | 28.6 | 325 | 23 | | | 100 | 1.22 | 0.009 | 6.70E-08 |
| ANL | DB-5 | M7929 | MA | 0 | None | CRDM | C-L | 296 | | 20 | 526 | CL | 29 | 325 | 23 | | | 100 | 1.22 | 0.062 | 2.20E-08 |
| ANL | DB-5 | M7929 | MA | 0 | None | CRDM | C-L | 296 | | 22 | 185 | PPU | 27.3 | 325 | 23 | 7200 | 0.5 | 100 | 1.22 | 0.036 | 4.89E-08 |
| ANL | DB-5 | M7929 | MA | 0 | None | CRDM | C-L | 296 | | 23 | 52 | PPU | 27.8 | 350 | 45 | 7200 | 0.5 | 100 | 1.22 | 0.021 | 1.20E-07 |
| ANL | DB-5 | M7929 | MA | 0 | None | CRDM | C-L | 296 | | 25 | 98 | PPU | 28 | 350 | 45 | 7200 | 0.5 | 100 | 1.22 | 0.063 | 8.57E-08 |
| ANL | DB-5 | M7929 | MA | 0 | None | CRDM | C-L | 296 | | 27 | 113 | PPU | 28.4 | 350 | 45 | 7200 | 0.5 | 100 | 1.22 | 0.014 | 4.68E-08 |
| ANL | DB-5 | M7929 | MA | 0 | None | CRDM | C-L | 296 | | 28 | 177 | PPU | 28.3 | 325 | 23 | 7200 | 0.5 | 100 | 1.22 | 0.057 | 1.40E-07 |
| ANL | DB-5 | M7929 | MA | 0 | None | CRDM | C-L | 296 | | 29 | 166 | CL | 28.4 | 325 | 23 | | | 100 | 1.22 | 0.040 | 7.02E-08 |
| ANL | N3CC-2 | M3935 | MA | 0 | None | CRDM | C-L | 334 | | 8 | 285 | PPU | 25.7 | 316 | 25 | 3600 | 0.5 | 100 | 1.74 | 0.039 | 6.92E-08 |
| ANL | N3CC-3 | M3935 | MA | 0 | None | CRDM | C-L | 334 | | 5b | 109 | CL | 20.9 | 316 | 23 | | | 100 | 1.57 | 0.094 | 1.25E-07 |
| ANL | N3CC-3 | M3935 | MA | 0 | None | CRDM | C-L | 334 | | 6a | 47 | CL | 26.4 | 316 | 23 | | | 100 | 1.57 | 0.085 | 2.28E-07 |
| ANL | N3CC-3 | M3935 | MA | 0 | None | CRDM | C-L | 334 | | 6b | 143 | CL | 26.7 | 316 | 23 | | | 100 | 1.57 | 0.106 | 1.55E-07 |
| Bettis | CB20-65 | NX5853G11 | HTMA | 0 | None | plate | L-T | 201 | | A | | bolt | 35.2 | 360 | 4.1 | | | | | | 5.01E-08 |
| Bettis | CB20-66 | NX5853G11 | HTMA | 0 | None | plate | L-T | 201 | | A | | bolt | 35.4 | 360 | 4.1 | | | | | | 5.56E-08 |
| Bettis | CB20-73 | NX5853G11 | HTMA | 0 | None | plate | L-T | 201 | | A | | bolt | 29.3 | 360 | 4.1 | | | | | | 3.93E-08 |
| Bettis | CB20-76 | NX5853G11 | HTMA | 0 | None | plate | L-T | 201 | | A | | bolt | 30.2 | 360 | 4.1 | | | | | | 5.79E-08 |
| Bettis | CPI-30 | LM-600 | MA | 0 | None | | | 287.3 | | A | | bolt | 60.7 | 338 | 40 | | | | | | 1.57E-07 |
| Bettis | CR28-19 | NX5853G11 | HTMA | 31.9 | CR | plate | L-T | 827 | | A | | PPU | 35.7 | 316 | 4.1 | 6000 | 0.7 | | | | 1.81E-07 |
| Bettis | CR28-20 | NX5853G11 | HTMA | 31.9 | CR | plate | L-T | 827 | | A | | PPU | 34.6 | 288 | 4.1 | 6000 | 0.7 | | | | 4.53E-08 |
| Bettis | CR28-5 | NX5853G11 | HTMA | 31.9 | CR | plate | L-T | 827 | | A | | bolt | 33.8 | 316 | 4.1 | | | | | | 1.06E-07 |
| Bettis | CR28-6 | NX5853G11 | HTMA | 31.9 | CR | plate | L-T | 827 | | A | | bolt | 34.1 | 316 | 4.1 | | | | | | 1.54E-07 |
| Bettis | CR28-8 | NX5853G11 | HTMA | 31.9 | CR | plate | L-T | 827 | | A | | bolt | 34.5 | 338 | 4.1 | | | | | | 3.03E-07 |

**Table A-1 (continued)**
**Alloy 600 CGR database–Scored-in data**

| Laboratory | Overall Test ID | Heat | As Received Condition | Thickness Reduction (%) | Processing Method | Product Form | Orientation | Yield Strength (MPa) | Hardness (HV) | Test Segment ID | Test Segment Duration (h) | Load Type | K (MPa√m) | Temperature (°C) | Dissolved $H_2$ (cc/kg) | Hold Time (s) | Load Ratio | % Engaged | Post-Test Correction Factor | Measured Δa (mm) | Reported SCC CGR (mm/s) |
|---|---|---|---|---|---|---|---|---|---|---|---|---|---|---|---|---|---|---|---|---|---|
| Bettis | CR28-9 | NX5853G11 | HTMA | 31.9 | CR | plate | L-T | 827 | | A | | bolt | 33.1 | 358 | 4.1 | | | | | | 6.98E-07 |
| Bettis | CV5-65 | LM-600 | MA | 0 | TT | | | 267.4 | | A | | bolt | 69.2 | 338 | 40 | | | | | | 1.18E-06 |
| Bettis | DG8-04 | LM-600 | MA | 0 | TT | | | 267.4 | | A | | bolt | 65.5 | 338 | 60 | | | | | | 4.80E-07 |
| Bettis | DG9-02 | LM-600 | MA | 0 | None | | | 287.3 | | A | | bolt | 60.2 | 338 | 60 | | | | | | 1.91E-07 |
| Bettis | ER6-02 | LM-600 | MA | 0 | None | | | 287.3 | | A | | bolt | 58 | 338 | 65 | | | | | | 9.00E-08 |
| Bettis | GK9-02 | LM-600 | MA | 0 | None | | | 287.3 | | A | | bolt | 57 | 338 | 64 | | | | | | 3.91E-08 |
| Bettis | LT1-11 | NX5853G11 | HTMA | 31.9 | CR | plate | L-T | 827 | | A | | bolt | 21.6 | 316 | 4.1 | | | | | | 9.82E-08 |
| Bettis | LT1-12 | NX5853G11 | HTMA | 31.9 | CR | plate | L-T | 827 | | A | | bolt | 21.1 | 316 | 4.1 | | | | | | 9.69E-08 |
| Bettis | LT1-13 | NX5853G11 | HTMA | 31.9 | CR | plate | L-T | 827 | | A | | bolt | 32.3 | 316 | 4.1 | | | | | | 2.22E-07 |
| Bettis | LT1-14 | NX5853G11 | HTMA | 31.9 | CR | plate | L-T | 827 | | A | | bolt | 39.7 | 316 | 4.1 | | | | | | 2.80E-07 |
| Bettis | LT1-15 | NX5853G11 | HTMA | 31.9 | CR | plate | L-T | 827 | | A | | bolt | 39.7 | 316 | 4.1 | | | | | | 2.68E-07 |
| Bettis | LT1-16 | NX5853G11 | HTMA | 31.9 | CR | plate | L-T | 827 | | A | | bolt | 52.3 | 316 | 4.1 | | | | | | 4.25E-07 |
| Bettis | LT1-17 | NX5853G11 | HTMA | 31.9 | CR | plate | L-T | 827 | | A | | bolt | 21.2 | 338 | 4.1 | | | | | | 1.87E-07 |
| Bettis | LT1-18 | NX5853G11 | HTMA | 31.9 | CR | plate | L-T | 827 | | A | | bolt | 32 | 338 | 4.1 | | | | | | 4.03E-07 |
| Bettis | LT1-19 | NX5853G11 | HTMA | 31.9 | CR | plate | L-T | 827 | | A | | bolt | 39.7 | 338 | 4.1 | | | | | | 5.87E-07 |
| Bettis | S16-10 | NX5853G11 | HTMA | 10.7 | TS | plate | L-T | 513 | | A | | bolt | 34.1 | 338 | 4.1 | | | | | | 7.59E-08 |
| Bettis | S16-11 | NX5853G11 | HTMA | 10.7 | TS | plate | L-T | 513 | | A | 6337 | bolt | 34.1 | 338 | 4.1 | | | | | | 8.13E-08 |
| Bettis | S16-12 | NX5853G11 | HTMA | 10.7 | TS | plate | L-T | 513 | | A | | bolt | 33.7 | 338 | 4.1 | | | | | | 5.53E-08 |
| Bettis | S16-13 | NX5853G11 | HTMA | 10.7 | TS | plate | L-T | 513 | | A | | bolt | 33.6 | 358 | 4.1 | | | | | | 1.52E-07 |
| Bettis | S16-14 | NX5853G11 | HTMA | 10.7 | TS | plate | L-T | 513 | | A | | bolt | 30.1 | 358 | 4.1 | | | | | | 1.19E-07 |
| Bettis | S16-47 | NX5853G11 | HTMA | 11.4 | TS | plate | L-T | 517 | | A | | PPU | 34.8 | 339 | 4.1 | 6000 | 0.7 | | | | 1.14E-07 |
| Bettis | S16-50 | NX5853G11 | HTMA | 11.4 | TS | plate | L-T | 517 | | A | | PPU | 34.2 | 288 | 4.1 | 6000 | 0.7 | | | | 3.62E-09 |
| Bettis | S16-52 | NX5853G11 | HTMA | 11.4 | TS | plate | L-T | 517 | | A | | PPU | 33.7 | 316 | 4.1 | 6000 | 0.7 | | | | 1.83E-08 |
| Bettis | S22-16 | NX5853G11 | HTMA | 17 | TS | plate | L-T | 630 | | A | | bolt | 34.2 | 338 | 4.1 | | | | | | 1.30E-07 |
| Bettis | S22-17 | NX5853G11 | HTMA | 17 | TS | plate | L-T | 630 | | A | | bolt | 32.4 | 358 | 4.1 | | | | | | 3.88E-07 |
| Bettis | S22-18 | NX5853G11 | HTMA | 17 | TS | plate | L-T | 630 | | A | 1254 | bolt | 33 | 358 | 4.1 | | | | | | 5.06E-07 |
| Bettis | S22-25 | NX5853G11 | HTMA | 17.3 | TS | plate | L-T | 633 | | A | | PPU | 33 | 339 | 4.1 | 6000 | 0.7 | | | | 3.06E-07 |
| Bettis | S22-27 | NX5853G11 | HTMA | 17.3 | TS | plate | L-T | 633 | | A | | PPU | 34 | 288 | 4.1 | 6000 | 0.7 | | | | 1.27E-08 |
| Bettis | S22-29 | NX5853G11 | HTMA | 17.3 | TS | plate | L-T | 633 | | A | | PPU | 34.5 | 316 | 4.1 | 6000 | 0.7 | | | | 7.99E-08 |
| Bettis | S34-22 | NX5853G11 | HTMA | 25.7 | TS | plate | L-T | 772 | | A | | PPU | 34.4 | 288 | 4.1 | 6000 | 0.7 | | | | 1.27E-08 |
| Bettis | S5-10 | NX5853G11 | HTMA | 3.5 | TS | plate | L-T | 345 | | A | | bolt | 34.1 | 360 | 4.1 | | | | | | 1.35E-07 |
| Bettis | S5-11 | NX5853G11 | HTMA | 3.5 | TS | plate | L-T | 345 | | A | | bolt | 34.3 | 358 | 4.1 | | | | | | 1.67E-07 |
| Bettis | S5-12 | NX5853G11 | HTMA | 3.5 | TS | plate | L-T | 345 | | A | | bolt | 34.2 | 358 | 4.1 | | | | | | 6.50E-08 |
| Bettis | ST1-10 | NX5853G11 | HTMA | 31.9 | CR | plate | S-T | 827 | | A | | CK | 20.4 | 288 | 4.1 | | | 100 | | | 1.02E-07 |
| Bettis | ST1-11 | NX5853G11 | HTMA | 31.9 | CR | plate | S-T | 827 | | A | | CK | 21.4 | 288 | 4.1 | | | 100 | | | 6.61E-08 |
| Bettis | ST1-12 | NX5853G11 | HTMA | 31.9 | CR | plate | S-T | 827 | | A | | CK | 32 | 288 | 4.1 | | | 100 | | | 1.16E-07 |
| Bettis | ST1-13 | NX5853G11 | HTMA | 31.9 | CR | plate | S-T | 827 | | A | | CK | 32.2 | 288 | 4.1 | | | 100 | | | 2.68E-07 |
| Bettis | ST1-14 | NX5853G11 | HTMA | 31.9 | CR | plate | S-T | 827 | | A | | CK | 31.9 | 288 | 4.1 | | | 100 | | | 8.90E-08 |
| Bettis | ST1-15 | NX5853G11 | HTMA | 31.9 | CR | plate | S-T | 827 | | A | | CK | 39.2 | 288 | 4.1 | | | 100 | | | 2.75E-07 |
| Bettis | ST1-16 | NX5853G11 | HTMA | 31.9 | CR | plate | S-T | 827 | | A | | CK | 39 | 288 | 4.1 | | | 100 | | | 2.64E-07 |
| Bettis | ST1-17 | NX5853G11 | HTMA | 31.9 | CR | plate | S-T | 827 | | A | | CK | 41.9 | 288 | 4.1 | | | 100 | | | 3.85E-07 |
| Bettis | ST1-18 | NX5853G11 | HTMA | 31.9 | CR | plate | S-T | 827 | | A | | CK | 52.7 | 288 | 4.1 | | | 100 | | | 8.06E-07 |
| Bettis | ST1-19 | NX5853G11 | HTMA | 31.9 | CR | plate | S-T | 827 | | A | | CK | 53.2 | 288 | 4.1 | | | 100 | | | 3.33E-07 |
| Bettis | ST1-20 | NX5853G11 | HTMA | 31.9 | CR | plate | S-T | 827 | | A | | CK | 53 | 288 | 4.1 | | | 100 | | | 6.18E-07 |

**Table A-1 (continued)**
**Alloy 600 CGR database–Scored-in data**

| Laboratory | Overall Test ID | Heat | As Received Condition | Thickness Reduction (%) | Processing Method | Product Form | Orientation | Yield Strength (MPa) | Hardness (HV) | Test Segment ID | Test Segment Duration (h) | Load Type | K (MPa√m) | Temperature (°C) | Dissolved $H_2$ (cc/kg) | Hold Time (s) | Load Ratio | % Engaged | Post-Test Correction Factor | Measured Δa (mm) | Reported SCC CGR (mm/s) |
|---|---|---|---|---|---|---|---|---|---|---|---|---|---|---|---|---|---|---|---|---|---|
| Bettis | ST1-21 | NX5853G11 | HTMA | 31.9 | CR | plate | S-T | 827 | | A | | CK | 21.4 | 316 | 4.1 | | | 100 | | | 1.37E-06 |
| Bettis | ST1-22 | NX5853G11 | HTMA | 31.9 | CR | plate | S-T | 827 | | A | | CK | 21.6 | 316 | 4.1 | | | 100 | | | 5.68E-07 |
| Bettis | ST1-23 | NX5853G11 | HTMA | 31.9 | CR | plate | S-T | 827 | | A | | CK | 21.2 | 316 | 4.1 | | | 100 | | | 5.78E-07 |
| Bettis | ST1-24 | NX5853G11 | HTMA | 31.9 | CR | plate | S-T | 827 | | A | | CK | 31.9 | 316 | 4.1 | | | 100 | | | 1.95E-06 |
| Bettis | ST1-6 | NX5853G11 | HTMA | 31.9 | CR | plate | S-T | 827 | | A | | CK | 54.7 | 252 | 4.1 | | | 100 | | | 4.72E-07 |
| Bettis | ST1-9 | NX5853G11 | HTMA | 31.9 | CR | plate | S-T | 827 | | A | | CK | 21.5 | 288 | 4.1 | | | 100 | | | 1.71E-07 |
| Bettis | ST2-25 | NX5853G11 | HTMA | 31.9 | CR | plate | S-T | 827 | | A | | CK | 33.9 | 316 | 4.1 | | | 100 | | | 1.82E-06 |
| Bettis | ST2-26 | NX5853G11 | HTMA | 31.9 | CR | plate | S-T | 827 | | A | | CK | 32.7 | 316 | 4.1 | | | 100 | | | 1.47E-06 |
| Bettis | ST2-27 | NX5853G11 | HTMA | 31.9 | CR | plate | S-T | 827 | | A | | CK | 39.9 | 316 | 4.1 | | | 100 | | | 2.56E-06 |
| Bettis | ST2-28 | NX5853G11 | HTMA | 31.9 | CR | plate | S-T | 827 | | A | | CK | 40.9 | 316 | 4.1 | | | 100 | | | 1.71E-06 |
| Bettis | ST2-29 | NX5853G11 | HTMA | 31.9 | CR | plate | S-T | 827 | | A | | CK | 41.7 | 316 | 4.1 | | | 100 | | | 2.37E-06 |
| Bettis | ST2-30 | NX5853G11 | HTMA | 31.9 | CR | plate | S-T | 827 | | A | | CK | 53.6 | 316 | 4.1 | | | 100 | | | 3.95E-06 |
| Bettis | ST2-31 | NX5853G11 | HTMA | 31.9 | CR | plate | S-T | 827 | | A | | CK | 49.1 | 316 | 4.1 | | | 100 | | | 3.14E-06 |
| Bettis | ST2-32 | NX5853G11 | HTMA | 31.9 | CR | plate | S-T | 827 | | A | | CK | 22.9 | 338 | 4.1 | | | 100 | | | 1.77E-06 |
| Bettis | ST2-33 | NX5853G11 | HTMA | 31.9 | CR | plate | S-T | 827 | | A | | CK | 22.2 | 338 | 4.1 | | | 100 | | | 1.57E-06 |
| Bettis | ST2-34 | NX5853G11 | HTMA | 31.9 | CR | plate | S-T | 827 | | A | | CK | 22 | 338 | 4.1 | | | 100 | | | 2.01E-06 |
| Bettis | ST2-35 | NX5853G11 | HTMA | 31.9 | CR | plate | S-T | 827 | | A | | CK | 32.8 | 338 | 4.1 | | | 100 | | | 3.78E-06 |
| Bettis | ST2-36 | NX5853G11 | HTMA | 31.9 | CR | plate | S-T | 827 | | A | | CK | 31 | 338 | 4.1 | | | 100 | | | 3.58E-06 |
| Bettis | ST2-37 | NX5853G11 | HTMA | 31.9 | CR | plate | S-T | 827 | | A | | CK | 34 | 338 | 4.1 | | | 100 | | | 3.93E-06 |
| Bettis | ST2-38 | NX5853G11 | HTMA | 31.9 | CR | plate | S-T | 827 | | A | | CK | 38.5 | 338 | 4.1 | | | 100 | | | 3.60E-06 |
| Bettis | ST2-39 | NX5853G11 | HTMA | 31.9 | CR | plate | S-T | 827 | | A | | CK | 40.4 | 338 | 4.1 | | | 100 | | | 4.42E-06 |
| Bettis | ST2-40 | NX5853G11 | HTMA | 31.9 | CR | plate | S-T | 827 | | A | | CK | 24.8 | 360 | 4.1 | | | 100 | | | 5.57E-06 |
| Bettis | ST2-41 | NX5853G11 | HTMA | 31.9 | CR | plate | S-T | 827 | | A | | CK | 24 | 360 | 4.1 | | | 100 | | | 4.35E-06 |
| Bettis | ST2-42 | NX5853G11 | HTMA | 31.9 | CR | plate | S-T | 827 | | A | | CK | 21.6 | 360 | 4.1 | | | 100 | | | 6.28E-06 |
| CEA | F112-1 | WH220 | MA | 0 | None | CRDM | C-L | 394 | | A | | | 34.8 | 330 | 37.5 | | | | | | 2.47E-07 |
| CEA | F122-1 | WH220 | MA | 0 | None | CRDM | C-L | 394 | | A | | CL | 14.4 | 330 | 37.5 | | | | | 0.3 | 6.10E-08 |
| CEA | F122-2 | WH220 | MA | 0 | None | CRDM | C-L | 394 | | A | | CL | 14.5 | 330 | 37.5 | | | | | 0.31 | 6.40E-08 |
| CEA | F222-2 | WH220 | MA | 0 | None | CRDM | C-L | 394 | | A | | | 14.3 | 310 | 37.5 | | | | | | 3.30E-08 |
| CEA | F312-1 | WH220 | MA | 0 | None | CRDM | C-L | 394 | | A | | | 31.6 | 310 | 37.5 | | | | | | 8.30E-08 |
| CEA | F312-2 | WH220 | MA | 0 | None | CRDM | C-L | 394 | | A | | | 31.1 | 310 | 37.5 | | | | | | 8.90E-08 |
| CEA | F322-1 | WH220 | MA | 0 | None | CRDM | C-L | 394 | | A | | | 14.5 | 310 | 37.5 | | | | | | 3.10E-08 |
| CEA | M6-1 | WF675 | MA | 0 | None | bar | C-L | 468 | | A | | | 35.3 | 330 | 37.5 | | | | | 1.4 | 4.86E-07 |
| CEA | M6-10 | WF675 | MA | 0 | None | bar | C-L | 468 | | A | | CL | 35.9 | 290 | 37.5 | | | | | 0.18 | 3.60E-08 |
| CEA | M6-22 | WF675 | MA | 0 | None | bar | C-L | 468 | | A | | | 38.3 | 330 | 37.5 | | | | | | 6.00E-07 |
| CEA | M6-3 | WF675 | MA | 0 | None | bar | C-L | 468 | | A | | | 36.1 | 330 | 37.5 | | | | | 1.45 | 5.00E-07 |
| CEA | M6-5 | WF675 | MA | 0 | None | bar | C-L | 468 | | A | | | 42.2 | 330 | 37.5 | | | | | | 5.81E-07 |
| CEA | M6-6 | WF675 | MA | 0 | None | bar | C-L | 468 | | A | | | 54 | 330 | 37.5 | | | | | | 5.83E-07 |
| CEA | M6-7 | WF675 | MA | 0 | None | bar | C-L | 468 | | A | | | 21.9 | 330 | 37.5 | | | | | | 4.86E-07 |
| CEA | M6-8 | WF675 | MA | 0 | None | bar | C-L | 468 | | A | | | 24.4 | 330 | 37.5 | | | | | | 5.22E-07 |
| CEA | M6-9 | WF675 | MA | 0 | None | bar | C-L | 468 | | A | | | 38.9 | 310 | 37.5 | | | | | 0.72 | 1.44E-07 |
| CEA | P6-1 | RA737 | MA | 0 | None | bar | C-L | 500 | | A | | | 34.5 | 310 | 37.5 | | | | | 0.73 | 1.47E-07 |
| CEA | P6-2 | RA737 | MA | 0 | None | bar | C-L | 500 | | A | | | 34.1 | 310 | 37.5 | | | | | 0.73 | 1.47E-07 |
| CEA | P6-3 | RA737 | MA | 0 | None | bar | C-L | 500 | | A | | | 33.8 | 290 | 37.5 | | | | | 0.2 | 3.90E-08 |
| CEA | P6-4 | RA737 | MA | 0 | None | bar | C-L | 500 | | A | | | 35.9 | 290 | 37.5 | | | | | 0.21 | 4.20E-08 |

**Table A-1 (continued)**
**Alloy 600 CGR database–Scored-in data**

| Laboratory | Overall Test ID | Heat | As Received Condition | Thickness Reduction (%) | Processing Method | Product Form | Orientation | Yield Strength (MPa) | Hardness (HV) | Test Segment ID | Test Segment Duration (h) | Load Type | K (MPa√m) | Temperature (°C) | Dissolved $H_2$ (cc/kg) | Hold Time (s) | Load Ratio | % Engaged | Post-Test Correction Factor | Measured Δa (mm) | Reported SCC CGR (mm/s) |
|---|---|---|---|---|---|---|---|---|---|---|---|---|---|---|---|---|---|---|---|---|---|
| CEA | T1 | WH220 | MA | 0 | None | CRDM | C-L | 394 | | A | | | 35.3 | 330 | 37.5 | | | | | 0.54 | 1.50E-07 |
| CEA | T2 | WH220 | MA | 0 | None | CRDM | C-L | 394 | | A | | | 34.4 | 330 | 37.5 | | | | | 0.42 | 1.16E-07 |
| CIEMAT | 1-1-L | 746301 | HTMA | 0 | None | CRDM | S-L | 301.5 | | A | 2000 | CL | 37.1 | 325 | 23 | | | | | | 9.46E-08 |
| CIEMAT | 1-1-T | 746301 | HTMA | 0 | None | CRDM | S-T | 301.5 | | A | 2000 | CL | 32.1 | 325 | 23 | | | | | | 3.01E-08 |
| CIEMAT | 1-2-L | 746301 | HTMA | 0 | None | CRDM | S-L | 301.5 | | A | 500 | CL | 31.7 | 325 | 23 | | | | | | 4.44E-08 |
| CIEMAT | 1-2-T | 746301 | HTMA | 0 | None | CRDM | S-T | 301.5 | | A | 2000 | CL | 35.4 | 325 | 23 | | | | | | 2.58E-08 |
| CIEMAT | 1-3-L | 746301 | HTMA | 0 | None | CRDM | S-L | 301.5 | | A | 3036 | CL | 34.8 | 325 | 23 | | | | | | 5.98E-08 |
| CIEMAT | 1-3-T | 746301 | HTMA | 0 | None | CRDM | S-T | 301.5 | | A | 2000 | CL | 32.5 | 325 | 23 | | | | | | 2.29E-08 |
| CIEMAT | 1H1 | NX8844 | HTMA | 0 | HAZ | plate | T-L | 455 | 210 | 7 | 750 | PPU | 28.7 | 340 | 15 | 9000 | 0.7 | 100 | 1.05 | 0.610 | 2.30E-07 |
| CIEMAT | 1H1 | NX8844 | HTMA | 0 | HAZ | plate | T-L | 455 | 210 | 10 | 573 | CL | 31.2 | 340 | 15 | | | 100 | 1.05 | 0.260 | 1.30E-07 |
| CIEMAT | 1H2 | NX8844 | HTMA | 0 | HAZ | plate | T-L | 455 | 210 | 7 | 750 | PPU | 27.3 | 340 | 15 | 9000 | 0.7 | 100 | 0.77 | 0.380 | 1.40E-07 |
| CIEMAT | 1H2 | NX8844 | HTMA | 0 | HAZ | plate | T-L | 455 | 210 | 10 | 573 | CL | 28.4 | 340 | 15 | | | 100 | 0.77 | 0.210 | 1.00E-07 |
| CIEMAT | 2-1-L | 746301 | HTMA | 0 | None | CRDM | S-L | 301.5 | | A | 800 | CL | 38.2 | 325 | 23 | | | | | | 4.52E-08 |
| CIEMAT | 2-1-L | 746301 | HTMA | 0 | None | CRDM | S-L | 301.5 | | B | 2000 | CL | 33 | 325 | 23 | | | | | | 3.58E-08 |
| CIEMAT | 2-2-L | 746301 | HTMA | 0 | None | CRDM | S-L | 301.5 | | A | 800 | CL | 35.8 | 325 | 23 | | | | | | 4.52E-08 |
| CIEMAT | 2-2-L | 746301 | HTMA | 0 | None | CRDM | S-L | 301.5 | | B | 2000 | CL | 31.3 | 325 | 23 | | | | | | 7.45E-08 |
| CIEMAT | 2-3-L | 746301 | HTMA | 0 | None | CRDM | S-L | 301.5 | | A | 3036 | CL | 39.6 | 325 | 23 | | | | | | 7.85E-08 |
| CIEMAT | 2-3-T | 746301 | HTMA | 0 | None | CRDM | S-T | 301.5 | | A | 3036 | CL | 29.3 | 325 | 23 | | | | | | 2.62E-08 |
| CIEMAT | 3-2-L | 746301 | HTMA | 0 | None | CRDM | S-L | 301.5 | | A | 500 | CL | 34.2 | 325 | 23 | | | | | | 5.39E-08 |
| CIEMAT | 3-2-T | 746301 | HTMA | 0 | None | CRDM | S-T | 301.5 | | A | 2000 | CL | 38.4 | 325 | 23 | | | | | | 5.16E-08 |
| CIEMAT | 3-3-T | 746301 | HTMA | 0 | None | CRDM | S-T | 301.5 | | A | 3036 | CL | 32.1 | 325 | 23 | | | | | | 2.52E-08 |
| CIEMAT | BH2 | NX8844 | HTMA | 0 | None | plate | T-L | 257 | 175 | 3 | 334 | PPU | 26.5 | 340 | 15 | 9000 | 0.7 | 100 | 0.57 | 0.200 | 1.70E-07 |
| CIEMAT | BH2 | NX8844 | HTMA | 0 | None | plate | T-L | 257 | 175 | 4 | 1008 | CL | 27.3 | 340 | 15 | | | 100 | 0.57 | 0.320 | 8.70E-08 |
| CIEMAT | BL2 | NX8844 | LTMA | 0 | None | plate | T-L | 340 | 185 | 3 | 334 | PPU | 27.2 | 340 | 15 | 9000 | 0.7 | 100 | 0.49 | 0.340 | 2.80E-07 |
| CIEMAT | BL2 | NX8844 | LTMA | 0 | None | plate | T-L | 340 | 185 | 4 | 1008 | CL | 28.5 | 340 | 15 | | | 100 | 0.49 | 0.480 | 1.30E-07 |
| CIEMAT | E-1 | NX8664 | AR | 0 | None | plate | S-L | 308 | | A | 1092 | CL | 36 | 330 | 23 | | | | | | 8.09E-08 |
| CIEMAT | E-1 | NX8664 | AR | 0 | None | plate | S-L | 308 | | B | 1983 | CL | 40.6 | 330 | 23 | | | | | | 1.39E-07 |
| CIEMAT | E-2 | NX8664 | AR | 0 | None | plate | S-L | 308 | | A | | CL | 36.9 | 290 | 23 | | | | | | 1.52E-08 |
| CIEMAT | E-3 | NX8664 | AR | 0 | None | plate | S-L | 308 | | A | | CL | 33.8 | 290 | 23 | | | | | | 1.01E-08 |
| CIEMAT | E-4 | NX8664 | AR | 0 | None | plate | S-L | 308 | | A | 1500 | CL | 31.9 | 330 | 23 | | | | | | 5.65E-08 |
| CIEMAT | E-5 | NX8664 | AR | 0 | None | plate | S-L | 308 | | A | 675 | CL | 39.3 | 330 | 23 | | | | | | 7.00E-08 |
| CIEMAT | E-5 | NX8664 | AR | 0 | None | plate | S-L | 308 | | B | 825 | CL | 44.5 | 330 | 23 | | | | | | 9.54E-08 |
| CIEMAT | E-6 | NX8664 | AR | 0 | None | plate | S-L | 308 | | A | 1500 | CL | 34.3 | 330 | 23 | | | | | | 7.04E-08 |
| CIEMAT | FC-1 | WA327 | AR | 0 | None | bar | S-L | 413 | | A | 3000 | CL | 44.6 | 330 | 23 | | | | | | 6.48E-08 |
| CIEMAT | FC-2 | WA327 | AR | 0 | None | bar | S-L | 413 | | A | 3300 | CL | 41.3 | 330 | 23 | | | | | | 8.75E-08 |
| CIEMAT | V-1L | 746301 | AR | 0 | None | CRDM | S-L | 301.5 | | A | | CL | 35.5 | 290 | 23 | | | | | | 1.04E-08 |
| CIEMAT | V-1L | 746301 | AR | 0 | None | CRDM | S-L | 301.5 | | B | | CL | 37.9 | 290 | 23 | | | | | | 1.19E-08 |
| CIEMAT | V1-T | 746301 | AR | 0 | None | CRDM | S-T | 301.5 | | A | | CL | 34.1 | 290 | 23 | | | | | | 6.92E-09 |
| CIEMAT | V-2L | 746301 | AR | 0 | None | CRDM | S-L | 301.5 | | A | | CL | 43 | 290 | 23 | | | | | | 7.37E-09 |
| CIEMAT | V2-T | 746301 | AR | 0 | None | CRDM | S-T | 301.5 | | A | | CL | 34.5 | 290 | 23 | | | | | | 4.88E-09 |
| CIEMAT | V-3L | 746301 | AR | 0 | None | CRDM | S-L | 301.5 | | A | | CL | 40.9 | 290 | 23 | | | | | | 1.18E-08 |
| CIEMAT | V-3L | 746301 | AR | 0 | None | CRDM | S-L | 301.5 | | B | | CL | 36.7 | 290 | 23 | | | | | | 9.26E-09 |
| CIEMAT | V-4L | 746301 | AR | 0 | None | CRDM | S-L | 301.5 | | A | | CL | 43.7 | 290 | 23 | | | | | | 1.35E-08 |
| CIEMAT | V-4L | 746301 | AR | 0 | None | CRDM | S-L | 301.5 | | B | | CL | 48.8 | 290 | 23 | | | | | | 8.96E-09 |

**Table A-1 (continued)**
**Alloy 600 CGR database–Scored-in data**

| Laboratory | Overall Test ID | Heat | As Received Condition | Thickness Reduction (%) | Processing Method | Product Form | Orientation | Yield Strength (MPa) | Hardness (HV) | Test Segment ID | Test Segment Duration (h) | Load Type | K (MPa√m) | Temperature (°C) | Dissolved $H_2$ (cc/kg) | Hold Time (s) | Load Ratio | % Engaged | Post-Test Correction Factor | Measured Δa (mm) | Reported SCC CGR (mm/s) |
|---|---|---|---|---|---|---|---|---|---|---|---|---|---|---|---|---|---|---|---|---|---|
| CIEMAT | V-5L | 746301 | AR | 0 | None | CRDM | S-L | 301.5 | | A | | CL | 31.9 | 290 | 23 | | | | | | 1.13E-08 |
| CIEMAT | V-5L | 746301 | AR | 0 | None | CRDM | S-L | 301.5 | | B | | CL | 35.5 | 290 | 23 | | | | | | 1.25E-08 |
| CIEMAT | V-6 | 746301 | AR | 0 | None | CRDM | T-S | 301.5 | | A | | CL | 34.9 | 330 | 23 | | | | | | 5.55E-08 |
| CIEMAT | W2-4 | NX8168G | AR | 0 | None | CRDM | S-L | 244.7 | | A | 2500 | CL | 44.3 | 330 | 23 | | | | | | 9.80E-09 |
| CIEMAT | W2-5 | NX8168G | AR | 0 | None | CRDM | S-L | 244.7 | | A | 3000 | CL | 49.7 | 330 | 23 | | | | | | 2.68E-08 |
| CIEMAT | Z-20 | HRH6503 | AR | 0 | None | bar | S-T | 280 | | A | 1250 | CL | 41.3 | 330 | 23 | | | | | | 3.80E-08 |
| CIEMAT | Z-21 | HRH6503 | AR | 0 | None | bar | S-T | 280 | | A | 1250 | CL | 35.9 | 330 | 23 | | | | | | 2.60E-08 |
| CIEMAT | Z-22 | HRH6503 | AR | 0 | None | bar | S-T | 280 | | A | 1250 | CL | 41.6 | 330 | 23 | | | | | | 7.10E-08 |
| EDF | B369-1 | RA737 | MA | 0 | None | bar | C-L | 500 | | A | | | 30 | 325 | 39 | | | | | 0.82 | 1.53E-07 |
| EDF | B369-15-2 | RA737 | MA | 0 | None | bar | C-L | 500 | | A | | | 29.9 | 325 | 27 | | | 80 | | 1.31 | 2.19E-07 |
| EDF | B369-TTD1 | RA737 | MA | 0 | None | bar | C-L | 500 | | A | | | 32.9 | 290 | 37.5 | | | 50 | | 0.23 | 1.94E-08 |
| EDF | B406-W2 | WJ797 | MA | 0 | HT | bar | C-L | 526 | | A | | CL | 31.8 | 325 | 25.2 | | | 61 | | 0.11 | 1.94E-08 |
| EDF | D722-4-1 | H3262 | MA | 0 | HT | plate | | 400 | | A | | CL | 33.1 | 325 | 37.5 | | | 93 | | 0.55 | 7.78E-08 |
| EDF | D725-Y1 | 2360 | MA | 0 | None | plate | | 211 | | A | | CL | 30.5 | 325 | 37.5 | | | 79 | | 0.92 | 1.28E-07 |
| EDF | D725-Y2 | 2360 | MA | 0 | None | plate | | 211 | | A | | CL | 30.4 | 325 | 37.5 | | | 61 | | 1.06 | 1.47E-07 |
| EDF | T64-1 | 2510 | MA | 0 | None | CRDM | C-L | 469 | | A | | CL | 31.5 | 325 | 25.2 | | | 100 | | 0.64 | 1.11E-07 |
| EDF | T64-2 | 2510 | MA | 0 | None | CRDM | C-L | 469 | | A | | | 24.9 | 290 | 25 | | | 72 | | 0.13 | 1.11E-08 |
| EDF | T65-1 | 2510 | MA | 0 | None | CRDM | C-L | 455 | | A | | CL | 24.4 | 290 | 25 | | | 100 | | 0.06 | 5.56E-09 |
| EDF | TL6 | WF675 | MA | 0 | None | bar | C-L | 468 | | A | | CL | 27.8 | 290 | 30 | | | | | 0.15 | 1.11E-08 |
| EDF | U559-2 CT | HB400 | MA | 0 | None | bar | C-L | 412 | | A | | | 29.9 | 315 | | | | | | | 1.67E-08 |
| EDF | U559-3 | HB400 | MA | 0 | None | bar | C-L | 412 | | A | | | 30.5 | 290 | | | | | | | 7.50E-09 |
| EDF | U589-4 | WF675 | MA | 0 | None | bar | C-L | 468 | | A | | CL | 29.9 | 325 | 28 | | | 50 | | 0.45 | 8.33E-08 |
| EDF | U589-5 | WF675 | MA | 0 | None | bar | C-L | 468 | | A | | CL | 32 | 325 | 25.2 | | | 100 | | 0.93 | 1.61E-07 |
| EDF | U589-6 | WF675 | MA | 0 | None | bar | C-L | 468 | | A | | CL | 32.9 | 290 | 25 | | | 85 | | 0.29 | 2.78E-08 |
| EDF | U589-7 | WF675 | MA | 0 | None | bar | C-L | 468 | | A | | CL | 33.3 | 290 | 25 | | | 100 | | 0.48 | 4.44E-08 |
| EDF | U589-8 | WF675 | MA | 0 | None | bar | C-L | 468 | | A | | CL | 32.8 | 290 | 37.5 | | | 68 | | 0.51 | 4.17E-08 |
| EDF | U589-9 | WF675 | MA | 0 | None | bar | C-L | 468 | | A | | CL | 33.2 | 290 | 37.5 | | | 75 | | 0.43 | 3.33E-08 |
| EDF | U589A | WF675 | MA | 0 | None | bar | C-L | 468 | | A | | | 20.6 | 360 | | | | | | | 1.19E-06 |
| EDF | U589B | WF675 | MA | 0 | None | bar | C-L | 468 | | A | | | 21.5 | 360 | | | | | | | 1.11E-06 |
| EDF | U589-TL13 | WF675 | MA | 0 | None | bar | C-L | 468 | | A | | CL | 35.3 | 325 | 30 | | | | | 1.03 | 2.67E-07 |
| EDF | U589-TL4 | WF675 | MA | 0 | None | bar | C-L | 468 | | A | | CL | 31.1 | 325 | 30 | | | | | 1.25 | 1.89E-07 |
| GE-GRC | c260 | 93510 | AR | 0 | None | CRDM | C-L | 269 | | A | 644 | CK | 27.5 | 340 | 18 | | | | | 0.747 | 3.80E-07 |
| GE-GRC | c260 | 93510 | AR | 0 | None | CRDM | C-L | 269 | | B | 481 | CK | 27.5 | 340 | 40 | | | | | 0.322 | 2.30E-07 |
| GE-GRC | c260 | 93510 | AR | 0 | None | CRDM | C-L | 269 | | C | 140 | CK | 27.5 | 340 | 80 | | | | | 0.051 | 1.10E-07 |
| GE-GRC | c261 | 93510 | AR | 0 | None | CRDM | C-L | 269 | | A | 817 | CK | 27.5 | 325 | 20 | | | | | 0.487 | 1.70E-07 |
| GE-GRC | c261 | 93510 | AR | 0 | None | CRDM | C-L | 269 | | B | 840 | CK | 27.5 | 325 | 40 | | | | | 0.333 | 1.30E-07 |
| GE-GRC | c261 | 93510 | AR | 0 | None | CRDM | C-L | 269 | | C | 853 | CK | 27.5 | 325 | 80 | | | | | 0.436 | 1.10E-07 |
| GE-GRC | c262 | 93510 | AR | 0 | None | CRDM | C-L | 269 | | A | 817 | CK | 27.5 | 325 | 20 | | | | | 0.260 | 1.10E-07 |
| GE-GRC | c262 | 93510 | AR | 0 | None | CRDM | C-L | 269 | | B | 840 | CK | 27.5 | 325 | 40 | | | | | 0.190 | 8.00E-08 |
| GE-GRC | c262 | 93510 | AR | 0 | None | CRDM | C-L | 269 | | C | 853 | CK | 27.5 | 325 | 80 | | | | | 0.206 | 6.80E-08 |
| GE-GRC | c283 | 93510 | AR | 0 | None | CRDM | C-L | 269 | | A | 2200 | CK | 27.5 | 325 | 30 | | | | | 0.640 | 8.30E-08 |
| GE-GRC | c284 | 93510 | AR | 0 | None | CRDM | T-L | 269 | | A | 2200 | CK | 27.5 | 325 | 30 | | | | | 0.970 | 1.40E-07 |
| GE-GRC | c292 | 93510 | AR | 0 | None | CRDM | C-L | 269 | | A | 1295 | CK | 16.5 | 325 | 18 | | | | | 0.119 | 3.20E-08 |
| GE-GRC | c292 | 93510 | AR | 0 | None | CRDM | C-L | 269 | | B | 1150 | CK | 16.5 | 325 | 18 | | | | | 0.058 | 5.60E-09 |

**Table A-1 (continued)**
**Alloy 600 CGR database–Scored-in data**

| Laboratory | Overall Test ID | Heat | As Received Condition | Thickness Reduction (%) | Processing Method | Product Form | Orientation | Yield Strength (MPa) | Hardness (HV) | Test Segment ID | Test Segment Duration (h) | Load Type | K (MPa√m) | Temperature (°C) | Dissolved $H_2$ (cc/kg) | Hold Time (s) | Load Ratio | % Engaged | Post-Test Correction Factor | Measured Δa (mm) | Reported SCC CGR (mm/s) |
|---|---|---|---|---|---|---|---|---|---|---|---|---|---|---|---|---|---|---|---|---|---|
| GE-GRC | c293 | 93510 | AR | 0 | None | CRDM | C-L | 269 | | A | 1295 | CK | 16.5 | 325 | 18 | | | | | 0.076 | 1.90E-08 |
| GE-GRC | c293 | 93510 | AR | 0 | None | CRDM | C-L | 269 | | B | 1150 | CK | 16.5 | 325 | 18 | | | | | 0.035 | 6.70E-09 |
| GE-GRC | c305 | 93510 | AR | 0 | None | CRDM | T-L | 269 | | A | 1041 | CK | 27.5 | 325 | 15 | | | | | 0.373 | 5.60E-08 |
| GE-GRC | c305 | 93510 | AR | 0 | None | CRDM | T-L | 269 | | B | 1050 | CK | 27.5 | 325 | 15 | | | | | 0.445 | 1.10E-07 |
| GE-GRC | c305 | 93510 | AR | 0 | None | CRDM | T-L | 269 | | C | 727 | CK | 27.5 | 325 | 15 | | | | | 0.441 | 1.70E-07 |
| GE-GRC | c306 | 93510 | AR | 0 | None | CRDM | C-L | 269 | | A | 1200 | CK | 27.5 | 325 | 15 | | | | | 0.410 | 9.80E-08 |
| GE-GRC | c306 | 93510 | AR | 0 | None | CRDM | C-L | 269 | | B | 615 | CK | 27.5 | 325 | 15 | | | | | 0.322 | 1.10E-07 |
| GE-GRC | c306 | 93510 | AR | 0 | None | CRDM | C-L | 269 | | C | 727 | CK | 27.5 | 325 | 15 | | | | | 0.325 | 1.20E-07 |
| GE-GRC | c311 | 93510 | AR | 0 | None | CRDM | T-L | 269 | | A | 1400 | CK | 27.5 | 325 | 15 | | | | | 0.362 | 6.00E-08 |
| GE-GRC | c315 | 93510 | AR | 0 | None | CRDM | C-L | 269 | | A | 314 | CK | 16.5 | 325 | 18 | | | | | 0.005 | 4.50E-09 |
| GE-GRC | c315 | 93510 | AR | 0 | None | CRDM | C-L | 269 | | B | 875 | CK | 16.5 | 325 | 18 | | | | | 0.017 | 6.00E-09 |
| GE-GRC | c316 | 93510 | AR | 0 | None | CRDM | C-L | 269 | | A | 314 | CK | 16.5 | 325 | 18 | | | | | 0.027 | 2.50E-08 |
| GE-GRC | c316 | 93510 | AR | 0 | None | CRDM | C-L | 269 | | B | 1575 | CK | 16.5 | 325 | 18 | | | | | 0.130 | 2.40E-08 |
| GE-GRC | c752 | 31907 | MA | 15 | HT+CF | bar | S-L | 372 | | 6 | 110 | CK | 33 | 360 | 26 | | | 100 | 1.09 | 7.000 | 1.20E-05 |
| GE-GRC | c753 | 93511 | MA | 15.9 | CF | CRDM | S-L | 605 | | 6 | 55 | CK | 40 | 360 | 26 | | | 100 | 1.33 | 1.000 | 3.10E-06 |
| GE-GRC | c753 | 93511 | MA | 15.9 | CF | CRDM | S-L | 605 | | 9 | 16 | CK | 55 | 360 | 26 | | | 100 | 1.33 | 1.900 | 2.00E-05 |
| GE-GRC | c757 | 93511 | MA | 15.9 | CF | CRDM | S-L | 605 | | 5 | 5 | CK | 31 | 360 | 26 | | | 100 | 1.7 | 0.210 | 1.10E-05 |
| GE-GRC | c757 | 93511 | MA | 15.9 | CF | CRDM | S-L | 605 | | 10 | 17 | CK | 27 | 360 | 26 | | | 100 | 1.7 | 0.210 | 3.20E-06 |
| GE-GRC | c757 | 93511 | MA | 15.9 | CF | CRDM | S-L | 605 | | 13 | 32 | CK | 23 | 360 | 26 | | | 100 | 1.7 | 0.180 | 1.50E-06 |
| GE-GRC | c757 | 93511 | MA | 15.9 | CF | CRDM | S-L | 605 | | 16 | 355 | CK | 20 | 360 | 26 | | | 100 | 1.7 | 0.160 | 1.00E-07 |
| Lockheed Martin | 0.6T-1 | NX5853G11 | MA | 0 | None | plate | L-T | 201 | | A | | CL | 29.5 | 338 | 40 | | | | | | 4.47E-08 |
| Lockheed Martin | 0.6T-2 | NX5853G11 | MA | 0 | None | plate | L-T | 201 | | A | | CL | 32 | 338 | 40 | | | | | | 3.87E-08 |
| Lockheed Martin | 0.6T-3 | NX5853G11 | MA | 0 | None | plate | L-T | 201 | | A | | CL | 67.8 | 338 | 40 | | | | | | 2.43E-07 |
| Lockheed Martin | 1T-1 | NX5853G11 | MA | 0 | None | plate | L-T | 201 | | A | | CL | 16.8 | 338 | 40 | | | | | | 2.06E-08 |
| Lockheed Martin | 1T-10 | NX5853G11 | MA | 0 | None | plate | L-T | 201 | | A | | CL | 38.6 | 338 | 40 | | | | | | 3.76E-08 |
| Lockheed Martin | 1T-11 | NX5853G11 | MA | 0 | None | plate | L-T | 201 | | A | | CL | 66.5 | 338 | 40 | | | | | | 7.49E-08 |
| Lockheed Martin | 1T-12 | NX5853G11 | MA | 0 | None | plate | L-T | 201 | | A | | CL | 67.8 | 338 | 40 | | | | | | 8.98E-08 |
| Lockheed Martin | 1T-13 | NX5853G11 | MA | 0 | None | plate | L-T | 201 | | A | | CL | 68.2 | 338 | 40 | | | | | | 1.07E-07 |
| Lockheed Martin | 1T-14 | NX5853G11 | MA | 0 | None | plate | L-T | 201 | | A | | CL | 67.9 | 338 | 40 | | | | | | 1.16E-07 |
| Lockheed Martin | 1T-2 | NX5853G11 | MA | 0 | None | plate | L-T | 201 | | A | | CL | 22.2 | 338 | 40 | | | | | | 2.25E-08 |
| Lockheed Martin | 1T-3 | NX5853G11 | MA | 0 | None | plate | L-T | 201 | | A | | CL | 22.1 | 338 | 40 | | | | | | 2.84E-08 |
| Lockheed Martin | 1T-4 | NX5853G11 | MA | 0 | None | plate | L-T | 201 | | A | | CL | 23.4 | 338 | 40 | | | | | | 3.24E-08 |
| Lockheed Martin | 1T-5 | NX5853G11 | MA | 0 | None | plate | L-T | 201 | | A | | CL | 22.2 | 338 | 40 | | | | | | 4.04E-08 |
| Lockheed Martin | 1T-6 | NX5853G11 | MA | 0 | None | plate | L-T | 201 | | A | | CL | 27.5 | 338 | 40 | | | | | | 2.54E-08 |
| Lockheed Martin | 1T-7 | NX5853G11 | MA | 0 | None | plate | L-T | 201 | | A | | CL | 27.4 | 338 | 40 | | | | | | 3.18E-08 |
| Lockheed Martin | 1T-8 | NX5853G11 | MA | 0 | None | plate | L-T | 201 | | A | | CL | 27.5 | 338 | 40 | | | | | | 3.88E-08 |
| Lockheed Martin | 1T-9 | NX5853G11 | MA | 0 | None | plate | L-T | 201 | | A | | CL | 28.4 | 338 | 40 | | | | | | 4.67E-08 |
| Lockheed Martin | 2T-1 | NX5853G11 | MA | 0 | None | plate | L-T | 201 | | A | | CL | 65.6 | 338 | 40 | | | | | | 5.65E-08 |
| Lockheed Martin | 2T-2 | NX5853G11 | MA | 0 | None | plate | L-T | 201 | | A | | CL | 66.6 | 338 | 40 | | | | | | 4.86E-08 |
| Lockheed Martin | Specimen 1 | 44639 | MA | 0 | HAZ | plate | S-L | 255 | 230 | A | | CL | 40 | 288 | 13 | | | | | | 2.53E-08 |
| Lockheed Martin | Specimen 10 | 44639 | MA | 0 | HAZ | plate | S-L | 255 | 230 | A | | CL | 42.6 | 338 | 22 | | | | | | 5.81E-07 |
| Lockheed Martin | Specimen 11 | 44639 | MA | 0 | HAZ | plate | S-L | 255 | 230 | A | | CL | 47.7 | 338 | 22 | | | | | | 6.35E-07 |
| Lockheed Martin | Specimen 12 | 44639 | MA | 0 | HAZ | plate | S-L | 255 | 230 | A | | CL | 47.3 | 338 | 22 | | | | | | 5.57E-07 |
| Lockheed Martin | Specimen 14 | 44639 | MA | 0 | HAZ | plate | S-L | 255 | 230 | A | | CL | 47.7 | 360 | 239 | | | | | | 9.19E-07 |

**Table A-1 (continued)**
**Alloy 600 CGR database–Scored-in data**

| Laboratory | Overall Test ID | Heat | As Received Condition | Thickness Reduction (%) | Processing Method | Product Form | Orientation | Yield Strength (MPa) | Hardness (HV) | Test Segment ID | Test Segment Duration (h) | Load Type | K (MPa√m) | Temperature (°C) | Dissolved $H_2$ (cc/kg) | Hold Time (s) | Load Ratio | % Engaged | Post-Test Correction Factor | Measured Δa (mm) | Reported SCC CGR (mm/s) |
|---|---|---|---|---|---|---|---|---|---|---|---|---|---|---|---|---|---|---|---|---|---|
| Lockheed Martin | Specimen 15 | 44639 | MA | 0 | HAZ | plate | S-L | 255 | 230 | A | | CL | 48.1 | 360 | 30 | | | | | | 1.07E-06 |
| Lockheed Martin | Specimen 5 | 44639 | MA | 0 | HAZ | plate | S-L | 255 | 230 | A | | CL | 44.1 | 338 | 3 | | | | | | 4.38E-07 |
| Lockheed Martin | Specimen 8 | 44639 | MA | 0 | HAZ | plate | S-L | 255 | 230 | A | | CL | 28.8 | 338 | 22 | | | | | | 2.96E-07 |
| Lockheed Martin | Specimen 9 | 44639 | MA | 0 | HAZ | plate | S-L | 255 | 230 | A | | CL | 38.7 | 338 | 20 | | | | | | 4.08E-07 |
| PNNL | CT063 (DB-1) | M7929 | MA | 0 | None | CRDM | C-R | 296 | 186.5 | 6 | 989 | CK | 21 | 325 | 29 | | | 100 | 1.10 | 0.098 | 3.10E-08 |
| PNNL | CT063 (DB-1) | M7929 | MA | 0 | None | CRDM | C-R | 296 | 186.5 | 7 | 117 | CK | 21 | 360 | 65 | | | 100 | 1.10 | 0.081 | 2.00E-07 |
| PNNL | CT063 (DB-1) | M7929 | MA | 0 | None | CRDM | C-R | 296 | 186.5 | 8 | 403 | CK | 21 | 325 | 29 | | | 100 | 1.10 | 0.090 | 6.80E-08 |
| PNNL | CT063 (DB-1) | M7929 | MA | 0 | None | CRDM | C-R | 296 | 186.5 | 9 | 484 | CK | 21 | 300 | 16 | | | 100 | 1.10 | 0.033 | 1.70E-08 |
| PNNL | CT063 (DB-1) | M7929 | MA | 0 | None | CRDM | C-R | 296 | 186.5 | 10 | 150 | CK | 21 | 325 | 29 | | | 100 | 1.10 | 0.046 | 6.20E-08 |
| PNNL | CT063 (DB-1) | M7929 | MA | 0 | None | CRDM | C-R | 296 | 186.5 | 12 | 164 | CK | 21 | 325 | 29 | | | 100 | 1.10 | 0.019 | 5.10E-08 |
| PNNL | CT063 (DB-1) | M7929 | MA | 0 | None | CRDM | C-R | 296 | 186.5 | 14 | 183 | CK | 33 | 325 | 29 | | | 100 | 1.10 | 0.162 | 1.80E-07 |
| PNNL | CT064 (DB-2) | M7929 | MA | 0 | None | CRDM | C-R | 296 | | 6 | 989 | CK | 21 | 325 | 29 | | | 100 | | 0.066 | 2.10E-08 |
| PNNL | CT064 (DB-2) | M7929 | MA | 0 | None | CRDM | C-R | 296 | | 7 | 117 | CK | 20 | 360 | 65 | | | 100 | | 0.024 | 6.00E-08 |
| PNNL | CT064 (DB-2) | M7929 | MA | 0 | None | CRDM | C-R | 296 | | 8 | 403 | CK | 20 | 325 | 29 | | | 100 | | 0.015 | 1.60E-08 |
| PNNL | CT064 (DB-2) | M7929 | MA | 0 | None | CRDM | C-R | 296 | | 9 | 484 | CK | 20 | 300 | 16 | | | 100 | | 0.008 | 4.40E-09 |
| PNNL | CT064 (DB-2) | M7929 | MA | 0 | None | CRDM | C-R | 296 | | 10 | 150 | CK | 20 | 325 | 29 | | | 100 | | 0.006 | 1.00E-08 |
| PNNL | CT064 (DB-2) | M7929 | MA | 0 | None | CRDM | C-R | 296 | | 14 | 183 | CK | 23 | 325 | 29 | | | 100 | | 0.014 | 1.90E-08 |
| PNNL | CT064 (DB-2) | M7929 | MA | 0 | None | CRDM | C-R | 296 | | 15 | 293 | CK | 25 | 325 | 29 | | | 100 | | 0.147 | 1.30E-07 |
| PNNL | CT064 (DB-2) | M7929 | MA | 0 | None | CRDM | C-R | 296 | | 17 | 491 | CK | 22 | 325 | 29 | | | 100 | | 0.086 | 6.10E-08 |
| PNNL | CT064 (DB-2) | M7929 | MA | 0 | None | CRDM | C-R | 296 | | 21 | 666 | CK | 30 | 325 | 29 | | | 100 | | 0.228 | 7.80E-08 |
| PNNL | CT064 (DB-2) | M7929 | MA | 0 | None | CRDM | C-R | 296 | | 23 | 136 | CK | 31 | 325 | 29 | | | 100 | | 0.047 | 1.00E-07 |
| PNNL | CT064 (DB-2) | M7929 | MA | 0 | None | CRDM | C-R | 296 | | 26 | 70 | CK | 32 | 325 | 29 | | | 100 | | 0.017 | 6.70E-08 |
| PNNL | CT064 (DB-2) | M7929 | MA | 0 | None | CRDM | C-R | 296 | | 28 | 186 | CK | 32 | 325 | 29 | | | 100 | | 0.039 | 5.90E-08 |
| PNNL | CT064 (DB-2) | M7929 | MA | 0 | None | CRDM | C-R | 296 | | 32 | 856 | CK | 41 | 325 | 29 | | | 100 | | 0.470 | 6.50E-08 |
| PNNL | CT090 (H1N1#1) | M3935 | MA | 0 | None | CRDM | C-L | 334 | 160.2 | 11 | 551 | CK | 15 | 325 | 11 | | | 100 | 1.00 | 0.029 | 1.30E-08 |
| PNNL | CT090 (H1N1#1) | M3935 | MA | 0 | None | CRDM | C-L | 334 | 160.2 | 15 | 554 | CK | 22 | 325 | 11 | | | 100 | 1.00 | 0.061 | 3.20E-08 |
| PNNL | CT091 (H1N1#2) | M3935 | MA | 0 | None | CRDM | C-L | 334 | | 11 | 551 | CK | 15 | 325 | 11 | | | 100 | 1.00 | 0.016 | 6.90E-09 |
| PNNL | CT091 (H1N1#2) | M3935 | MA | 0 | None | CRDM | C-L | 334 | | 15 | 554 | CK | 22 | 325 | 11 | | | 100 | 1.00 | 0.034 | 1.60E-08 |
| Studsvik | 167-1:53 | NX8664 | AR | 0 | None | plate | L-T | 308 | | A | 259 | PPU | 33.2 | 330 | 25 | 10000 | 0.75 | | | 0.11 | 1.10E-07 |
| Studsvik | 167-1:54 | NX8664 | AR | 0 | None | plate | L-T | 308 | | A | 330 | PPU | 33.2 | 330 | 25 | 100000 | 0.75 | | | 0.06 | 4.90E-08 |
| Studsvik | 167-2:76 | NX8664 | AR | 0 | None | plate | L-T | 308 | | A | 339 | PPU | 36 | 320 | 25 | 10000 | 0.75 | | | 0.03 | 2.30E-08 |
| Studsvik | 167-2:77 | NX8664 | AR | 0 | None | plate | L-T | 308 | | A | 279 | PPU | 36.4 | 320 | 25 | 100000 | 0.75 | | | 0.04 | 3.90E-08 |
| Studsvik | 173-3 | PYE7704 | AR | 0 | None | bar | C-R | 278 | | A | 2608 | CK | 34.4 | 343 | 25 | | | | | 0.21 | 2.30E-08 |
| Studsvik | 196-19 | 22474 | MA | 0 | None | plate | L-T | 311 | 169 | 4 | 815 | CK | 22.8 | 328.3 | 25.5 | | | | | 0.202 | 6.40E-08 |
| Studsvik | 196-19 | 22474 | MA | 0 | None | plate | L-T | 311 | 169 | 5 | 599 | CK | 22 | 327.9 | 24.8 | | | | | 0.123 | 5.70E-08 |
| Studsvik | 196-19 | 22474 | MA | 0 | None | plate | L-T | 311 | 169 | 6 | 504 | CK | 21 | 328 | 25 | | | | | 0.016 | 9.00E-09 |
| Studsvik | 196-19 | 22474 | MA | 0 | None | plate | L-T | 311 | 169 | 3b | 307 | CK | 23.3 | 328.5 | 24.9 | | | | | 0.122 | 1.08E-07 |
| Studsvik | 196-2 | 22474 | MA | 0 | None | plate | L-T | 311 | 169 | 2 | 439 | CK | 23.3 | 328.4 | 23.2 | | | | | 0.075 | 4.80E-08 |
| Studsvik | 196-2 | 22474 | MA | 0 | None | plate | L-T | 311 | 169 | 1a | 133 | CK | 23.2 | 328.4 | 27 | | | | | 0.085 | 1.76E-07 |
| Studsvik | 196-2 | 22474 | MA | 0 | None | plate | L-T | 311 | 169 | 1b | 253 | CK | 22.9 | 328.4 | 27 | | | | | 0.037 | 5.80E-08 |
| Studsvik | 196-2 | 22474 | MA | 0 | None | plate | L-T | 311 | 169 | 3a | 426 | CK | 23.8 | 328.5 | 25.6 | | | | | 0.016 | 1.60E-08 |
| Studsvik | 196-53 | 22474 | MA | 0 | None | plate | L-T | 311 | 169 | 4 | 4746 | CL | 8.9 | 340 | 25 | | | | | 0.032 | 1.87E-09 |
| Studsvik | 196-54 | 22474 | MA | 0 | None | plate | L-T | 311 | 169 | 4 | 6381 | CL | 10.9 | 340 | 25 | | | | | 0.080 | 3.48E-09 |
| Studsvik | 196-55 | 22474 | MA | 0 | None | plate | L-T | 311 | 169 | 4 | 6381 | CL | 12.1 | 340 | 25 | | | | | 0.051 | 2.22E-09 |

**Table A-1 (continued)**
**Alloy 600 CGR database–Scored-in data**

| Laboratory | Overall Test ID | Heat | As Received Condition | Thickness Reduction (%) | Processing Method | Product Form | Orientation | Yield Strength (MPa) | Hardness (HV) | Test Segment ID | Test Segment Duration (h) | Load Type | K (MPa√m) | Temperature (°C) | Dissolved $H_2$ (cc/kg) | Hold Time (s) | Load Ratio | % Engaged | Post-Test Correction Factor | Measured Δa (mm) | Reported SCC CGR (mm/s) |
|---|---|---|---|---|---|---|---|---|---|---|---|---|---|---|---|---|---|---|---|---|---|
| Studsvik | 196-56 | 22474 | MA | 0 | None | plate | L-T | 311 | 169 | 4 | 6381 | CL | 16.4 | 340 | 25 | | | | | 0.100 | 4.35E-09 |
| Studsvik | 196-57 | 22474 | MA | 0 | None | plate | L-T | 311 | 169 | 4 | 4774 | CL | 7.2 | 340 | 25 | | | | | 0.020 | 1.16E-09 |
| Studsvik | 1FCT1 | SG1 | MA | 0 | None | plate | | 336 | | 5 | 2000 | CK | 33.9 | 350 | 25 | | | 100 | 52 | 1.137 | 2.99E-08 |
| Studsvik | 1FCT2 | SG1 | MA | 0 | None | plate | | 336 | | 1 | 7000 | CK | 32.8 | 350 | 25 | | | 98 | 17 | 0.585 | 2.69E-08 |
| Studsvik | 2D1 | SG1 | MA | 0 | HAZ | plate | | 336 | | 5 | 2000 | CK | 32.1 | 350 | 25 | | | 100 | 21 | 0.767 | 3.17E-08 |
| Studsvik | 2D2 | SG1 | MA | 0 | HAZ | plate | | 336 | | 1 | 7000 | CK | 31.3 | 350 | 25 | | | 100 | 41 | 0.834 | 3.83E-08 |
| Studsvik | BABA1 | SG2 | MA | 0 | HAZ | plate | | 305 | | 5 | 2000 | CK | 35.5 | 350 | 25 | | | 100 | 50 | 1.520 | 3.87E-08 |
| Studsvik | BABA2 | SG2 | MA | 0 | HAZ | plate | | 305 | | 1 | 7000 | CK | 34.8 | 350 | 25 | | | 100 | 51 | 1.692 | 6.54E-08 |
| Studsvik | BABA3 | SG2 | MA | 0 | None | plate | | 305 | | 5 | 2000 | CK | 32.6 | 350 | 25 | | | 100 | 30 | 0.578 | 8.25E-09 |
| Studsvik | BABA4 | SG2 | MA | 0 | None | plate | | 305 | | 1 | 7000 | CK | 32.4 | 350 | 25 | | | 98 | 18 | 0.400 | 1.25E-08 |
| Studsvik | S20-21 | NX6420G | AR | 0 | None | CRDM | C-L | 248.4 | | A | 1486 | CK | 25 | 329.7 | 25 | | | | | 0.11 | 2.10E-08 |
| Studsvik | S510-1 | 93510 | AR | 0 | None | CRDM | C-L | 297.2 | | A | 1486 | CK | 21.4 | 329.7 | 25 | | | | | 0.92 | 1.40E-07 |
| Studsvik | S510-2 | 93510 | AR | 0 | None | CRDM | C-L | 297.2 | | A | 1486 | CK | 21.4 | 329.7 | 25 | | | | | 1.05 | 1.70E-07 |
| Studsvik | S510-3 | 93510 | AR | 0 | None | CRDM | C-L | 297.2 | | A | 1486 | CK | 26.2 | 329.7 | 25 | | | | | 1.27 | 2.10E-07 |
| Studsvik | S511-1 | 93511 | MA | 0 | None | CRDM | C-L | 329 | | A | 1486 | CK | 20.4 | 329.7 | 25 | | | | | 0.82 | 1.20E-07 |
| Studsvik | S511-2 | 93511 | MA | 0 | None | CRDM | C-L | 329 | | A | 1486 | CK | 27.1 | 329.7 | 25 | | | | | 1.15 | 2.00E-07 |
| Studsvik | S69-40 | 91069 | AR | 0 | None | CRDM | C-L | 273.8 | | A | 1486 | CK | 20 | 329.7 | 25 | | | | | 0.79 | 1.40E-07 |
| Studsvik | S69-41 | 91069 | AR | 0 | None | CRDM | C-L | 273.8 | | A | 1486 | CK | 27.5 | 329.7 | 25 | | | | | 1.21 | 1.90E-07 |
| Westinghouse | 13-1 | D2604DE | AR | 0 | None | CRDM | | 165.5 | | A | | PPU | 19.05 | 326.4 | 25 | 3600 | 0.7 | | | | 1.56E-08 |
| Westinghouse | 20-12 | NX6420G | AR | 0 | None | CRDM | | 248.4 | | A | | PPU | 20.05 | 325.1 | 25 | 3600 | 0.7 | | | | 8.69E-09 |
| Westinghouse | 20-16 | NX6420G | AR | 0 | None | CRDM | | 248.4 | | A | | CL | 30.75 | 325.4 | 25 | | | | | | 1.58E-08 |
| Westinghouse | 20-17 | NX6420G | AR | 0 | None | CRDM | | 248.4 | | A | | PPU | 20.85 | 328.1 | 25 | 3600 | 0.7 | | | | 9.77E-09 |
| Westinghouse | 20-18 | NX6420G | AR | 0 | None | CRDM | | 248.4 | | A | | PPU | 21 | 328.4 | 25 | 3600 | 0.7 | | | | 3.27E-08 |
| Westinghouse | 20-19 | NX6420G | AR | 0 | None | CRDM | | 248.4 | | A | | PPU | 23.85 | 353.3 | 25 | 3600 | 0.7 | | | | 3.53E-08 |
| Westinghouse | 20-20 | NX6420G | AR | 0 | None | CRDM | | 248.4 | | A | | PPU | 23.75 | 340.2 | 25 | 3600 | 0.7 | | | | 1.14E-08 |
| Westinghouse | 20-3 | NX6420G | AR | 0 | None | CRDM | | 248.4 | | A | | PPU | 22.3 | 302.6 | 25 | 3600 | 0.7 | | | | 6.14E-09 |
| Westinghouse | 20-3 | NX6420G | AR | 0 | None | CRDM | | 248.4 | | B | | PPU | 22.3 | 340.2 | 25 | 3600 | 0.7 | | | | 1.02E-07 |
| Westinghouse | 20-4 | NX6420G | AR | 0 | None | CRDM | | 248.4 | | A | | | 22.05 | 326.1 | 25 | | | | | | 5.56E-09 |
| Westinghouse | 20-5 | NX6420G | AR | 0 | None | CRDM | | 248.4 | | A | | CL | 21.1 | 326.9 | 25 | | | | | | 1.78E-08 |
| Westinghouse | 49-1 | C2649 | AR | 0 | None | CRDM | | 309.6 | | A | | PPU | 25.15 | 325.3 | 25 | 3600 | 0.7 | | | | 6.78E-08 |
| Westinghouse | 5-1 | NX8664-5 | AR | 0 | None | plate | | 308.2 | | A | 1291 | PPU | 23 | 327.7 | 25 | 3600 | 0.85 | | | | 3.47E-08 |
| Westinghouse | 510-1 | 93510 | AR | 0 | None | CRDM | | 297.2 | | A | 926 | PPU | 21.4 | 327.7 | 25 | 3600 | 0.7 | | | | 5.10E-08 |
| Westinghouse | 511-1 | 93511 | MA | 0 | None | CRDM | | 329 | | A | 1061 | PPU | 23.6 | 327.6 | 25 | 3600 | 0.7 | | | | 1.09E-07 |
| Westinghouse | 511-2 | 93511 | MA | 0 | None | CRDM | | 329 | | A | | CL | 24.65 | 325.6 | 25 | | | | | | 8.55E-08 |
| Westinghouse | 559-1 | HB400 | MA | 0 | None | bar | | 412 | | A | | PPU | 21.95 | 327 | 25 | 3600 | 0.7 | | | | 1.97E-09 |
| Westinghouse | 559-1 | HB400 | MA | 0 | None | bar | | 412 | | B | | PPU | 21.95 | 340.8 | 25 | 3600 | 0.7 | | | | 1.93E-08 |
| Westinghouse | 589-1 | WF675 | MA | 0 | None | bar | | 468 | | A | | PPU | 26.9 | 323.8 | 25 | 3600 | 0.7 | | | | 3.63E-08 |
| Westinghouse | 62015-1 | NX9240 | AR | 0 | None | plate | | 392 | | A | | PPU | 26.75 | 323.5 | 25 | 3600 | 0.7 | | | | 1.31E-08 |
| Westinghouse | 69-10 | 91069 | AR | 0 | None | CRDM | | 273.8 | | A | | PPU | 24.95 | 328.2 | 25 | 3600 | 0.7 | | | | 1.98E-07 |
| Westinghouse | 69-11 | 91069 | AR | 0 | None | CRDM | | 273.8 | | A | | PPU | 19.65 | 325.5 | 25 | 3600 | 0.7 | | | | 1.27E-07 |
| Westinghouse | 69-11 | 91069 | AR | 0 | None | CRDM | | 273.8 | | B | | PPU | 19.65 | 325.5 | 25 | 18000 | 0.7 | | | | 6.51E-08 |
| Westinghouse | 69-11 | 91069 | AR | 0 | None | CRDM | | 273.8 | | E | | PPU | 19.65 | 325.5 | 25 | 3600 | 0.7 | | | | 1.72E-08 |
| Westinghouse | 69-13 | 91069 | AR | 0 | None | CRDM | | 273.8 | | A | | | 21.3 | 328.3 | 25 | 3600 | 0.7 | | | | 8.13E-08 |
| Westinghouse | 69-14 | 91069 | AR | 0 | None | CRDM | | 273.8 | | A | | PPU | 22.2 | 326.6 | 25 | 3600 | 0.7 | | | | 3.18E-08 |

**Table A-1 (continued)**
**Alloy 600 CGR database–Scored-in data**

| Laboratory | Overall Test ID | Heat | As Received Condition | Thickness Reduction (%) | Processing Method | Product Form | Orientation | Yield Strength (MPa) | Hardness (HV) | Test Segment ID | Test Segment Duration (h) | Load Type | K (MPa√m) | Temperature (°C) | Dissolved $H_2$ (cc/kg) | Hold Time (s) | Load Ratio | % Engaged | Post-Test Correction Factor | Measured Δa (mm) | Reported SCC CGR (mm/s) |
|---|---|---|---|---|---|---|---|---|---|---|---|---|---|---|---|---|---|---|---|---|---|
| Westinghouse | 69-17 | 91069 | AR | 0 | None | CRDM | | 273.8 | | A | | PPU | 23.45 | 363.3 | 25 | 3600 | 0.7 | | | | 1.61E-07 |
| Westinghouse | 69-18 | 91069 | AR | 0 | None | CRDM | | 273.8 | | A | | PPU | 23.1 | 291.1 | 25 | 3600 | 0.7 | | | | 7.68E-09 |
| Westinghouse | 69-18 | 91069 | AR | 0 | None | CRDM | | 273.8 | | B | | PPU | 23.1 | 327.5 | 25 | 3600 | 0.7 | | | | 1.71E-07 |
| Westinghouse | 69-19 | 91069 | AR | 0 | None | CRDM | | 273.8 | | A | | PPU | 23.5 | 341.6 | 25 | 3600 | 0.7 | | | | 2.22E-07 |
| Westinghouse | 69-20 | 91069 | AR | 0 | None | CRDM | | 273.8 | | A | | PPU | 23.3 | 339.6 | 25 | 3600 | 0.7 | | | | 7.61E-08 |
| Westinghouse | 69-21 | 91069 | AR | 0 | None | CRDM | | 273.8 | | A | | PPU | 24.6 | 337.9 | 25 | 3600 | 0.7 | | | | 9.33E-08 |
| Westinghouse | 69-22 | 91069 | AR | 0 | None | CRDM | | 273.8 | | A | | PPU | 15.6 | 326.1 | 25 | 3600 | 0.7 | | | | 3.53E-08 |
| Westinghouse | 69-23 | 91069 | AR | 0 | None | CRDM | | 273.8 | | A | | PPU | 24.35 | 325.3 | 25 | 3600 | 0.7 | | | | 1.36E-07 |
| Westinghouse | 69-26 | 91069 | AR | 0 | None | CRDM | | 273.8 | | A | | PPU | 24.1 | 360.6 | 25 | 3600 | 0.7 | | | | 1.34E-07 |
| Westinghouse | 69-27 | 91069 | AR | 0 | None | CRDM | | 273.8 | | A | | PPU | 24 | 353.5 | 25 | 3600 | 0.7 | | | | 7.06E-08 |
| Westinghouse | 69-29 | 91069 | AR | 0 | None | CRDM | | 273.8 | | A | | | 37.65 | 326.3 | 25 | | | | | | 1.87E-07 |
| Westinghouse | 69-5 | 91069 | AR | 0 | None | CRDM | | 273.8 | | A | | PPU | 22.5 | 331.1 | 25 | 3600 | 0.7 | | | | 1.29E-07 |
| Westinghouse | 69-5 | 91069 | AR | 0 | None | CRDM | | 273.8 | | C | | PPU | 22.5 | 331.1 | 25 | 10800 | 0.7 | | | | 5.00E-08 |
| Westinghouse | 69-5 | 91069 | AR | 0 | None | CRDM | | 273.8 | | D | | PPU | 22.5 | 331.1 | 25 | 72000 | 0.7 | | | | 4.00E-08 |
| Westinghouse | 69-5 | 91069 | AR | 0 | None | CRDM | | 273.8 | | E | | PPU | 22.5 | 331.1 | 25 | 3600 | 0.85 | | | | 3.44E-08 |
| Westinghouse | 69-5 | 91069 | AR | 0 | None | CRDM | | 273.8 | | F | 164 | CK | 22.5 | 331.1 | 25 | | | | | | 1.97E-08 |
| Westinghouse | 69-6 | 91069 | AR | 0 | None | CRDM | | 273.8 | | A | | PPU | 22.85 | 309.2 | 25 | 3600 | 0.7 | | | | 5.28E-08 |
| Westinghouse | 69-9 | 91069 | AR | 0 | None | CRDM | | 273.8 | | A | | PPU | 21.1 | 325.6 | 25 | 3600 | 0.7 | | | | 4.96E-08 |
| Westinghouse | 7-1 | NX8664-7 | AR | 0 | None | plate | | 298.5 | | A | 924 | PPU | 22.3 | 327.5 | 25 | 3600 | 0.7 | | | | 2.98E-08 |

## Table A-2
## Alloy 600 CGR database–Scored-out data

| Laboratory | Overall Test ID | Heat | As Received Condition | Thickness Reduction (%) | Processing Method | Product Form | Orientation | Yield Strength (MPa) | Hardness (HV) | Test Segment ID | Test Segment Duration (h) | Load Type | K (MPa√m) | Temperature (°C) | Dissolved $H_2$ (cc/kg) | Hold Time (s) | Load Ratio | % Engaged | Post-Test Correction Factor | Measured Δa (mm) | Reported SCC CGR (mm/s) |
|---|---|---|---|---|---|---|---|---|---|---|---|---|---|---|---|---|---|---|---|---|---|
| ANL | DB-3 | M7929 | MA | 0 | None | CRDM | C-R | 296 | | 4 | 89 | CL | 12.6 | 320 | 23 | | | 100 | 1.11 | 0.002 | 2.53E-09 |
| ANL | DB-3 | M7929 | MA | 0 | None | CRDM | C-R | 296 | | 18 | 18 | PPU | 19.5 | 320 | 23 | 3600 | 0.5 | 100 | 1.11 | 0.003 | 2.32E-08 |
| ANL | DB-4 | M7929 | MA | 0 | None | CRDM | C-L | 296 | | 8 | 28 | PPU | 24.3 | 320 | 23 | 7200 | 0.7 | 100 | 1.31 | 0.000 | 1.69E-08 |
| ANL | DB-4 | M7929 | MA | 0 | None | CRDM | C-L | 296 | | 18 | 167 | CL | 30.2 | 290 | 11 | | | 100 | 1.31 | 0.001 | 4.07E-09 |
| ANL | N3CC-2 | M3935 | MA | 0 | None | CRDM | C-L | 334 | | 10 | 165 | CL | 24.7 | 316 | 25 | | | 100 | 1.74 | 0.007 | 1.44E-09 |
| ANL | N3CC-3 | M3935 | MA | 0 | None | CRDM | C-L | 334 | | 7 | 119 | CL | 31.9 | 316 | 23 | | | 100 | 1.57 | 0.000 | 1.00E-10 |
| ANL | N3CC-3 | M3935 | MA | 0 | None | CRDM | C-L | 334 | | 5a | 56 | CL | 20.5 | 316 | 23 | | | 100 | 1.57 | 0.016 | 7.85E-08 |
| Bettis | 1-2 | Bettis-600 | HTMA | 32 | TS | plate | S-T | 851.9 | | A | | PPU | 21.1 | 316 | 50 | 600 | 0.7 | | | | 1.60E-07 |
| Bettis | 1-2 | Bettis-600 | HTMA | 32 | TS | plate | S-T | 851.9 | | A | | PPU | 21.1 | 316 | 50 | 600 | 0.7 | | | | 1.72E-07 |
| Bettis | 1-2 | Bettis-600 | HTMA | 32 | TS | plate | S-T | 851.9 | | A | | PPU | 34.0 | 316 | 50 | 600 | 0.7 | | | | 2.39E-07 |
| Bettis | 1-2 | Bettis-600 | HTMA | 32 | TS | plate | S-T | 851.9 | | A | | PPU | 33.9 | 316 | 50 | 600 | 0.7 | | | | 2.81E-07 |
| Bettis | 1-5 | Bettis-600 | HTMA | 24 | CR | plate | S-T | 850.1 | | A | | PPU | 10.6 | 316 | 50 | 600 | 0.7 | | | | 1.29E-07 |
| Bettis | 1-5 | Bettis-600 | HTMA | 24 | CR | plate | S-T | 850.1 | | A | | PPU | 21.1 | 316 | 50 | 600 | 0.7 | | | | 3.43E-07 |
| Bettis | CB20-61 | NX5853G11 | HTMA | 0 | None | plate | L-T | 201 | | A | | bolt | 35.8 | 288 | 4.1 | | | | | 0.000 | 1.00E-10 |
| Bettis | CB20-63 | NX5853G11 | HTMA | 0 | None | plate | L-T | 201 | | A | | bolt | 35.7 | 338 | 4.1 | | | | | 0.000 | 1.00E-10 |
| Bettis | CR28-10 | NX5853G11 | HTMA | 31.9 | CR | plate | L-T | 827 | | A | | PPU | 35.1 | 288 | 4.1 | 600 | 0.7 | | | | 8.42E-08 |
| Bettis | CR28-11 | NX5853G11 | HTMA | 31.9 | CR | plate | L-T | 827 | | A | | PPU | 33.6 | 316 | 4.1 | 600 | 0.7 | | | | 4.97E-08 |
| Bettis | CR28-18 | NX5853G11 | HTMA | 31.9 | CR | plate | L-T | 827 | | A | | PPU | 34.9 | 316 | 4.1 | 600 | 0.7 | | | | 2.39E-08 |
| Bettis | S16-43 | NX5853G11 | HTMA | 11.4 | TS | plate | L-T | 517 | | A | | PPU | 34.8 | 288 | 4.1 | 600 | 0.7 | | | | 1.00E-10 |
| Bettis | S16-44 | NX5853G11 | HTMA | 11.4 | TS | plate | L-T | 517 | | A | | PPU | 34.5 | 316 | 4.1 | 600 | 0.7 | | | | 2.05E-08 |
| Bettis | S16-48 | NX5853G11 | HTMA | 11.4 | TS | plate | L-T | 517 | | A | | PPU | 33.3 | 338 | 4.1 | 600 | 0.7 | | | | 2.65E-07 |
| Bettis | S16-53 | NX5853G11 | HTMA | 11.4 | TS | plate | L-T | 517 | | A | | PPU | 33.7 | 316 | 4.1 | 600 | 0.7 | | | | 2.74E-08 |
| Bettis | S22-19 | NX5853G11 | HTMA | 17.3 | TS | plate | L-T | 633 | | A | | PPU | 34.4 | 288 | 4.1 | 600 | 0.7 | | | | 2.73E-08 |
| Bettis | S22-20 | NX5853G11 | HTMA | 17.3 | TS | plate | L-T | 633 | | A | | PPU | 34.6 | 316 | 4.1 | 600 | 0.7 | | | | 5.00E-08 |
| Bettis | S22-23 | NX5853G11 | HTMA | 17.3 | TS | plate | L-T | 633 | | A | | PPU | 34.2 | 316 | 4.1 | 600 | 0.7 | | | | 7.80E-08 |
| Bettis | S22-24 | NX5853G11 | HTMA | 17.3 | TS | plate | L-T | 633 | | A | | PPU | 34.3 | 338 | 4.1 | 600 | 0.7 | | | | 3.44E-07 |
| Bettis | S34-15 | NX5853G11 | HTMA | 25.7 | TS | plate | L-T | 772 | | A | | PPU | 34.2 | 288 | 4.1 | 600 | 0.7 | | | | 2.19E-08 |
| Bettis | S34-20 | NX5853G11 | HTMA | 25.7 | TS | plate | L-T | 772 | | A | | PPU | 34.5 | 316 | 4.1 | 600 | 0.7 | | | | 4.31E-08 |
| Bettis | S34-50 | NX5853G11 | HTMA | 25.7 | TS | plate | L-T | 772 | | A | | bolt | 33.1 | 252 | 4.1 | | | | | | 1.00E-10 |
| Bettis | S5-6 | NX5853G11 | HTMA | 3.5 | TS | plate | L-T | 345 | | A | | PPU | 38.2 | 338 | 4.1 | 600 | 0.7 | | | | 1.83E-07 |
| EDF | 1533-55 | 1b | TT | 10 | TS | plate | T-L | | | A | | | 40.8 | 345 | | | | | | 0.902 | 1.36E-07 |
| EDF | 1533-56 | 1a | TT | 7 | TS | plate | T-L | | | A | | | 39.5 | 345 | | | | | | 0.050 | 8.33E-09 |
| EDF | 1533-57 | 1a | TT | 13 | TS | plate | T-L | | | A | 1824 | | 41.3 | 345 | | | | 100 | | 0.980 | 1.50E-07 |
| EDF | 1533-59 | 2b | TT | 8 | TS | plate | T-L | | | A | 1600 | | 40.0 | 345 | | | | | | 0.400 | 6.94E-08 |
| EDF | 1533-78 | 2a | TT | 12 | TS | plate | T-L | | | A | | | 40.0 | 360 | | | | | | 1.370 | 5.08E-07 |
| EDF | 1533-79 | 2a | TT | 12 | TS | plate | T-L | | | A | | | 35.5 | 360 | | | | | | 0.580 | 2.14E-07 |
| EDF | 1533-80 | 2a | TT | 19 | TS | plate | T-L | | | A | | | 40.0 | 360 | | | | | | 8.000 | 2.97E-06 |
| EDF | 1533-82 | 2a | TT | 19 | TS | plate | T-L | | | A | | | 36.5 | 360 | | | | | | 2.480 | 9.19E-07 |
| EDF | 1571-07 | RA737 | TT | 0 | HT | bar | L-R | 536 | | A | | | 10.0 | 325 | | | | | | 0.204 | 2.78E-08 |
| EDF | 1571-08 | RA737 | TT | 0 | HT | bar | L-R | 536 | | A | | | 13.1 | 325 | | | | | | 1.028 | 1.47E-07 |
| EDF | 1571-09 | RA737 | TT | 0 | HT | bar | L-R | 536 | | A | | | 21.8 | 325 | | | | | | 2.502 | 3.56E-07 |
| EDF | 1571-10 | RA737 | TT | 0 | HT | bar | L-R | 536 | | A | | | 35.4 | 325 | | | | | | 3.167 | 4.50E-07 |
| EDF | 1571-11 | RA737 | TT | 0 | HT | bar | L-R | 536 | | A | | | 80.3 | 325 | | | | | | 8.655 | 1.21E-06 |
| EDF | 1571-12 | RA737 | TT | 0 | HT | bar | C-R | 536 | | A | | | 42.1 | 325 | | | | | | 1.447 | 2.03E-07 |

**Table A-2 (continued)**
**Alloy 600 CGR database–Scored-out data**

| Laboratory | Overall Test ID | Heat | As Received Condition | Thickness Reduction (%) | Processing Method | Product Form | Orientation | Yield Strength (MPa) | Hardness (HV) | Test Segment ID | Test Segment Duration (h) | Load Type | K (MPa√m) | Temperature (°C) | Dissolved $H_2$ (cc/kg) | Hold Time (s) | Load Ratio | % Engaged | Post-Test Correction Factor | Measured Δa (mm) | Reported SCC CGR (mm/s) |
|---|---|---|---|---|---|---|---|---|---|---|---|---|---|---|---|---|---|---|---|---|---|
| EDF | 1571-13 | RA737 | TT | 0 | HT | bar | L-R | 541 | | A | | | 26.1 | 325 | | | | | | 0.639 | 9.17E-08 |
| EDF | 1571-14 | RA737 | TT | 0 | HT | bar | L-R | 541 | | A | | | 35.4 | 325 | | | | | | 1.674 | 2.39E-07 |
| EDF | 1571-15 | RA737 | TT | 0 | HT | bar | L-R | 541 | | A | | | 41.8 | 325 | | | | | | 1.214 | 1.69E-07 |
| EDF | 1571-16 | RA737 | TT | 0 | HT | bar | C-R | 541 | | A | | | 40.4 | 325 | | | | | | 0.289 | 4.17E-08 |
| EDF | D725-X1 | 3 | TT | 9 | TS | plate | T-L | | | A | | | 29.5 | 325 | | | | | | 0.300 | 4.17E-08 |
| EDF | D725-X2 | 3 | TT | 9 | TS | plate | T-L | | | A | | | 30.0 | 325 | | | | | | 0.310 | 4.44E-08 |
| EDF | D725-Y1 | 3 | TT | 19 | TS | plate | T-L | | | A | | | 30.5 | 325 | | | | | | 1.180 | 1.64E-07 |
| EDF | D725-Y2 | 3 | TT | 19 | TS | plate | T-L | | | A | | | 30.5 | 325 | | | | | | 1.760 | 2.44E-07 |
| Lockheed Martin | Specimen 13 | 44639 | MA | 0 | HAZ | plate | S-L | 255 | | A | | CL | 46.6 | 338 | 147 | | | | | | 2.01E-07 |
| Lockheed Martin | Specimen 2 | 44639 | MA | 0 | HAZ | plate | S-L | 255 | | A | | CL | 40.2 | 288 | 13 | | | | | | 2.91E-08 |
| Lockheed Martin | Specimen 3 | 44639 | MA | 0 | HAZ | plate | S-L | 255 | | A | | CL | 45.1 | 316 | 12 | | | | | | 1.68E-07 |
| Lockheed Martin | Specimen 4 | 44639 | MA | 0 | HAZ | plate | S-L | 255 | | A | | CL | 45.2 | 316 | 12 | | | | | | 1.50E-07 |
| Lockheed Martin | Specimen 6 | 44639 | MA | 0 | HAZ | plate | S-L | 255 | | A | | CL | 17.3 | 338 | 22 | | | | | | 1.99E-07 |
| Lockheed Martin | Specimen 7 | 44639 | MA | 0 | HAZ | plate | S-L | 255 | | A | | CL | 17.0 | 338 | 22 | | | | | | 1.89E-07 |
| PNNL | CT064 (DB-2) | M7929 | MA | 0 | None | CRDM | C-R | 296 | | 30 | 48 | CK | 32.0 | 325 | 29 | | | 100 | | 0.008 | 1.60E-08 |
| Westinghouse | 147-1 | WF147 | AR | 0 | None | bar | | 329 | | A | 939 | PPU | 37.2 | 326.6 | | 1200 | 0.67 | | | | 8.35E-08 |
| Westinghouse | 151-1 | WF151 | AR | 0 | None | bar | | 441 | | A | 1701 | PPU | 36.9 | 327.4 | | 1200 | 0.7 | | | | 1.68E-07 |
| Westinghouse | 20-1 | NX6420G | AR | 0 | None | CRDM | | 248.4 | | A | 1075 | PPU | 23.6 | 326.8 | | 1200 | 0.6 | | | | 5.71E-08 |
| Westinghouse | 22-3 | 7-74592-23 | AR | 0 | None | CRDM | | 352.2 | | A | 703 | PPU | 37.6 | 326.7 | | 1200 | 0.61 | | | | 1.31E-08 |
| Westinghouse | 22-4 | 7-74592-23 | AR | 0 | None | CRDM | | 352.2 | | A | 809 | PPU | 24.8 | 326.8 | | 1200 | 0.7 | | | | 5.10E-09 |
| Westinghouse | 43-2 | EO-6843 | AR | 0 | None | bar | | 376 | | A | 1251 | PPU | 36.1 | 326.7 | | 1200 | 0.62 | | | | 4.49E-08 |
| Westinghouse | 69-1 | 91069 | AR | 0 | None | CRDM | | 273.8 | | A | 1426 | PPU | 38.2 | 326.8 | | 1200 | 0.67 | | | | 4.04E-07 |
| Westinghouse | 69-1 | 91069 | AR | 0 | None | CRDM | | 273.8 | | B | 1426 | PPU | 44.9 | 326.8 | | 1200 | 0.67 | | | | 4.74E-07 |
| Westinghouse | 69-11 | 91069 | AR | 0 | None | CRDM | | 273.8 | | C | | PPU | 19.7 | 325.5 | | 1200 | 0.7 | | | | 2.85E-08 |
| Westinghouse | 69-11 | 91069 | AR | 0 | None | CRDM | | 273.8 | | D | | PPU | 19.7 | 325.5 | | 612 | 0.7 | | | | 3.93E-08 |
| Westinghouse | 69-3 | 91069 | AR | 0 | None | CRDM | | 273.8 | | A | 813 | PPU | 23.6 | 324.0 | | 1200 | 0.6 | | | | 1.37E-07 |
| Westinghouse | 69-5 | 91069 | AR | 0 | None | CRDM | | 273.8 | | B | | PPU | 14.8 | 331.1 | | 900 | 0.7 | | | | 7.89E-08 |
| Westinghouse | 75-4 | NX8101 | AR | 0 | None | CRDM | | 286.2 | | A | 2412 | PPU | 40.5 | 325.6 | | 1200 | 0.7 | | | | 7.70E-08 |

**Table A-3**
**Chemical compositions of all Alloy 600 heats tested in the CGR database, for which information was available**

| Heat | Composition | | | | | | | | | | | | | | | | | | |
|---|---|---|---|---|---|---|---|---|---|---|---|---|---|---|---|---|---|---|---|
| | Al | B | C | Co | Cr | Cu | Fe | Mg | Mn | Mo | N | Nb | Ni | O | P | S | Si | Ta | Ti |
| 2360 | — | — | 0.072 | 0.05 | 16.2 | 0.26 | 9.8 | — | 0.46 | — | — | — | — | — | <0.001 | <0.001 | 0.33 | — | — |
| 2510 | — | — | 0.015 | — | — | — | — | — | — | — | — | — | — | — | — | — | — | — | — |
| 22474 | 0.22 | — | 0.04 | 0.18 | 15.25 | 0.09 | 7.34 | — | 0.24 | — | — | 0.01 | 75.94 | — | 0.010 | 0.002 | 0.18 | 0.01 | 0.28 |
| 31907 | 0.22 | 0.0023 | 0.01 | 0.011 | 15.6 | <0.01 | 7.92 | — | 0.46 | 0.03 | — | — | 75.1 | — | 0.009 | 0.0002 | 0.22 | — | 0.28 |
| 91069 | — | — | 0.054 | 0.047 | 16.03 | 0.01 | 7.17 | — | 0.27 | — | — | — | 75.93 | — | — | 0.002 | 0.31 | — | — |
| 93510 | — | — | 0.047 | 0.057 | 15.4 | 0.01 | 8.94 | — | 0.23 | — | — | — | 74.4 | — | 0.005 | 0.002 | 0.3 | — | — |
| 93511 | — | — | 0.03 | 0.057 | 15.5 | 0.02 | 8.69 | — | 0.22 | — | — | — | 74.7 | — | 0.005 | 0.002 | 0.29 | — | — |
| 746301 | 0.27 | — | 0.051 | 0.013 | 15.8 | 0.006 | 10 | — | 0.79 | — | — | — | 72.3 | — | 0.008 | 0.003 | 0.41 | — | 0.41 |
| 7-74592-23 | — | — | 0.054 | 0.013 | 15.8 | 0.01 | 9.6 | — | 0.87 | — | — | — | 724 | — | 0.01 | 0.003 | 0.34 | — | — |
| C2649 | — | — | 0.047 | 0.015 | 15.30 | 0.02 | 8.93 | — | 0.39 | — | — | — | 74.4 | — | 0.002 | 0.002 | 0.36 | — | — |
| D2604DE | — | — | 0.03 | — | 16.73 | 0.01 | 7.67 | — | 0.29 | — | — | — | 75.5 | — | 0.008 | 0.001 | 0.29 | — | — |
| EO-6843 | — | — | 0.077 | 0.06 | 15.5 | 0.02 | 8.8 | — | 0.77 | — | — | — | 74.2 | — | 0.008 | 0.001 | 0.17 | — | — |
| H3262 | — | — | 0.052 | — | — | — | — | — | — | — | — | — | — | — | — | — | — | — | — |
| HB400 | — | — | 0.019 | 0.14 | 16.05 | 0.05 | 9.1 | — | 0.89 | — | — | — | 73.38 | — | <0.001 | <0.001 | 0.39 | — | — |
| HRH6503 | — | — | 0.067 | 0.86 | 15.14 | 0.32 | 9.79 | — | 0.31 | — | — | — | 73.26 | — | — | 0.004 | 0.24 | — | — |
| LM-600 | 0.17 | 0.003 | 0.07 | 0.04 | 15.54 | 0.11 | 7.76 | 0.01 | 0.25 | — | — | — | 75.4 | — | 0.007 | <0.001 | 0.29 | — | 0.35 |
| M3935 | — | — | 0.28 | 0.01 | 15.58 | 0.01 | 6.25 | — | 0.27 | — | — | — | 77.89 | — | 0.004 | 0.002 | 0.37 | — | 0.25 |
| NX8101 | — | — | 0.07 | 0.03 | 15.42 | 0.28 | 9.04 | — | 0.29 | — | — | — | 74.59 | — | — | 0.003 | 0.2 | — | — |
| NX8168G | — | — | 0.07 | 0.09 | 15.16 | 0.35 | 8.52 | — | 0.31 | — | — | — | 75.37 | — | — | 0.003 | 0.24 | — | — |
| NX9240 | — | — | 0.053 | 0.04 | 15.27 | 0.12 | 8.32 | — | 0.25 | — | — | — | 75.08 | — | 0.008 | <0.001 | 0.3 | — | — |
| PYE7704 | — | — | 0.08 | 0.1 | 15.49 | 0.11 | 8.35 | — | 0.24 | — | — | — | 75.537 | — | — | 0.002 | 0.19 | — | — |
| RA737 | — | 0.049 | 0.01 | 16.2 | 0.0 | 9.7 | — | 0.87 | — | — | — | — | — | <0.001 | <0.001 | 0.3 | — | — | — |
| WA327 | — | — | 0.024 | 0.01 | 15.91 | 0.01 | 8.1 | — | 0.75 | — | — | — | 74.6 | — | — | 0.001 | 0.28 | — | — |
| WF147 | — | — | 0.033 | 0.18 | 15.69 | 0.02 | 9.65 | — | 0.78 | — | — | — | 73.07 | — | 0.009 | 0.001 | 0.29 | — | — |
| WF151 | — | — | 0.029 | 0.022 | 15.83 | 0.02 | 9.46 | — | 0.78 | — | — | — | 73.18 | — | 0.009 | 0.0007 | 0.25 | — | — |
| WF675 | — | — | 0.061 | 0.047 | 16.03 | 0.02 | 8.63 | — | 0.78 | — | — | — | 73.6 | — | 0.011 | 0.001 | 0.34 | — | — |
| WH220 | — | — | 0.030 | <0.001 | 15.8 | 0.01 | 9.30 | — | 0.79 | — | — | — | — | — | — | <0.001 | 0.31 | — | — |
| WJ797 | — | — | 0.061 | — | — | — | — | — | — | — | — | — | — | — | — | — | — | — | — |

**Table A-4**
**Alloy 82/182/132 CGR database–Scored-in data**

| Laboratory | Alloy | Overall Test ID | Weld | Post-Supplier Processing | Orientation | Segment ID | Test Segment Duration (h) | Load Type | K (MPa√m) | Temperature (°C) | Dissolved $H_2$ (cc/kg) | Hold Time (s) | Load Ratio | % Engaged | Post-Test Correction Factor | Measured Δa (mm) | Reported SCC CGR (mm/s) |
|---|---|---|---|---|---|---|---|---|---|---|---|---|---|---|---|---|---|
| ANL | 182 | A182-1 | A182-1 | AW | T-S | 4 | 597 | CL | 33.7 | 322.1 | 23 | | | 100 | 2.60 | 0.991 | 5.88E-07 |
| ANL | 182 | A182-1 | A182-1 | AW | T-S | 5 | 1312 | CL | 34.5 | 307.3 | 15 | | | 100 | 2.60 | 0.500 | 1.23E-07 |
| ANL | 182 | A182-1 | A182-1 | AW | T-S | 6 | 1206 | CL | 35.2 | 291.1 | 11 | | | 100 | 2.60 | 0.356 | 3.63E-08 |
| ANL | 182 | A182-1 | A182-1 | AW | T-S | 7 | 837 | CL | 37.8 | 321.4 | 23 | | | 100 | 2.60 | 1.505 | 4.95E-07 |
| ANL | 182 | BCR-01 | VCS-182 | AW | C-R | 1 | 311 | CL | 20.8 | 320 | 23 | | | 100 | 1.34 | 0.043 | 2.35E-08 |
| ANL | 182 | BCR-01 | VCS-182 | AW | C-R | 4 | 332 | CL | 25.4 | 320 | 23 | | | 100 | 1.34 | 0.016 | 2.34E-08 |
| ANL | 182 | BCR-01 | VCS-182 | AW | C-R | 8 | 401 | CL | 30.2 | 320 | 23 | | | 100 | 1.34 | 0.025 | 4.49E-08 |
| ANL | 182 | BCR-01 | VCS-182 | AW | C-R | 12 | 356 | CL | 33.9 | 320 | 23 | | | 100 | 1.34 | 0.029 | 4.31E-08 |
| ANL | 182 | CT31-W01 | CT31 | AW | T-S | 10 | 356 | PPU | 29 | 320 | 23 | 3600 | 0.7 | 90 | 2.10 | 0.103 | 9.79E-08 |
| ANL | 182 | CT31-W02 | CT31 | AW | T-S | 3 | 240 | CL | 30.5 | 320 | 23 | | | 100 | 2.60 | 0.134 | 1.55E-07 |
| ANL | 182 | CT31-W02 | CT31 | AW | T-S | 4 | 213 | CL | 36.4 | 320 | 23 | | | 100 | 2.60 | 0.122 | 1.59E-07 |
| ANL | 182 | CT31-W02 | CT31 | AW | T-S | 5 | 345 | CL | 49.5 | 320 | 23 | | | 100 | 2.60 | 1.088 | 7.29E-07 |
| ANL | 182 | CT933H-1 | CT933 | AW | T-S | 4 | 1967 | CL | 26 | 310 | 18 | | | 60 | 4.30 | 0.334 | 5.88E-08 |
| ANL | 182 | CT933H-1 | CT933 | AW | T-S | 5 | 1609 | CL | 26.7 | 300 | 14 | | | 60 | 4.30 | 0.075 | 1.25E-08 |
| ANL | 182 | CT933H-1 | CT933 | AW | T-S | 6 | 674 | CL | 26.8 | 290 | 11 | | | 60 | 4.30 | 0.048 | 2.68E-08 |
| ANL | 182 | CT933H-1 | CT933 | AW | T-S | 7 | 1902 | CL | 27.1 | 310 | 18 | | | 60 | 4.30 | 0.148 | 3.62E-08 |
| ANL | 182 | CT933H-2 | CT933 | AW | T-S | 6 | 660 | CL | 23.4 | 351 | 47 | | | 100 | 3.00 | 0.170 | 6.49E-08 |
| ANL | 182 | CT933H-2 | CT933 | AW | T-S | 9 | 67 | CL | 25.9 | 351 | 47 | | | 100 | 3.00 | 0.046 | 1.06E-07 |
| ANL | 182 | CT933H-2 | CT933 | AW | T-S | 12 | 375 | CL | 26.8 | 351 | 47 | | | 100 | 3.00 | 0.034 | 4.65E-08 |
| ANL | 182 | CT933H-2 | CT933 | AW | T-S | 13 | 711 | CL | 27 | 320 | 23 | | | 100 | 3.00 | 0.424 | 1.36E-07 |
| ANL | 182 | CT933H-2 | CT933 | AW | T-S | 14 | 812 | CL | 28.8 | 291 | 11 | | | 100 | 3.00 | 0.082 | 2.72E-08 |
| ANL | 182 | CT933H-2 | CT933 | AW | T-S | 15 | 162 | CL | 29.3 | 352 | 47 | | | 100 | 3.00 | 0.138 | 4.53E-07 |
| ANL | 182 | CT933H-2 | CT933 | AW | T-S | 17 | 860 | CL | 35.2 | 352 | 47 | | | 100 | 3.00 | 0.044 | 6.59E-08 |
| ANL | 182 | CT933-LS | CT933 | AW | L-S | 3 | 619 | CL | 28.7 | 320 | 23 | | | 100 | 2.30 | 0.244 | 1.10E-07 |
| ANL | 182 | CT933-LS | CT933 | AW | L-S | 4 | 829 | CL | 44.8 | 320 | 23 | | | 100 | 2.30 | 1.965 | 6.54E-07 |
| ANL | 182 | CT933-TL | CT933 | AW | T-L | 5 | 262 | CL | 21.8 | 320 | 23 | | | 100 | 1.06 | 0.078 | 4.46E-08 |
| ANL | 182 | CT933-TL | CT933 | AW | T-L | 11 | 266 | CL | 31 | 320 | 23 | | | 100 | 1.06 | 0.089 | 9.04E-08 |
| ANL | 182 | CT933-TL | CT933 | AW | T-L | 15 | 194 | CL | 35.4 | 320 | 23 | | | 100 | 1.06 | 0.154 | 8.10E-08 |
| ANL | 182 | CT933-TL | CT933 | AW | T-L | 20 | 474 | CL | 50 | 320 | 23 | | | 100 | 1.06 | 0.270 | 1.57E-07 |
| ANL | 182 | CT933-TS | CT933 | AW | T-S | 6 | 260 | PPU | 28.6 | 320 | 23 | 3600 | 0.7 | 50 | 1.65 | 0.063 | 1.05E-07 |
| ANL | 182 | CT933-TS | CT933 | AW | T-S | 7 | 168 | CL | 28.7 | 320 | 23 | | | 50 | 1.65 | 0.063 | 1.05E-07 |
| ANL | 182 | CT933-TS | CT933 | AW | T-S | 10 | 343 | CL | 36.9 | 320 | 23 | | | 50 | 1.65 | 0.763 | 2.53E-07 |
| ANL | 182 | J11CC-1 | Davis-Besse-182 | AW | C-R | 13 | 400 | CL | 30.3 | 316 | 23 | | | 50 | 1.60 | 0.050 | 1.63E-08 |
| ANL | 82 | WLR-01 | VCS-82 | AW | L-R | 4 | 337 | CL | 24.7 | 320 | 23 | | | 100 | 1.91 | 0.005 | 2.07E-08 |
| ANL | 82 | WLR-01 | VCS-82 | AW | L-R | 14 | 835 | CL | 49.8 | 320 | 23 | | | 100 | 1.91 | 0.218 | 7.71E-08 |
| AREVA | 82 | 82.08 | MNPK3 | AW | T-S | 6 | 400 | CL | 27.3 | 340 | 25 | | | 97 | 1.2 | 2.411 | 3.72E-08 |
| AREVA | 82 | 82.09 | MNPK3 | HT | T-S | 6 | 400 | CL | 27.3 | 340 | 25 | | | 99 | 1.2 | 1.879 | 2.90E-08 |

**Table A-4 (continued)**
**Alloy 82/182/132 CGR database–Scored-in data**

| Laboratory | Alloy | Overall Test ID | Weld | Post-Supplier Processing | Orientation | Segment ID | Test Segment Duration (h) | Load Type | K (MPa√m) | Temperature (°C) | Dissolved $H_2$ (cc/kg) | Hold Time (s) | Load Ratio | % Engaged | Post-Test Correction Factor | Measured Δa (mm) | Reported SCC CGR (mm/s) |
|---|---|---|---|---|---|---|---|---|---|---|---|---|---|---|---|---|---|
| Bettis | 82H | 21.01 | Bettis-82H | HT | | A | 1750 | PPU | 22.3 | 338 | 50 | 6000 | 0.7 | | | | 9.91E-09 |
| Bettis | 82H | 21.02 | Bettis-82H | HT | | A | 1750 | PPU | 22.7 | 338 | 50 | 6000 | 0.7 | | | | 1.13E-08 |
| Bettis | 82H | 21.03 | Bettis-82H | HT | | A | 1750 | PPU | 35.1 | 338 | 50 | 6000 | 0.7 | | | | 2.56E-08 |
| Bettis | 82H | 21.04 | Bettis-82H | HT | | A | 1750 | PPU | 36.2 | 338 | 50 | 6000 | 0.7 | | | | 2.92E-08 |
| Bettis | 82H | 21.05 | Bettis-82H | HT | | A | 1750 | PPU | 23 | 316 | 50 | 6000 | 0.7 | | | | 4.58E-09 |
| Bettis | 82H | 21.07 | Bettis-82H | HT | | A | 1750 | PPU | 35.3 | 316 | 50 | 6000 | 0.7 | | | | 1.22E-08 |
| Bettis | 82H | 21.08 | Bettis-82H | HT | | A | 1750 | PPU | 37.1 | 316 | 50 | 6000 | 0.7 | | | | 1.17E-08 |
| Bettis | 82 | 16AW-1 | 16 | AW | T-S | A | | | 28.8 | 338 | 25 | 86400 | 0.7 | | | | 1.42E-07 |
| Bettis | 82 | 16AW-10 | 16 | AW | T-S | A | | | 46.6 | 338 | 50 | 86400 | 0.7 | | | | 1.55E-07 |
| Bettis | 82 | 16AW-11 | 16 | AW | T-S | A | | | 44.5 | 338 | 50 | 86400 | 0.7 | | | | 3.34E-07 |
| Bettis | 82 | 16AW-2 | 16 | AW | T-S | A | | | 28.4 | 338 | 25 | 86400 | 0.7 | | | | 1.07E-07 |
| Bettis | 82 | 16AW-3 | 16 | AW | T-S | A | | | 43.3 | 338 | 25 | 86400 | 0.7 | | | | 3.73E-07 |
| Bettis | 82 | 16AW-4 | 16 | AW | T-S | A | | | 44.5 | 338 | 25 | 86400 | 0.7 | | | | 4.44E-07 |
| Bettis | 82 | 16AW-5 | 16 | AW | T-S | A | | | 44.3 | 338 | 25 | 86400 | 0.7 | | | | 4.96E-07 |
| Bettis | 82 | 16AW-6 | 16 | AW | T-S | A | | | 50 | 338 | 25 | 86400 | 0.7 | | | | 3.57E-07 |
| Bettis | 82 | 16AW-7 | 16 | AW | T-S | A | | | 54.5 | 338 | 25 | 86400 | 0.7 | | | | 4.96E-07 |
| Bettis | 82 | 16AW-8 | 16 | AW | T-S | A | | | 28 | 338 | 50 | 86400 | 0.7 | | | | 7.36E-08 |
| Bettis | 82 | 16AW-9 | 16 | AW | T-S | A | | | 27.8 | 338 | 50 | 86400 | 0.7 | | | | 6.31E-08 |
| Bettis | 82 | 16SR-1 | 16 | HT | T-S | A | | | 27.8 | 338 | 25 | 86400 | 0.7 | | | | 6.04E-08 |
| Bettis | 82 | 16SR-2 | 16 | HT | T-S | A | | | 27.5 | 338 | 25 | 86400 | 0.7 | | | | 3.06E-08 |
| Bettis | 82 | 16SR-3 | 16 | HT | T-S | A | | | 26.9 | 338 | 25 | 86400 | 0.7 | | | | 1.55E-08 |
| Bettis | 82 | 16SR-4 | 16 | HT | T-S | A | | | 27 | 338 | 25 | 86400 | 0.7 | | | | 1.12E-08 |
| Bettis | 82 | 16SR-5 | 16 | HT | T-S | A | | | 43.2 | 338 | 25 | 86400 | 0.7 | | | | 5.41E-08 |
| Bettis | 82 | 16SR-6 | 16 | HT | T-S | A | | | 44 | 338 | 25 | 86400 | 0.7 | | | | 7.20E-08 |
| Bettis | 82 | 16SR-7 | 16 | HT | T-S | A | | | 26.9 | 338 | 50 | 86400 | 0.7 | | | | 1.19E-08 |
| Bettis | 82 | 16SR-8 | 16 | HT | T-S | A | | | 43.8 | 338 | 50 | 86400 | 0.7 | | | | 1.00E-08 |
| Bettis | 82 | 16SR-9 | 16 | HT | T-S | A | | | 43.7 | 338 | 50 | 86400 | 0.7 | | | | 3.73E-08 |
| Bettis | 82H | 21TSL-4 | Bettis-82H | HT | | A | 1750 | PPU | 23.2 | 316 | 50 | 6000 | 0.7 | | | | 7.33E-09 |
| Bettis | 82 | 23HT-1 | 7D | HT | T-S | A | | | 33 | 338 | 52 | 86400 | 0.7 | | | | 4.70E-08 |
| Bettis | 82 | 23HT-2 | 7D | HT | T-S | A | | | 32.1 | 338 | 52 | 86400 | 0.7 | | | | 8.72E-08 |
| Bettis | 82 | 23HT-3 | 7D | HT | T-S | A | | | 34.1 | 338 | 52 | 86400 | 0.7 | | | | 1.02E-07 |
| Bettis | 82 | 23HT-4 | 7D | HT | T-S | A | | | 35.2 | 338 | 52 | 86400 | 0.7 | | | | 9.34E-08 |
| Bettis | 82 | 23TLL-1 | 7D | AW | T-L | A | 2042 | PPU | 38.9 | 338 | 52 | 6000 | 0.7 | 100 | | 1.750 | 2.38E-07 |
| Bettis | 82 | 23TLL-2 | 7D | AW | T-L | A | 4272 | PPU | 22 | 338 | 50 | 6000 | 0.7 | 94 | | 0.874 | 5.67E-08 |
| Bettis | 82 | 23TLL-3 | 7D | AW | T-L | A | 4001 | PPU | 35.5 | 316 | 52 | 6000 | 0.7 | 92 | | 0.711 | 4.94E-08 |
| Bettis | 82 | 23TSL-1 | 7D | AW | T-S | A | 4272 | PPU | 22 | 338 | 50 | 6000 | 0.7 | 81 | | 0.836 | 5.44E-08 |
| Bettis | 82 | 23TSL-2 | 7D | AW | T-S | A | 2042 | PPU | 38.2 | 338 | 52 | 6000 | 0.7 | 89 | | 2.370 | 3.23E-07 |

**Table A-4 (continued)**
**Alloy 82/182/132 CGR database–Scored-in data**

| Laboratory | Alloy | Overall Test ID | Weld | Post-Supplier Processing | Orientation | Segment ID | Test Segment Duration (h) | Load Type | K (MPa√m) | Temperature (°C) | Dissolved $H_2$ (cc/kg) | Hold Time (s) | Load Ratio | % Engaged | Post-Test Correction Factor | Measured Δa (mm) | Reported SCC CGR (mm/s) |
|---|---|---|---|---|---|---|---|---|---|---|---|---|---|---|---|---|---|
| Bettis | 82 | 23TSL-3 | 7D | AW | T-S | A | 4001 | PPU | 32.9 | 316 | 51 | 6000 | 0.7 | 78 | | 0.716 | 4.97E-08 |
| Bettis | 82 | 23TSL-7 | 7D | AW | T-S | A | 2059 | PPU | 32.9 | 338 | 51 | 6000 | 0.7 | 94 | | 1.690 | 2.29E-07 |
| Bettis | 82 | 8DAW-1 | 8D | AW | T-S | A | | | 29.1 | 338 | 25 | 86400 | 0.7 | | | | 8.10E-08 |
| Bettis | 82 | 8DAW-10 | 8D | AW | T-S | A | | | 40.1 | 338 | 50 | 86400 | 0.7 | | | | 4.59E-08 |
| Bettis | 82 | 8DAW-2 | 8D | AW | T-S | A | | | 30.1 | 338 | 25 | 86400 | 0.7 | | | | 7.29E-08 |
| Bettis | 82 | 8DAW-3 | 8D | AW | T-S | A | | | 30.8 | 338 | 25 | 86400 | 0.7 | | | | 1.62E-07 |
| Bettis | 82 | 8DAW-4 | 8D | AW | T-S | A | | | 39.4 | 338 | 25 | 86400 | 0.7 | | | | 2.80E-07 |
| Bettis | 82 | 8DAW-5 | 8D | AW | T-S | A | | | 43.4 | 338 | 25 | 86400 | 0.7 | | | | 5.73E-07 |
| Bettis | 82 | 8DAW-6 | 8D | AW | T-S | A | | | 34.1 | 338 | 50 | 86400 | 0.7 | | | | 3.35E-08 |
| Bettis | 82 | 8DAW-7 | 8D | AW | T-S | A | | | 35.7 | 338 | 50 | 86400 | 0.7 | | | | 4.79E-08 |
| Bettis | 82 | 8DAW-8 | 8D | AW | T-S | A | | | 36.6 | 338 | 50 | 86400 | 0.7 | | | | 4.13E-08 |
| Bettis | 82 | 8DAW-9 | 8D | AW | T-S | A | | | 39.4 | 338 | 50 | 86400 | 0.7 | | | | 4.69E-08 |
| Bettis | 82 | 8DSR-1 | 8D | HT | T-S | A | | | 29.1 | 338 | 25 | 86400 | 0.7 | | | | 7.29E-08 |
| Bettis | 82 | 8DSR-2 | 8D | HT | T-S | A | | | 31.5 | 338 | 25 | 86400 | 0.7 | | | | 8.10E-08 |
| Bettis | 82 | 8DSR-3 | 8D | HT | T-S | A | | | 31.3 | 338 | 25 | 86400 | 0.7 | | | | 1.66E-07 |
| Bettis | 82 | 8DSR-4 | 8D | HT | T-S | A | | | 41.5 | 338 | 25 | 86400 | 0.7 | | | | 2.80E-07 |
| Bettis | 82 | 8DSR-5 | 8D | HT | T-S | A | | | 46.3 | 338 | 25 | 86400 | 0.7 | | | | 5.73E-07 |
| Bettis | 82 | 8DSR-6 | 8D | HT | T-S | A | | | 34.1 | 338 | 50 | 86400 | 0.7 | | | | 3.96E-08 |
| Bettis | 82 | 8DSR-7 | 8D | HT | T-S | A | | | 42.5 | 338 | 50 | 86400 | 0.7 | | | | 6.43E-08 |
| Bettis | 182 | 8N12TS-1 | Bettis-182 | AW | T-S | A | 1171 | PPU | 22.5 | 337 | 49 | 6000 | 0.7 | 82 | | 0.478 | 1.13E-07 |
| Bettis | 182 | 8N12TS-10 | Bettis-182 | AW | T-S | A | 1867 | PPU | 32 | 316 | 52 | 6000 | 0.7 | 56 | | 0.178 | 2.68E-08 |
| Bettis | 182 | 8N12TS-2 | Bettis-182 | AW | T-S | A | 1171 | PPU | 34.8 | 337 | 49 | 6000 | 0.7 | 100 | | 1.170 | 2.79E-07 |
| Bettis | 182 | 8N12TS-3 | Bettis-182 | AW | T-S | A | 2484 | PPU | 21.2 | 315 | 51 | 6000 | 0.7 | 78 | | 0.323 | 3.59E-08 |
| Bettis | 182 | 8N12TS-4 | Bettis-182 | AW | T-S | A | 2484 | PPU | 34.2 | 315 | 51 | 6000 | 0.7 | 100 | | 0.838 | 9.38E-08 |
| Bettis | 182 | 8N12TS-7 | Bettis-182 | AW | T-S | A | 1682 | PPU | 22 | 337 | 49 | 6000 | 0.7 | 81 | | 0.544 | 8.97E-08 |
| Bettis | 182 | 8N12TS-8 | Bettis-182 | AW | T-S | A | 1682 | PPU | 34.4 | 337 | 49 | 6000 | 0.7 | 100 | | 1.270 | 2.09E-07 |
| Bettis | 82H | A-1 | A-1 | AW | T-L | A | | CL/CK | 47.1 | 338 | 50 | | | 100 | | | 2.85E-07 |
| Bettis | 82H | A-1 | A-1 | AW | T-L | B | | CL/CK | 44.3 | 338 | 50 | | | 100 | | | 2.78E-07 |
| Bettis | 82H | A-1 | A-1 | AW | T-L | C | | CL/CK | 41.5 | 338 | 50 | | | 94 | | | 1.17E-07 |
| Bettis | 82H | C-1 | C-1 | AW | T-L | A | | CL/CK | 51.3 | 338 | 50 | | | 100 | | | 6.43E-07 |
| Bettis | 82H | C-1 | C-1 | AW | T-L | B | | CL/CK | 53 | 338 | 50 | | | 100 | | | 2.35E-07 |
| Bettis | 82H | C-1 | C-1 | AW | T-L | C | | CL/CK | 40.2 | 338 | 50 | | | 98 | | | 2.14E-07 |
| Bettis | 82H | C-2 | C-2 | AW | T-L | A | | CL/CK | 49.5 | 338 | 50 | | | 98 | | | 4.03E-07 |
| Bettis | 82H | C-2 | C-2 | AW | T-L | B | | CL/CK | 48.3 | 338 | 50 | | | 69 | | | 7.81E-08 |
| Bettis | 82H | C-3 | C-3 | AW | T-S | A | | CL/CK | 52.5 | 338 | 50 | | | 100 | | | 7.29E-07 |
| Bettis | 82H | C-4 | C-4 | AW | T-S | A | | CL/CK | 56.8 | 338 | 50 | | | 100 | | | 3.14E-07 |
| Bettis | 82H | C-4 | C-4 | AW | T-S | B | | PPU | 55.6 | 338 | 50 | 6000 | 0.65 | 75 | | | 1.69E-07 |

**Table A-4 (continued)**
**Alloy 82/182/132 CGR database–Scored-in data**

| Laboratory | Alloy | Overall Test ID | Weld | Post-Supplier Processing | Orientation | Segment ID | Test Segment Duration (h) | Load Type | K (MPa√m) | Temperature (°C) | Dissolved $H_2$ (cc/kg) | Hold Time (s) | Load Ratio | % Engaged | Post-Test Correction Factor | Measured Δa (mm) | Reported SCC CGR (mm/s) |
|---|---|---|---|---|---|---|---|---|---|---|---|---|---|---|---|---|---|
| Bettis | 82H | C-4 | C-4 | AW | T-S | C | | PPU | 49.4 | 338 | 50 | 6000 | 0.65 | 94 | | | 1.48E-07 |
| Bettis | 82H | C-4 | C-4 | AW | T-S | D | | CL/CK | 46.1 | 338 | 50 | | | 96 | | | 1.27E-07 |
| Bettis | 82H | C-4 | C-4 | AW | T-S | E | | CL/CK | 46.1 | 338 | 50 | | | 100 | | | 9.44E-08 |
| Bettis | 82H | C-4 | C-4 | AW | T-S | F | | CL/CK | 46.5 | 338 | 50 | | | 88 | | | 8.67E-08 |
| Bettis | 82 | M2AW-1 | NGW-2 | AW | T-S | A | | | 42.7 | 338 | 25 | 86400 | 0.7 | | | | 1.77E-07 |
| Bettis | 82 | M2AW-2 | NGW-2 | AW | T-S | A | | | 42.5 | 338 | 25 | 86400 | 0.7 | | | | 2.28E-07 |
| Bettis | 82 | M2AW-3 | NGW-2 | AW | T-S | A | | | 43.1 | 338 | 25 | 86400 | 0.7 | | | | 2.43E-07 |
| Bettis | 82 | M2SR-1 | NGW-2 | HT | T-S | A | | | 40.5 | 338 | 25 | 86400 | 0.7 | | | | 3.63E-08 |
| Bettis | 82 | M2SR-2 | NGW-2 | HT | T-S | A | | | 40.2 | 338 | 25 | 86400 | 0.7 | | | | 4.21E-08 |
| Bettis | 82 | M2SR-3 | NGW-2 | HT | T-S | A | | | 40.7 | 338 | 25 | 86400 | 0.7 | | | | 5.09E-08 |
| Bettis | 82 | M2SR-4 | NGW-2 | HT | T-S | A | | | 41.5 | 338 | 25 | 86400 | 0.7 | | | | 4.58E-08 |
| Bettis | 82 | MAW-1 | NGW-1 | AW | T-S | A | | | 27.6 | 338 | 25 | 86400 | 0.7 | | | | 5.29E-08 |
| Bettis | 82 | MAW-2 | NGW-1 | AW | T-S | A | | | 27.8 | 338 | 25 | 86400 | 0.7 | | | | 6.82E-08 |
| Bettis | 82 | MAW-3 | NGW-1 | AW | T-S | A | | | 28.9 | 338 | 25 | 86400 | 0.7 | | | | 8.44E-08 |
| Bettis | 82 | MAW-4 | NGW-1 | AW | T-S | A | | | 28.4 | 338 | 25 | 86400 | 0.7 | | | | 1.02E-07 |
| Bettis | 82 | MAW-5 | NGW-1 | AW | T-S | A | | | 41.3 | 338 | 25 | 86400 | 0.7 | | | | 3.35E-07 |
| Bettis | 82 | MAW-6 | NGW-1 | AW | T-S | A | | | 42.4 | 338 | 25 | 86400 | 0.7 | | | | 3.21E-07 |
| Bettis | 82 | MAW-7 | NGW-1 | AW | T-S | A | | | 43.4 | 338 | 25 | 86400 | 0.7 | | | | 3.08E-07 |
| Bettis | 82 | MAW-8 | NGW-1 | AW | T-S | A | | | 43.4 | 338 | 25 | 86400 | 0.7 | | | | 4.23E-07 |
| Bettis | 82 | MSR-1 | NGW-1 | HT | T-S | A | | | 24.9 | 338 | 25 | 86400 | 0.7 | | | | 9.48E-09 |
| Bettis | 82 | MSR-2 | NGW-1 | HT | T-S | A | | | 25.1 | 338 | 25 | 86400 | 0.7 | | | | 1.15E-08 |
| Bettis | 82 | MSR-3 | NGW-1 | HT | T-S | A | | | 25.6 | 338 | 25 | 86400 | 0.7 | | | | 1.61E-08 |
| Bettis | 82 | MSR-4 | NGW-1 | HT | T-S | A | | | 40.6 | 338 | 25 | 86400 | 0.7 | | | | 1.58E-08 |
| Bettis | 82 | MSR-5 | NGW-1 | HT | T-S | A | | | 40.8 | 338 | 25 | 86400 | 0.7 | | | | 1.65E-08 |
| Bettis | 82 | MSR-6 | NGW-1 | HT | T-S | A | | | 40.5 | 338 | 25 | 86400 | 0.7 | | | | 2.31E-08 |
| GE-GRC | 182 | c346 | 414998 | AW | T-S | A | 650 | CK | 27.5 | 325 | 80 | | | | | 0.012 | 5.00E-09 |
| GE-GRC | 182 | c370 | 414998 | AW | T-S | A | 383 | CK | 30.8 | 325 | 10.4 | | | | | 0.267 | 2.10E-07 |
| GE-GRC | 182 | c370 | 414998 | AW | T-S | B | 769 | CK | 30.8 | 325 | 26 | | | | | 0.302 | 9.10E-08 |
| GE-GRC | 182 | c370 | 414998 | AW | T-S | C | 1705 | CK | 35.2 | 325 | 80 | | | | | 0.043 | 2.00E-08 |
| GE-GRC | 182 | c370 | 414998 | AW | T-S | D | 1587 | CK | 35.2 | 325 | 10.4 | | | | | 0.674 | 1.00E-07 |
| GE-GRC | 182 | c370 | 414998 | AW | T-S | E | 696 | CK | 36.5 | 325 | 1.35 | | | | | 0.064 | 1.30E-08 |
| GE-GRC | 182 | c370 | 414998 | AW | T-S | F | 1078 | CK | 38.5 | 325 | 10.4 | | | | | 0.310 | 8.30E-08 |
| GE-GRC | 182 | c370 | 414998 | AW | T-S | G | 1078 | CK | 38.5 | 325 | 10.4 | | | | | 0.050 | 1.30E-08 |
| GE-GRC | 182 | c380 | 414998 | AW | T-S | A | 620 | CK | 37.4 | 325 | 10.4 | | | | | 0.255 | 1.20E-07 |
| GE-GRC | 182 | c380 | 414998 | AW | T-S | B | 1079 | CK | 38 | 325 | 26 | | | | | 0.173 | 3.80E-08 |
| GE-GRC | 182 | c380 | 414998 | AW | T-S | D | 694 | CK | 39.6 | 325 | 10.4 | | | | | 0.532 | 2.50E-07 |
| GE-GRC | 182 | c380 | 414998 | AW | T-S | E | 1073 | CK | 43 | 325 | 4.16 | | | | | 0.264 | 1.20E-07 |

**Table A-4 (continued)**
**Alloy 82/182/132 CGR database–Scored-in data**

| Laboratory | Alloy | Overall Test ID | Weld | Post-Supplier Processing | Orientation | Segment ID | Test Segment Duration (h) | Load Type | K (MPa√m) | Temperature (°C) | Dissolved $H_2$ (cc/kg) | Hold Time (s) | Load Ratio | % Engaged | Post-Test Correction Factor | Measured Δa (mm) | Reported SCC CGR (mm/s) |
|---|---|---|---|---|---|---|---|---|---|---|---|---|---|---|---|---|---|
| GE-GRC | 182 | c380 | 414998 | AW | T-S | F | 1079 | CK | 44 | 325 | 10.4 | | | | | 0.623 | 2.00E-07 |
| GE-GRC | 182 | c380 | 414998 | AW | T-S | G | 802 | CK | 44 | 325 | 10.4 | | | | | 0.216 | 8.40E-08 |
| GE-GRC | 182 | c385 | 414998 | AW | T-S | A | 756 | CK | 32 | 325 | 10.4 | | | | | 0.394 | 1.10E-07 |
| GE-GRC | 182 | c386 | 414998 | AW | T-S | A | 359 | CK | 27.5 | 325 | 80 | | | | | 0.007 | 6.00E-09 |
| GE-GRC | 182 | c398 | 414998 | AW | T-S | A | 167 | CK | 38 | 325 | 10.4 | | | | | 0.084 | 1.40E-07 |
| GE-GRC | 182 | c398 | 414998 | AW | T-S | B | 344 | CK | 38 | 325 | 25 | | | | | 0.104 | 9.50E-08 |
| GE-GRC | 182 | c398 | 414998 | AW | T-S | C | 1028 | CK | 39 | 325 | 41 | | | | | 0.004 | 2.00E-09 |
| GE-GRC | 182 | c398 | 414998 | AW | T-S | D | 620 | CK | 39 | 325 | 10.4 | | | | | 0.509 | 2.10E-07 |
| GE-GRC | 182 | c398 | 414998 | AW | T-S | E | 574 | CK | 40 | 325 | 2.6 | | | | | 0.101 | 1.00E-07 |
| GE-GRC | 182 | c398 | 414998 | AW | T-S | F | 935 | CK | 41 | 325 | 5.2 | | | | | 0.050 | 3.00E-09 |
| GE-GRC | 182 | c398 | 414998 | AW | T-S | G | 1923 | CK | 42 | 325 | 10.4 | | | | | 0.647 | 1.00E-07 |
| GE-GRC | 182 | c399 | 414998 | AW | T-S | A | 167 | CK | 46 | 340 | 15.3 | | | | | 0.089 | 1.30E-07 |
| GE-GRC | 182 | c399 | 414998 | AW | T-S | B | 341 | CK | 47 | 340 | 35 | | | | | 0.092 | 7.00E-08 |
| GE-GRC | 182 | c399 | 414998 | AW | T-S | C | 742 | CK | 47 | 340 | 52 | | | | | 0.016 | 2.00E-08 |
| GE-GRC | 182 | c399 | 414998 | AW | T-S | D | 282 | CK | 47 | 340 | 15.3 | | | | | 0.217 | 1.60E-07 |
| GE-GRC | 182 | c408 | 414998 | AW | T-S | A | 406 | CK | 31 | 340 | 5.2 | | | | | 0.058 | 9.20E-08 |
| GE-GRC | 182 | c408 | 414998 | AW | T-S | B | 400 | CK | 31 | 340 | 15.3 | | | | | 0.483 | 5.40E-07 |
| GE-GRC | 182 | c408 | 414998 | AW | T-S | C | 360 | CK | 31 | 340 | 41 | | | | | 0.247 | 1.80E-07 |
| GE-GRC | 182 | c408 | 414998 | AW | T-S | D | 1487 | CK | 31 | 340 | 80 | | | | | 0.197 | 8.00E-08 |
| GE-GRC | 182 | c408 | 414998 | AW | T-S | E | 366 | CK | 31 | 340 | 15.3 | | | | | 0.305 | 5.00E-07 |
| GE-GRC | 182 | c410 | 414998 | AW | T-S | A | 856 | CK | 29.7 | 325 | 10.4 | | | | | 0.119 | 4.70E-08 |
| GE-GRC | 182 | c410 | 414998 | AW | T-S | B | 323 | CK | 29.7 | 325 | 10.4 | | | | | 0.056 | 4.70E-08 |
| GE-GRC | 182 | c410 | 414998 | AW | T-S | C | 2199 | CK | 29.7 | 325 | 10.4 | | | | | 0.233 | 2.70E-08 |
| GE-GRC | 82H | c419 | HD78-1 | AW | T-S | A | 600 | CK | 30.8 | 340 | 15.3 | | | | | 0.266 | 1.30E-07 |
| GE-GRC | 82H | c419 | HD78-1 | AW | T-S | B | 672 | CK | 31.5 | 340 | 30 | | | | | 0.088 | 2.50E-08 |
| GE-GRC | 82H | c419 | HD78-1 | AW | T-S | F | 743 | CK | 32.5 | 340 | 10 | | | | | 0.384 | 2.80E-07 |
| GE-GRC | 82H | c419 | HD78-1 | AW | T-S | G | 527 | CK | 33.3 | 340 | 7.1 | | | | | 0.182 | 8.00E-08 |
| GE-GRC | 82H | c419 | HD78-1 | AW | T-S | H | 2789 | CK | 34 | 340 | 15.3 | | | | | 0.456 | 4.00E-08 |
| GE-GRC | 82H | c419 | HD78-1 | AW | T-S | I | 1696 | CK | 34.8 | 340 | 0.71 | | | | | 0.158 | 3.00E-10 |
| GE-GRC | 82H | c419 | HD78-1 | AW | T-S | J | 2501 | CK | 35.2 | 340 | 15.3 | | | | | 0.096 | 1.20E-08 |
| GE-GRC | 82H | c420 | HD78-1 | AW | T-S | A | 600 | CK | 28.9 | 340 | 15.3 | | | | | 0.322 | 1.50E-07 |
| GE-GRC | 82H | c420 | HD78-1 | AW | T-S | B | 672 | CK | 29.8 | 340 | 30 | | | | | 0.072 | 3.30E-08 |
| GE-GRC | 82H | c420 | HD78-1 | AW | T-S | D | 1586 | CK | 29.9 | 340 | 45 | | | | | 0.031 | 6.00E-09 |
| GE-GRC | 82H | c420 | HD78-1 | AW | T-S | E | 429 | CK | 30 | 340 | 15.3 | | | | | 0.173 | 1.20E-07 |
| GE-GRC | 82H | c420 | HD78-1 | AW | T-S | F | 743 | CK | 30.8 | 340 | 10 | | | | | 0.243 | 6.00E-08 |
| GE-GRC | 82H | c420 | HD78-1 | AW | T-S | G | 527 | CK | 31.6 | 340 | 7.1 | | | | | 0.050 | 2.00E-08 |
| GE-GRC | 82H | c420 | HD78-1 | AW | T-S | H | 2789 | CK | 31.4 | 340 | 15.3 | | | | | 0.240 | 2.00E-08 |

**Table A-4 (continued)**
**Alloy 82/182/132 CGR database–Scored-in data**

| Laboratory | Alloy | Overall Test ID | Weld | Post-Supplier Processing | Orientation | Segment ID | Test Segment Duration (h) | Load Type | K (MPa√m) | Temperature (°C) | Dissolved $H_2$ (cc/kg) | Hold Time (s) | Load Ratio | % Engaged | Post-Test Correction Factor | Measured Δa (mm) | Reported SCC CGR (mm/s) |
|---|---|---|---|---|---|---|---|---|---|---|---|---|---|---|---|---|---|
| GE-GRC | 82H | c420 | HD78-1 | AW | T-S | I | 1696 | CK | 31.8 | 340 | 0.71 | | | | | 0.113 | 6.00E-09 |
| GE-GRC | 82H | c420 | HD78-1 | AW | T-S | J | 2501 | CK | 32.2 | 340 | 15.3 | | | | | 0.080 | 3.00E-08 |
| GE-GRC | 182 | c423 | 688879 | AW | T-S | A | 505 | CK | 27.5 | 325 | 10.5 | | | | | 0.128 | 7.80E-08 |
| GE-GRC | 182 | c423 | 688879 | AW | T-S | B | 365 | CK | 28.6 | 325 | 5 | | | | | 0.059 | 4.60E-08 |
| GE-GRC | 182 | c423 | 688879 | AW | T-S | C | 641 | CK | 28.6 | 325 | 2.5 | | | | | 0.059 | 6.00E-09 |
| GE-GRC | 182 | c423 | 688879 | AW | T-S | D | 848 | CK | 28.6 | 325 | 1 | | | | | 0.055 | 1.90E-08 |
| GE-GRC | 182 | c423 | 688879 | AW | T-S | E | 1676 | CK | 28.6 | 325 | 10.5 | | | | | 0.262 | 5.40E-08 |
| GE-GRC | 182 | c423 | 688879 | AW | T-S | F | 833 | CK | 28.6 | 325 | 18 | | | | | 0.143 | 4.70E-08 |
| GE-GRC | 182 | c423 | 688879 | AW | T-S | G | 2092 | CK | 28.6 | 325 | 30 | | | | | 0.209 | 1.60E-08 |
| GE-GRC | 182 | c424 | 414988 | AW | T-S | A | 505 | CK | 31 | 325 | 10.5 | | | | | 0.517 | 3.20E-07 |
| GE-GRC | 182 | c424 | 414988 | AW | T-S | B | 365 | CK | 32 | 325 | 5 | | | | | 0.313 | 2.40E-07 |
| GE-GRC | 182 | c424 | 414988 | AW | T-S | C | 641 | CK | 33 | 325 | 2.5 | | | | | 0.203 | 9.60E-08 |
| GE-GRC | 182 | c424 | 414988 | AW | T-S | D | 848 | CK | 35 | 325 | 1 | | | | | 0.142 | 4.60E-08 |
| GE-GRC | 182 | c424 | 414988 | AW | T-S | E | 1676 | CK | 38 | 325 | 10.5 | | | | | 1.461 | 2.40E-07 |
| GE-GRC | 182 | c424 | 414988 | AW | T-S | F | 833 | CK | 44 | 325 | 18 | | | | | 0.830 | 2.80E-07 |
| GE-GRC | 182 | c424 | 414988 | AW | T-S | G | 2092 | CK | 53 | 325 | 30 | | | | | 2.042 | 1.30E-07 |
| GE-GRC | 82H | c437 | HD78-1 | AW | T-S | A | 793 | CK | 27.5 | 340 | 15.3 | | | | | 0.074 | 2.50E-08 |
| GE-GRC | 82H | c437 | HD78-1 | AW | T-S | B | 673 | CK | 27.5 | 340 | 30 | | | | | 0.029 | 1.10E-08 |
| GE-GRC | 82H | c437 | HD78-1 | AW | T-S | C | 983 | CK | 27.5 | 340 | 45 | | | | | 0.027 | 7.00E-09 |
| GE-GRC | 182 | c458 | 058895 | AW | T-S | A | 1474 | CK | 65 | 325 | 10.4 | | | | | 1.204 | 2.00E-07 |
| GE-GRC | 182 | c458 | 058895 | AW | T-S | B | 1439 | CK | 77 | 325 | 0.7 | | | | | 0.058 | 6.00E-09 |
| GE-GRC | 182 | c459 | 1Z182DA801 | AW | T-S | A | 1474 | CK | 25.6 | 325 | 10.4 | | | | | 0.282 | 5.00E-08 |
| GE-GRC | 182 | c459 | 1Z182DA801 | AW | T-S | B | 1439 | CK | 24.8 | 325 | 0.7 | | | | | 0.042 | 3.00E-09 |
| Lockheed Martin | 182 | LM182-1 | LM182-1 | AW | T-S | A | | CL/CK | 33.4 | 328 | 35 | | | 100 | | | 2.59E-07 |
| Lockheed Martin | 182 | LM182-1 | LM182-1 | AW | T-S | B | | CL/CK | 35.7 | 328 | 35 | | | 100 | | | 1.87E-07 |
| Lockheed Martin | 182 | LM182-1 | LM182-1 | AW | T-S | C | | CL/CK | 35.9 | 328 | 35 | | | 100 | | | 1.30E-07 |
| Lockheed Martin | 182 | LM182-1 | LM182-1 | AW | T-S | D | | CL/CK | 36.5 | 328 | 35 | | | 100 | | | 1.69E-07 |
| Lockheed Martin | 182 | LM182-1 | LM182-1 | AW | T-S | E | | CL/CK | 36.4 | 328 | 35 | | | 100 | | | 1.20E-07 |
| Lockheed Martin | 182 | LM182-2a | LM182-2a | AW | T-S | A | | CL/CK | 40.3 | 338 | 40 | | | 100 | | | 2.11E-07 |
| Lockheed Martin | 182 | LM182-2a | LM182-2a | AW | T-S | B | | CL/CK | 40.5 | 338 | 40 | | | 100 | | | 2.65E-07 |
| Lockheed Martin | 182 | LM182-2a | LM182-2a | AW | T-S | C | | CL/CK | 41.1 | 338 | 40 | | | 90 | | | 2.20E-07 |
| Lockheed Martin | 182 | LM182-2b | LM182-2b | AW | T-S | A | | CL/CK | 45.3 | 338 | 40 | | | 100 | | | 5.43E-07 |
| Lockheed Martin | 182 | LM182-2b | LM182-2b | AW | T-S | B | | CL/CK | 45.8 | 338 | 40 | | | 100 | | | 5.40E-07 |
| Lockheed Martin | 182 | LM182-2b | LM182-2b | AW | T-S | C | | CL/CK | 46.5 | 338 | 40 | | | 100 | | | 5.94E-07 |
| Lockheed Martin | 82 | LM82-1 | LM82-1 | AW | T-S | A | | CL/CK | 55 | 360 | 40 | | | 90 | | | 2.66E-07 |
| Lockheed Martin | 82 | LM82-1 | LM82-1 | AW | T-S | B | | CL/CK | 55 | 360 | 40 | | | 70 | | | 2.04E-07 |
| Lockheed Martin | 82 | LM82-2 | LM82-2 | AW | T-S | A | | CL/CK | 28.1 | 338 | 40 | | | 60 | | | 4.47E-08 |

**Table A-4 (continued)**
**Alloy 82/182/132 CGR database–Scored-in data**

| Laboratory | Alloy | Overall Test ID | Weld | Post-Supplier Processing | Orientation | Segment ID | Test Segment Duration (h) | Load Type | K (MPa√m) | Temperature (°C) | Dissolved $H_2$ (cc/kg) | Hold Time (s) | Load Ratio | % Engaged | Post-Test Correction Factor | Measured Δa (mm) | Reported SCC CGR (mm/s) |
|---|---|---|---|---|---|---|---|---|---|---|---|---|---|---|---|---|---|
| Lockheed Martin | 82 | LM82-2 | LM82-2 | AW | T-S | B | | CL/CK | 28.3 | 338 | 40 | | | 70 | | | 5.54E-08 |
| Lockheed Martin | 82 | LM82-2 | LM82-2 | AW | T-S | C | | CL/CK | 29.1 | 338 | 40 | | | 60 | | | 7.14E-08 |
| Lockheed Martin | 82 | LM82-2 | LM82-2 | AW | T-S | D | | CL/CK | 39 | 338 | 20 | | | 100 | | | 5.40E-07 |
| Lockheed Martin | 82 | LM82-2 | LM82-2 | AW | T-S | E | | CL/CK | 39.4 | 338 | 20 | | | 87 | | | 6.19E-07 |
| Lockheed Martin | 82 | LM82-2 | LM82-2 | AW | T-S | F | | CL/CK | 39.8 | 338 | 20 | | | 97 | | | 5.60E-07 |
| Lockheed Martin | 82 | LM82-3 | LM82-3 | AW | T-S | A | | CL/CK | 28 | 316 | 40 | | | 80 | | | 3.32E-08 |
| Lockheed Martin | 82 | LM82-3 | LM82-3 | AW | T-S | B | | CL/CK | 47.7 | 316 | 40 | | | 60 | | | 1.35E-08 |
| Lockheed Martin | 82 | LM82-3 | LM82-3 | AW | T-S | C | | CL/CK | 33 | 328 | 35 | | | 70 | | | 1.67E-08 |
| Lockheed Martin | 82 | LM82-3 | LM82-3 | AW | T-S | D | | CL/CK | 38.9 | 328 | 35 | | | 90 | | | 5.28E-08 |
| Lockheed Martin | 82 | LM82-3 | LM82-3 | AW | T-S | E | | CL/CK | 36.3 | 328 | 35 | | | 60 | | | 2.24E-08 |
| Lockheed Martin | 82 | LM82-3 | LM82-3 | AW | T-S | F | | CL/CK | 28.2 | 338 | 40 | | | 60 | | | 7.04E-08 |
| Lockheed Martin | 82 | LM82-3 | LM82-3 | AW | T-S | G | | CL/CK | 28.4 | 338 | 40 | | | 70 | | | 7.70E-08 |
| Lockheed Martin | 82 | LM82-3 | LM82-3 | AW | T-S | H | | CL/CK | 28.6 | 338 | 40 | | | 80 | | | 6.52E-08 |
| Lockheed Martin | 82 | LM82-3 | LM82-3 | AW | T-S | I | | CL/CK | 40.5 | 338 | 40 | | | 70 | | | 2.69E-07 |
| Lockheed Martin | 82 | LM82-3 | LM82-3 | AW | T-S | J | | CL/CK | 50.5 | 338 | 40 | | | 55 | | | 3.68E-07 |
| Lockheed Martin | 82 | LM82-3 | LM82-3 | AW | T-S | K | | CL/CK | 48.8 | 360 | 30 | | | 92 | | | 6.30E-07 |
| MHI | 132 | 132-2 | MHI-132 | AW | L-S | A | 200 | PPU | 35 | 325 | 30 | 9000 | 0.7 | | | 0.040 | 5.56E-08 |
| MHI | 132 | 132LS-1 | MHI-132 | AW | L-S | A | 439 | PPU | 60 | 325 | 30 | 9000 | 0.7 | 68 | | 0.632 | 4.00E-07 |
| MHI | 132 | 132-LT2 | MHI-132 | AW | L-T | A | 300 | PPU | 35 | 325 | 30 | 9000 | 0.7 | | | 0.030 | 2.80E-08 |
| MHI | 132 | MG7-2 | MHI-MG7 | AW | T-S | A | 950 | PPU | 35 | 325 | 30 | 9000 | 0.7 | 76 | | 0.828 | 2.42E-07 |
| MHI | 132 | MG7-5 | MHI-MG7 | AW | T-S | A | 650 | CL/CK | 35 | 325 | 30 | | | | | 0.257 | 1.10E-07 |
| MHI | 132 | MG7-5 | MHI-MG7 | AW | T-S | A | 800 | PPU | 35 | 325 | 30 | 9000 | 0.7 | 65 | | 0.720 | 2.50E-07 |
| MHI | 132 | MG7L-1 | MHI-MG7 | AW | L-T | A | 950 | PPU | 35 | 325 | 30 | 9000 | 0.7 | | | 0.075 | 2.20E-08 |
| MHI | 132 | MG7L-1 | MHI-MG7 | AW | L-T | B | 600 | CL/CK | 35 | 325 | 30 | | | | | 0.054 | 2.50E-08 |
| MHI | 132 | MG7T-2 | MHI-MG7 | AW | L-S | A | 800 | PPU | 35 | 325 | 30 | 9000 | 0.7 | 62 | | 1.575 | 5.47E-07 |
| PNNL | 182 | CT012 | 8T | AW | | 1 | 850 | CK | 35 | 325 | 29 | | | | | 0.019 | 7.00E-09 |
| PNNL | 182 | CT012 | 8T | AW | | 2 | 390 | CK | 35 | 325 | 12 | | | | | 0.073 | 4.20E-08 |
| PNNL | 182 | CT012 | 8T | AW | | 3 | 430 | CK | 35 | 325 | 29 | | | | | 0.007 | 5.30E-09 |
| PNNL | 182 | CT012 | 8T | AW | | 4 | 370 | CK | 35 | 325 | 5 | | | | | 0.070 | 9.50E-08 |
| PNNL | 182 | CT012 | 8T | AW | | 7 | 150 | CK | 35 | 325 | 29 | | | | | 0.009 | 9.50E-09 |
| PNNL | 182 | CT012 | 8T | AW | | 9 | 730 | CK | 35 | 325 | 5 | | | | | 0.039 | 2.50E-08 |
| PNNL | 182 | CT012 | 8T | AW | | 10 | 430 | CK | 35 | 325 | 12 | | | | | 0.046 | 2.80E-08 |
| PNNL | 182 | CT012 | 8T | AW | | 12b | 310 | CK | 35 | 325 | 5 | | | | | 0.020 | 1.80E-08 |
| PNNL | 182 | CT012 | 8T | AW | | 6b | 400 | CK | 35 | 325 | 1.5 | | | | | 0.005 | 4.20E-09 |
| PNNL | 182 | CT012 | 8T | AW | | 8b | 320 | CK | 35 | 325 | 1.5 | | | | | 0.007 | 3.90E-09 |
| Studsvik | 182 | 1 | WC05F8 | AW | T-S | A | 2616 | CL/CK | 19.7 | 318.7 | 29.6 | | | 67 | | 0.590 | 6.30E-08 |
| Studsvik | 182 | 2 | WC05F8 | AW | T-S | A | 2616 | CL/CK | 23.7 | 318.7 | 29.6 | | | 84 | | 1.400 | 1.49E-07 |

**Table A-4 (continued)**
**Alloy 82/182/132 CGR database–Scored-in data**

| Laboratory | Alloy | Overall Test ID | Weld | Post-Supplier Processing | Orientation | Segment ID | Test Segment Duration (h) | Load Type | K (MPa√m) | Temperature (°C) | Dissolved $H_2$ (cc/kg) | Hold Time (s) | Load Ratio | % Engaged | Post-Test Correction Factor | Measured Δa (mm) | Reported SCC CGR (mm/s) |
|---|---|---|---|---|---|---|---|---|---|---|---|---|---|---|---|---|---|
| Studsvik | 182 | 3 | WC05F8 | AW | T-S | A | 2616 | CL/CK | 30.6 | 318.7 | 29.6 | | | 80 | | 1.380 | 1.47E-07 |
| Studsvik | 182 | 4 | WC05F8 | AW | T-S | A | 2616 | CL/CK | 36.7 | 318.7 | 29.6 | | | 72 | | 0.660 | 7.00E-08 |
| Studsvik | 182 | 5 | WC05F8 | AW | T-S | A | 2616 | CL/CK | 41.9 | 318.7 | 29.6 | | | 60 | | 1.210 | 1.28E-07 |
| Studsvik | 182 | 6 | WC05F8 | AW | T-S | A | 2616 | CL/CK | 43.7 | 318.7 | 29.6 | | | 85 | | 1.670 | 1.77E-07 |
| Studsvik | 182 | 7 | WC05F8 | AW | T-S | A | 2616 | CL/CK | 49.8 | 318.7 | 29.6 | | | 67 | | 1.580 | 1.68E-07 |
| Studsvik | 182 | 8 | WC05F8 | AW | T-S | A | 2616 | CL/CK | 56.1 | 318.7 | 29.6 | | | 85 | | 1.510 | 1.60E-07 |
| Studsvik | 182 | 169-1:54-55 | 26B2 | AW | T-S | A | 1750 | PPU | 51.1 | 345 | 28.8 | 100000 | 0.75 | 100 | | 11.400 | 1.81E-06 |
| Studsvik | 182 | 169-15:1-2 | 26B2 | AW | T-S | A | 2608 | CL/CK | 30 | 343 | 29.5 | | | 100 | | 5.520 | 5.88E-07 |
| Studsvik | 182 | 169-16:1-3 | 26B2 | AW | T-S | A | 2608 | CL/CK | 50.7 | 343 | 29.5 | | | 100 | | 6.100 | 6.50E-07 |
| Studsvik | 182 | 169-17:1-2 | 26B2 | AW | T-S | A | 2608 | CL/CK | 24.5 | 343 | 29.5 | | | 100 | | 5.330 | 5.68E-07 |
| Studsvik | 182 | 169-18:1-2 | 26B2 | AW | T-S | A | 1940 | CL/CK | 30 | 343 | 30.4 | | | 100 | | 3.490 | 5.00E-07 |
| Studsvik | 182 | 169-5:29 | 26B2 | AW | T-S | A | 67 | PPU | 41 | 344 | 25.5 | 100000 | 0.75 | | | 0.470 | 1.95E-06 |
| Studsvik | 182 | 169-5:38a-c | 26B2 | AW | T-S | A | 97 | PPU | 31 | 345 | 30.8 | 100000 | 0.75 | | | 0.410 | 1.17E-06 |
| Studsvik | 182 | 186A-12 | 33644 | AW | T-S | A | 5798 | CMOD | 17.8 | 340 | 25 | | | 76 | | 1.260 | 6.04E-08 |
| Studsvik | 182 | 186A-13 | 33644 | AW | T-S | A | 5798 | CMOD | 20.5 | 340 | 25 | | | 61 | | 1.530 | 7.33E-08 |
| Studsvik | 182 | 194-01 | 194 | AW | T-S | A | 2616 | CL | 19.7 | 318.7 | 29.6 | | | 100 | | 0.590 | 6.30E-08 |
| Studsvik | 182 | 194-02 | 194 | AW | T-S | A | 2616 | CL | 23.7 | 318.7 | 29.6 | | | 100 | | 1.400 | 1.49E-07 |
| Studsvik | 182 | 194-03 | 194 | AW | T-S | A | 2616 | CL | 30.6 | 318.7 | 29.6 | | | 100 | | 2.080 | 2.21E-07 |
| Studsvik | 182 | 194-04 | 194 | AW | T-S | A | 2616 | CL | 36.7 | 318.7 | 29.6 | | | 100 | | 0.660 | 7.00E-08 |
| Studsvik | 182 | 194-05 | 194 | AW | T-S | A | 2616 | CL | 41.9 | 318.7 | 29.6 | | | 100 | | 1.840 | 1.95E-07 |
| Studsvik | 182 | 194-06 | 194 | AW | T-S | A | 2616 | CL | 43.7 | 318.7 | 29.6 | | | 100 | | 1.670 | 1.77E-07 |
| Studsvik | 182 | 194-07 | 194 | AW | T-S | A | 2616 | CL | 49.8 | 318.7 | 29.6 | | | 100 | | 2.030 | 2.16E-07 |
| Studsvik | 182 | 194-08 | 194 | AW | T-S | A | 2616 | CL | 56.1 | 318.7 | 29.6 | | | 100 | | 1.800 | 1.91E-07 |
| Studsvik | 182 | 194-09 | 194 | AW | T-S | A | 1029 | CL | 32.4 | 305 | 24.9 | | | 100 | | 0.520 | 1.40E-07 |
| Studsvik | 182 | 194-10 | 194 | AW | T-S | A | 1029 | CL | 33 | 305 | 24.9 | | | 100 | | 0.690 | 1.90E-07 |
| Studsvik | 182 | 194-11 | 194 | AW | T-S | A | 1000 | CL | 33.7 | 320 | 26.2 | | | 100 | | 0.860 | 2.40E-07 |
| Studsvik | 182 | 194-12 | 194 | AW | T-S | A | 1000 | CL | 34.3 | 320 | 26.2 | | | 100 | | 1.120 | 3.10E-07 |
| Studsvik | 182 | 194-13 | 194 | AW | T-S | A | 999 | CL | 39.1 | 340 | 24.8 | | | 100 | | 2.700 | 7.50E-07 |
| Studsvik | 182 | 194-14 | 194 | AW | T-S | A | 999 | CL | 34.1 | 340 | 24.8 | | | 100 | | 1.460 | 4.00E-07 |
| Studsvik | 182 | 194-15 | 194 | AW | T-S | A | 2010 | CL | 33.6 | 290 | 27.1 | | | 100 | | 0.560 | 7.70E-08 |
| Studsvik | 182 | 194-16 | 194 | AW | T-S | A | 2010 | CL | 33.4 | 290 | 27.1 | | | | | 0.440 | 6.10E-08 |
| Studsvik | 182 | 194-34 | 194 | AW | T-S | A | 5798 | CMOD | 13.8 | 340 | 25 | | | 55 | | 1.180 | 5.65E-08 |
| Studsvik | 182 | 194-35 | 194 | AW | T-S | A | 5798 | CMOD | 16.6 | 340 | 25 | | | 62 | | 1.660 | 7.95E-08 |
| Studsvik | 182 | 194-36 | 194 | AW | T-S | A | 5798 | CMOD | 18.3 | 340 | 25 | | | 68 | | 1.520 | 7.28E-08 |
| Studsvik | 182 | 194-38 | 194 | AW | T-S | A | 5798 | CMOD | 20.7 | 340 | 25 | | | 78 | | 2.130 | 1.02E-07 |
| Studsvik | 182 | 2332:1-3 | 6892 | AW | T-S | A | 1819 | PPU | 58 | 343 | 29.5 | 100000 | 0.7 | 100 | | 10.860 | 1.66E-06 |
| Studsvik | 182 | 2333:1-3 | 6892 | AW | T-S | B | 2608 | CL/CK | 56 | 343 | 29.5 | | | 100 | | 8.110 | 8.64E-07 |

**Table A-4 (continued)**
**Alloy 82/182/132 CGR database–Scored-in data**

| Laboratory | Alloy | Overall Test ID | Weld | Post-Supplier Processing | Orientation | Segment ID | Test Segment Duration (h) | Load Type | K (MPa√m) | Temperature (°C) | Dissolved $H_2$ (cc/kg) | Hold Time (s) | Load Ratio | % Engaged | Post-Test Correction Factor | Measured Δa (mm) | Reported SCC CGR (mm/s) |
|---|---|---|---|---|---|---|---|---|---|---|---|---|---|---|---|---|---|
| Westinghouse | 182 | 182-RT | D545/582 | AW | L-S | A | 1510 | PPU | 29.5 | 324 | 25 | 3600 | 0.7 | 89 | | 1.816 | 3.34E-07 |
| Westinghouse | 182 | 182-RT | D545/582 | AW | L-S | B | 1510 | PPU | 37.6 | 324.2 | 25 | 3600 | 0.7 | 89 | | 3.022 | 5.56E-07 |
| Westinghouse | 182 | 182-RW | D545/582 | AW | T-L | A | 2021 | PPU | 27.3 | 325.7 | 25 | 3600 | 0.7 | 100 | | 1.535 | 2.11E-07 |
| Westinghouse | 182 | 182-TS1 | D545/582 | AW | T-S | A | 1600 | PPU | 21.9 | 326.1 | 25 | 3600 | 0.7 | 100 | | 0.622 | 1.08E-07 |
| Westinghouse | 182 | 182-TS2 | D545/582 | AW | T-S | A | 906 | PPU | 30.2 | 326.3 | 25 | 3600 | 0.7 | 100 | | 1.406 | 4.31E-07 |
| Westinghouse | 182 | 182-TS3 | D545/582 | AW | T-S | A | 987 | PPU | 26 | 324.2 | 25 | 3600 | 0.7 | 100 | | 2.207 | 6.21E-07 |
| Westinghouse | 182 | 182-TS4 | D545/582 | AW | T-S | A | 1625 | CL/CK | 30.4 | 326.3 | 25 | | | 100 | | 4.042 | 6.91E-07 |
| Westinghouse | 182 | 182-TS5 | D545/582 | AW | T-S | A | 1565 | PPU | 26.5 | 325 | 25 | 3600 | 0.7 | 100 | | 3.414 | 6.06E-07 |
| Westinghouse | 182 | 182-WR | D545/582 | AW | L-T | A | 1237 | PPU | 26.7 | 326.6 | 25 | 3600 | 0.85 | | | 0.071 | 1.59E-08 |
| Westinghouse | 182 | S182-1 | 33644 | AW | T-S | A | 910 | PPU | 25.2 | 325.9 | 25 | 3600 | 0.7 | 91 | | 1.035 | 3.16E-07 |
| Westinghouse | 182 | S182-2 | 33644 | AW | T-S | A | 1366 | PPU | 25.6 | 323.1 | 25 | 3600 | 0.7 | 70 | | 1.274 | 2.59E-07 |
| Westinghouse | 182 | WTS-10 | PP751 | AW | T-S | A | 974 | PPU | 23.7 | 326.1 | 25 | 3600 | 0.7 | | | 0.417 | 1.19E-07 |
| Westinghouse | 182 | WTS-11 | PP751 | AW | T-S | A | 2398 | PPU | 17.3 | 324 | 25 | 3600 | 0.7 | | | 0.194 | 2.25E-08 |
| Westinghouse | 182 | WTS-12 | PP751 | AW | T-S | A | 2981 | PPU | 23.1 | 295 | 25 | 3600 | 0.7 | | | 0.118 | 1.10E-08 |
| Westinghouse | 182 | WTS-6 | PP751 | AW | T-S | A | 3686 | PPU | 22.5 | 290 | 25 | 3600 | 0.7 | | | 0.045 | 3.37E-09 |
| Westinghouse | 182 | WTS-7 | PP751 | AW | T-S | A | 1392 | PPU | 32.1 | 324 | 25 | 3600 | 0.7 | 80 | | 1.288 | 2.57E-07 |
| Westinghouse | 182 | WTS-8 | PP751 | AW | T-S | A | 1191 | PPU | 24.2 | 342 | 25 | 3600 | 0.7 | 60 | | 0.905 | 2.11E-07 |
| Westinghouse | 182 | WTS-9 | PP751 | AW | T-S | A | 1342 | PPU | 22 | 325 | 25 | 3600 | 0.7 | 100 | | 0.850 | 1.76E-07 |

## Table A-5
## Alloy 82/182/132 CGR database–Scored-out data

| Laboratory | Alloy | Overall Test ID | Weld | Post-Supplier Processing | Orientation | Segment ID | Test Segment Duration (h) | Load Type | K (MPa√m) | Temperature (°C) | Dissolved $H_2$ (cc/kg) | Hold Time (s) | Load Ratio | % Engaged | DCPD Correction Factor | Measured Δa (mm) | Reported SCC CGR (mm/s) | Scored Out Reason |
|---|---|---|---|---|---|---|---|---|---|---|---|---|---|---|---|---|---|---|
| ANL | 182 | CT933-TL | CT933 | AW | T-L | 2 | 194 | CL | 21.6 | 320 | 23 | | | 100 | 1.06 | 0.043 | 2.68E-09 | Poor score |
| ANL | 182 | J11CC-1 | Davis-Besse-182 | AW | C-R | 6 | 119 | PPU | 23.9 | 316 | 23 | 3600 | 0.5 | 50 | 1.60 | 0.001 | 0 | Poor score |
| ANL | 182 | J11CC-1 | Davis-Besse-182 | AW | C-R | 9 | 167 | PPU | 24.3 | 316 | 23 | 3600 | 0.75 | 50 | 1.60 | 0 | 0 | No growth |
| ANL | 182 | J11CC-1 | Davis-Besse-182 | AW | C-R | 12 | 35 | PPU | 29.3 | 316 | 23 | 3600 | 0.5 | 50 | 1.60 | 0.005 | 4.00E-08 | Poor score |
| ANL | 182 | J11CC-3 | Davis-Besse-182 | AW | C-R | 3 | 95 | CL | 20.0 | 316 | 23 | | | 15 | 2.00 | 0.023 | 3.92E-08 | Poor score |
| ANL | 182 | J11CC-3 | Davis-Besse-182 | AW | C-R | 8 | 138 | PPU | 28.2 | 316 | 23 | 3600 | 0.7 | 15 | 2.00 | 0 | 0 | No growth |
| ANL | 182 | J11CC-3 | Davis-Besse-182 | AW | C-R | 10 | 164 | PPU | 32.7 | 316 | 23 | 3600 | 0.7 | 15 | 2.00 | 0.015 | 4.65E-08 | <50% eng. |
| ANL | 182 | J11CC-3 | Davis-Besse-182 | AW | C-R | 12 | 167 | PPU | 32.6 | 316 | 23 | 3600 | 0.7 | 15 | 2.00 | 0 | 0 | No growth |
| ANL | 182 | J11CC-3 | Davis-Besse-182 | AW | C-R | 6a | 122 | CL | 22.2 | 316 | 23 | | | 15 | 2.00 | 0 | 0 | No growth |
| ANL | 182 | J11CC-3 | Davis-Besse-182 | AW | C-R | 6b | 70 | PPU | 22.2 | 316 | 23 | 3600 | 0.5 | 15 | 2.00 | 0.036 | 3.93E-08 | Poor score |
| ANL | 82 | WCR-01 | VCS-82 | AW | C-R | 4 | 70 | CL | 24.2 | 320 | 23 | | | 100 | 2.60 | 0.010 | 4.11E-08 | Poor score |
| ANL | 82 | WLR-01 | VCS-82 | AW | L-R | 5 | 241 | CL | 33.2 | 320 | 23 | | | 100 | 1.91 | 0.059 | 5.43E-09 | Poor score |
| AREVA | 82 | 82.10 | MNPK3 | AW | T-S | 6 | 3600 | CL | 20.0 | 340 | 25 | | | 100 | 1.2 | 0.204 | 2.95E-09 | Poor score |
| AREVA | 82 | 82.11 | MNPK3 | HT | T-S | 6 | 3600 | CL | 20.0 | 340 | 25 | | | 100 | 1.2 | 0.156 | 2.25E-09 | Poor score |
| Bettis | 82 | 23TSL-4 | 7D | AW | T-S | A | 6115 | PPU | 21.2 | 316 | 52 | 6000 | 0.7 | 36 | | 0.198 | 8.82E-09 | <50% eng. |
| Bettis | 82 | 24HT-1 | 7D | CW+HT | T-S | A | | PPU | 36.2 | 338 | 52 | 86400 | 0.7 | | | | 2.23E-07 | Cold worked |
| Bettis | 82 | 24HT-2 | 7D | CW+HT | T-S | A | | PPU | 40.1 | 338 | 52 | 86400 | 0.7 | | | | 3.13E-07 | Cold worked |
| Bettis | 82 | 24TLL-10 | 7D | CW | T-L | A | 907 | PPU | 37.7 | 338 | 48 | 6000 | 0.7 | 100 | | 1.970 | 6.03E-07 | Cold worked |
| Bettis | 82 | 24TLL-11 | 7D | CW | T-L | A | 4246 | PPU | 35.3 | 288 | 49 | 86400 | 0.7 | 94 | | 0.455 | 2.98E-08 | Cold worked |
| Bettis | 82 | 24TLL-3 | 7D | CW | T-L | A | 1975 | PPU | 25.1 | 338 | 55 | 6000 | 0.7 | 100 | | 1.890 | 2.66E-07 | Cold worked |
| Bettis | 82 | 24TLL-4 | 7D | CW | T-L | A | 1963 | PPU | 41.8 | 316 | 52 | 6000 | 0.7 | 100 | | 2.230 | 3.16E-07 | Cold worked |
| Bettis | 82 | 24TLL-5 | 7D | CW | T-L | A | 3019 | PPU | 22.7 | 316 | 56 | 6000 | 0.7 | 94 | | 0.516 | 4.76E-08 | Cold worked |
| Bettis | 82 | 24TLL-6 | 7D | CW | T-L | A | 583 | PPU | 53.2 | 338 | 27 | 6000 | 0.7 | 100 | | 4.690 | 2.24E-06 | Cold worked |
| Bettis | 82 | 24TLL-9 | 7D | CW | T-L | A | 242 | PPU | 30.2 | 338 | 25 | 6000 | 0.7 | 86 | | 0.445 | 5.12E-07 | Cold worked |
| Bettis | 82 | 24TSL-12 | 7D | CW | T-S | A | 907 | PPU | 44.6 | 338 | 48 | 6000 | 0.7 | 100 | | 3.570 | 1.09E-06 | Cold worked |
| Bettis | 82 | 24TSL-2 | 7D | CW | T-S | A | 1975 | PPU | 28.2 | 338 | 55 | 6000 | 0.7 | 100 | | 2.460 | 3.44E-07 | Cold worked |
| Bettis | 82 | 24TSL-3 | 7D | CW | T-S | A | 1963 | PPU | 43.0 | 316 | 52 | 6000 | 0.7 | 100 | | 2.930 | 4.14E-07 | Cold worked |
| Bettis | 82 | 24TSL-4 | 7D | CW | T-S | A | 3019 | PPU | 25.1 | 316 | 56 | 6000 | 0.7 | 100 | | 1.920 | 1.76E-07 | Cold worked |
| Bettis | 82 | 24TSL-5 | 7D | CW | T-S | A | 4246 | PPU | 37.6 | 288 | 49 | 86400 | 0.7 | 69 | | 0.566 | 3.71E-08 | Cold worked |
| Bettis | 82 | 24TSL-8 | 7D | CW | T-S | A | 242 | PPU | 32.9 | 338 | 25 | 6000 | 0.7 | 100 | | 1.280 | 1.46E-06 | Cold worked |
| Bettis | 182 | 8N12TS-5 | Bettis-182 | AW | T-S | A | 3043 | PPU | 21.4 | 288 | 54 | 86400 | 0.7 | 11 | | 0.023 | 2.09E-09 | <50% eng. |
| Bettis | 182 | 8N12TS-6 | Bettis-182 | AW | T-S | A | 3043 | PPU | 33.4 | 288 | 54 | 86400 | 0.7 | 42 | | 0.079 | 7.06E-09 | <50% eng. |
| Bettis | 182 | 8N12TS-9 | Bettis-182 | AW | T-S | A | 1867 | PPU | 22.0 | 316 | 52 | 6000 | 0.7 | 42 | | 0.132 | 1.97E-08 | <50% eng. |
| Bettis | 82H | 22.01 | Bettis-82H | HT+CW | | A | 1750 | PPU | 23.1 | 316 | 50 | 6000 | 0.7 | | | | 4.37E-08 | Cold worked |
| Bettis | 82H | 22.02 | Bettis-82H | HT+CW | | A | 1750 | PPU | 23.7 | 316 | 50 | 6000 | 0.7 | | | | 6.02E-08 | Cold worked |
| Bettis | 82H | 22.03 | Bettis-82H | HT+CW | | A | 1750 | PPU | 34.8 | 316 | 50 | 6000 | 0.7 | | | | 6.37E-08 | Cold worked |
| Bettis | 82H | 22.04 | Bettis-82H | HT+CW | | A | 1750 | PPU | 35.7 | 316 | 50 | 6000 | 0.7 | | | | 6.61E-08 | Cold worked |
| Bettis | 82H | 22.05 | Bettis-82H | HT+CW | | A | 1750 | PPU | 28.1 | 338 | 50 | 6000 | 0.7 | | | | 3.00E-07 | Cold worked |
| Bettis | 82H | 22.06 | Bettis-82H | HT+CW | | A | 1750 | PPU | 29.6 | 338 | 50 | 6000 | 0.7 | | | | 3.91E-07 | Cold worked |

**Table A-5 (continued)**
**Alloy 82/182/132 CGR database–Scored-out data**

| Laboratory | Alloy | Overall Test ID | Weld | Post-Supplier Processing | Orientation | Segment ID | Test Segment Duration (h) | Load Type | K (MPa√m) | Temperature (°C) | Dissolved $H_2$ (cc/kg) | Hold Time (s) | Load Ratio | % Engaged | DCPD Correction Factor | Measured Δa (mm) | Reported SCC CGR (mm/s) | Scored Out Reason |
|---|---|---|---|---|---|---|---|---|---|---|---|---|---|---|---|---|---|---|
| Bettis | 82H | 22.07 | Bettis-82H | HT+CW | | A | 1750 | PPU | 36.3 | 338 | 50 | 6000 | 0.7 | | | | 3.49E-07 | Cold worked |
| Bettis | 82H | 22.08 | Bettis-82H | HT+CW | | A | 1750 | PPU | 36.9 | 338 | 50 | 6000 | 0.7 | | | | 3.24E-07 | Cold worked |
| Bettis | 82H | A-1 | A-1 | AW | T-L | | | PPU | 43 | 338 | 50 | 600 | 0.65 | | | | 2.53E-07 | Short hold time |
| Bettis | 82H | A-1 | A-1 | AW | T-L | | | PPU | 43 | 338 | 50 | 600 | 0.65 | | | | 2.50E-07 | Short hold time |
| Bettis | 82H | A-1 | A-1 | AW | T-L | | | PPU | 43 | 338 | 50 | 600 | 0.65 | | | | 2.05E-07 | Short hold time |
| Bettis | 82H | A-1 | A-1 | AW | T-L | | | CL/CK | 40 | 360 | 150 | | | | | | 2.38E-07 | 150 cc/kg $H_2$ |
| Bettis | 82H | A-1 | A-1 | AW | T-L | | | CL/CK | 48 | 360 | 150 | | | | | | 1.48E-07 | 150 cc/kg $H_2$ |
| Bettis | 82H | A-1 | A-1 | AW | T-L | | | CL/CK | 41 | 360 | 150 | | | | | | 5.86E-08 | 150 cc/kg $H_2$ |
| Bettis | 82H | A-2 | A-2 | AW | T-S | | | CL/CK | 54 | 360 | 150 | | | | | | 7.83E-07 | 150 cc/kg $H_2$ |
| Bettis | 82H | A-2 | A-2 | AW | T-S | | | flutter | 48 | 360 | 150 | | 0.9 | | | | 5.35E-07 | Flutter load; 150 cc/kg $H_2$ |
| Bettis | 82H | A-2 | A-2 | AW | T-S | | | CL/CK | 65 | 360 | 150 | | | | | | 1.02E-06 | Outside LEFM; 150 $H_2$ |
| Bettis | 82H | A-2 | A-2 | AW | T-S | | | CL/CK | 65 | 360 | 150 | | | | | | 2.08E-07 | Outside LEFM; 150 $H_2$ |
| Bettis | 82H | B-1 | B-1 | AW | T-L | | | CL/CK | 31 | 360 | 150 | | | | | | 1.94E-07 | 150 cc/kg $H_2$ |
| Bettis | 82H | B-1 | B-1 | AW | T-L | | | CL/CK | 30 | 360 | 150 | | | | | | 1.78E-07 | 150 cc/kg $H_2$ |
| Bettis | 82H | B-1 | B-1 | AW | T-L | | | flutter | 27 | 338 | 150 | | 0.9 | | | | 3.66E-08 | Flutter load; 150 cc/kg $H_2$ |
| Bettis | 82H | B-1 | B-1 | AW | T-L | | | CL/CK | 62 | 360 | 150 | | | | | | 7.77E-07 | Outside LEFM; 150 $H_2$ |
| Bettis | 82H | C-1 | C-1 | AW | T-L | | | CL/CK | 63 | 338 | 50 | | | | | | 3.24E-07 | Outside LEFM |
| Bettis | 82H | C-1 | C-1 | AW | T-L | | | CL/CK | 62 | 360 | 150 | | | | | | 7.15E-07 | Outside LEFM; 150 $H_2$ |
| Bettis | 82H | C-3 | C-3 | AW | T-S | | | CL/CK | 54 | 338 | 50 | | | | | | 8.66E-07 | Outside LEFM |
| Bettis | 82H | C-4 | C-4 | AW | T-S | | | PPU | 33 | 288 | 50 | 600 | 0.65 | | | | 2.48E-08 | Short hold time |
| Bettis | 82H | C-4 | C-4 | AW | T-S | | | PPU | 34 | 288 | 50 | 600 | 0.65 | | | | 2.06E-08 | Short hold time |
| Bettis | 82H | C-4 | C-4 | AW | T-S | | | PPU | 32 | 288 | 50 | 600 | 0.65 | | | | 2.04E-08 | Short hold time |
| Bettis | 82H | C-4 | C-4 | AW | T-S | | | PPU | 28 | 316 | 50 | 6000 | 0.65 | | | | 2.17E-08 | <50% eng. |
| Bettis | 82H | C-4 | C-4 | AW | T-S | | | PPU | 61 | 338 | 50 | 600 | 0.65 | | | | 8.71E-07 | Outside LEFM; short hold time |
| Bettis | 82H | C-4 | C-4 | AW | T-S | | | PPU | 67 | 338 | 50 | 600 | 0.65 | | | | 4.13E-07 | Outside LEFM; short hold time |
| Bettis | 82H | C-4 | C-4 | AW | T-S | | | PPU | 60 | 338 | 50 | 600 | 0.65 | | | | 3.07E-07 | Outside LEFM; short hold time |
| Bettis | 82H | C-4 | C-4 | AW | T-S | | | PPU | 31 | 316 | 50 | 6000 | 0.65 | | | | 2.64E-08 | Low crack increment |
| Bettis | 82H | C-4 | C-4 | AW | T-S | | | PPU | 32 | 316 | 50 | 6000 | 0.65 | | | | 2.38E-08 | Low crack increment |
| Bettis | 82H | C-4 | C-4 | AW | T-S | | | PPU | 32 | 316 | 50 | 6000 | 0.65 | | | | 2.24E-08 | Low crack increment |
| CEA | 182 | D545 | D545/582 | AW | T-L | | 800 | CL/CK | 25 | 330 | 55 | | | | | | N/A | No avg growth reported |
| CEA | 182 | D545 | D545/582 | AW | T-L | | 800 | CL/CK | 22 | 330 | 55 | | | | | | N/A | No avg growth reported |
| CEA | 182 | D545 | D545/582 | AW | T-L | | 1383 | CL/CK | 20 | 310 | 40 | | | | | | N/A | No avg growth reported |
| CEA | 182 | D545 | D545/582 | AW | T-L | | 1383 | CL/CK | 21 | 290 | 40 | | | | | | N/A | No avg growth reported |
| CEA | 182 | D545 | D545/582 | SR | T-L | | 1200 | CL/CK | 22 | 330 | 35 | | | | | | N/A | No avg growth reported |
| CEA | 182 | D545 | D545/582 | SR | T-L | | 1200 | CL/CK | 22 | 330 | 35 | | | | | | N/A | No avg growth reported |
| CEA | 82 | EP554 | EP | AW | T-S | A | 1970 | CL | 37.0 | 325 | 38 | | | 1 | | 0.200 | 2.80E-08 | <50% eng.; $\Delta a_{avg}$ not reported |
| CEA | 82 | EP555 | EP | AW | T-S | A | 6440 | CL | 38.3 | 325 | 38 | | | 10 | | 1.000 | 4.30E-08 | <50% eng.; $\Delta a_{avg}$ not reported |
| CEA | 82 | EP556 | EP | AW | T-S | A | 1970 | CL | 30.0 | 325 | 38 | | | 1 | | 0.350 | 5.00E-08 | <50% eng.; $\Delta a_{avg}$ not reported |
| CEA | 82 | EP560 | EP | AW | T-L | A | 6440 | CL | 41.5 | 325 | 38 | | | 0 | | 0 | 0 | No growth |

**Table A-5 (continued)**
**Alloy 82/182/132 CGR database–Scored-out data**

| Laboratory | Alloy | Overall Test ID | Weld | Post-Supplier Processing | Orientation | Segment ID | Test Segment Duration (h) | Load Type | K (MPa√m) | Temperature (°C) | Dissolved $H_2$ (cc/kg) | Hold Time (s) | Load Ratio | % Engaged | DCPD Correction Factor | Measured Δa (mm) | Reported SCC CGR (mm/s) | Scored Out Reason |
|---|---|---|---|---|---|---|---|---|---|---|---|---|---|---|---|---|---|---|
| CEA | 82 | EP562 | EP | AW | T-L | A | 6440 | CL | 29.6 | 325 | 38 | | | 20 | | 0.750 | 3.20E-08 | <50% eng.; $\Delta a_{avg}$ not reported |
| CEA | 82 | EP564 | EP | HT | T-S | A | 6440 | CL | 14.0 | 325 | 38 | | | 0 | | 0 | 0 | No growth |
| CEA | 82 | EP565 | EP | HT | T-S | A | 1970 | CL | 36.5 | 325 | 38 | | | 0 | | 0 | 0 | No growth |
| CEA | 82 | EP566 | EP | HT | T-S | A | 4470 | CL | 24.0 | 325 | 38 | | | 0 | | 0 | 0 | No growth |
| CEA | 82 | EP567 | EP | HT | T-S | A | 4470 | CL | 29.0 | 325 | 38 | | | 0 | | 0 | 0 | No growth |
| CEA | 82 | EP568 | EP | HT | T-L | A | 6440 | CL | 16.0 | 325 | 38 | | | 0 | | 0 | 0 | No growth |
| CEA | 82 | EP569 | EP | HT | T-L | A | 4470 | CL | 30.0 | 325 | 38 | | | 1 | | 0.100 | 1.20E-12 | <50% eng.; $\Delta a_{avg}$ not reported |
| CEA | 82 | EP570 | EP | HT | T-L | A | 1970 | CL | 32.1 | 325 | 38 | | | 0 | | 0 | 0 | No growth |
| CEA | 82 | EP785 | EP | AW | T-S | A | 8064 | CL | 31.5 | 325 | 38 | | | 48 | | 3.000 | 1.03E-07 | <50% eng.; $\Delta a_{avg}$ not reported |
| CEA | 82 | EP786 | EP | AW | T-S | A | 8064 | CL | 30.5 | 325 | 38 | | | 28 | | 2.200 | 7.58E-08 | <50% eng.; $\Delta a_{avg}$ not reported |
| CEA | 82 | EP787 | EP | AW | T-S | A | 8064 | CL | 39.7 | 325 | 38 | | | 40 | | 3.150 | 1.09E-07 | <50% eng.; $\Delta a_{avg}$ not reported |
| CEA | 82 | EP788 | EP | AW | T-S | A | 8064 | CL | 31.7 | 325 | 38 | | | 45 | | 3.100 | 1.07E-07 | <50% eng.; $\Delta a_{avg}$ not reported |
| CEA | 82 | EP839 | EP | AW | T-S | A | 8064 | CL | 39.2 | 325 | 38 | | | 34 | | 2.500 | 8.62E-08 | <50% eng.; $\Delta a_{avg}$ not reported |
| CEA | 82 | EP840 | EP | AW | T-S | A | 8064 | CL | 37.0 | 325 | 38 | | | 60 | | 3.700 | 1.27E-07 | $\Delta a_{avg}$ not reported |
| CEA | 182 | Product 1 | Product 1 | AW | T-L | | 1367 | CL/CK | 30 | 330 | 45 | | | | | | N/A | $\Delta a_{avg}$ not reported |
| CEA | 182 | Product 1 | Product 1 | AW | T-L | | 1367 | CL/CK | 18 | 330 | 45 | | | | | | N/A | $\Delta a_{avg}$ not reported |
| CEA | 182 | Product 1 | Product 1 | SR | T-L | | 1367 | CL/CK | 29 | 330 | 45 | | | | | | N/A | $\Delta a_{avg}$ not reported |
| CEA | 182 | Product 1 | Product 1 | SR | T-L | | 1367 | CL/CK | 18 | 330 | 45 | | | | | | N/A | $\Delta a_{avg}$ not reported |
| CEA | 182 | Product 2 | Product 2 | AW | T-L | | 1383 | CL/CK | 22 | 330 | 40 | | | | | | N/A | $\Delta a_{avg}$ not reported |
| CEA | 182 | Product 2 | Product 2 | AW | T-L | | 1383 | CL/CK | 21 | 330 | 40 | | | | | | N/A | $\Delta a_{avg}$ not reported |
| CEA | 182 | Product 2 | Product 2 | SR | T-L | | 1383 | CL/CK | 23 | 330 | 40 | | | | | | N/A | $\Delta a_{avg}$ not reported |
| CEA | 182 | Product 2 | Product 2 | SR | T-L | | 1383 | CL/CK | 21 | 330 | 40 | | | | | | N/A | $\Delta a_{avg}$ not reported |
| CEA | 182 | Product 4 | Product 4 | AW | T-L | | 1500 | CL/CK | 23 | 330 | 35 | | | | | | N/A | $\Delta a_{avg}$ not reported |
| CEA | 182 | Product 4 | Product 4 | AW | T-L | | 1500 | CL/CK | 33 | 330 | 35 | | | | | | N/A | $\Delta a_{avg}$ not reported |
| CEA | 182 | Product 4 | Product 4 | SR | T-L | | 900 | CL/CK | 22 | 330 | 30 | | | | | | N/A | $\Delta a_{avg}$ not reported |
| CEA | 182 | Product 4 | Product 4 | SR | T-L | | 900 | CL/CK | 22 | 330 | 30 | | | | | | N/A | $\Delta a_{avg}$ not reported |
| EDF | 182 | D545.12 | D545/582 | AW | T-L | | 2200 | CL/CK | 40 | 360 | 38 | | | | | | N/A | $\Delta a_{avg}$ not reported |
| EDF | 182 | D545.2 | D545/582 | AW | T-S | | 2394 | CL/CK | 30 | 360 | 38 | | | | | | N/A | $\Delta a_{avg}$ not reported |
| EDF | 182 | D545.4 | D545/582 | SR | T-L | | 2000 | CL/CK | 20 | 360 | 38 | | | | | | N/A | $\Delta a_{avg}$ not reported |
| EDF | 182 | D545.S1A | D545/582 | AW | T-L | | 2680 | CL/CK | 30 | 360 | 38 | | | | | | N/A | $\Delta a_{avg}$ not reported |
| EDF | 182 | D545.S3A | D545/582 | AW | T-S | | 2705 | CL/CK | 20 | 360 | 38 | | | | | | N/A | $\Delta a_{avg}$ not reported |
| EDF | 182 | D545S3B | D545/582 | AW | T-S | | 2000 | CL/CK | 20 | 325 | 38 | | | | | | N/A | $\Delta a_{avg}$ not reported |
| EDF | 182 | D545T7 | D545/582 | AW | L-T | | 2394 | CL/CK | 30 | 360 | 38 | | | | | | N/A | $\Delta a_{avg}$ not reported |
| EDF | 182 | D582.1TL | D545/582 | AW | T-L | | 3180 | CL/CK | 40 | 315 | 38 | | | | | | N/A | $\Delta a_{avg}$ not reported |
| EDF | 182 | D582.1TS | D545/582 | AW | T-S | | 2000 | CL/CK | 20 | 360 | 38 | | | | | | N/A | $\Delta a_{avg}$ not reported |
| EDF | 182 | D582.2TTL | D545/582 | SR | T-L | | 2153 | CL/CK | 30 | 360 | 38 | | | | | | N/A | $\Delta a_{avg}$ not reported |
| EDF | 182 | D582.2TTS | D545/582 | SR | T-S | | 2394 | CL/CK | 32 | 360 | 38 | | | | | | N/A | $\Delta a_{avg}$ not reported |
| EDF | 182 | D582.3TTS | D545/582 | SR | T-S | | 2394 | CL/CK | 30 | 360 | 38 | | | | | | N/A | $\Delta a_{avg}$ not reported |
| EDF | 182 | D582.3TTS | D545/582 | SR | T-S | | 1600 | CL/CK | 20 | 360 | 38 | | | | | | N/A | $\Delta a_{avg}$ not reported |

**Table A-5 (continued)**
**Alloy 82/182/132 CGR database–Scored-out data**

| Laboratory | Alloy | Overall Test ID | Weld | Post-Supplier Processing | Orientation | Segment ID | Test Segment Duration (h) | Load Type | K (MPa√m) | Temperature (°C) | Dissolved $H_2$ (cc/kg) | Hold Time (s) | Load Ratio | % Engaged | DCPD Correction Factor | Measured Δa (mm) | Reported SCC CGR (mm/s) | Scored Out Reason |
|---|---|---|---|---|---|---|---|---|---|---|---|---|---|---|---|---|---|---|
| EDF | 182 | D582.4TS | D545/582 | AW | T-S | | 2026 | CL/CK | 20 | 360 | 38 | | | | | | N/A | $\Delta a_{avg}$ not reported |
| EDF | 182 | D582.4TTS | D545/582 | SR | T-S | | 2069 | CL/CK | 20 | 325 | 38 | | | | | | N/A | $\Delta a_{avg}$ not reported |
| EDF | 182 | D582.5TS | D545/582 | AW | T-S | | 2026 | CL/CK | 20 | 360 | 38 | | | | | | N/A | $\Delta a_{avg}$ not reported |
| EDF | 182 | D582.6TS | D545/582 | AW | T-S | | 2026 | CL/CK | 20 | 360 | 38 | | | | | | N/A | $\Delta a_{avg}$ not reported |
| EDF | 182 | D582.7TS | D545/582 | AW | T-S | | 2026 | CL/CK | 20 | 360 | 38 | | | | | | N/A | $\Delta a_{avg}$ not reported |
| EDF | 182 | D582.7TTS | D545/582 | SR | T-S | | 2026 | CL/CK | 20 | 360 | 38 | | | | | | N/A | $\Delta a_{avg}$ not reported |
| EDF | 182 | D582.8TTS | D545/582 | SR | T-S | | 2026 | CL/CK | 20 | 360 | 38 | | | | | | N/A | $\Delta a_{avg}$ not reported |
| EDF | 182 | D582.9TTS | D545/582 | SR | T-S | | 2026 | CL/CK | 20 | 360 | 38 | | | | | | N/A | $\Delta a_{avg}$ not reported |
| ETH | 182 | 2991 | D545/582 | AW | T-L | | 2600 | CL/CK | 17 | 350 | 38 | | | | | | N/A | $\Delta a_{avg}$ not reported |
| ETH | 182 | 2992 | D545/582 | AW | T-L | | 3200 | CL/CK | 20 | 350 | 38 | | | | | | N/A | $\Delta a_{avg}$ not reported |
| ETH | 182 | 2993 | D545/582 | AW | T-L | | 2600 | CL/CK | 26 | 350 | 38 | | | | | | N/A | $\Delta a_{avg}$ not reported |
| ETH | 182 | 2994 | D545/582 | AW | T-L | | 2600 | CL/CK | 31 | 350 | 38 | | | | | | N/A | $\Delta a_{avg}$ not reported |
| ETH | 182 | 2995 | D545/582 | AW | T-L | | 3200 | CL/CK | 40 | 350 | 38 | | | | | | N/A | $\Delta a_{avg}$ not reported |
| ETH | 182 | 2996 | D545/582 | AW | T-L | | 2600 | CL/CK | 53 | 350 | 38 | | | | | | N/A | $\Delta a_{avg}$ not reported |
| ETH | 182 | 3113 | D545/582 | AW | T-L | | 4320 | CL/CK | 17 | 290 | 38 | | | | | | N/A | $\Delta a_{avg}$ not reported |
| ETH | 182 | 3114 | D545/582 | AW | T-L | | 4320 | CL/CK | 19 | 290 | 38 | | | | | | N/A | $\Delta a_{avg}$ not reported |
| ETH | 182 | 3115 | D545/582 | AW | T-L | | 1310 | CL/CK | 27 | 290 | 38 | | | | | | N/A | $\Delta a_{avg}$ not reported |
| ETH | 182 | 3116 | D545/582 | AW | T-L | | 4320 | CL/CK | 30 | 290 | 38 | | | | | | N/A | $\Delta a_{avg}$ not reported |
| ETH | 182 | 3117 | D545/582 | AW | T-L | | 14250 | CL/CK | 41 | 290 | 38 | | | | | | N/A | $\Delta a_{avg}$ not reported |
| ETH | 182 | 3118 | D545/582 | AW | T-L | | 4320 | CL/CK | 57 | 290 | 38 | | | | | | N/A | $\Delta a_{avg}$ not reported |
| ETH | 182 | 3132 | D545/582 | AW | T-L | | 2150 | CL/CK | 20 | 320 | 38 | | | | | | N/A | $\Delta a_{avg}$ not reported |
| ETH | 182 | 3133 | D545/582 | AW | T-L | | 2105 | CL/CK | 28 | 320 | 38 | | | | | | N/A | $\Delta a_{avg}$ not reported |
| ETH | 182 | 3134 | D545/582 | AW | T-L | | 11300 | CL/CK | 40 | 320 | 38 | | | | | | N/A | $\Delta a_{avg}$ not reported |
| ETH | 182 | 3135 | D545/582 | AW | T-L | | 2150 | CL/CK | 50 | 320 | 38 | | | | | | N/A | $\Delta a_{avg}$ not reported |
| ETH | 182 | 3511 | D545/582 | AW | T-L | | 850 | CL/CK | 15 | 350 | 38 | | | | | | N/A | $\Delta a_{avg}$ not reported |
| ETH | 182 | 3512 | D545/582 | AW | T-L | | 850 | CL/CK | 30 | 350 | 38 | | | | | | N/A | $\Delta a_{avg}$ not reported |
| ETH | 182 | 3513 | D545/582 | SR | T-L | | 850 | CL/CK | 64 | 350 | 38 | | | | | | N/A | $\Delta a_{avg}$ not reported |
| ETH | 182 | 3519 | D545/582 | SR | T-L | | 5873 | CL/CK | 63 | 290 | 38 | | | | | | N/A | $\Delta a_{avg}$ not reported |
| ETH | 182 | 3520 | D545/582 | SR | T-L | | 5873 | CL/CK | 14 | 290 | 38 | | | | | | N/A | $\Delta a_{avg}$ not reported |
| ETH | 182 | 3521 | D545/582 | SR | T-L | | 5873 | CL/CK | 33 | 290 | 38 | | | | | | N/A | $\Delta a_{avg}$ not reported |
| ETH | 182 | 3522 | D545/582 | AW | T-L | | 5873 | CL/CK | 55 | 290 | 38 | | | | | | N/A | $\Delta a_{avg}$ not reported |
| ETH | 182 | 3523 | D545/582 | SR | T-L | | 3400 | CL/CK | 59 | 320 | 38 | | | | | | N/A | $\Delta a_{avg}$ not reported |
| ETH | 182 | 3525 | D545/582 | SR | T-L | | 3400 | CL/CK | 31 | 320 | 38 | | | | | | N/A | $\Delta a_{avg}$ not reported |
| ETH | 182 | 3526 | D545/582 | AW | T-L | | 6080 | CL/CK | 24 | 320 | 38 | | | | | | N/A | $\Delta a_{avg}$ not reported |
| ETH | 182 | 3527 | D545/582 | AW | T-L | | 3400 | CL/CK | 52 | 320 | 38 | | | | | | N/A | $\Delta a_{avg}$ not reported |
| ETH | 182 | 3621 | D545/582 | SR | T-L | | 1840 | CL/CK | 39 | 350 | 38 | | | | | | N/A | $\Delta a_{avg}$ not reported |
| ETH | 182 | 3630 | D545/582 | AW | T-L | | 1840 | CL/CK | 21 | 350 | 38 | | | | | | N/A | $\Delta a_{avg}$ not reported |
| ETH | 182 | 3631 | D545/582 | AW | T-L | | 1840 | CL/CK | 58 | 350 | 38 | | | | | | N/A | $\Delta a_{avg}$ not reported |
| ETH | 182 | 3632 | D545/582 | AW | T-L | | 1840 | CL/CK | 14 | 350 | 38 | | | | | | N/A | $\Delta a_{avg}$ not reported |

**Table A-5 (continued)**
**Alloy 82/182/132 CGR database–Scored-out data**

| Laboratory | Alloy | Overall Test ID | Weld | Post-Supplier Processing | Orientation | Segment ID | Test Segment Duration (h) | Load Type | K (MPa√m) | Temperature (°C) | Dissolved $H_2$ (cc/kg) | Hold Time (s) | Load Ratio | % Engaged | DCPD Correction Factor | Measured Δa (mm) | Reported SCC CGR (mm/s) | Scored Out Reason |
|---|---|---|---|---|---|---|---|---|---|---|---|---|---|---|---|---|---|---|
| ETH | 182 | 3640 | D545/582 | SR | T-L | | 4560 | CL/CK | 41 | 320 | 38 | | | | | | N/A | $\Delta a_{avg}$ not reported |
| ETH | 182 | 3641 | D545/582 | SR | T-L | | 4560 | CL/CK | 15 | 320 | 38 | | | | | | N/A | $\Delta a_{avg}$ not reported |
| ETH | 182 | 3651 | D545/582 | AW | T-L | | 4530 | CL/CK | 39 | 320 | 38 | | | | | | N/A | $\Delta a_{avg}$ not reported |
| ETH | 182 | 3652 | D545/582 | AW | T-L | | 1830 | CL/CK | 62 | 320 | 38 | | | | | | N/A | $\Delta a_{avg}$ not reported |
| ETH | 182 | 3653 | D545/582 | AW | T-L | | 1830 | CL/CK | 21 | 320 | 38 | | | | | | N/A | $\Delta a_{avg}$ not reported |
| ETH | 182 | 3654 | D545/582 | AW | T-L | | 1830 | CL/CK | 16 | 320 | 38 | | | | | | N/A | $\Delta a_{avg}$ not reported |
| ETH | 182 | 3655 | D545/582 | SR | T-L | | 4506 | CL/CK | 30 | 320 | 38 | | | | | | N/A | $\Delta a_{avg}$ not reported |
| ETH | 182 | 3656 | D545/582 | AW | T-L | | 6449 | CL/CK | 22 | 290 | 38 | | | | | | N/A | $\Delta a_{avg}$ not reported |
| ETH | 182 | 3657 | D545/582 | AW | T-L | | 4440 | CL/CK | 40 | 290 | 38 | | | | | | N/A | $\Delta a_{avg}$ not reported |
| ETH | 182 | 3668 | D545/582 | AW | T-L | | 6449 | CL/CK | 20 | 290 | 38 | | | | | | N/A | $\Delta a_{avg}$ not reported |
| ETH | 182 | 3669 | D545/582 | AW | T-L | | 6449 | CL/CK | 72 | 290 | 38 | | | | | | N/A | $\Delta a_{avg}$ not reported |
| ETH | 182 | 3670 | D545/582 | AW | T-L | | 4440 | CL/CK | 42 | 290 | 38 | | | | | | N/A | $\Delta a_{avg}$ not reported |
| ETH | 182 | 3734 | D545/582 | SR | T-L | | 2700 | CL/CK | 40 | 350 | 38 | | | | | | N/A | $\Delta a_{avg}$ not reported |
| ETH | 182 | 3735 | D545/582 | SR | T-L | | 2700 | CL/CK | 25 | 350 | 38 | | | | | | N/A | $\Delta a_{avg}$ not reported |
| ETH | 182 | 3746 | D545/582 | SR | T-L | | 2630 | CL/CK | 30 | 320 | 38 | | | | | | N/A | $\Delta a_{avg}$ not reported |
| ETH | 182 | 3747 | D545/582 | SR | T-L | | 2630 | CL/CK | 14 | 320 | 38 | | | | | | N/A | $\Delta a_{avg}$ not reported |
| ETH | 182 | 3748 | D545/582 | SR | T-L | | 2630 | CL/CK | 38 | 320 | 38 | | | | | | N/A | $\Delta a_{avg}$ not reported |
| ETH | 182 | 3759 | D545/582 | SR | T-L | | 4719 | CL/CK | 40 | 290 | 38 | | | | | | N/A | $\Delta a_{avg}$ not reported |
| ETH | 182 | 3760 | D545/582 | SR | T-L | | 4719 | CL/CK | 25 | 290 | 38 | | | | | | N/A | $\Delta a_{avg}$ not reported |
| ETH | 182 | 3762 | D545/582 | AW | T-L | | 4719 | CL/CK | 16 | 290 | 38 | | | | | | N/A | $\Delta a_{avg}$ not reported |
| ETH | 182 | 3763 | D545/582 | AW | T-L | | 4719 | CL/CK | 29 | 290 | 38 | | | | | | N/A | $\Delta a_{avg}$ not reported |
| ETH | 182 | 3833 | D545/582 | SR | T-L | | 1600 | CL/CK | 20 | 350 | 38 | | | | | | N/A | $\Delta a_{avg}$ not reported |
| ETH | 182 | 3834 | D545/582 | SR | T-L | | 1600 | CL/CK | 35 | 350 | 38 | | | | | | N/A | $\Delta a_{avg}$ not reported |
| ETH | 182 | 3835 | D545/582 | SR | T-L | | 1600 | CL/CK | 59 | 350 | 38 | | | | | | N/A | $\Delta a_{avg}$ not reported |
| ETH | 182 | 3844 | D545/582 | SR | T-L | | 1600 | CL/CK | 49 | 350 | 38 | | | | | | N/A | $\Delta a_{avg}$ not reported |
| GE-GRC | 82H | c419 | HD78-1 | AW | T-S | C | 1512 | CK | 31.9 | 340 | 60 | | | | | 0 | 1.00E-10 | No growth; $H_2$ changes |
| GE-GRC | 82H | c419 | HD78-1 | AW | T-S | D | 1586 | CK | 31.9 | 340 | 45 | | | | | 0 | 1.00E-10 | No growth; $H_2$ changes |
| GE-GRC | 82H | c419 | HD78-1 | AW | T-S | E | 429 | CK | 31.9 | 340 | 15.3 | | | | | 0.129 | 1.20E-07 | $H_2$ changes |
| GE-GRC | 82H | c420 | HD78-1 | AW | T-S | C | 1512 | CK | 30.0 | 340 | 60 | | | | | 0 | 1.00E-10 | No growth |
| Lockheed Martin | 82 | LM82-2 | LM82-2 | AW | T-S | | | CL/CK | 50 | 338 | 40 | | | | | | 1.93E-07 | Low crack increment |
| MHI | 132 | 132-2 | MHI-132 | AW | L-S | | 200 | PPU | 35 | 325 | 30 | 1080 | 0.7 | | | 0.120 | 1.67E-07 | Short hold time |
| MHI | 132 | 132-LT2 | MHI-132 | AW | L-T | | 800 | PPU | 35 | 325 | 30 | 360 | 0.7 | | | 0.239 | 8.30E-08 | Short hold time |
| MHI | 82 | 82-2 | MHI-82 | AW | L-S | | 400 | PPU | 35 | 325 | 30 | 9000 | 0.7 | | | 0.048 | 3.30E-08 | <50% eng. |
| MHI | 82 | 82-2 | MHI-82 | AW | L-S | | 100 | CL/CK | 35 | 325 | 30 | | | | | 0.012 | 3.30E-08 | <50% eng. |
| MHI | 82 | 82-3 | MHI-82 | AW | L-S | | 349 | PPU | 35 | 325 | 30 | 9000 | 0.7 | | | 0.006 | 4.90E-09 | <50% eng. |
| MHI | 132 | MG7-1 | MHI-MG7 | AW | T-S | | 1000 | PPU | 20 | 325 | 30 | 9000 | 0.7 | | | 0.020 | 5.60E-09 | No growth |
| MHI | 132 | MG7-1 | MHI-MG7 | AW | T-S | | 200 | CL/CK | 20 | 325 | 30 | | | | | 0 | 0 | No growth |
| MHI | 132 | MG7-2 | MHI-MG7 | AW | T-S | | 200 | CL/CK | 35 | 325 | 30 | | | | | 0 | 0 | No growth |
| MHI | 132 | MG7L-1 | MHI-MG7 | AW | L-T | | 350 | PPU | 35 | 325 | 30 | 1080 | 0.7 | | | 0.105 | 8.30E-08 | Short hold time |

**Table A-5 (continued)**
**Alloy 82/182/132 CGR database–Scored-out data**

| Laboratory | Alloy | Overall Test ID | Weld | Post-Supplier Processing | Orientation | Segment ID | Test Segment Duration (h) | Load Type | K (MPa√m) | Temperature (°C) | Dissolved $H_2$ (cc/kg) | Hold Time (s) | Load Ratio | % Engaged | DCPD Correction Factor | Measured Δa (mm) | Reported SCC CGR (mm/s) | Scored Out Reason |
|---|---|---|---|---|---|---|---|---|---|---|---|---|---|---|---|---|---|---|
| MHI | 132 | MG7T-1 | MHI-MG7 | AW | L-S | | 1000 | PPU | 20 | 325 | 30 | 9000 | 0.7 | | | 0.020 | 5.60E-09 | No growth |
| MHI | 132 | MG7T-1 | MHI-MG7 | AW | L-S | | 200 | CL/CK | 20 | 325 | 30 | | | | | 0 | 0 | No growth |
| MHI | 132 | MG7T-2 | MHI-MG7 | AW | L-S | | 200 | CL/CK | 35 | 325 | 30 | | | | | 0 | 0 | No growth |
| Studsvik | 182 | 169-4:10-11 | 26B2 | AW | T-S | | 115 | PPU | 42 | 320 | 30 | 1000 | 0.75 | | | 0 | 0 | $\Delta a_{avg}$ not reported |
| Studsvik | 182 | 169-4:18-23 | 26B2 | AW | T-S | | 903 | PPU | 47 | 335 | 33 | 100000 | 0.75 | | | 2.390 | 7.35E-07 | Test conditions changed |
| Studsvik | 182 | 169-5:25-26 | 26B2 | AW | T-S | | 238 | PPU | 38 | 344 | 21 | 1000 | 0.75 | | | 1.310 | 1.53E-06 | Short hold time |
| Studsvik | 182 | 169-5:31 | 26B2 | AW | T-S | | 229 | PPU | 32 | 344 | 28 | 1000 | 0.75 | | | 0.590 | 7.16E-07 | Short hold time |
| Studsvik | 182 | 186B-27 | 33644 | AW | T-S | 4a | 4005 | CMOD | 8.6 | 340 | 25 | | | 11.1 | | 0.090 | 6.24E-09 | <50% eng. |
| Studsvik | 182 | 194-32 | 194 | AW | T-S | A | 5798 | CMOD | 8.9 | 340 | 25 | | | 17.1 | | 0.350 | 1.68E-08 | <50% eng. |
| Studsvik | 182 | 194-33 | 194 | AW | T-S | A | 5798 | CMOD | 12.1 | 340 | 25 | | | 45.3 | | 0.680 | 3.26E-08 | <50% eng. |
| Studsvik | 82 | A82-06 | MNPK3 | AW | T-S | 4a-4c | 6381 | CMOD | 10.8 | 340 | 25 | | | 7 | | 0.088 | 3.83E-09 | <50% eng. |
| Studsvik | 82 | A82-07 | MNPK3 | AW | T-S | 4a-4c | 6381 | CMOD | 16.9 | 340 | 25 | | | 12.3 | | 0.099 | 4.31E-09 | <50% eng. |
| Westinghouse | 182 | 182-1 | S 182 | AW | T-L | | | PPU | 20 | 325 | 33 | 1080 | 0.7 | | | | 4.80E-08 | Loading changes |
| Westinghouse | 182 | 182-1 | S 182 | AW | T-L | | | PPU | 21 | 325 | 33 | 1080 | 0.7 | | | | 1.60E-07 | Loading changes |
| Westinghouse | 182 | 182-1 | S 182 | AW | T-L | | | PPU | 22 | 325 | 33 | 1080 | 0.7 | | | | 1.60E-07 | Loading changes |
| Westinghouse | 182 | 182-1 | S 182 | AW | T-L | | | PPU | 22 | 325 | 33 | 1080 | 0.7 | | | | 1.60E-07 | Loading changes |
| Westinghouse | 182 | 182-2 | S 182 | AW | T-L | | | PPU | 34 | 325 | 33 | 9000 | 0.7 | | | | 2.60E-07 | Loading changes |
| Westinghouse | 182 | 182-2 | S 182 | AW | T-L | | | PPU | 35 | 325 | 33 | 9000 | 0.7 | | | | 2.60E-07 | Loading changes |
| Westinghouse | 182 | 182-2 | S 182 | AW | T-L | | | PPU | 36 | 325 | 33 | 9000 | 0.7 | | | | 2.60E-07 | Loading changes |
| Westinghouse | 182 | 182-2 | S 182 | AW | T-L | | | PPU | 37 | 325 | 33 | 9000 | 0.7 | | | | 2.60E-07 | Loading changes |
| Westinghouse | 82 | 82-1 | S 82 | AW | T-S | | | CL/CK | 20 | 325 | 33 | | | | | | 6.00E-08 | Loading changes |
| Westinghouse | 82 | 82-1 | S 82 | AW | T-S | | | CL/CK | 21 | 325 | 33 | | | | | | 1.85E-07 | Loading changes |
| Westinghouse | 82 | 82-1 | S 82 | AW | T-S | | | CL/CK | 22 | 325 | 33 | | | | | | 1.85E-07 | Loading changes |
| Westinghouse | 82 | 82-1 | S 82 | AW | T-S | | | CL/CK | 23 | 325 | 33 | | | | | | 1.85E-07 | Loading changes |
| Westinghouse | 82 | 82-2 | S 82 | AW | T-S | | | PPU | 38 | 325 | 33 | 9000 | 0.7 | | | | 2.70E-07 | Loading changes |
| Westinghouse | 82 | 82-2 | S 82 | AW | T-S | | | PPU | 39 | 325 | 33 | 9000 | 0.7 | | | | 2.45E-07 | Loading changes |
| Westinghouse | 82 | 82-2 | S 82 | AW | T-S | | | PPU | 41 | 325 | 33 | 9000 | 0.7 | | | | 1.70E-07 | Loading changes |
| Westinghouse | 82 | 82-2 | S 82 | AW | T-S | | | PPU | 42 | 325 | 33 | 9000 | 0.7 | | | | 3.20E-07 | Loading changes |

**Table A-6**
**Chemical compositions of all Alloy 82/182/132 welds tested in the CGR database, for which information was available**

| Weld | Alloy | Composition | | | | | | | | | | | | | | | | | |
|---|---|---|---|---|---|---|---|---|---|---|---|---|---|---|---|---|---|---|---|
| | | Al | B | C | Co | Cr | Cu | Fe | Mg | Mn | Mo | N | Nb | Ni | P | S | Si | Ta | Ti |
| 16 | 82 | — | — | 0.0345 | — | 19.5 | 0.04 | 0.99 | — | 2.9 | — | — | 2.6 | 73.0 | <0.001 | <0.001 | 0.06 | — | 0.42 |
| 194 | 182 | — | — | 0.044 | — | 14.6 | 0.01 | 7.75 | — | 5.66 | — | — | 1.34 | 69.8 | 0.005 | 0.005 | 0.39 | — | 0.29 |
| 6892 | 182 | — | — | 0.04 | 0.02 | 13.9 | 0.01 | 7.86 | — | 7.24 | — | — | 1.7 | 68.3 | 0.011 | 0.004 | 0.46 | 0.01 | 0.44 |
| 33644 | 182 | — | — | 0.025 | 0.01 | 16.3 | 0.04 | 5.1 | — | 5.6 | — | — | — | 69.7 | 0.008 | 0.005 | 0.38 | — | — |
| 26B2 | 182 | — | — | 0.04 | <0.01 | 14.1 | 1.63 | 7.36 | — | 7.3 | — | — | 0.44 | 68.64 | 0.01 | 0.003 | 0.46 | <0.07 | 0.01 |
| 7D | 82 | 0.04 | — | 420 | — | 19.2 | 0.097 | 1.31 | — | 2.76 | — | — | 2.42 | 73.2 | <0.001 | <0.001 | 0.17 | — | 0.36 |
| 8D | 82 | — | — | 345 | — | 19.8 | 0.03 | 1.18 | — | 2.87 | — | — | 2.37 | 72.9 | <0.001 | <0.001 | 0.08 | — | 0.35 |
| Davis-Besse-182 | 182 | — | — | 0.045 | 0.04 | 13.5 | <0.04 | 7.64 | — | 7.38 | — | — | 1.81 | bal | — | 0.017 | 0.52 | — | 0.27 |
| HD78-1 | 82H | 0.053 | 0.0002 | 0.0341 | 0.02 | 19.5 | 0.0021 | 0.4 | 0.0008 | 3.1 | 0.01 | 0.0151 | 2.4 | 74.15 | 0.0013 | 0.0004 | 0.11 | 0.2 | 0.0039 |
| LM182-1 | 182 | 0.02 | — | 0.029 | 0.015 | 14.8 | 0.04 | 7.35 | — | 7.55 | 0.05 | 0.017 | 2.13 | bal | <0.004 | 0.004 | 0.42 | — | 0.08 |
| LM182-2a | 182 | — | — | 0.030 | 0.03 | 15 | 0.0 | 7.2 | — | 5.9 | — | — | 2.00 | bal | — | 0.005 | 0.7 | — | 0.5 |
| LM182-2b | 182 | — | — | 0.02 | 0.03 | 15.10 | 0.000 | 7.00 | — | 6.00 | — | — | 1.9 | 68.7 | 0.01 | 0.005 | 0.8 | — | 0.5 |
| LM82-1 | 82 | — | — | 0.047 | 0.04 | 17.5 | 0.05 | 1.7 | — | 3.14 | — | — | 3.64 | 73.4 | — | 0.005 | 0.26 | — | 0.17 |
| LM82-2 | 82 | — | — | 0.045 | 0.0400 | 19 | 0.05 | 1.46 | — | 2.8 | — | — | 2.32 | 73.5 | 0.013 | 0.001 | 0.12 | — | 0.3 |
| LM82-3 | 82 | — | — | 0.045 | 0.0400 | 20.6 | 0.31 | 1.27 | — | 2.81 | — | — | 2.44 | 71.5 | 0.012 | 0.002 | 0.14 | — | 0.35 |
| MHI-132 | 132 | — | — | 0.04 | — | 14.5 | 0.02 | 9.49 | — | 2.9 | — | — | 1.85 | 71 | 0.003 | 0.001 | 0.22 | — | — |
| MHI-82 | 82 | — | — | 0.04 | — | 19.03 | 0.03 | bal | — | 2.86 | — | — | 2.44 | 72.87 | 0.005 | 0.001 | 0.25 | — | 0.4 |
| MNPK3 | 82 | — | — | 0.03 | <0.01 | 16.9 | 0.06 | 2.9 | — | 5.7 | 1.36 | 0.021 | 2.3 | — | <0.01 | 0.005 | 0.45 | — | 0.05 |
| NGW-1 | 82 | — | — | 400 | — | 18.5 | <0.01 | 1.3 | — | 2.61 | — | — | 2.6 | 74.4 | <0.001 | <0.001 | 0.1 | — | 0.36 |
| NGW-2 | 82 | — | — | 320 | — | 19.6 | <0.05 | 0.97 | — | 2.98 | — | — | 2.48 | 73.2 | <0.001 | <0.001 | <0.1 | — | 0.39 |
| PP751 | 182 | — | — | 0.053 | 0.02 | 14.6 | 0.03 | 9.9 | — | 5.96 | — | — | — | 67.26 | 0.014 | 0.006 | 0.35 | — | — |
| VCS-182 | 182 | — | — | 0.049 | 0.05 | 14.4 | 0.10 | 7.94 | — | 7.09 | — | — | 1.62 | bal | — | 0.010 | 0.66 | — | 0.72 |
| VCS-82 | 82 | — | — | 0.038 | 0.04 | 18.6 | 0.19 | 2.76 | — | 2.87 | — | — | 2.51 | bal | — | 0.001 | 0.18 | — | 0.44 |

# B
# HARDNESS, COLD WORK, AND YIELD STRENGTH RELATIONSHIPS FOR ALLOY 690

Relationships between cold work (CW), yield strength (YS), and hardness (HV) were developed from data in the Alloy 690 PWSCC CGR database compiled in MRP-386 [1]. The data are plotted in Figure B-1, Figure B-2, and Figure B-3, and the relationships between the properties are described by the following equations:

$$\boldsymbol{YS\ (MPa) = -0.501 \cdot \%CW^2 + 32.0 \cdot \%CW + 282} \qquad \textbf{Eq. B-1}$$

$$\boldsymbol{HV = -0.067 \cdot \%CW^2 + 5.88 \cdot \%CW + 181} \qquad \textbf{Eq. B-2}$$

$$\boldsymbol{HV = 0.248 \cdot YS(MPa) + 95.8} \qquad \textbf{Eq. B-3}$$

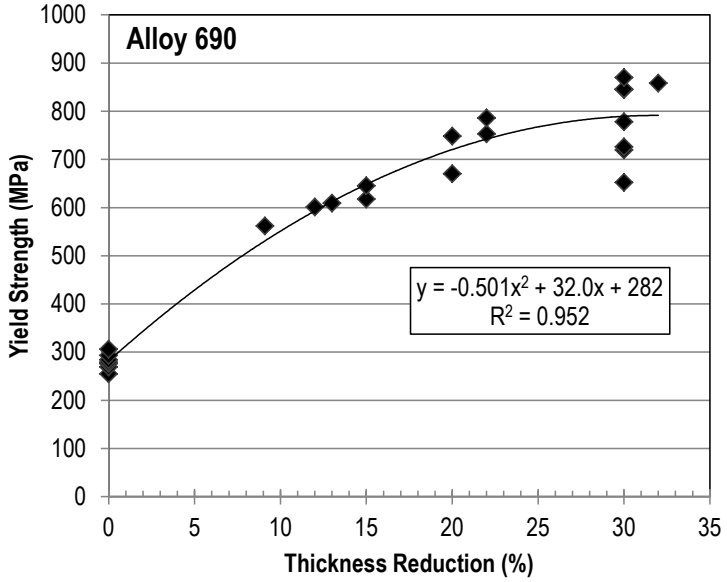


**Figure B-1**
**Relationship between yield strength and thickness reduction (i.e., cold work level) for Alloy 690**

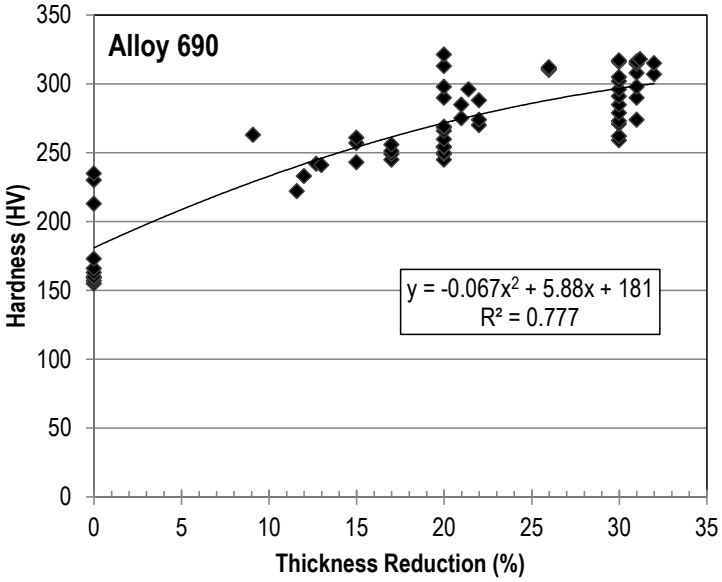


**Figure B-2**
**Relationship between Vickers hardness and thickness reduction (i.e., cold work level) for Alloy 690**

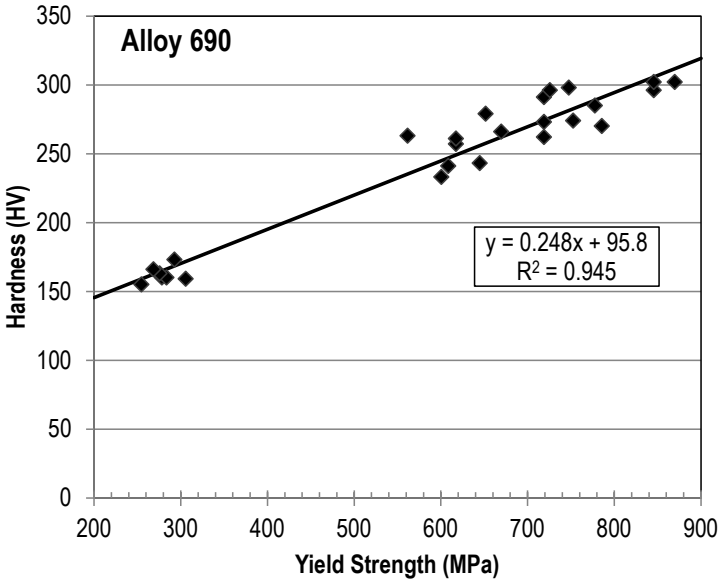


**Figure B-3**
**Relationship between Vickers hardness and yield strength for Alloy 690**

## B.1 References

*Materials Reliability Program: Crack Growth Rates for PWSCC of Alloy 690 and Alloy 52, 152, and Variants Welds (MRP-386).* EPRI, Palo Alto, CA: 2017. 3002010756.

# C
# UPDATED DISSOLVED HYDROGEN PARAMETER DEPENDENCIES IN REVISION 1

MRP-420 Rev. 0, which was published in December 2017 and is now obsolete, presented revised primary water stress corrosion cracking (PWSCC) crack growth rate (CGR) disposition equations for Alloy 600 wrought material and Alloy 82/182/132 weld metals. These equations updated those originally published in MRP-55 [1] and MRP-115 [2], respectively, based on a reevaluation of the functional dependencies determined in those reports and the addition of a dissolved hydrogen term for both the Alloy 600 and Alloy 82/182/132 equations. Later assessment of the practical implications of the MRP-420 Rev. 0 equations concluded that the magnitude of the dissolved hydrogen effect in the new Alloy 82/182/132 equation at reactor vessel cold leg temperatures ($T_{cold}$) was not sufficiently defensible. In particular, a distinct bias in the model residuals (i.e., $\log(CGR_{measured}) - \log(CGR_{predicted})$) versus temperature was apparent.

As a result, the basis for the Alloy 82/182/132 dissolved hydrogen model parameters was revisited for this Revision 1 of MRP-420. The parameter values presented in Section 5.3 and the CGR equations presented in Section 6.2 of the body of this report reflect this reassessment. No parameter values or equations for Alloy 600 were changed from Rev. 0.

The following Section C.1 contrasts the original (Rev. 0) and new (Rev. 1) approaches for selecting the parameter values for the hydrogen model. Section C.2 then assesses the bias in the model residuals induced by the hydrogen term on the temperature effect for both approaches. The revised MRP-420 Rev. 1 equation is shown to address the concern and hence represents a defensible temperature dependence.

## C.1 Approaches for Evaluating the Alloy 82/182/132 Dissolved Hydrogen Model Parameters

The MRP-420 Rev. 0 values for the dissolved hydrogen effect were determined from 10 datasets where CGR measurements were obtained at least at both the Ni/NiO transition concentration (i.e., $\Delta ECP_{Ni/NiO} = 0$ mV, referred to as the "peak") and far from this concentration (i.e., $|\Delta ECP_{Ni/NiO}| > 25$ mV, referred to as the "shelf"). The ratio of the CGRs measured at the peak and at the shelf were calculated for each dataset, and the median of these ratios was selected as the overall P value. Eight of the datasets included additional points at mid-range ΔECP values that could be used to determine the width of the Gaussian distribution, c. The median width was taken as the overall c value. In this way, the final parameter values were identified as P=14 and c=15 mV.

Due to the distinct bias in the overall disposition equation induced by the hydrogen term, a different approach was used for MRP-420 Rev. 1 with a goal to obtain parameter values that were more representative of all data. In this regard, five datasets were identified that showed an obvious Gaussian dependence along an extended ΔECP range, often, although not always, on

both sides of the Ni/NiO transition. Statistical best-fit P and c values were identified for each dataset using Microsoft Excel's Solver function to perform a least squares fit to the nonlinear equation form, as described in Section 5.3.3. The median of the fitted P values from each set was then assumed for all datasets and the Gaussian distributions were re-fit to each dataset to determine c. Taking the median of the resulting c values from each set resulted in final parameter values of P=7.5 and c=14 mV. This more modest hydrogen effect is most consistent with the totality of data and addresses, although it does not fully eliminate, the observed modeling bias in the predictions as a function of temperature, as shown in Section C.2. The statistical fitting approach for the Gaussian distributions is concluded to result in a more representative dependence on ΔECP than the approach taken in MRP-420 Rev. 0, in which the deduced value of P was based on the full range of reported CGRs for a given dataset and thus is susceptible to capturing some of the inherent random data scatter.

## C.2 Bias in the Temperature Effect Induced by the Hydrogen Model

Subsequent to the publication of MRP-420 Rev. 0 in December 2017, assessment of the practical implications of the MRP-420 Rev. 0 equations revealed a bias in the model residuals on the temperature dependence of the Alloy 82/182/132 equation. This bias has the greatest impact for components operating at reactor cold leg temperatures ($T_{cold}$), as such applications require extrapolation from the bulk of the laboratory testing conditions. Specifically, most of the Alloy 82/182/132 laboratory data were obtained at temperatures above 325°C (617°F), whereas reactor vessel cold leg temperatures are predominantly 285-294°C (545-561°F).

The trends in model residuals with respect to temperature were investigated for all data (top subfigures in Figure C-1 through Figure C-4), as well as for the specific welds/heats that include data obtained below 300°C (572°F) (bottom subfigures). The residuals presented here are evaluated at the 50$^{th}$ percentile, or best estimate, of material variability per the standard approach of calculating model residuals. The same bias trends versus temperature would be apparent when making predictions using the 75$^{th}$ percentile CGR equations recommended in Section 6.2.2.

An assessment of these residuals, as shown in Figure C-1, demonstrates that there exists significant bias in the temperature effect for the MRP-420 Rev. 0 equation for Alloy 82/182/132. In general, the Rev. 0 equation has a tendency to under-predict data for lower temperatures that are relevant to reactor vessel cold leg temperatures (i.e., $CGR_{meas} > CGR_{pred}$). This can be seen acutely in the bottom subfigure of Figure C-1, which includes only the welds for which data were obtained below 300°C (572°F) (in addition to data at higher temperatures as well). The slopes for three of these welds are negative with respect to increasing temperature, exemplifying this bias. Such a bias is not readily apparent for the MRP-420 Rev. 0 equation for Alloy 600 (see Figure C-2) or when comparing the MRP-420 data with predictions made using the MRP-115 [2] equation in Figure C-3.

Temperature dependencies in the CGR disposition equations are included in both the explicit Arrhenius temperature term and in the dissolved hydrogen term, so either or both terms could have been adjusted to address the observed bias. The alternative, more statistically meaningful approach to fitting P and c was investigated first. Subsequently, the new hydrogen parameter values were used to reevaluate the inherent activation energy, $Q_{inh}$, described in Section 5.3.2, the results of which support maintaining the MRP-420 Rev. 0 Q value of 120 kJ/mol (29 kcal/mol). Using the revised hydrogen terms presented in Section C.1 for the MRP-420 Rev. 1

equation results in the trends with respect to temperature shown in Figure C-4. This approach was selected to resolve the bias concern because it meets the theoretical expectation of the same inherent activation energy for Alloy 600 and its weld metals and because it reflects a more statistically meaningful approach to fitting the ΔECP dependence.

A comparison of the trends for the four low-temperature welds with respect to temperature for the three Alloy 82/182/132 equations – MRP-115, MRP-420 Rev. 0, and MRP-420 Rev. 1 – is shown in Table C-1. As shown in the table, the MRP-420 Rev. 0 equation results in trends with slopes that both have the maximum value of the three equations and has the largest median, when comparing absolute values. With the revised hydrogen parameters, the MRP-420 Rev. 1 equation has both the lowest median and average trends, and it is close to the MRP-115 equation in terms of the greatest magnitude of bias for these four welds.

Based on the reduced bias produced, it is therefore concluded that the reduced magnitude of the hydrogen effect included in the MRP-420 Rev. 1 equation for Alloy 82/182/132 is most appropriate for use.

For reference, as mentioned above, the bias in the overall temperature effect has the greatest impact on predictions made for reactor cold leg temperatures. Over the main K values of interest at $T_{cold}$, the MRP-420 Rev. 1 equation predicts CGRs that are a factor of ~3 lower than those predicted by MRP-115 for the same conditions, whereas the MRP-420 Rev. 0 equation is lower than the MRP-115 equation by a factor of about 5-6.

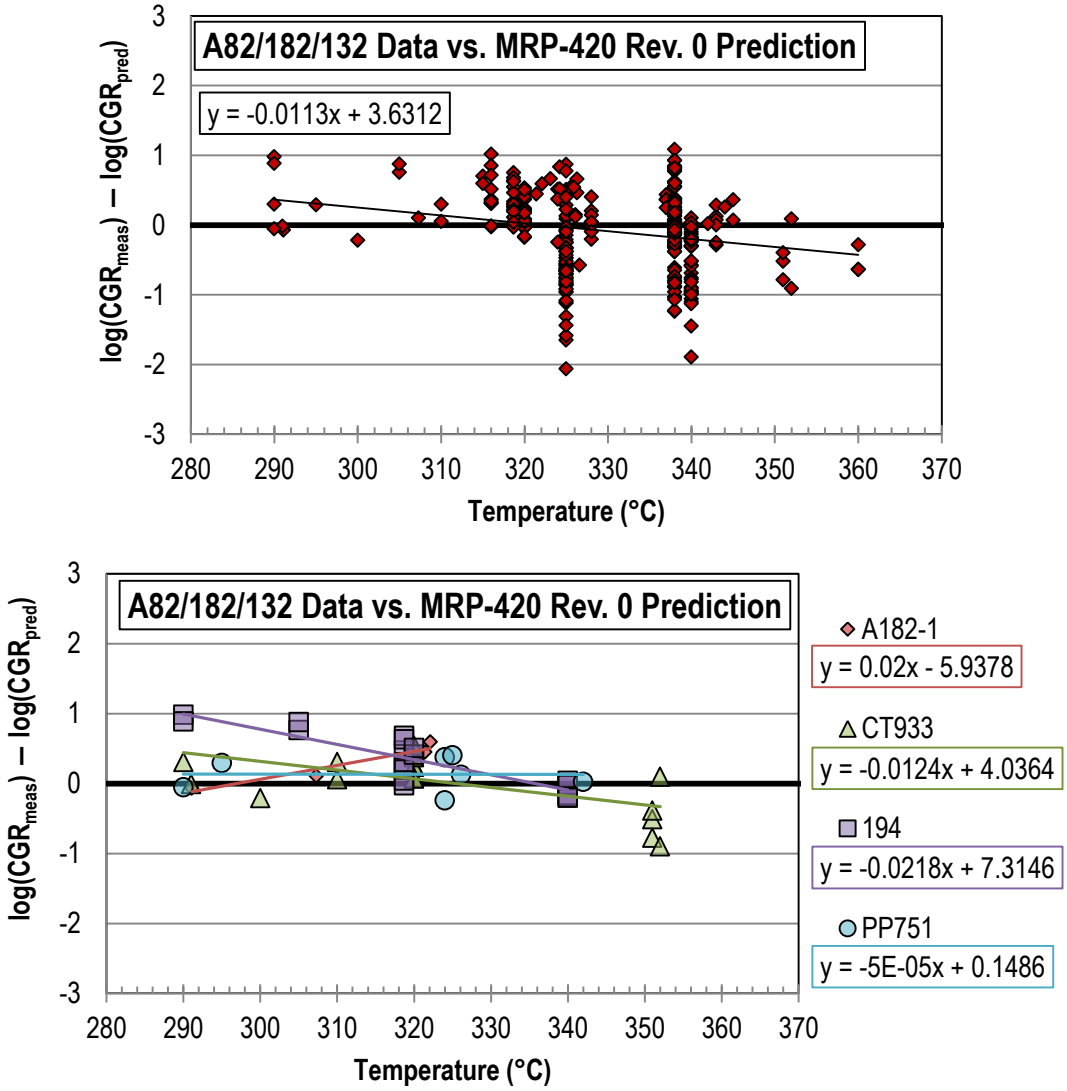


**Figure C-1**
**Residuals for the MRP-420 Rev. 0 Alloy 82/182/132 temperature effect, evaluated at the 50th percentile of weld variability. Top: All scored-in Alloy 82/182/132 data. Bottom: Welds for which data were obtained below 300°C (572°F) (in addition to higher temperatures).**

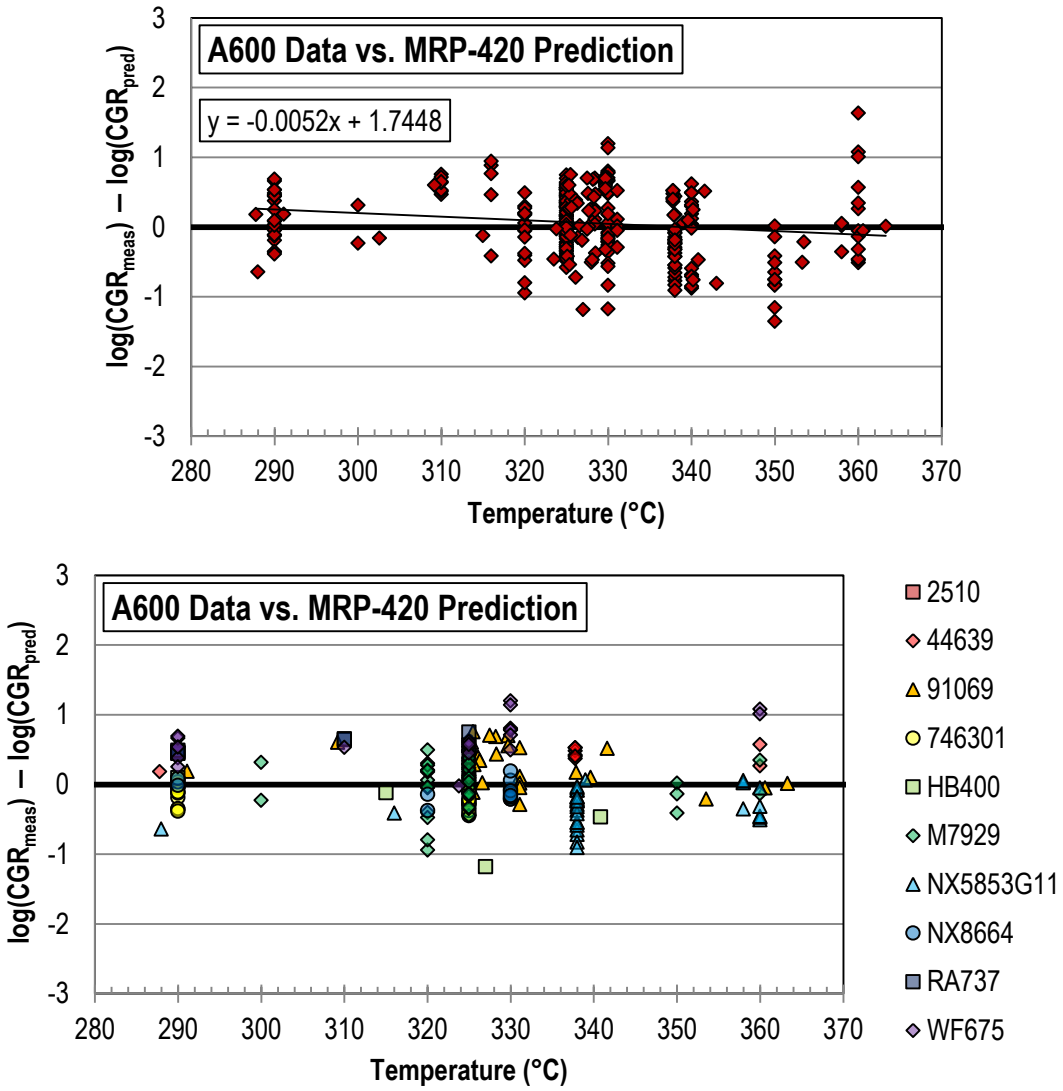


**Figure C-2**
**Residuals for the MRP-420 Alloy 600 temperature effect, evaluated at the 50th percentile of heat variability. Top: All scored-in Alloy 600 data. Bottom: Heats for which data were obtained below 300°C (572°F) (in addition to higher temperatures).**

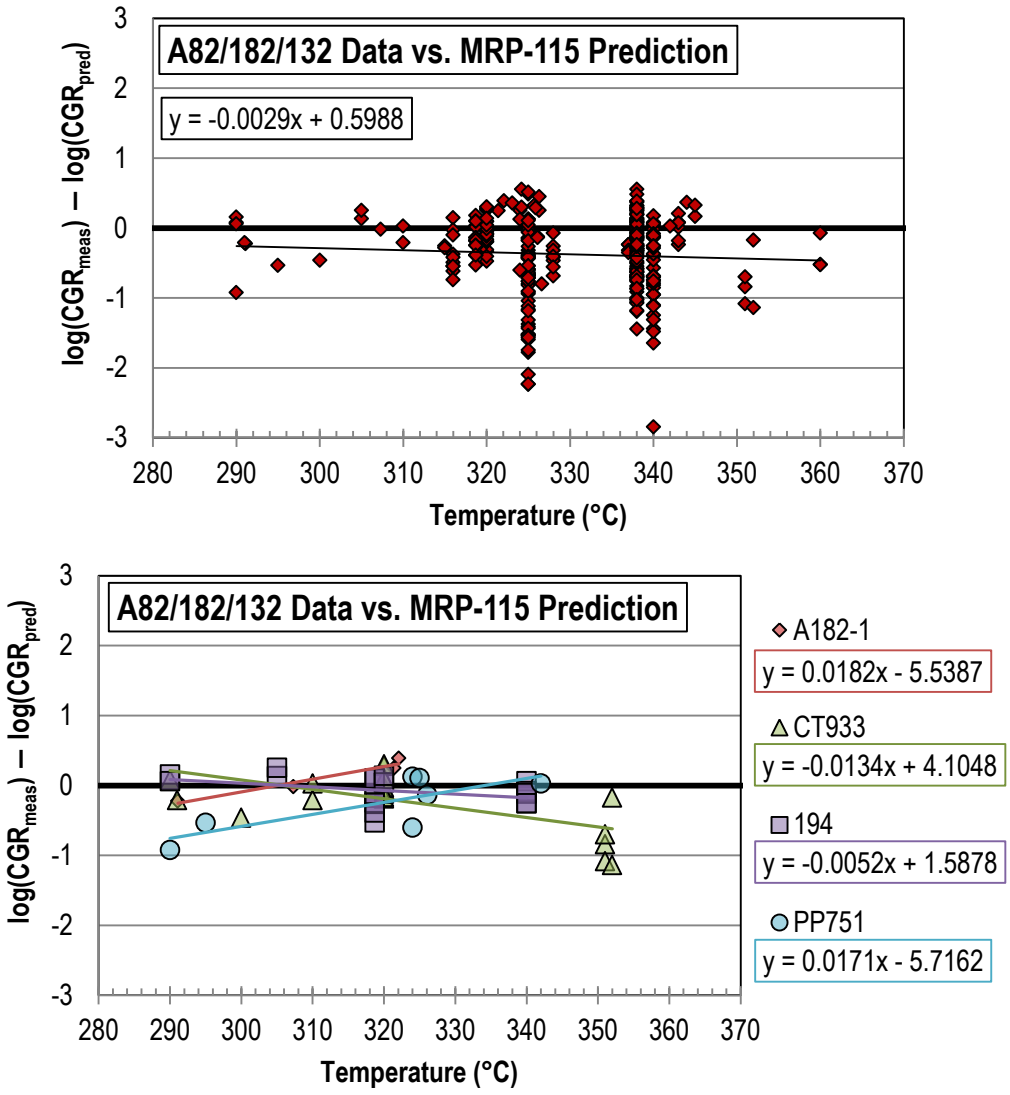


**Figure C-3**
**Residuals for the MRP-420 Alloy 82/182/132 data and MRP-115 equation versus temperature, evaluated at the 50th percentile of weld variability. Top: All scored-in Alloy 82/182/132 data. Bottom: Welds for which data were obtained below 300°C (572°F) (in addition to higher temperatures).**

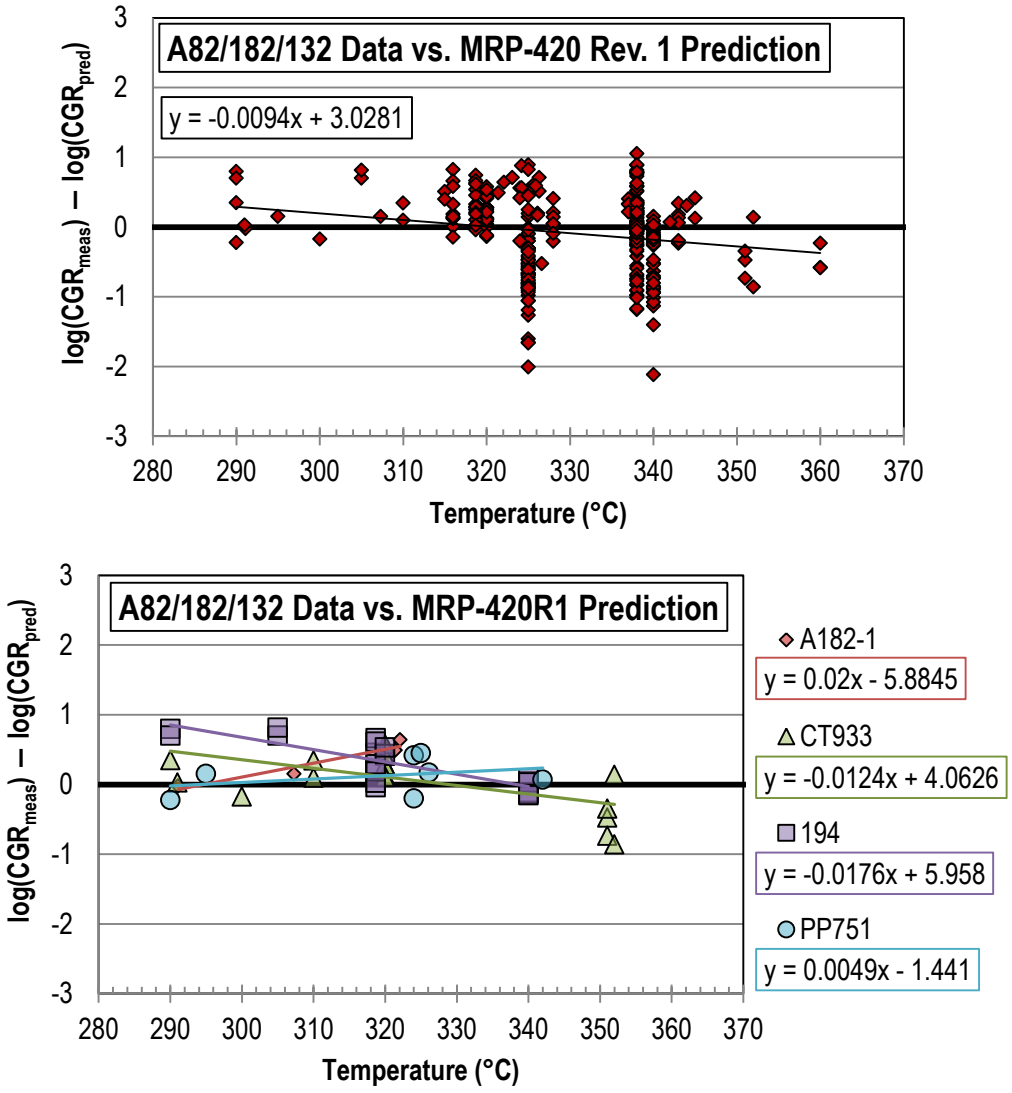


**Figure C-4**
**Residuals for the MRP-420 Rev. 1 Alloy 82/182/132 temperature effect, evaluated at the 50th percentile of weld variability. Top: All scored-in Alloy 82/182/132 data. Bottom: Welds for which data were obtained below 300°C (572°F) (in addition to higher temperatures).**

**Table C-1**
**Comparison of temperature effect trends for the four Alloy 82/182/132 welds shown in Figure C-1, Figure C-3, and Figure C-4. Bolded values are the lowest absolute values across the three equations.**

| Weld | Trend Slope | | |
|---|---|---|---|
| | MRP-115 Equation | MRP-420 R0 Equation | MRP-420 R1 Equation |
| A182-1 | 0.0182 | 0.0200 | 0.0200 |
| CT933 | -0.0134 | -0.0124 | -0.0124 |
| 194 | -0.0052 | -0.0218 | -0.0176 |
| PP751 | 0.0171 | -0.0001 | 0.0049 |
| Max Abs Value | **0.0182** | 0.0218 | 0.0200 |
| Median | 0.0060 | -0.0063 | **-0.0038** |
| Average | 0.0042 | -0.0036 | **-0.0013** |
| All Data | -0.0029 | -0.0113 | -0.0094 |

## C.3 References

1. *Materials Reliability Program (MRP) Crack Growth Rates for Evaluating Primary Water Stress Corrosion Cracking (PWSCC) of Thick-Wall Alloy 600 Materials (MRP-55) Revision 1*, EPRI, Palo Alto, CA: 2002. 1006695.
2. *Materials Reliability Program Crack Growth Rates for Evaluating Primary Water Stress Corrosion Cracking (PWSCC) of Alloy 82, 182, and 132 Welds (MRP-115)*, EPRI, Palo Alto, CA: 2004. 1006696.

**The Electric Power Research Institute, Inc.** (EPRI, www.epri.com) conducts research and development relating to the generation, delivery and use of electricity for the benefit of the public. An independent, nonprofit organization, EPRI brings together its scientists and engineers as well as experts from academia and industry to help address challenges in electricity, including reliability, efficiency, affordability, health, safety and the environment. EPRI members represent 90% of the electric utility revenue in the United States with international participation in 35 countries. EPRI's principal offices and laboratories are located in Palo Alto, Calif.; Charlotte, N.C.; Knoxville, Tenn.; and Lenox, Mass.

Together...Shaping the Future of Electricity

***Program:***

Pressurized Water Reactor Materials Reliability Program (MRP)



3002014244

**Electric Power Research Institute**
3420 Hillview Avenue, Palo Alto, California 94304-1338 • PO Box 10412, Palo Alto, California 94303-0813 USA
800.313.3774 • 650.855.2121 • askepri@epri.com • www.epri.com